

CALIFORNIA INSTITUTE OF TECHNOLOGY

EARTHQUAKE ENGINEERING RESEARCH LABORATORY

SPECTRUM ANALYSES OF STRONG-MOTION
EARTHQUAKES

by

J. L. Alford, G. W. Housner, and R. R. Martel

A REPORT ON RESEARCH CONDUCTED UNDER
CONTRACT WITH THE OFFICE OF NAVAL RESEARCH

August 1951

(Revised August 1964)

SPECTRUM ANALYSES OF STRONG-MOTION
EARTHQUAKES

by

J. L. ALFORD, G. W. HOUSNER, and R. R. MARTEL

FIRST TECHNICAL REPORT

under

OFFICE OF NAVAL RESEARCH
Contract N6onr-244
Task Order 25
PROJECT DESIGNATION NR-081-095

CALIFORNIA INSTITUTE OF TECHNOLOGY
PASADENA, CALIFORNIA
AUGUST 1951

(Revised August, 1964)

Spectrum Analyses of Strong-Motion Earthquakes

Table of Contents

	Preface	
	Abstract	iv
I	Introduction	1
II	Analytical Outline of the Earthquake Problem	3
III	Evaluation of the Spectrum	5
IV	Description of the Analog Computer Technique	10
V	Results of the Investigation	23
VI	Discussion of the Results	96
VII	Summary and Conclusions	104
	Appendix A. Damping in multiple-degree-of-freedom systems	106
	Acknowledgments	108
	References	109
	San Francisco Earthquakes of March, 1957	111
	Appendix I	118
	Appendix II	120
	Appendix III	123

PREFACE

SPECTRUM ANALYSES OF STRONG-MOTION EARTHQUAKES

This report, first issued in 1951, contained the response spectra of all of the larger recorded ground accelerations. It was the first time that damped response spectrum curves had been calculated. Actually, earlier spectrum curves, calculated by means of a torsion pendulum, which were thought to be the zero damped curves, were later found to be damped curves as the torsion pendulums had a not insignificant amount of damping.

Since the report contains a convenient collection of spectrum curves, together with the accelerograms from which they were calculated, there has been a large demand for copies, and there have been a number of reprintings. When it was decided to make the present reprinting, later pertinent results were added. The Taft 1952 accelerograms and spectra have been included as it was a large and important earthquake. The accelerograms and spectra of the Port Hueneme shock of 28 March 1957 have been included as this was an interesting example of a single displacement pulse earthquake. The accelerograms and spectra of the San Francisco earthquake of 22 March 1957 have been included as this is the only case where as many as four accelerometers were in the epicentral region. The spectra of Mexico City ground motions have been included because of the extremely soft ground at this site, whose natural period is exhibited in the spectra.

The original spectra were calculated on an analog computer, perhaps the first machine to have suitable capability. Since then, the development of large digital computers has led to spectrum calculations being performed in many places. This raised the question of reproducibility of results, that is, if two persons, starting with the accelerogram of ground motion, were to calculate the spectrum independently, how great a discrepancy would result? Such calculations were performed on the first 60 seconds of recorded ground motion at Taft, 1952, at the University of California (R. W. Clough), the University of Michigan (G. V. Berg), the University of Illinois (A. Veletsos), and the California Institute of Technology (D. E. Hudson). The results, which were obtained by means of digital computers, are also included in Appendix I of the present report. It may be noted that when spectrum curves are calculated without special regard to accuracy, discrepancies of 25% or more have been exhibited. However, careful checks on these discrepancies indicates that the original spectrum curves of this report are accurate to within 10%.

Integrated ground velocities and ground displacements have been included in Appendix III to the report to round out the picture.

In Appendix II there is shown a comparison of the spectra as calculated by means of an analog computer and as calculated by means of a digital computer. In view of the close relationship between the velocity response spectrum and the Fourier spectrum a comparison of these is also given in Appendix III.

George W. Housner

August 1964

LIST OF TABLES

<u>TABLE</u>	<u>TITLE</u>	<u>PAGE</u>
I.	Mechanical-electrical Relations for Analog	14
II.	Summary of Spectra and Earthquake Data	25

LIST OF FIGURES

<u>FIG. NO.</u>	<u>TITLE</u>	<u>PAGE</u>
1	Torsion-pendulum analyzer	7
2	Basic electro-mechanical analog	11
3	Electric analog computer :	12
4	Plotting Table for film records	15
5	Typical computer solutions. Los Angeles Subway Terminal, Oct. 2, 1933. Component N 51 W	18
6	Computer circuit diagram	20
7 - 27	Accelerograms. (see Table II)	26 - 46
28 - 48	Velocity Spectra. (see Table II)	47 - 67
49 - 76	Acceleration Spectra. (see Table II)	68 - 95

ABSTRACT

The problem of the dynamic response of a structure to an earthquake has been formulated in a manner which permits separation of the characteristics of particular structures from the characteristics of the earthquake. The expression involving the characteristics of the earthquake is defined as the "spectrum" of the earthquake and it is shown that the spectrum is simply a plot of the response of a simple oscillator versus the period of the oscillator. Eighty-eight such spectra were computed by means of an electric analog computer and are presented in this report.

It is found that damping is a very important parameter in the overall problem; relatively small amounts of damping reduce structural response sharply. It is shown that, when damping is considered, the spectra are consistent with the hypothesis of a distribution about a mean value. It is concluded that the concept of a "dominant ground period" is not valid for the purpose of aseismic structural design. Further research on damping in buildings is recommended, and it is proposed that the mean value of a damped spectrum be used as a quantitative measure of earthquake intensity.

I. INTRODUCTION

When an earthquake takes place the base of a structure is subjected to a variable acceleration, and dynamic stresses are developed throughout the structure. The destructive effect of the stronger earthquakes on structures not specifically designed to withstand such stresses has demonstrated the need for methods of aseismic structural design. In order that these methods be as realistic as possible it is desirable to have an understanding of the dynamic response of structures to earthquake motions.

The attack on this problem has utilized three principal approaches: the accumulation of empirical data by study of actual earthquake damage, the performance of experiments on structures and structural models, and the making of analytical studies. This report is of the last type and presents an analysis of certain phases of the earthquake problem.

The response of a structure to an earthquake is essentially a vibration problem; hence an analytical solution would be possible which depends on the mass, rigidity, and damping of the structure and on the nature of the soil which supports the structure. However, certain practical difficulties are encountered which obviate a straightforward approach. First, it is not possible to know the intensity and characteristics of a future earthquake so that even if a complete analytical solution were possible it would not suffice for a predetermination of earthquake stresses. Second, the precise physical properties of the structure with which the engineer must deal are not readily determined; it is questionable at present whether all the dynamic properties can be determined precisely before a structure is built. It is not possible, therefore, to predict what stresses will be produced by an unknown earthquake acting upon a structure whose properties are not known precisely.

If we wish to obtain meaningful results it is necessary to restate the problem; instead of asking for the actual magnitudes of the earthquake stresses, we may legitimately ask the following question. Assuming that future earthquakes will have approximately the same characteristics as past earthquakes, how should structures be designed so that all parts have approximately the same factor of safety?

To answer this question it is necessary, first, to determine the significant characteristics of past earthquakes and, then, to deduce the significant dynamic behavior of structures when subjected to such earthquakes. An investigation of these two questions constitutes the present project; this report is a statement of progress on the first phase of the problem.

II. ANALYTICAL OUTLINE OF THE EARTHQUAKE PROBLEM

In order to investigate the characteristics of an earthquake as regards its effect upon structures it is necessary to formulate the problem in such a manner that the proper approach is clarified. For this purpose we shall consider the general class of structures which have linearly elastic damped vibrations. If the damping be subject to certain restrictions, which are discussed in Appendix A, it is known (1)* that during free vibrations of such a structure the displacement, y , at any point can be represented by the sum of the normal modes of vibration

$$y = \sum_i c_i \phi_i e^{-n_i p_i t} \sin p_i t \quad (1)$$

in which

- c_i = undetermined coefficient
- ϕ_i = i^{th} normal mode
- p_i = 2π times the frequency of vibration of the i^{th} mode
- n_i = ratio of damping in i^{th} mode to critical damping
- t = time

If the free vibrations are initiated in such a fashion that at time $t = 0$, the displacement is zero and the velocity is v_0 at every point of the structure, then the coefficients c_i are evaluated in the Fourier manner, namely,

$$c_i = \frac{v_0}{p_i} \cdot \frac{\int \phi_i \rho}{\int \phi_i^2 \rho} = \frac{v_0}{p_i} W_i \quad (2)$$

in which ρ is the density and the integrals are taken over the entire mass of the structure. The corresponding free vibrations are then

$$y = \sum_i \frac{v_0}{p_i} W_i \phi_i e^{-n_i p_i t} \sin p_i t \quad (3)$$

*Numbers in parentheses refer to the Bibliography at the end of this report.

If now the base of the structure be subjected to a variable acceleration, a , the displacement at time t , is given (2) by

$$y = \sum_i \frac{W_i}{P_i} \phi_i \int_0^t a e^{-n_i P_i (t-\tau)} \sin p_i (t-\tau) d\tau \quad (4)$$

This may be written as

$$y = \sum_i \frac{W_i}{P_i} \phi_i X_i \quad (5)$$

in which

$$X_i = \int_0^t a e^{-n_i P_i (t-\tau)} \sin p_i (t-\tau) d\tau \quad (6)$$

It should be noted that the factor W_i/P_i is a function only of the physical properties of the structure, that is, mass, rigidity, and dimensions. The factor ϕ_i is a function of the space coordinates and the factor X_i is a function of the earthquake (ground acceleration). The physical significance of Equation (6) is that X_i^2 is a measure of the kinetic energy of an oscillator with frequency $P_i/2\pi$ which is subjected to the ground acceleration.

From Equation (5) it can be seen that in order to investigate the significant characteristics of earthquakes it is necessary to evaluate X as a function of p and n for past earthquakes and determine its behavior. We shall refer to the factor X as the spectrum of the earthquake.

A study of the factors $\frac{W_i}{P_i}$ and ϕ_i , on the other hand, would reveal the effect of the physical properties of particular types of structure.

III. EVALUATION OF THE SPECTRUM

A. General Considerations

The accelerograms of fourteen strong-motion earthquakes are presented in Figures 7 through 27; X_i is to be evaluated for these earthquakes. It will be noted from Equation 6 that X_i is a function not only of the ground acceleration, a , but also of n_i , the damping ratio; of p_i , which is equal to 2π divided by the period of vibration of the i^{th} mode; and of t , the time at which the integral is evaluated.

For a complete examination of X_i , it is necessary to evaluate the integral in Equation 6 for all periods of vibration which are pertinent to the structural problem. In practice the calculations are made for periods of vibration between 0.1 and 3.0 seconds. Since the damping in structures may vary widely, all of the spectra have been computed for several values of damping ratio.

When X_i is computed for particular values of p_i and n_i , there is obtained a time-history of the displacement of a simple oscillator of the specified period and damping ratio as it responds to the recorded ground acceleration. This response passes through a maximum at some time prior to the end of the earthquake and it is this maximum value which is of interest for aseismic design. The spectrum will therefore consist of a plot of such maximum responses versus period of vibration, with damping ratio as a parameter.

B. Analytical Methods

Several methods have been used in the past for calculating the response; one of the first was a direct numerical integration of Equation 6 using finite time intervals. Another was a semi-graphical procedure in which an integrator was used. These methods have been described in a previous paper (3). Both methods are excessively laborious and time-consuming, and both have the disadvantage of being feasible only for the case of zero damping.

C. The Torsion Pendulum Analog

A more convenient method is based upon the use of a physical model of a simple oscillator, rather than a mathematical process, for performing the integration in Equation 6. This is possible because, once the period and damping values are particularized as they must be in any method of calculation, Equation 4 represents simply the response of a simple oscillator, such as the one shown in Fig. 2, to the earthquake acceleration "a". Several investigators have applied this technique to the zero-damping case, with a torsion pendulum as the physical model of the simple oscillator. The method has been described by Biot (4), but a brief description will be given here in the interest of completeness. The equipment which was used in earlier spectrum analysis at the California Institute of Technology is shown in Figure 1. It consists basically of a torsion pendulum, an input function device, and a means for measuring the angular displacement. The torsion pendulum comprises a vertical torsion element which supports a horizontal inertia bar, the whole being supported on a ball thrust-bearing. Gross changes in period are made by assembling torsion elements of different diameter; fine changes by changing the separation of the masses on the inertia bar.

The input device consists of a table which is translated at a uniform speed by means of a lead screw, and a tracer-arm linkage which imparts to the upper end of the torsion element an angular motion proportional to the ground acceleration. The angular displacement of the pendulum's lower end is indicated by a beam of light which is reflected from a mirror attached to the inertia bar and focused on a circular scale. Lateral oscillations of the pendulum are damped by a thin-walled cylinder suspended in oil from the bottom of the inertia bar.

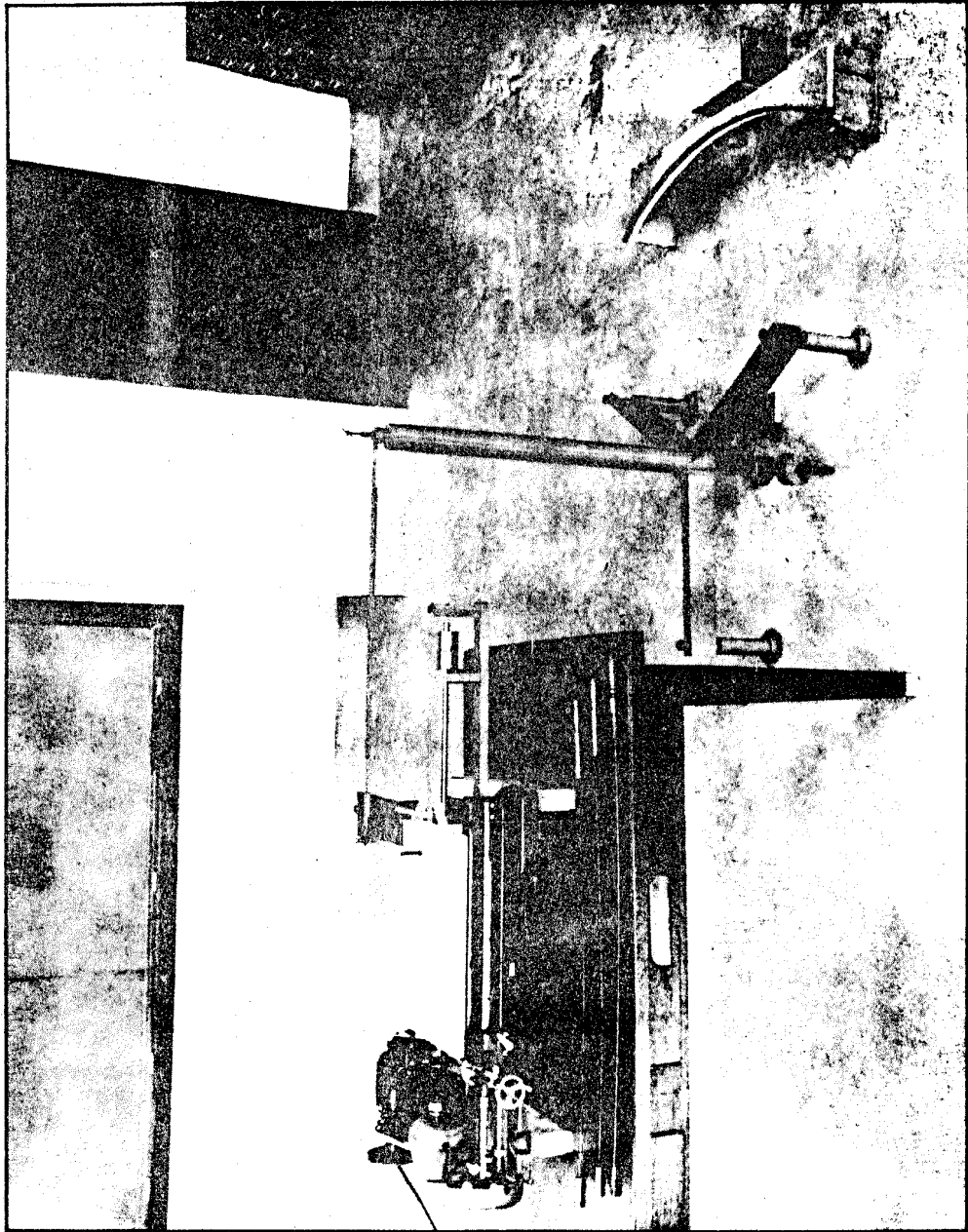


Figure 1. Torsion-pendulum analyzer.

The differential equation of this system is

$$I \ddot{\alpha} + c (\alpha - \alpha_0) = 0 \quad (7)$$

in which

- α = Angular displacement of inertia bar
- α_0 = impressed displacement of upper end
- I = polar moment of inertia
- c = spring constant of torsion element

This can be rewritten as

$$I \ddot{\alpha} + c \alpha = c \alpha_0 \quad (8)$$

Equation 8 shows that the response of the pendulum to the base motion α_0 is mathematically equivalent to its response to a torque $c \alpha_0$. The undamped response is given by

$$\alpha = \frac{1}{p} \int_0^t \frac{c \alpha_0}{I} \sin p (t-\tau) d \tau \quad (9)$$

Noting that $\frac{c}{I} = p^2$ and that $\alpha_0 = a \cdot \frac{K}{L}$, where K is the scale of the accelerometer and L is the length of the tracer arm, this becomes

$$\alpha = \frac{pK}{L} \int_0^t a \sin p (t-\tau) d \tau = \frac{pK}{L} \cdot X \quad (10)$$

Therefore

$$X_{\max} = \frac{L}{pK} \cdot \alpha_{\max} \quad (11)$$

Thus, by performing the experiment for a large number of periods, a reasonable approximation to the undamped spectrum could be obtained. It would be possible to extend this method to the damped spectra; that this has not been done is largely due to the development of a more convenient physical model for determining both undamped and damped spectra.

D. The Electric Circuit Analog

A physical model of the simple oscillator which is more convenient in use than the torsion pendulum is an electric circuit. Since the electric analog technique was used in this investigation, a detailed description of it will be given in the following section.

IV. DESCRIPTION OF THE ANALOG COMPUTER TECHNIQUE

The basis of the electric analog method of solution is shown in Figure 2, in which it can be seen that the equation which governs the behavior of the single loop circuit is of the same form as the equation of motion of the simple mechanical oscillator. If the circuit constants are made proportional to the corresponding coefficients of the mechanical equation, the mechanical solution can be found to an appropriate scale by measuring the corresponding electrical variable. The electric analog computer at the California Institute of Technology is a general-purpose machine for the rapid solution of problems by means of such analogies. The computer and its application to earthquake problems have been described in the literature (5, 6, 7); however, a description will be given here in detail sufficient for the continuity of this report.

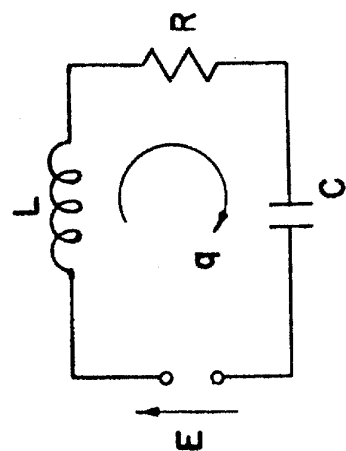
The electric analog computer used in these studies is shown in Figure 3. It comprises complete facilities for the electrical simulation of a wide variety of physical systems, the generation of steady-state or arbitrary excitation functions, and the observation and recording of the dependent variables.

A. Simulation of the Physical System.

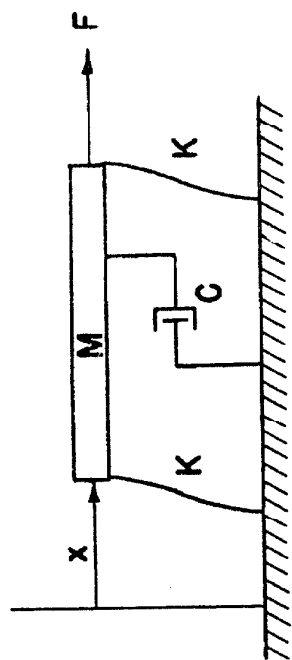
The physical system to be simulated in this study is the simple mechanical oscillator of Figure 2, in which it is assumed that the damping is viscous in character (see Appendix A). The analogous circuit is shown in the same figure.

If an arbitrary ground displacement be applied to the simple mechanical oscillator of Fig. 2 the equation of motion will be

$$m \frac{d^2}{dt^2} (x + z) + c \frac{dx}{dt} + kx = 0 \quad (12)$$



$$E = L\ddot{q} + R\dot{q} + \frac{1}{C}q$$



$$F = M\ddot{x} + C\dot{x} + Kx$$

$$2\pi\sqrt{\frac{M}{K}} \text{ PERIOD}$$

$$50 C \sqrt{\frac{1}{KM}} \text{ \% DAMPING}$$

Figure 2. Basic electro-mechanical analog.

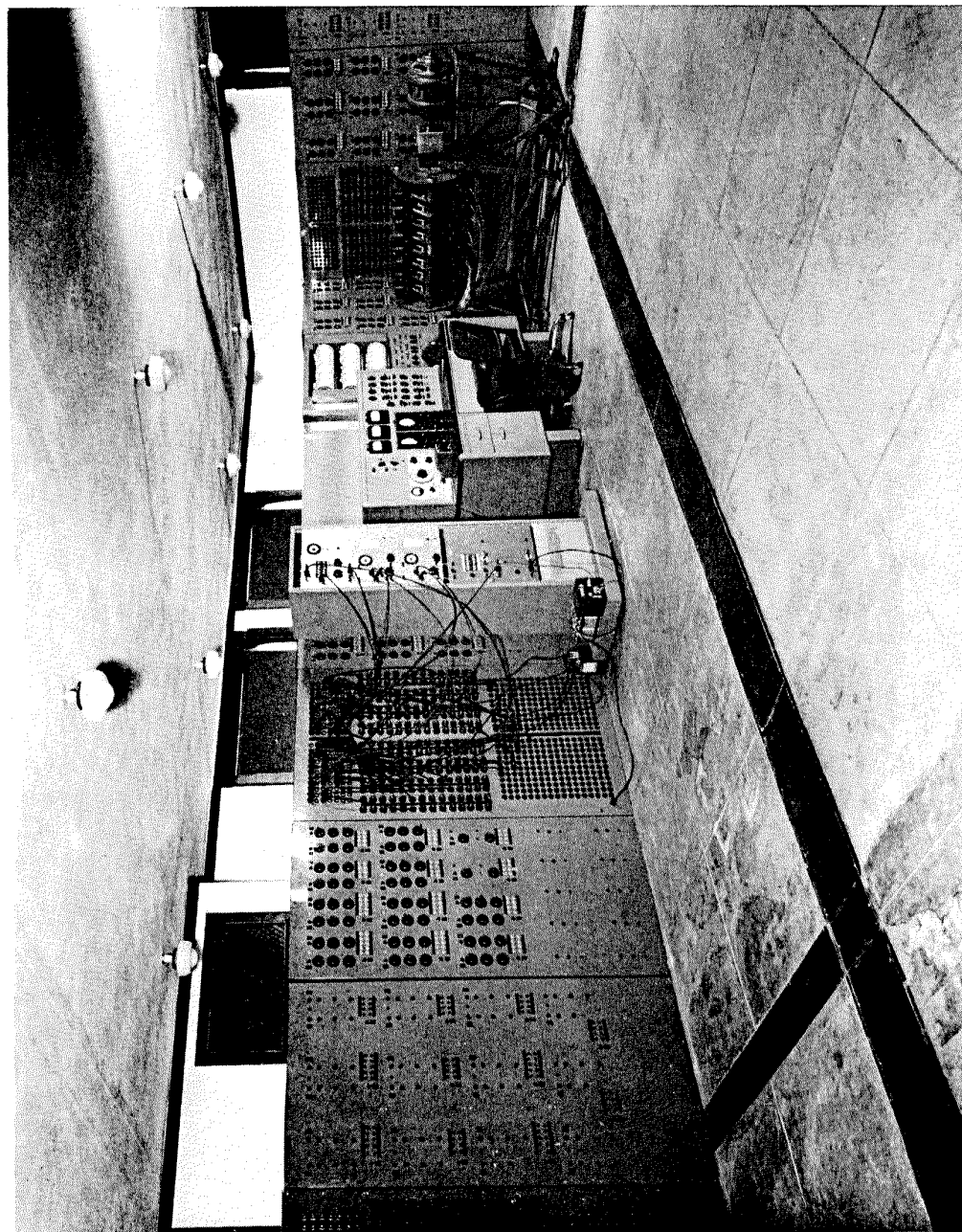


Figure 3. Electric analog computer.

in which

z = ground displacement

x = displacement relative to ground

m = mass of simple oscillator

c = viscous damping coefficient

k = spring constant

Rewriting Equation 12 in the form

$$m\ddot{x} + c\dot{x} + kx = -m\ddot{z} \quad (13)$$

it can be seen that the left-hand side of Equation 13 contains the constants which characterize the physical system, while the right-hand side represents an exciting force which is proportional to the ground acceleration. Simulation of the mechanical oscillator, then, consists in choosing circuit components which are proportional to the mechanical constants. The relation between mechanical and electrical quantities is shown in Table I. The factor "N" is applied so that the time scale in the analog will be appropriate to an electric circuit; the factor "a" serves to adjust the values of circuit components to those available in the computer. In use the electrical values are readily changed by means of switches so that effects of changes in natural period or damping are immediately apparent.

B. Introduction of the Excitation Function.

It was pointed out above that the effect of the ground acceleration, \ddot{z} , is mathematically equivalent to an external force, $-m\ddot{z}$. This force corresponds to an applied voltage, $E(t)$, in the electric analog. It is necessary, therefore, to apply to the electric circuit a voltage which has the same form as the recorded ground acceleration; this end is accomplished by means of the following scheme.

A carefully scaled drawing is made of the earthquake record and mounted on the drum of a plotting table as shown in Figure 4. At the upper

TABLE I

MECHANICAL-ELECTRICAL RELATIONS FOR ANALOG

Mechanical System	Electrical Analog
m = mass of system	L = inductance = $\frac{a}{N^2} m$
k = spring constant	c = capacitance = $\frac{1}{ak}$
c = damping constant	R = resistance = $\frac{a c}{N}$
τ = period of vibration	τ^1 = simulated period = $\frac{\tau}{N}$
F = exciting force	E = applied voltage
x = displacement	q = electrical charge
v = velocity	i = current

$$x = a \frac{F}{E} q$$

N = time scale change factor

a = impedance change factor

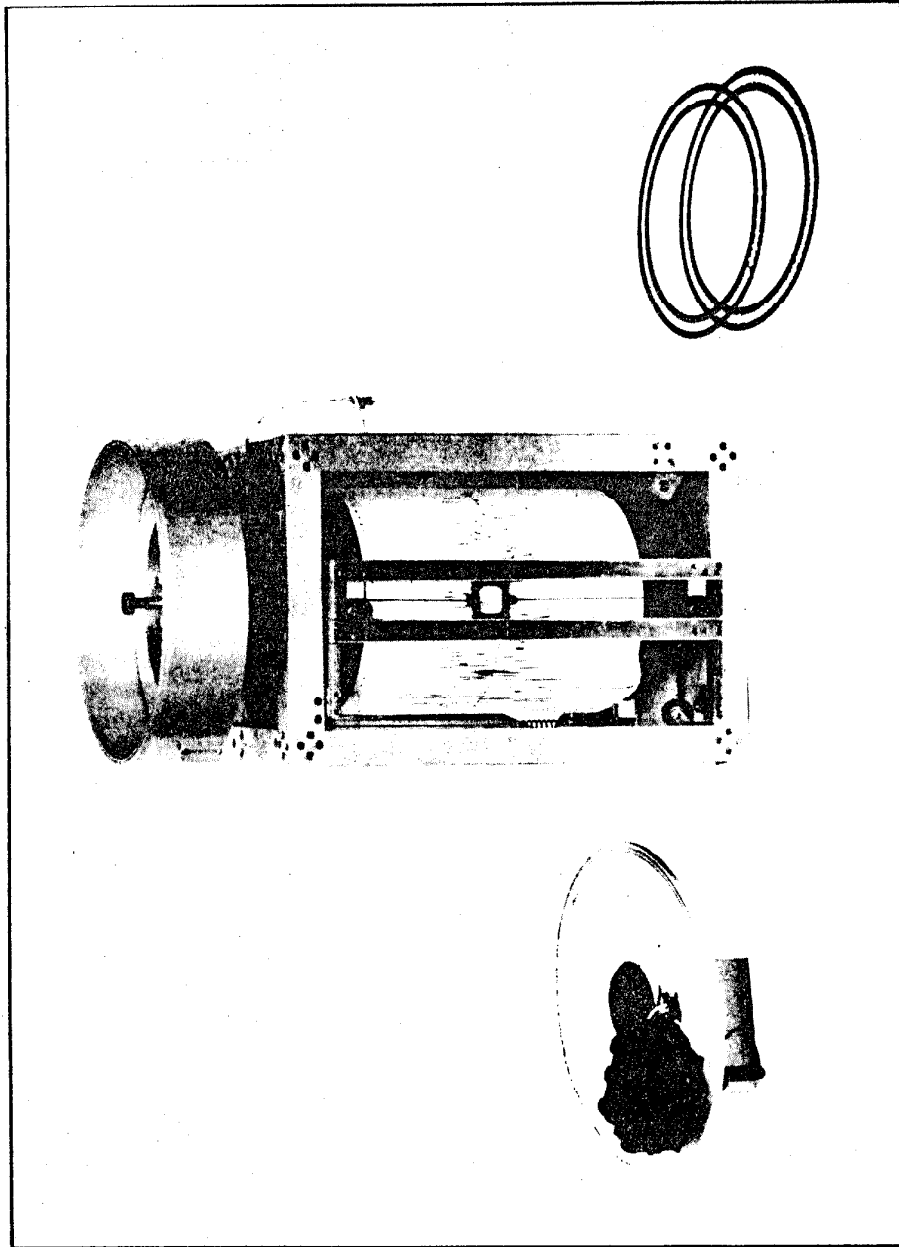


Figure 4. Plotting table for film records.

end of the plotting-table drum shaft is a disc which carries a circular photographic film. While the drum is revolved slowly by a motor, an operator follows the ordinate of the accelerogram with a cross-hair. Through a cable linkage the motion of the cross-hair is fed into a selsyn transmitter. The selsyn receiver is located inside the cover of the upper cylinder (lower left, Figure 4) where it controls the opening of a light valve. Thus, as the film revolves, a variable-width "sound track" is exposed, resulting in the typical records shown at lower right in Figure 4. In use one of these records is mounted on a constant-speed turntable in such a way that the variable-width "sound track" meters the light in a photocell circuit. The output of the photocell circuit is then amplified to provide a voltage which, over a finite time interval, has the required form.

C. Observation and Measurement of the Response

Observation of the response of the system to the forcing function involves detecting the electrical variable which is analogous to the required mechanical variable and displaying it on the screen of a cathode ray oscilloscope. Since the oscilloscope is a voltage-sensitive device, the observation process is direct only for force, which corresponds to voltage in the analogy used for these studies. If velocity is sought, the analogous current is detected by measuring the voltage drop across a known resistance. Charge, which is analogous to displacement, is proportional to the voltage across a condenser.

In practice, the transient voltage is applied to the analog circuit repeatedly, punctuated by intervals during which electrical charges are permitted to leak off circuit components or are removed by short-circuiting the components by means of synchronous switches, thus insuring that the initial conditions are the same for each application of the transient. When the ensuing responses are displayed on the oscilloscope, the persistence of the screen material causes the response to appear as a stationary pattern which can be photographed or from which measurements can be made directly. Typical oscillograms of ground acceleration and oscillator response are shown in Figure 5.

D. Procedure for Earthquake Studies.

If Equation 5 be applied to the case of the simple oscillator, we obtain

$$y = \frac{1}{p} X \quad (14)$$

It can be seen from Equation 14 that the maximum value of X will be just " p " times the maximum displacement; by observing the maximum displacement and multiplying by the appropriate value of " p ", we obtain a point of the spectrum.

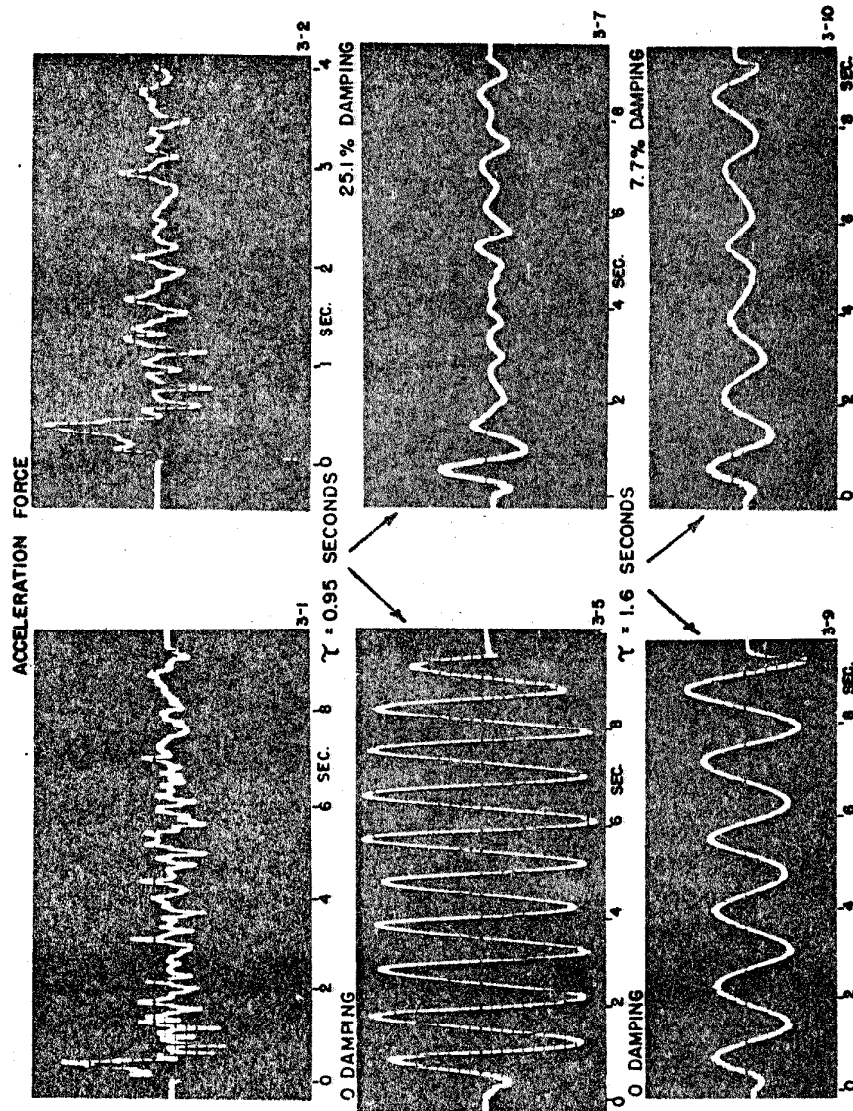


Figure 5. Typical computer solutions.
Los Angeles Subway Terminal, Oct. 2, 1933. Component N51W.

This has the practical disadvantage that the observed displacement is very small at the short periods and large at the longer periods, with consequent adverse effect on the relative accuracy of reading. This difficulty is avoided by observing directly the maximum velocity of response. If the motion of the oscillator were simple harmonic, the maximum velocity would be exactly "p" times the maximum displacement. Actually the response of the oscillator is a harmonic motion of variable amplitude, but within the range of periods studied the error involved in observing maximum velocity for "p" times maximum displacement is small.

Since velocity is analogous to current it was necessary to insert in the circuit a resistor across which the voltage drop could be measured. This resistor is shown at R_1 in Figure 6. The box labeled "A" is an amplifier which has the effect of a negative resistance, cancelling the voltage drop in R_1 . In this manner the current-detecting resistor is made independent of the resistor R , which is varied to provide the desired fraction of critical damping in the circuit. During the determination of the undamped spectra the amplifier gain was adjusted until an oscillation initiated by closing the battery switch at the left of Figure 6 would persist without growth or decay, indicating that the damping was not merely "small" but actually zero.

Gross changes in oscillator period were made by changing inductance; fine changes by changing capacitance in small steps. With the excitation function being applied continuously, fine changes in period were made and the resulting effect on response viewed on the oscilloscope. In general, only local maxima or minima of response were recorded, in the interest of a reasonable definition of the spectrum with a minimum number of points.

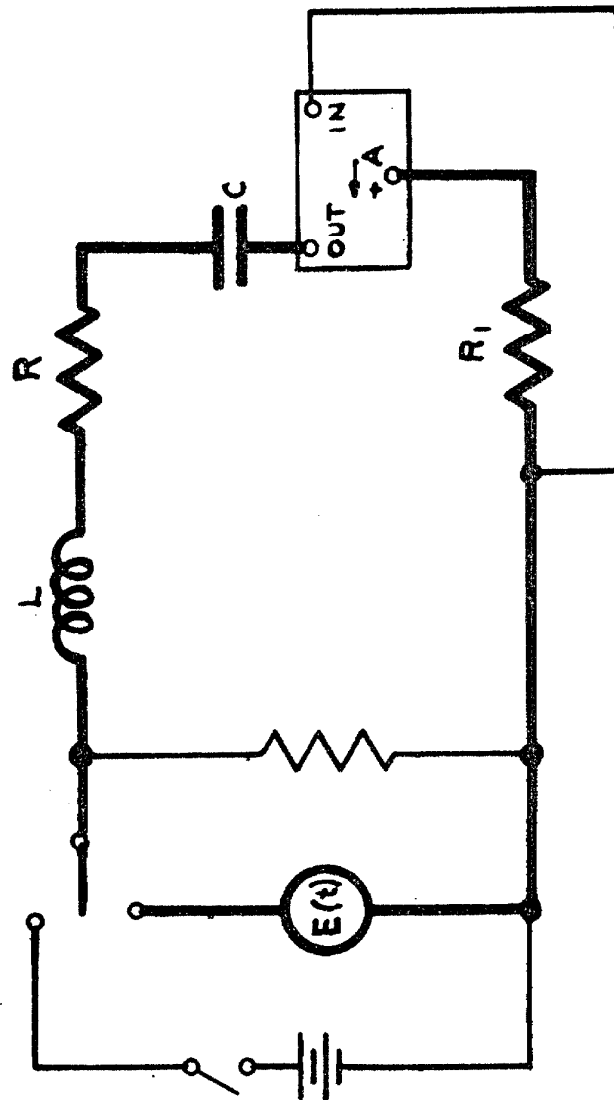


Figure 6. Computer circuit diagram.

E. Discussion of Accuracy and Reproducibility

There are several stages in the process of spectrum analysis, which has been outlined, above at which errors may arise. The first of these is the preparation of the photographic film which serves as the excitation function in the computer. Manual errors and errors in the selsyn link introduce certain errors in reproducing the record. In view of the nature of the earthquake and of the inevitable instrumental errors involved in the original earthquake record, however, this is not regarded as significant. Of greater importance is the fact that a film record is made only once for each earthquake and is used thereafter in unchanged form. The most serious error in the preparation of the film record would be the introduction of a harmonic component. There is no reason to expect such a periodic error, and the absence of any resonant oscillations in the undamped responses indicates that there was none in the range of period studied.

Errors in either speed or amplitude of successive applications of the excitation function would cause the pattern to drift or flicker on the oscilloscope, hence this source of error was readily detected and avoided.

The approximation involved in reading maximum velocity for "p" times maximum displacement was investigated by means of detailed calculations on the Los Angeles Subway Terminal earthquake of October 2, 1933. These comparisons indicated that the assumption resulted in maximum errors of 5 percent at medium periods.

The average error involved in reading magnitudes from the oscilloscope screen is estimated at 3 percent.

Reproducibility of the analog computer results was checked by taking duplicate data on a particular earthquake on different days. Comparison of these data revealed an extreme difference of 10 percent; throughout most of

the spectrum, however, the difference between the two determinations was well within the reading error. This is regarded as important since previous methods of spectrum analysis have been very sensitive to computational errors.

V. RESULTS OF THE INVESTIGATION

The U. S. Coast and Geodetic Survey records of 14 strong-motion earthquakes were chosen as suitable for the spectrum calculations. These were:

1. Vernon, California	March 10, 1933
2. Vernon, California	October 2, 1933
3. Los Angeles Subway Terminal	March 10, 1933
4. Los Angeles Subway Terminal	October 2, 1933
5. El Centro, California	December 30, 1934
6. El Centro, California	May 18, 1940
7. Helena, Montana	October 31, 1935
8. Ferndale, California	September 11, 1938
9. Ferndale, California	February 9, 1941
10. Ferndale, California	October 3, 1941
11. Santa Barbara, California	June 30, 1941
12. Hollister, California	March 9, 1949
13. Olympia, Washington	April 13, 1949
14. Seattle, Washington	April 13, 1949

For each of these earthquakes, both horizontal components were analyzed. The 28 accelerograms are shown in Figures 7 to 27.

By means of the analog computer technique described in the foregoing section, the spectrum, X , was determined for each accelerogram using several values of damping ratio. The resulting 88 spectra are presented in Figures 28 to 48. These spectra, showing maximum velocity versus period, are graphs of the maximum value of Equation 6.

As an aid in visualizing the significance of the velocity spectra, accelerations have been calculated from the maximum velocities on the assumption of simple harmonic motion. These acceleration spectra are presented in Figures 49 to 76.

For cross-reference Table II lists the figure numbers of accelero-gram, velocity spectrum and acceleration spectrum, the damping ratios investigated, and the essential data for each earthquake component.

TABLE II

SUMMARY OF SPECTRA AND EARTHQUAKE DATA

Location	Mag.	Date	Component	Damping Ratios				Figure Numbers	
				0	.02	.1	.2	Accelerogram Spectrum	Velocity Acceleration Spectrum
Vernon, Calif.	6.3	March 10, 1933	N 08 E	x	x	x	x	7	28
"	"	"	S 82 E	x	x	x	x	8	29
"	5.3	Oct. 2, 1933	N 08 E	x	x	x	x	9	30
"	"	"	S 82 E	x	x	x	x	10	31
Los Angeles Subway Terminal	6.3	March 10, 1933	N 39 E	x	x	x	x	11	32
"	"	"	N 51 W	x	x	x	x	11	32
"	5.3	Oct. 2, 1933	N 39 E	x	x	x	x	12	33
"	"	"	N 51 W	x	x	x	x	12	33
El Centro, Calif.	6.5	Dec. 30, 1934	N-S	x	x	x	x	13	34
"	"	"	E-W	x	x	x	x	14	35
"	7.0	May 18, 1940	N-S	x	x	x	x	15	36
"	"	"	E-W	x	x	x	x	16	37
Helena, Montana	6.0	Oct. 31, 1935	N-S	x	x	x	x	17	38
"	"	"	E-W	x	x	x	x	18	39
Ferndale, Calif.	5.5	Sept. 11, 1938	N 45 E	x	x	x	x	19	40
"	6.6	Feb. 9, 1941	S 45 E	x	x	x	x	19	40
"	"	"	N 45 E	x	x	x	x	20	41
"	6.4	Oct. 3, 1941	S 45 E	x	x	x	x	20	41
"	"	"	N 45 E	x	x	x	x	21	42
Santa Barbara, Cal.	5.9	June 30, 1941	S 45 E	x	x	x	x	21	42
"	"	"	N 45 E	x	x	x	x	22	43
Hollister, Calif.	5.3	March 9, 1949	S 45 E	x	x	x	x	23	44
"	"	"	N 89 W	x	x	x	x	24	45
Olympia, Wash.	7.1	April 13, 1949	S 10 E	x	x	x	x	24	45
"	"	"	S 80 W	x	x	x	x	25	46
*Seattle, Wash.	7.1	April 13, 1949	N 88 W	x	x	x	x	26	47
"	"	"	S 02 W	x	x	x	x	27	48
Taft, Calif.	7.7	July 21, 1952	S 69 E	x	x	x	x	27	48
"	"	"	N 21 E	x	x	x	x	27a	48a
Port Hueneme, Cal.	5.0	Mar. 18, 1957	N-S	x	x	x	x	27b	48b
"	"	"	E-W	x	x	x	x	27c	48c
San Francisco, Cal.	"	Mar. 22, 1957	"	x	x	x	x	27c	48c
*Mexico City	"	May 11, 19, 1962	"	x	x	x	x	111	76c
* Recorded on very soft ground.									67d

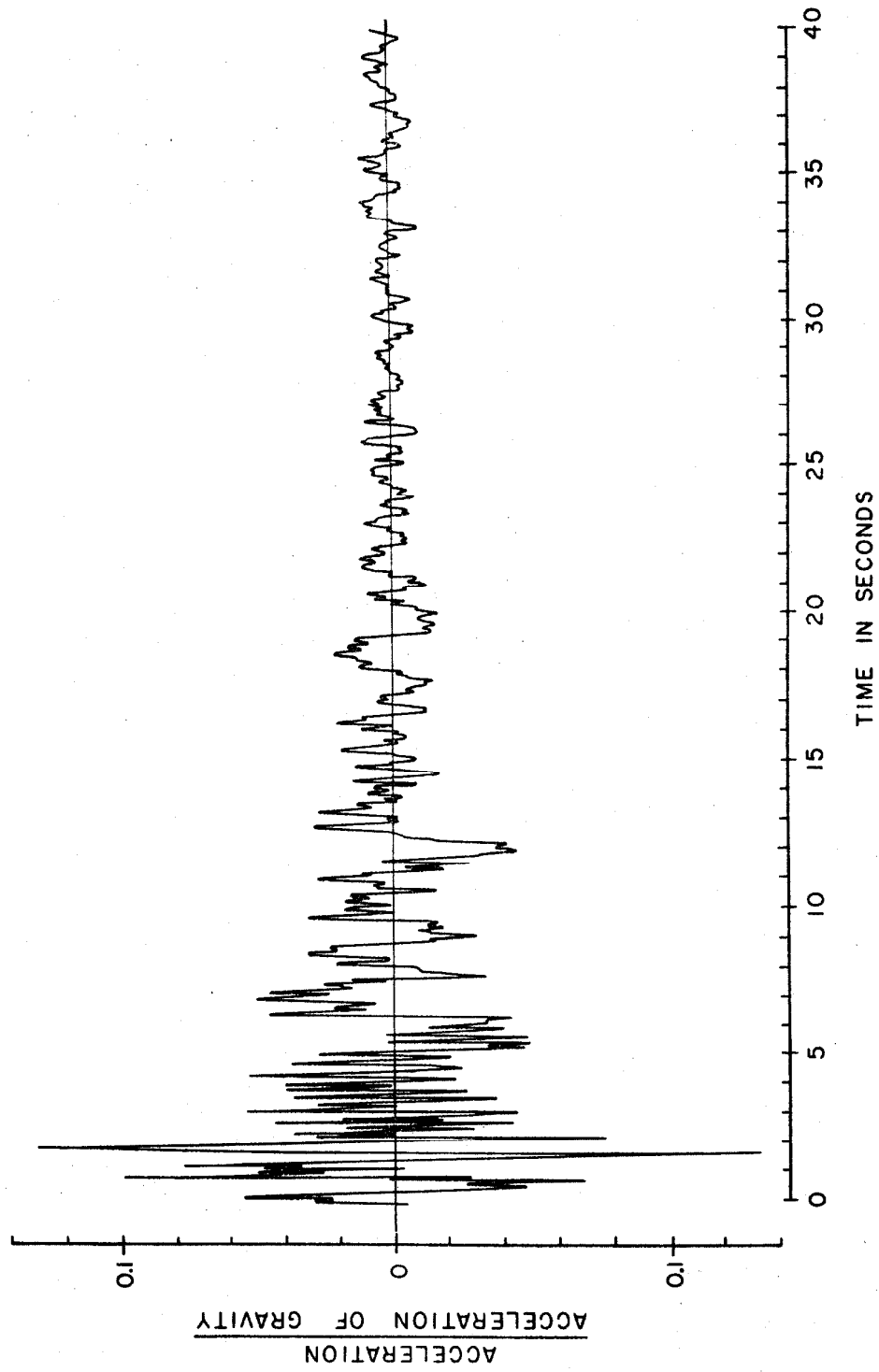


Figure 7. Accelerogram for Vernon, California; earthquake of March 10, 1933. Component N 08 E.

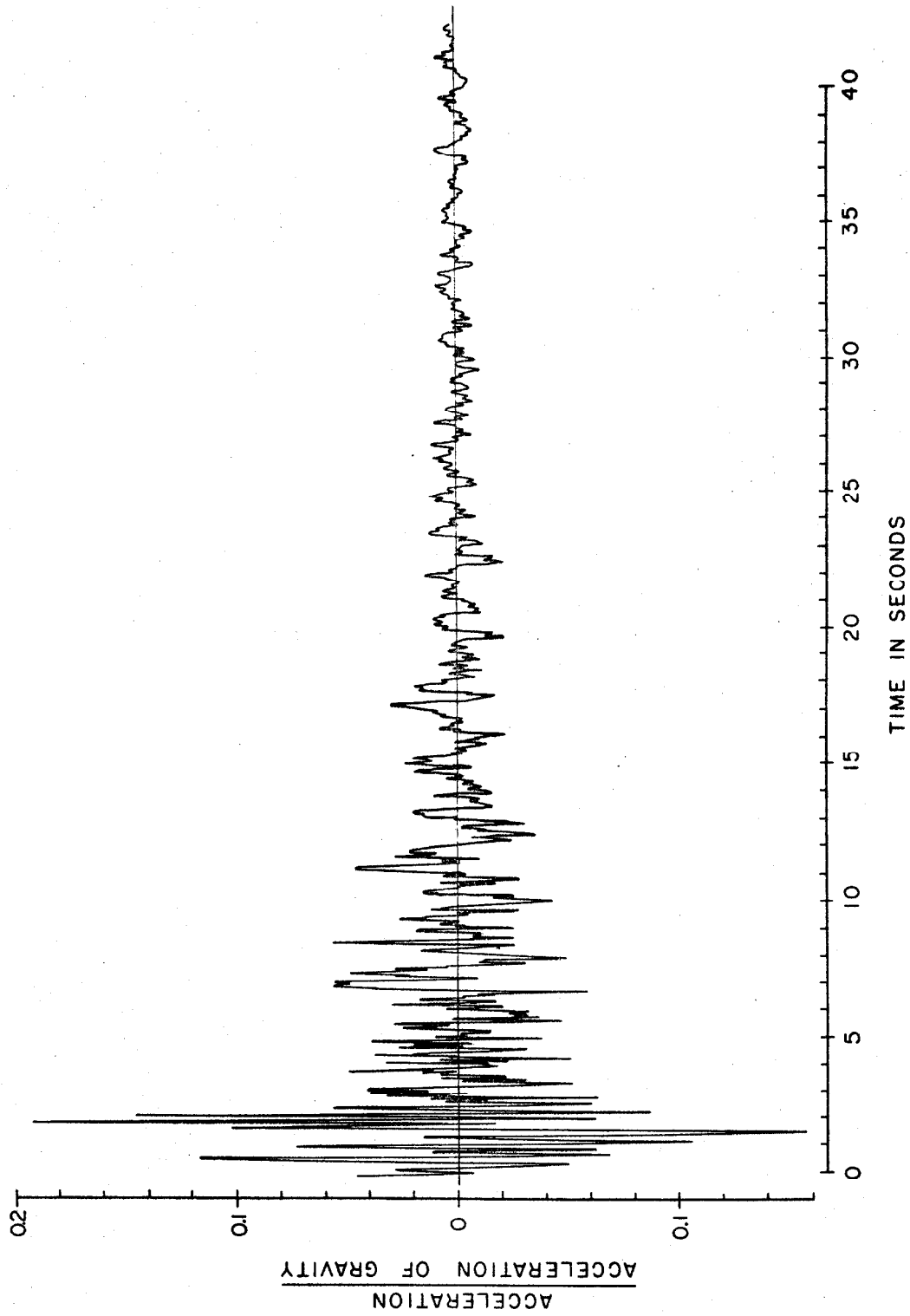


Figure 8. Accelerogram for Vernon, California; earthquake of March 10, 1933. Component S 82 E.

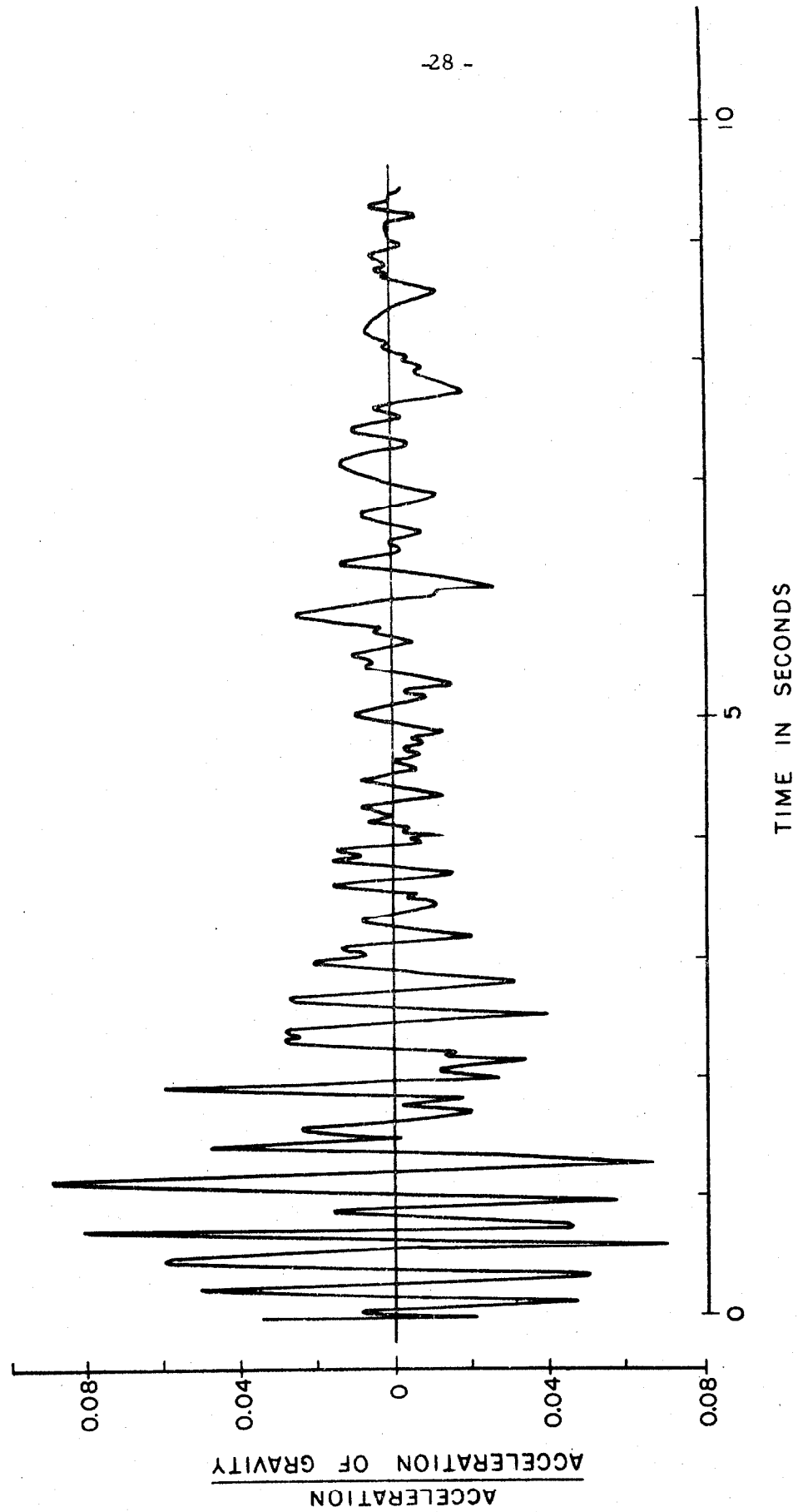


Figure 9. Accelerogram for Vernon, California; earthquake of October 2, 1933. Component N 08 E.

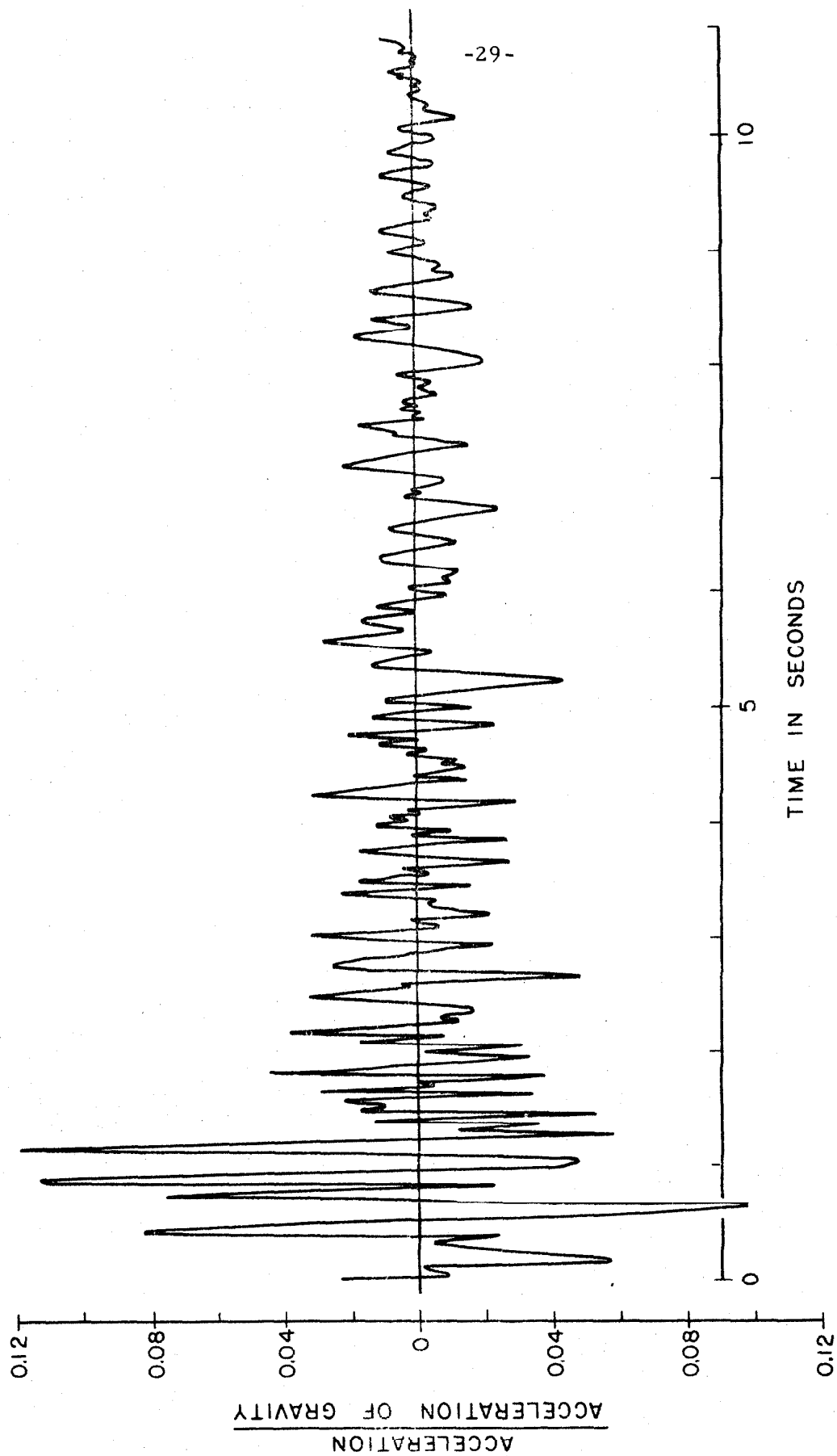


Figure 10. Accelerogram for Vernon, California; earthquake of October 2, 1933. Component S 82 E.

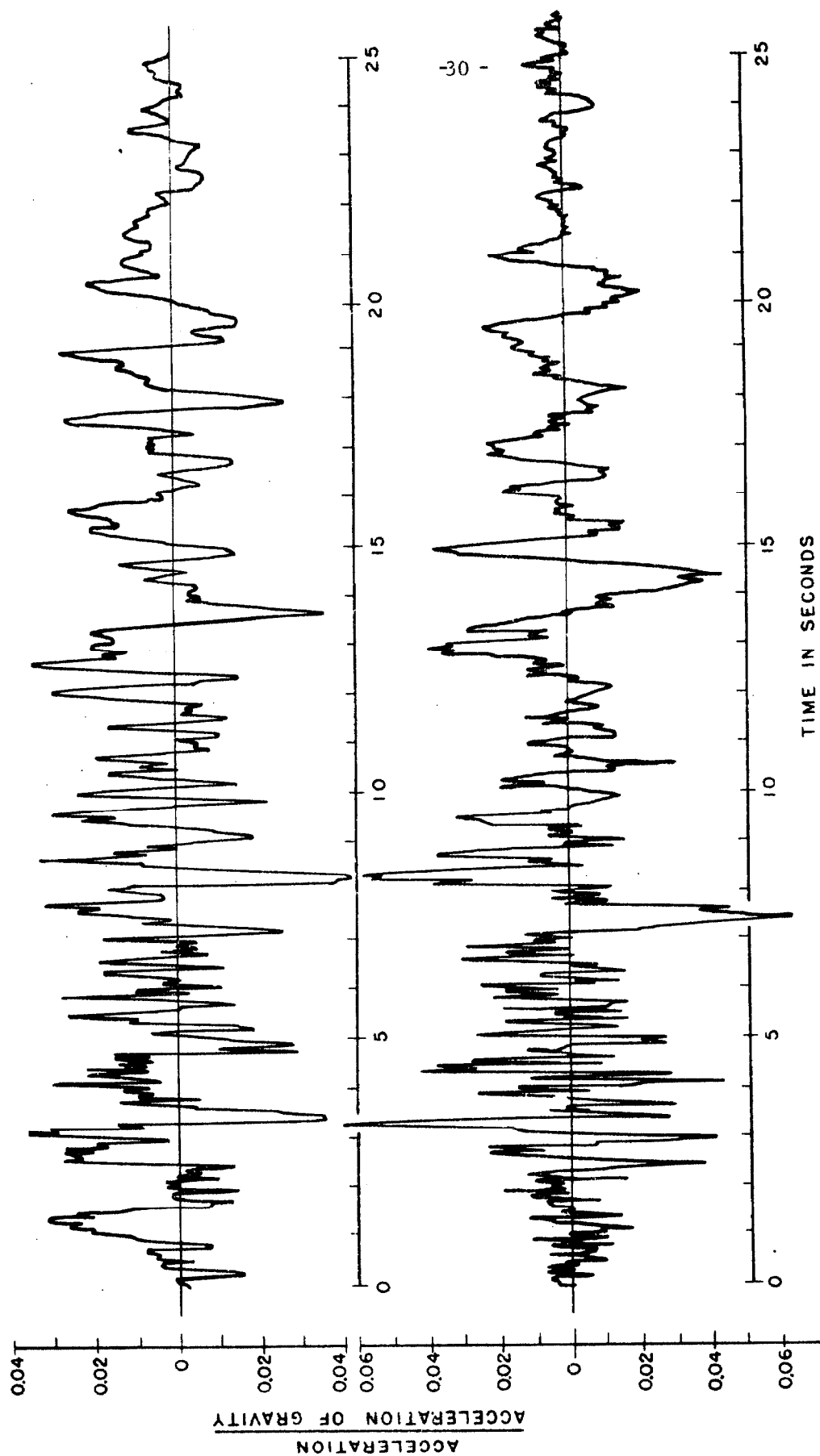


Figure 11. Accelerograms for Los Angeles Subway Terminal; earthquake of March 10, 1933. Components: N 39 E (lower), N 51 W (upper).

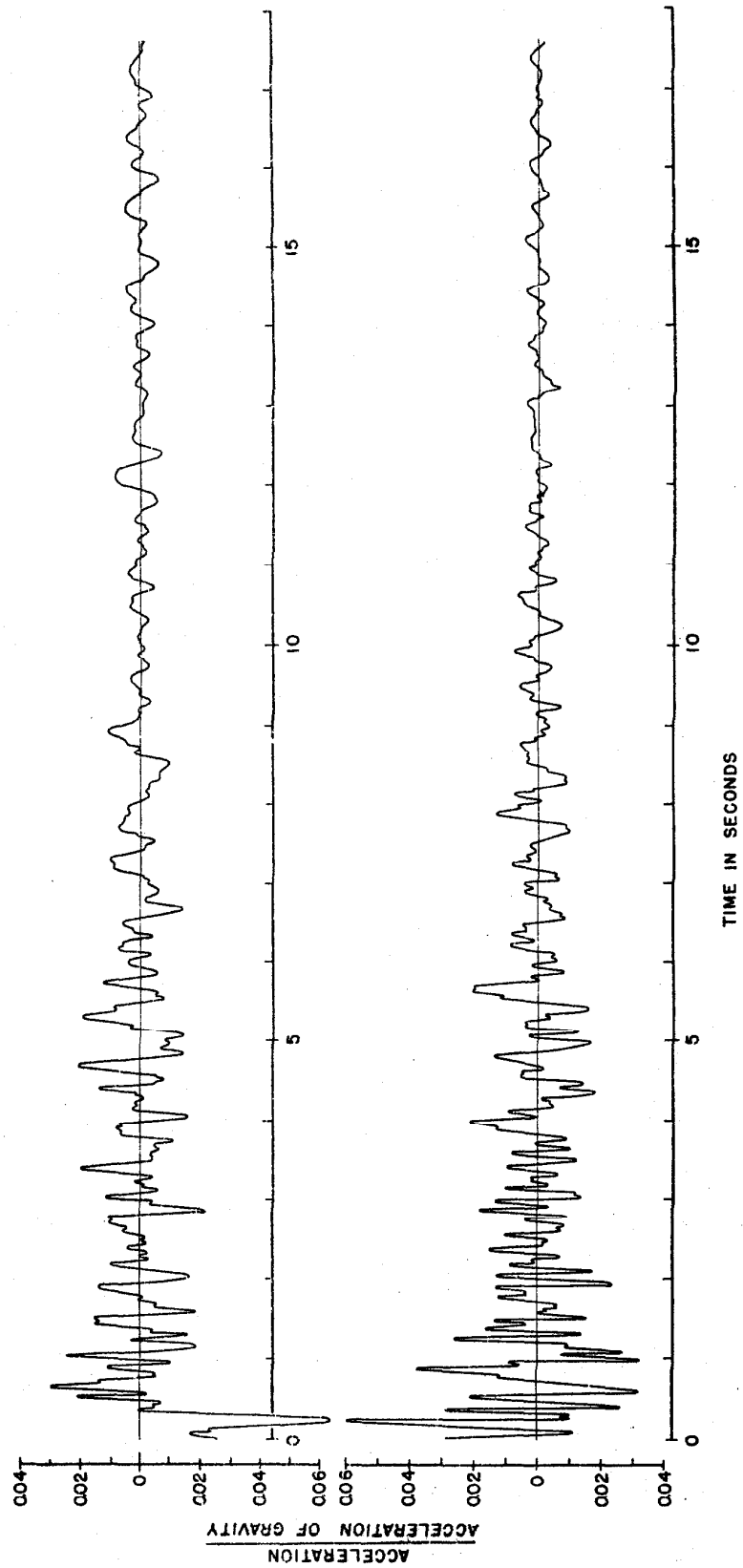


Figure 12: Accelerograms for Los Angeles Subway Terminal; earthquake of October 2, 1933. Components: N 39 E (lower), N 51 W (upper).

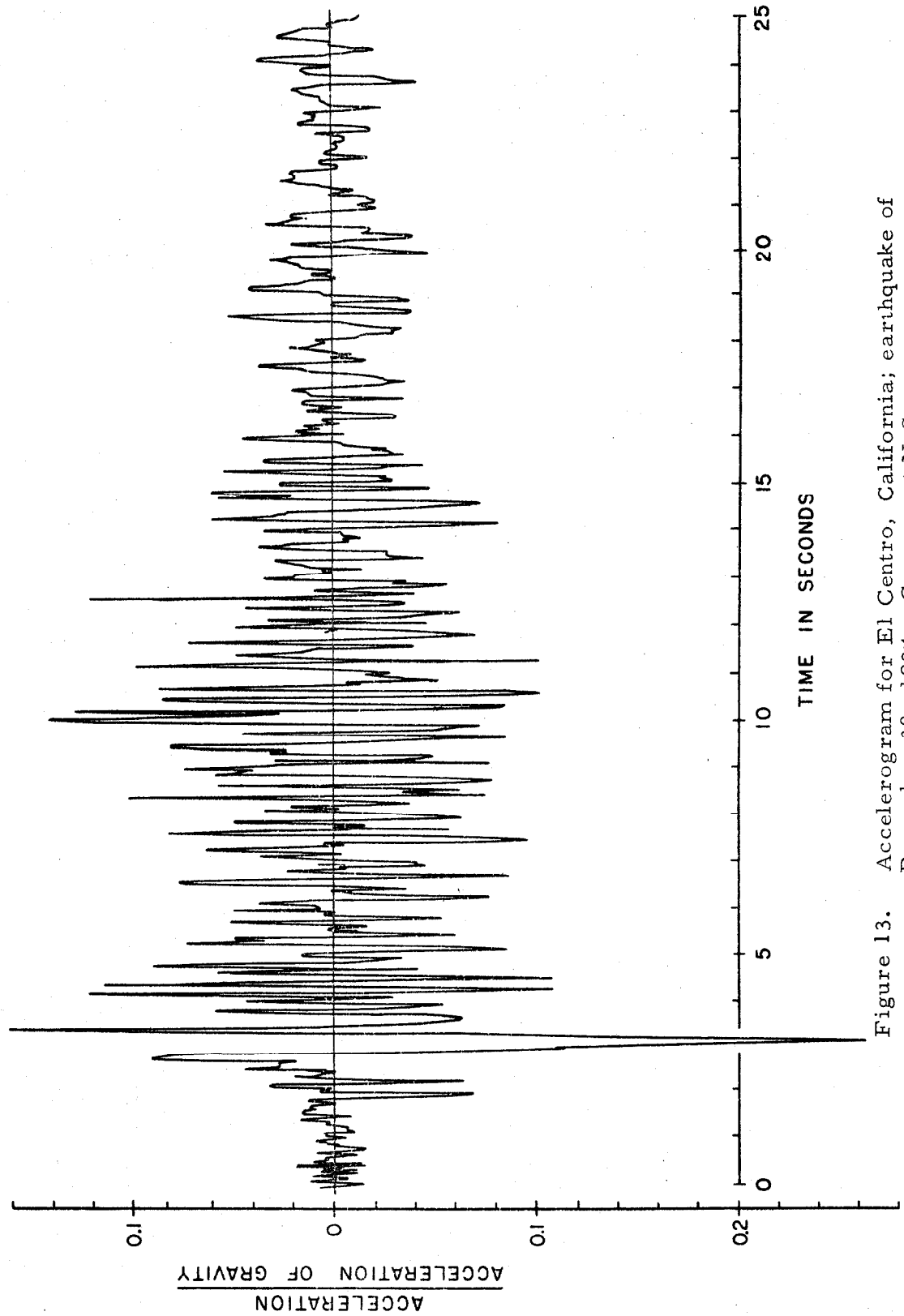


Figure 13. Accelerogram for El Centro, California; earthquake of December 30, 1934. Component N-S.

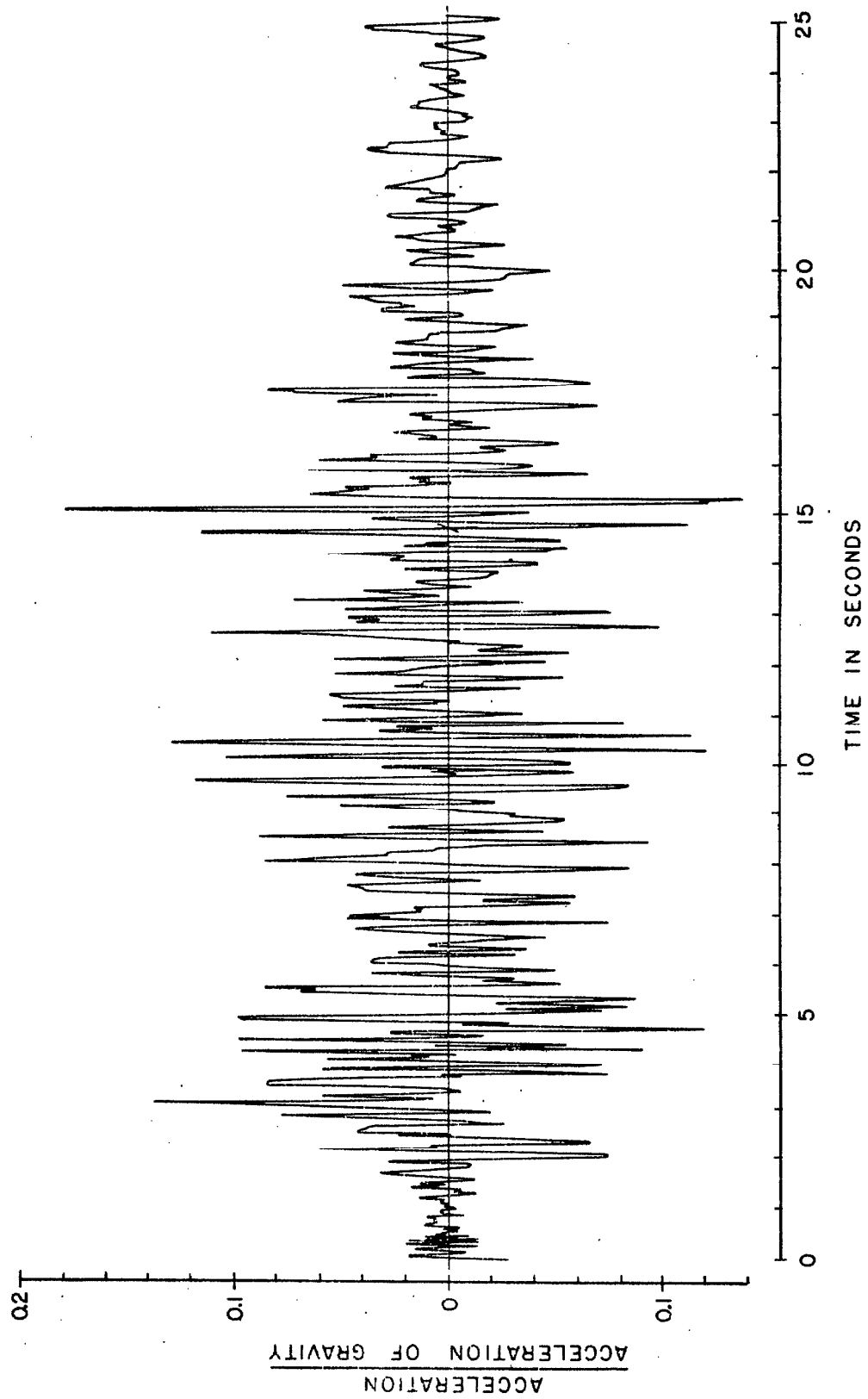


Figure 14. Accelerogram for El Centro, California; earthquake of December 30, 1934. Component E-W.

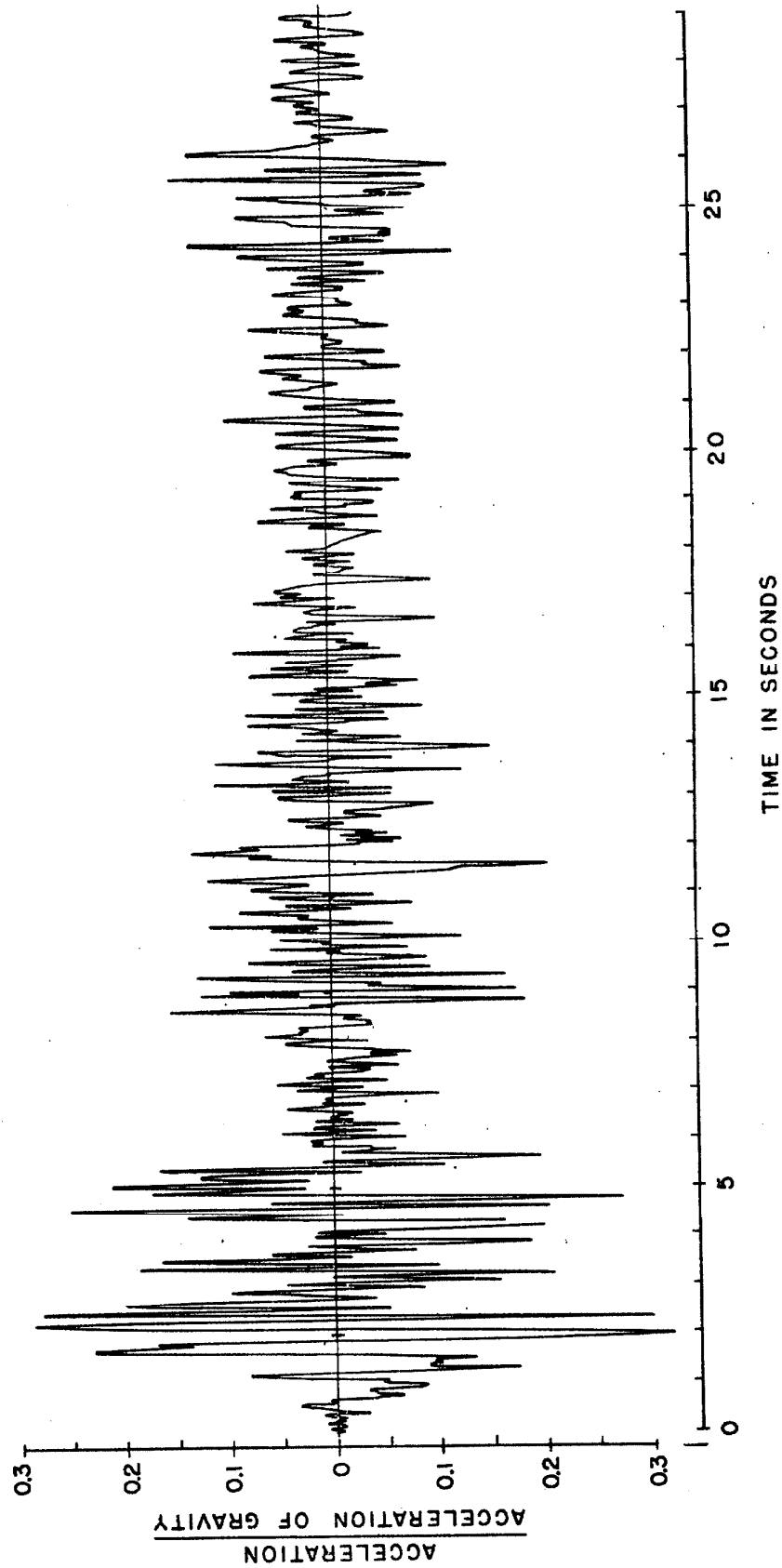


Figure 15. Accelerogram for El Centro, California; earthquake of May 18, 1940. Component N-S.

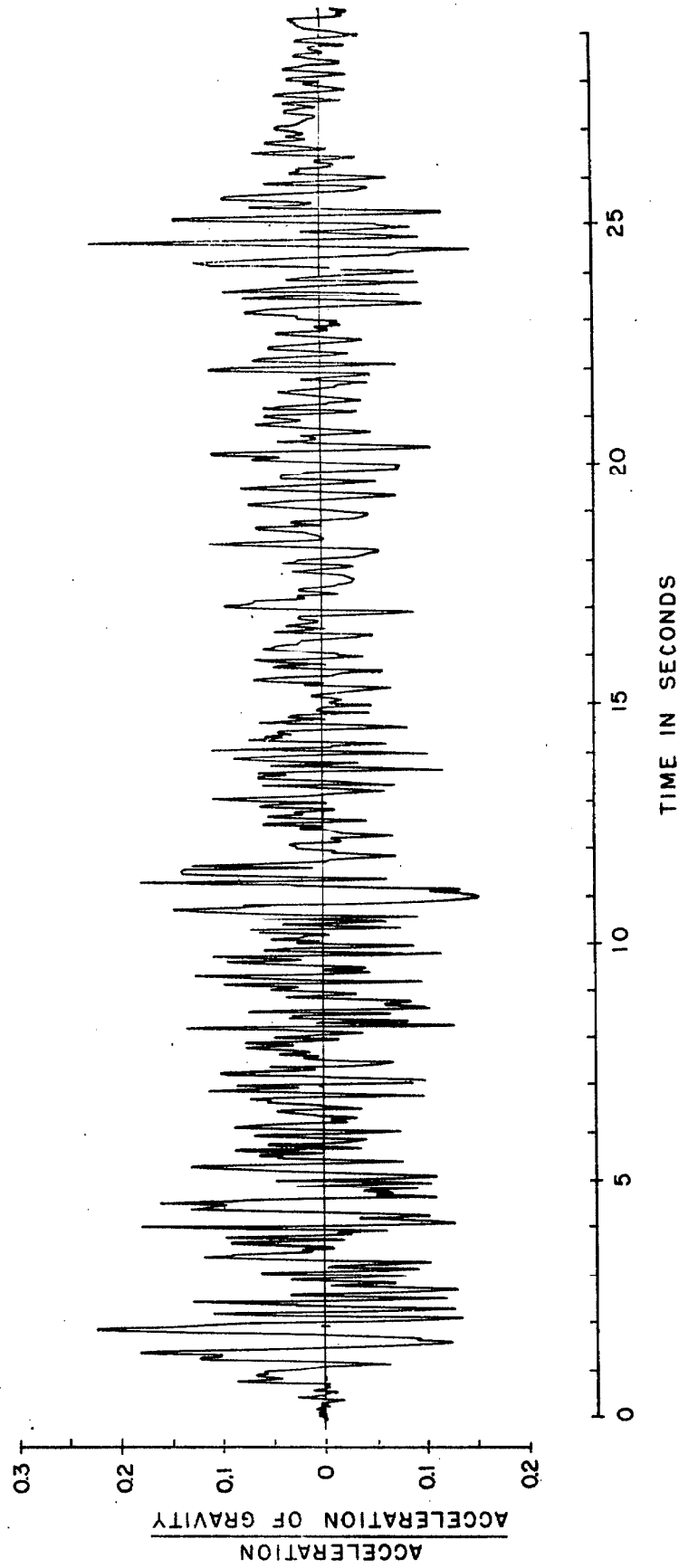


Figure 16. Accelerogram for El Centro, California; earthquake of May 18, 1940. Component E-W.

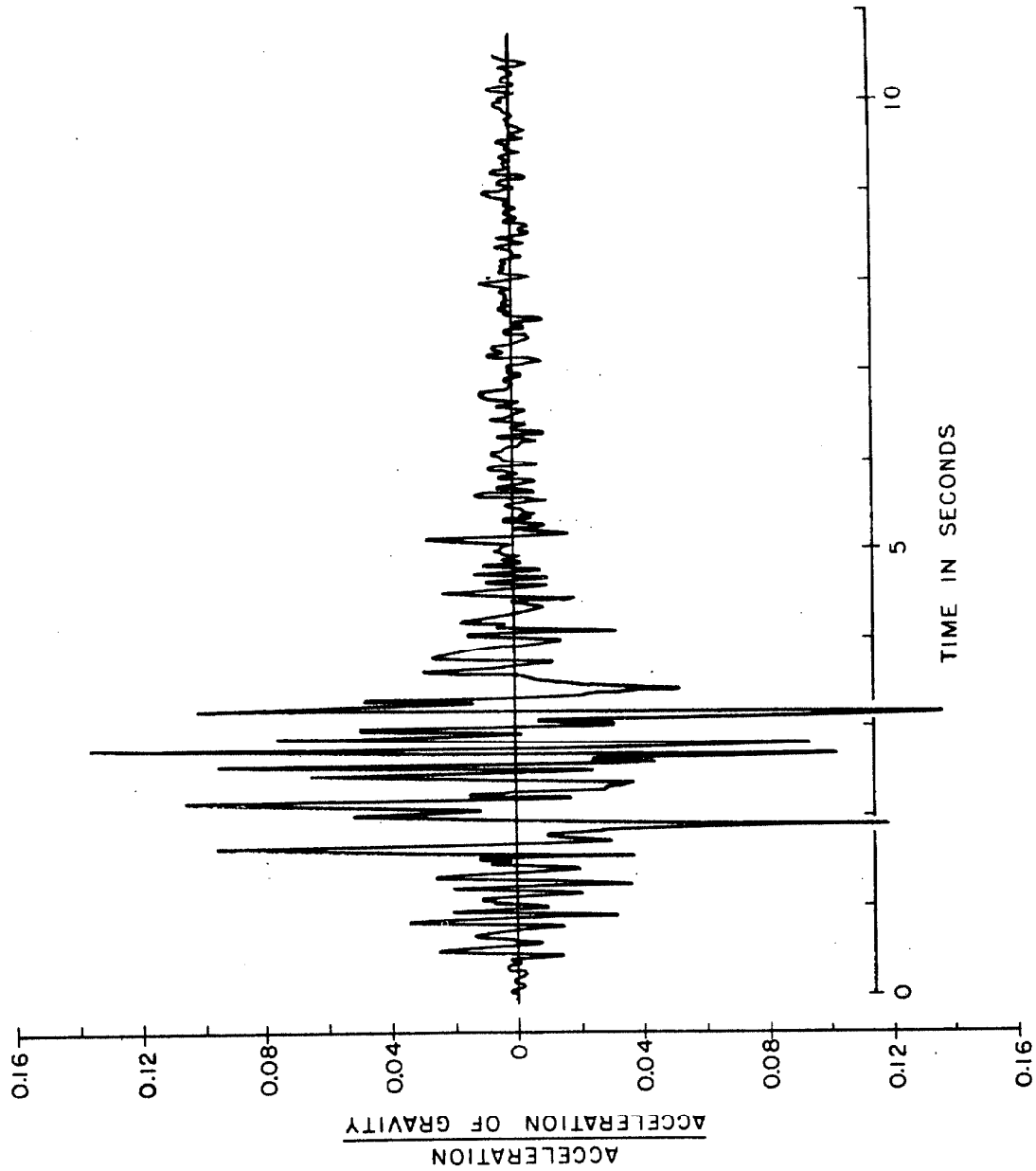


Figure 17. Accelerogram for Helena, Montana; earthquake of October 31, 1935. Component N-S.

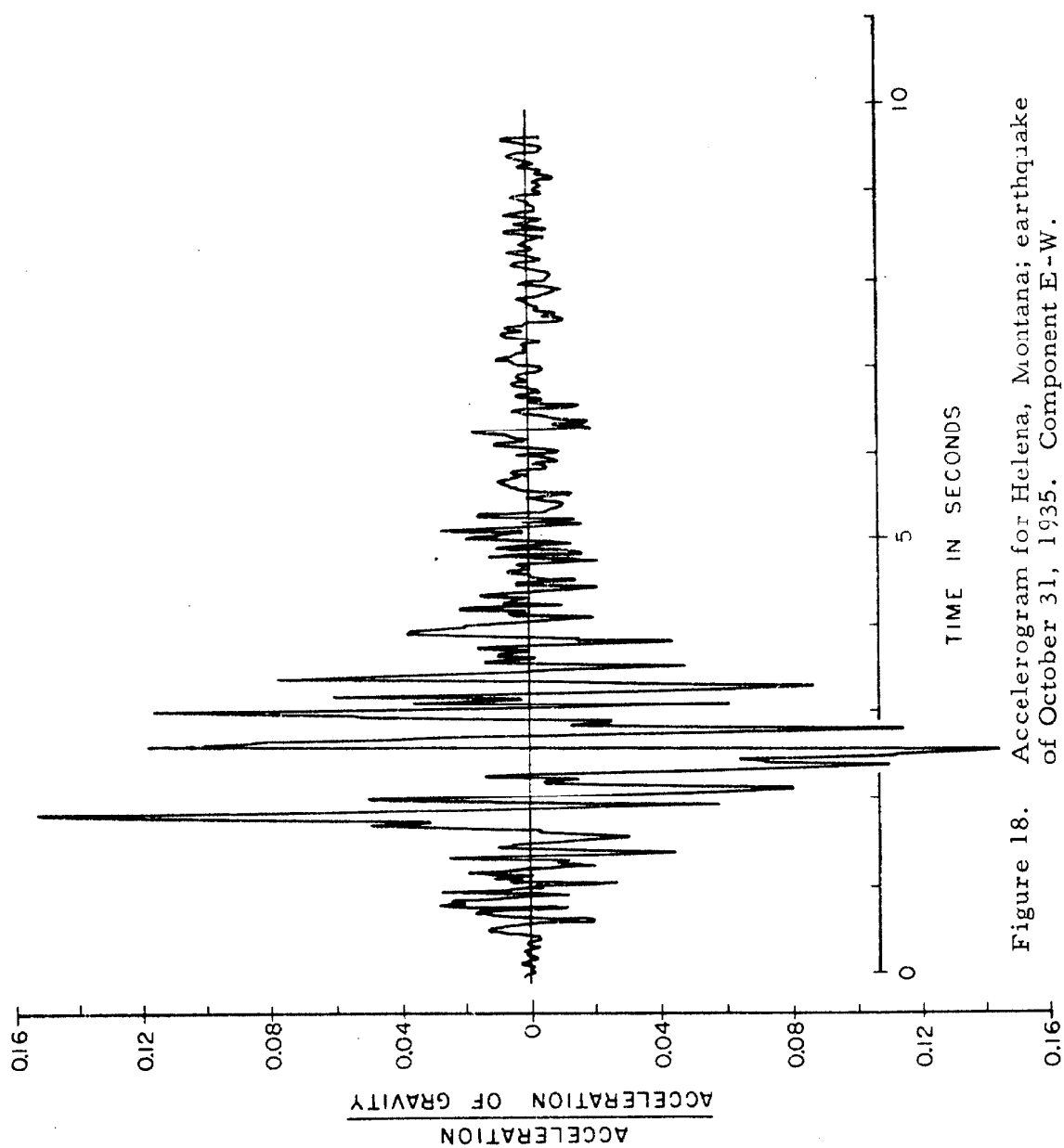


Figure 18. Accelerogram for Helena, Montana; earthquake of October 31, 1935. Component E-W.

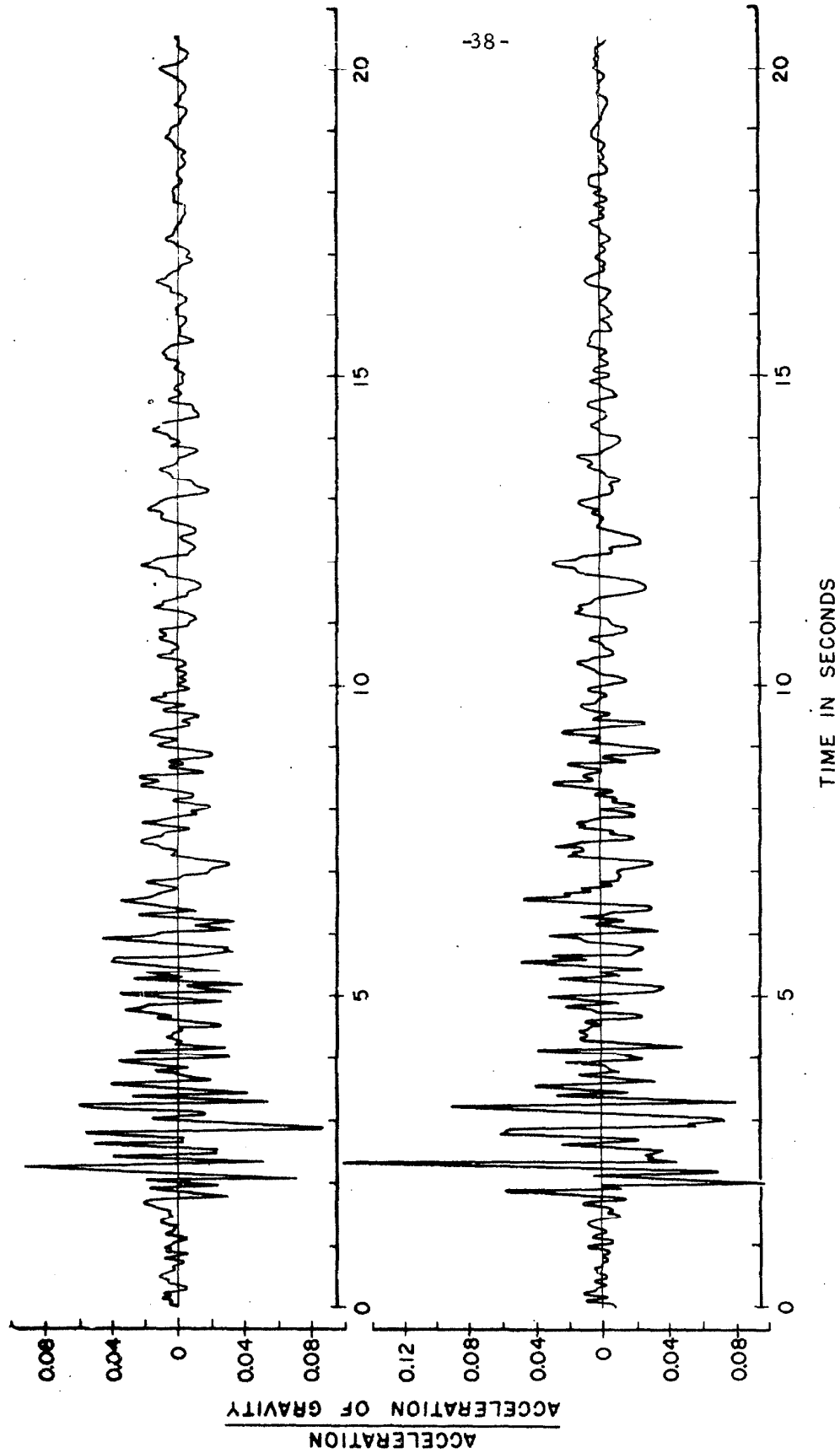


Figure 19. Accelerograms for Ferndale, California; earthquake of Sept. 11, 1938. Components: N 45 E (lower), S 45 E (upper).

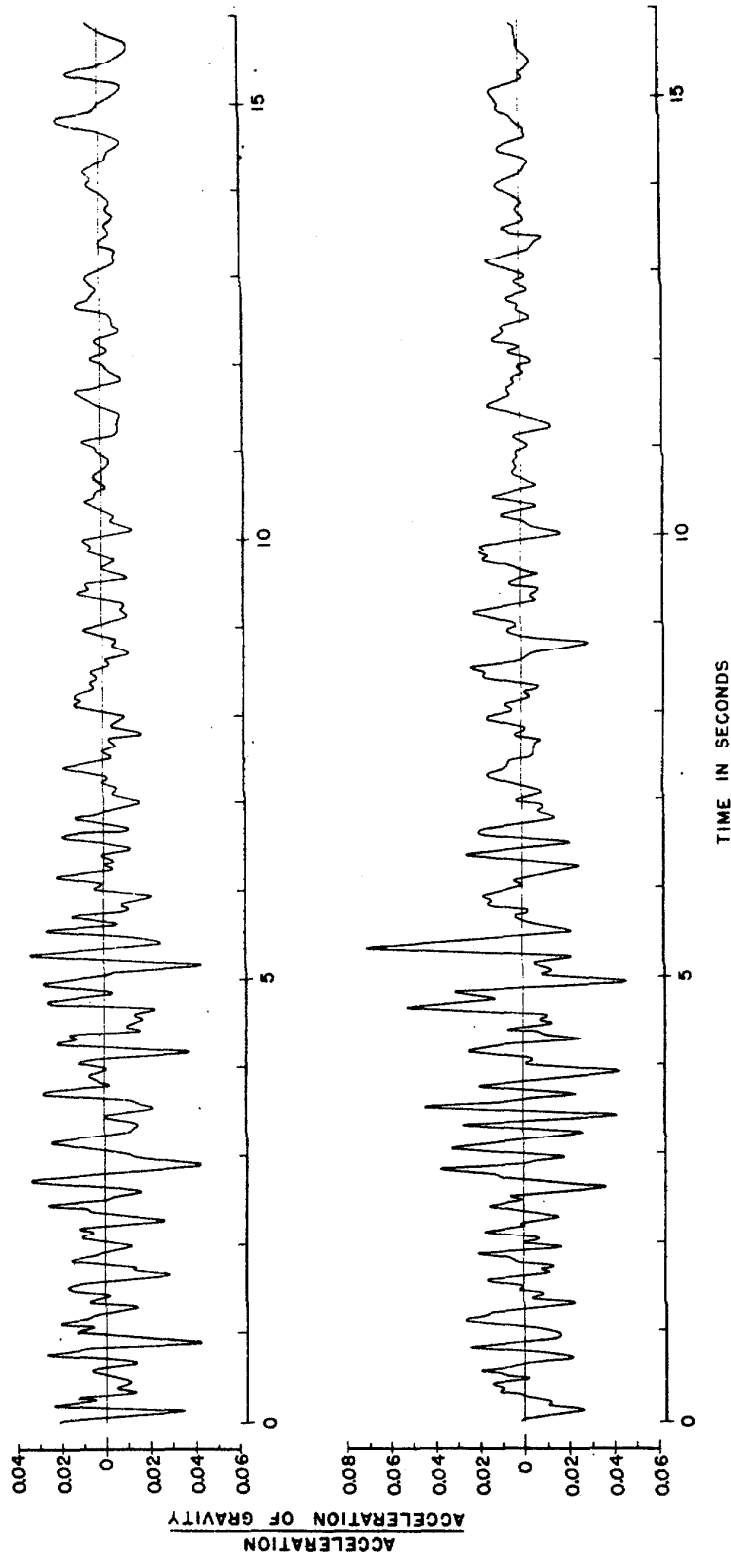


Figure 20. Accelerograms for Ferndale, California; earthquake of Feb. 9, 1941. Components: N 45 E (lower), S 45 E (upper).

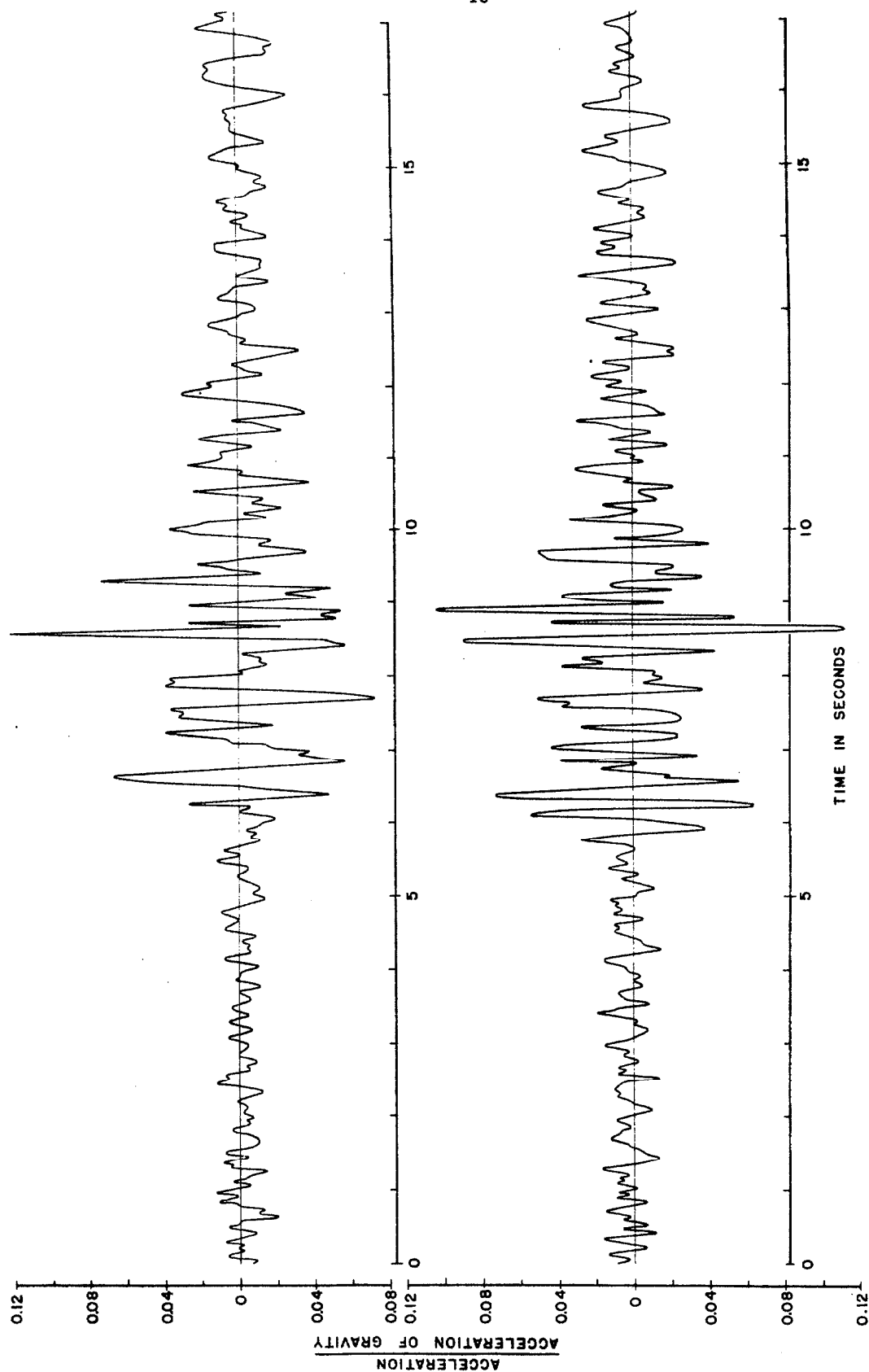


Figure 21. Accelerograms for Ferndale, California; earthquake of Oct. 3, 1941. Components: N 45 E (lower), S 45 E (upper).

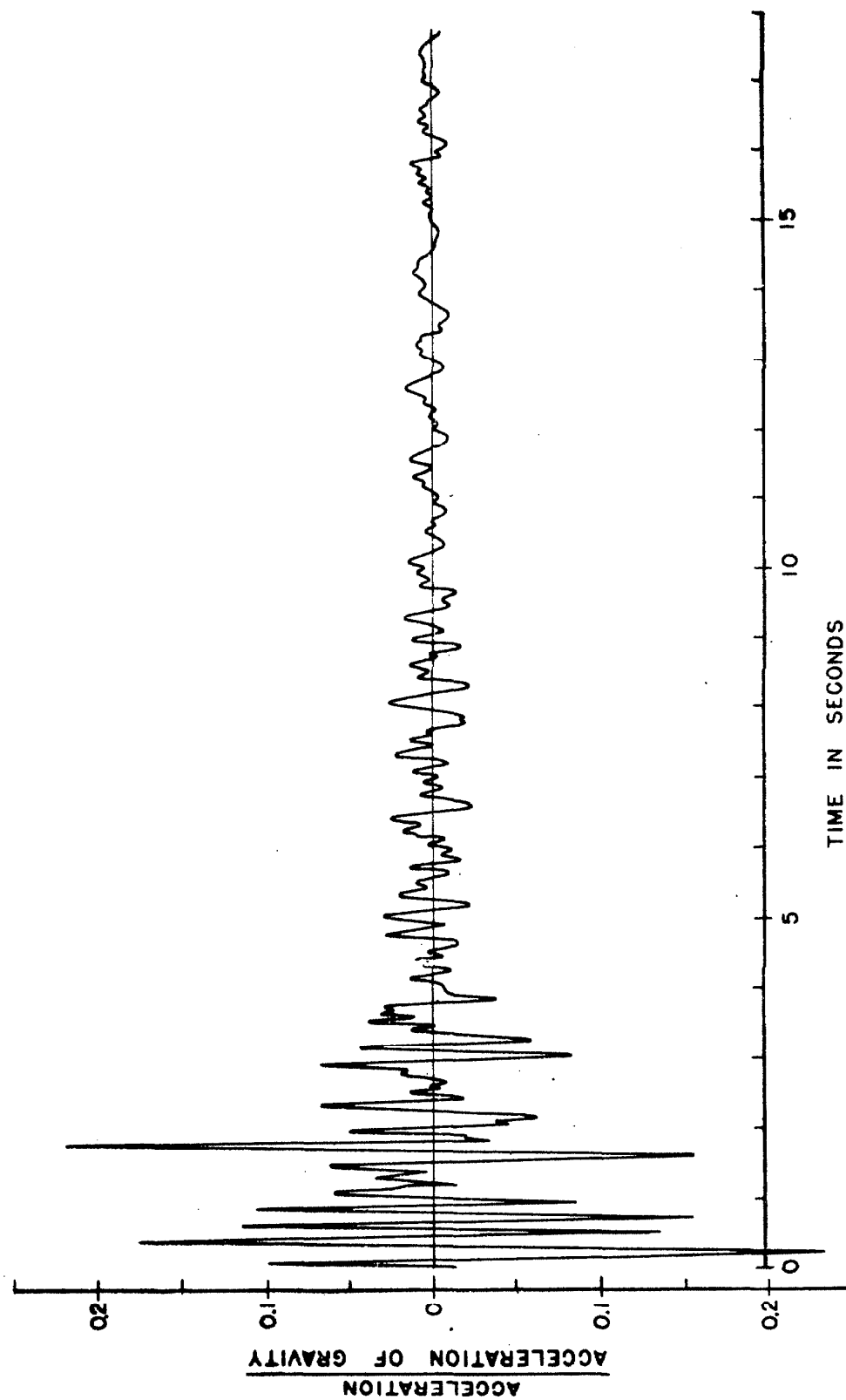


Figure 22. Accelerogram for Santa Barbara, California; earthquake of June 30, 1941. Component N 45 E.

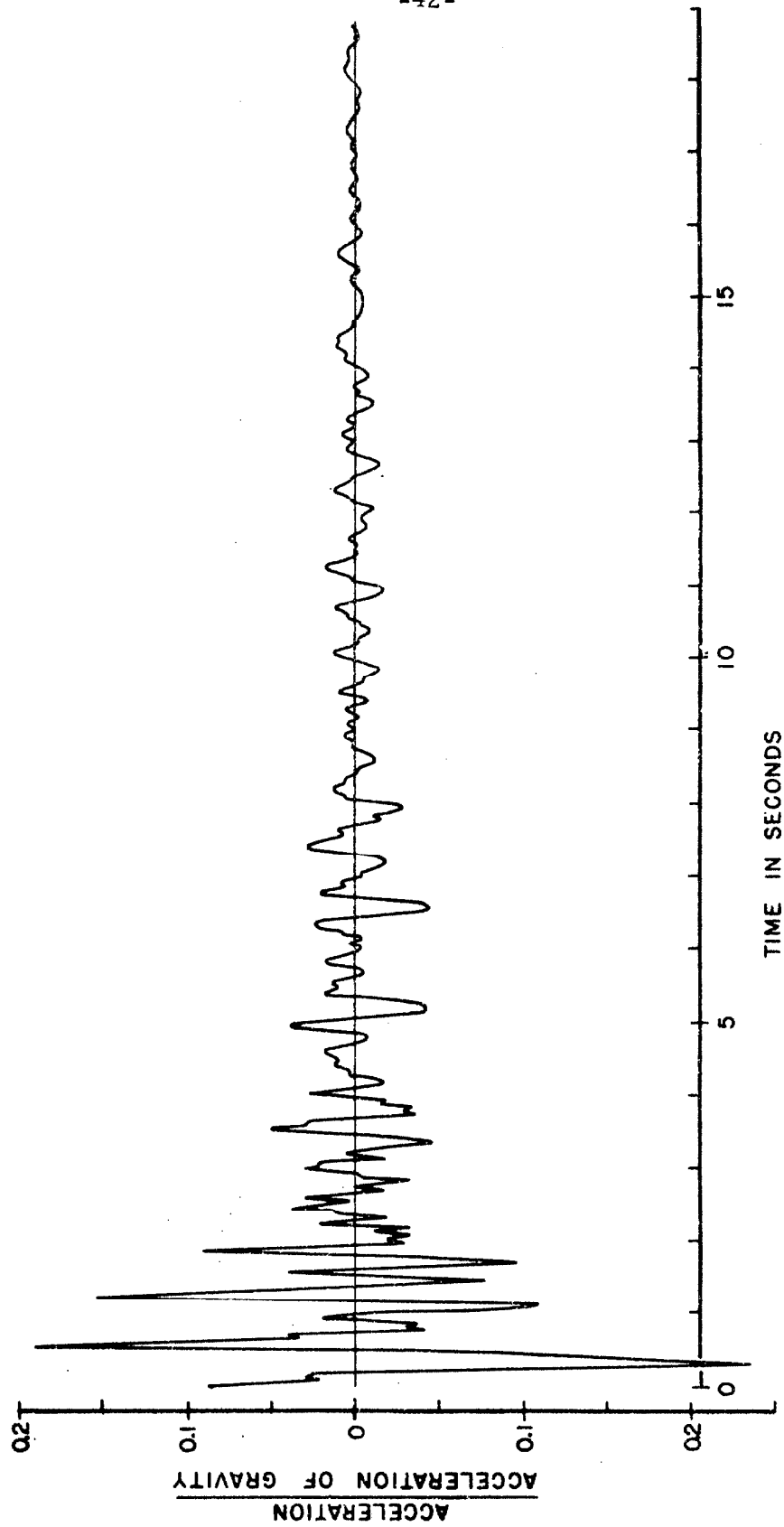


Figure 23. Accelerogram for Santa Barbara, California; earthquake of June 30, 1941. Component S 45 E.

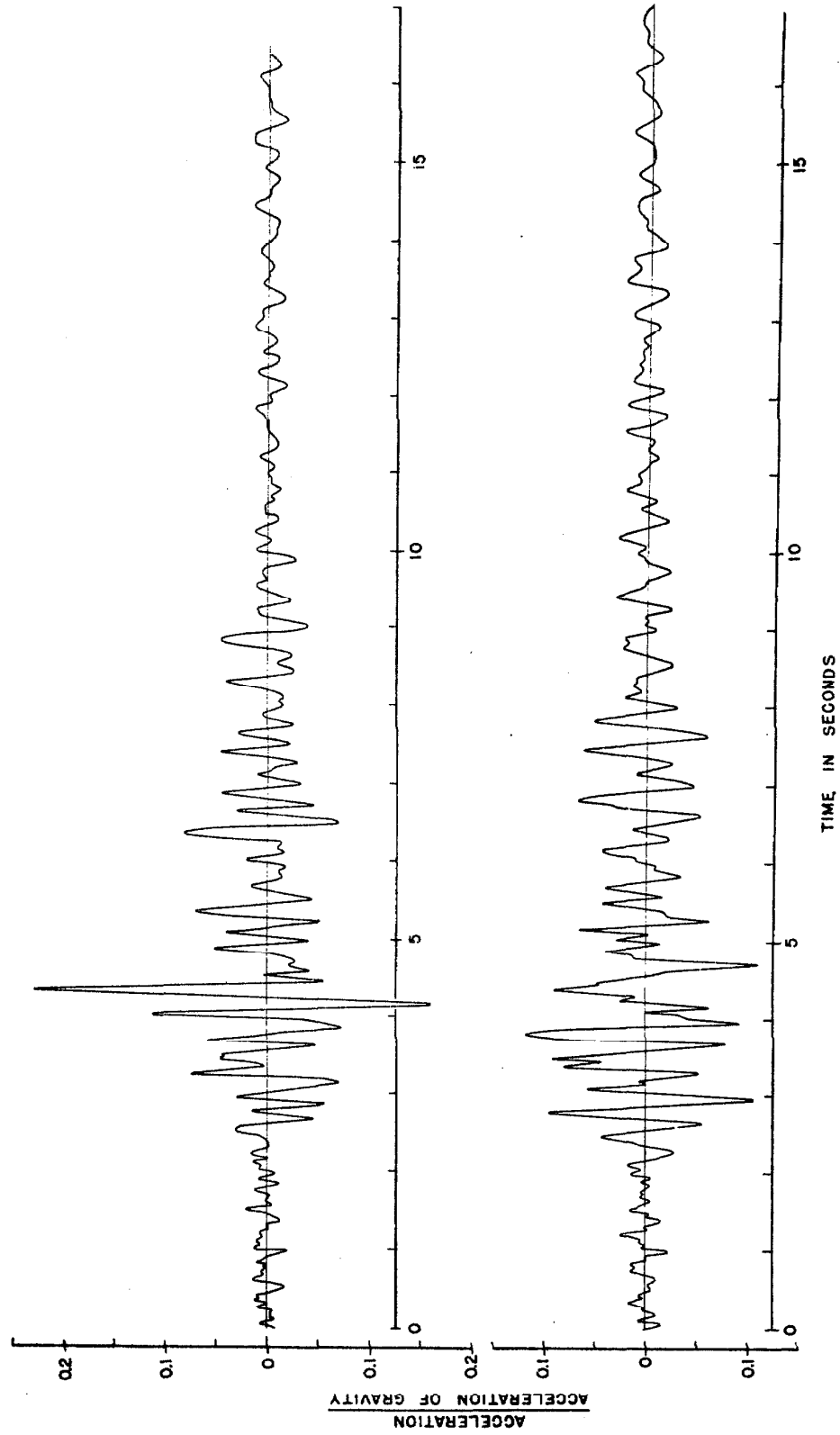


Figure 24. Accelerograms for Hollister, California; earthquake of March 9, 1949. Components: S 01 W(lower), N 89 W (upper).

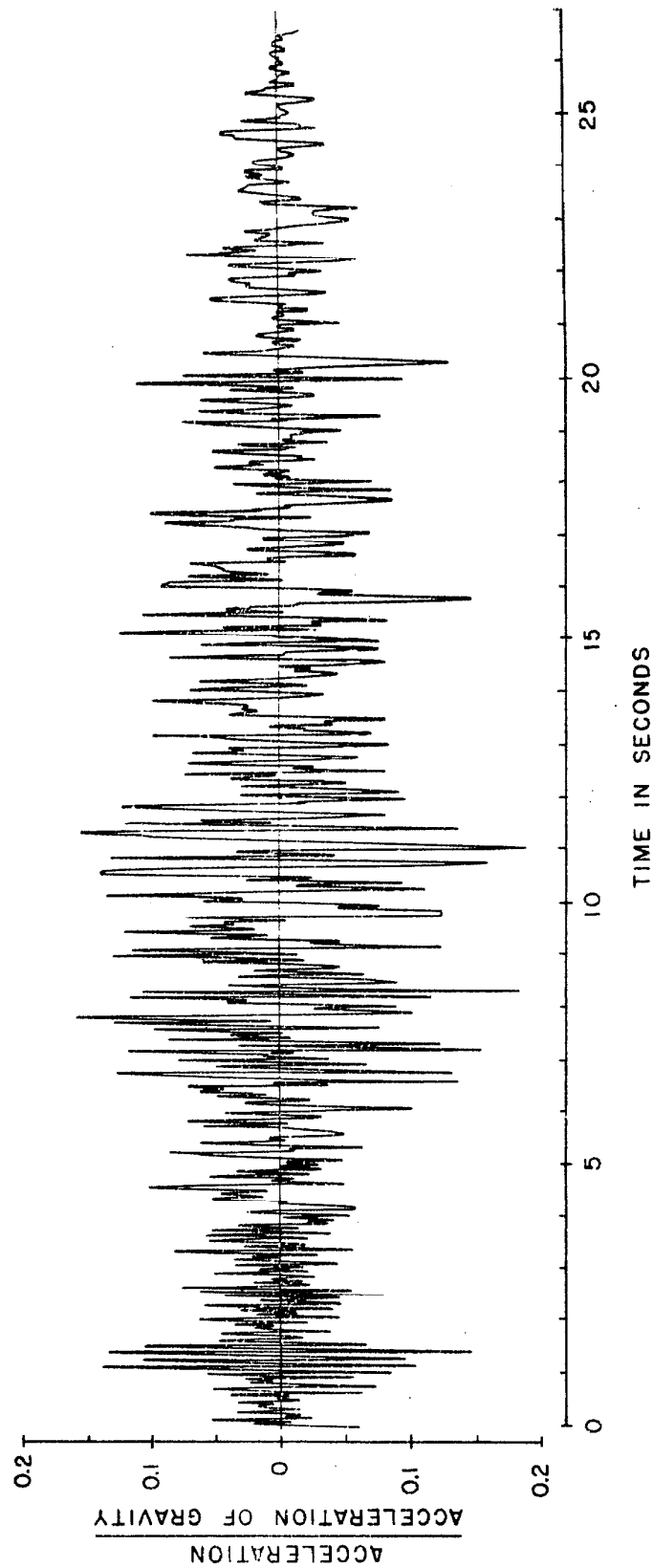


Figure 25. Accelerogram for Olympia, Washington; earthquake of April 13, 1949. Component S 10 E.

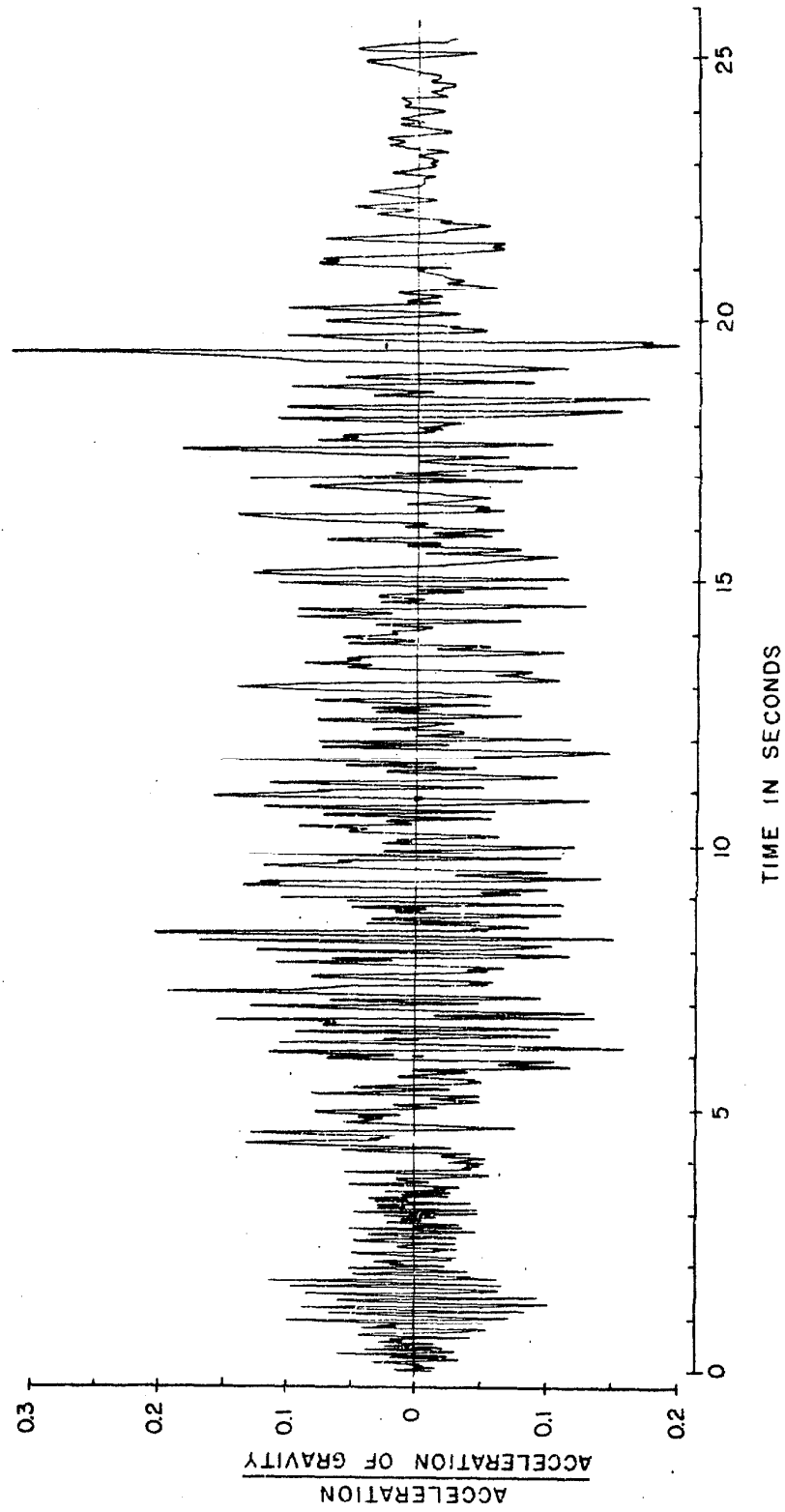


Figure 26. Accelerogram for Olympia, Washington; earthquake of April 13, 1949. Component S 80 W.

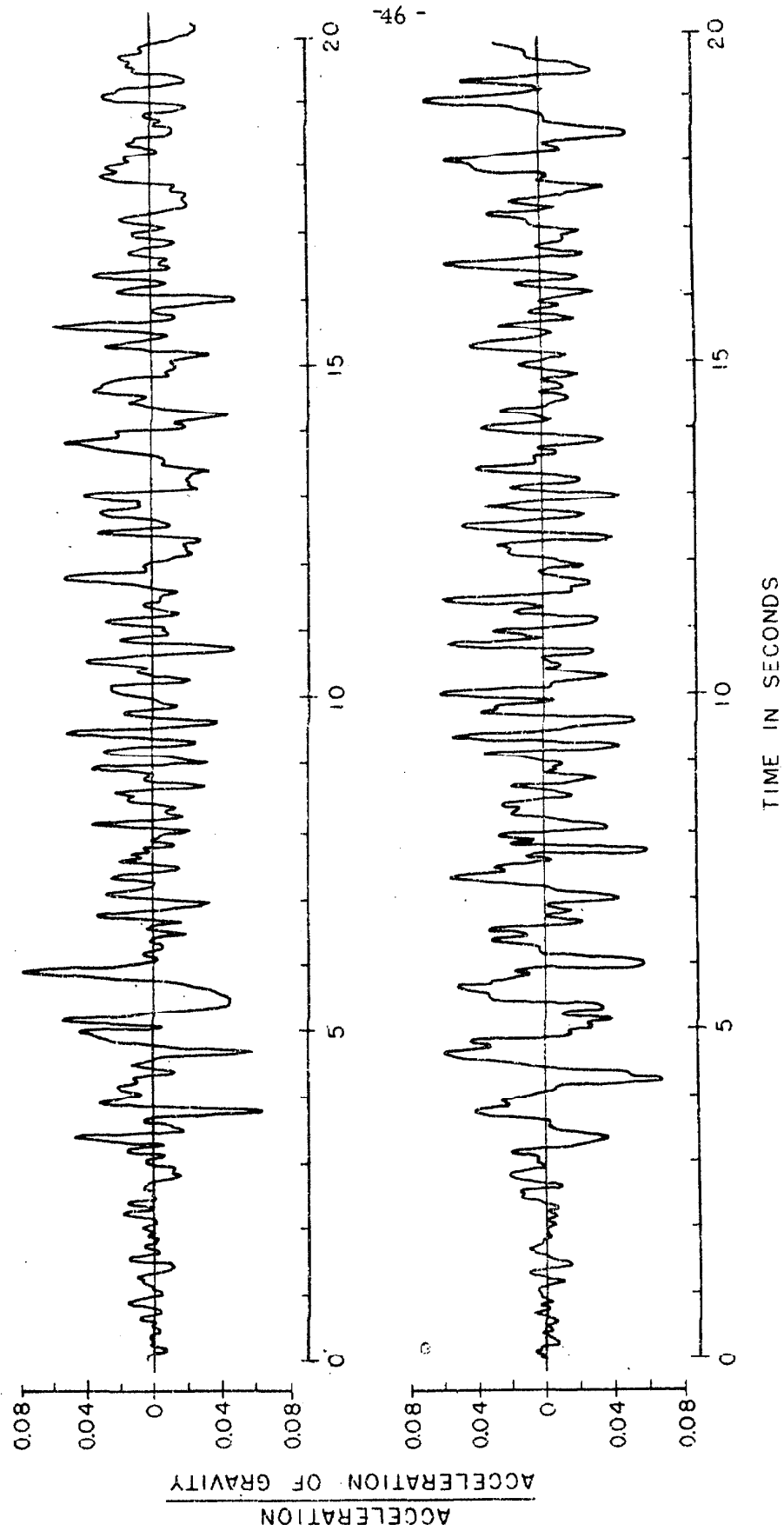


Figure 27. Accelerograms for Seattle, Washington; earthquake of April 13, 1949. Components: N 88 W (upper), S 02 W (lower).

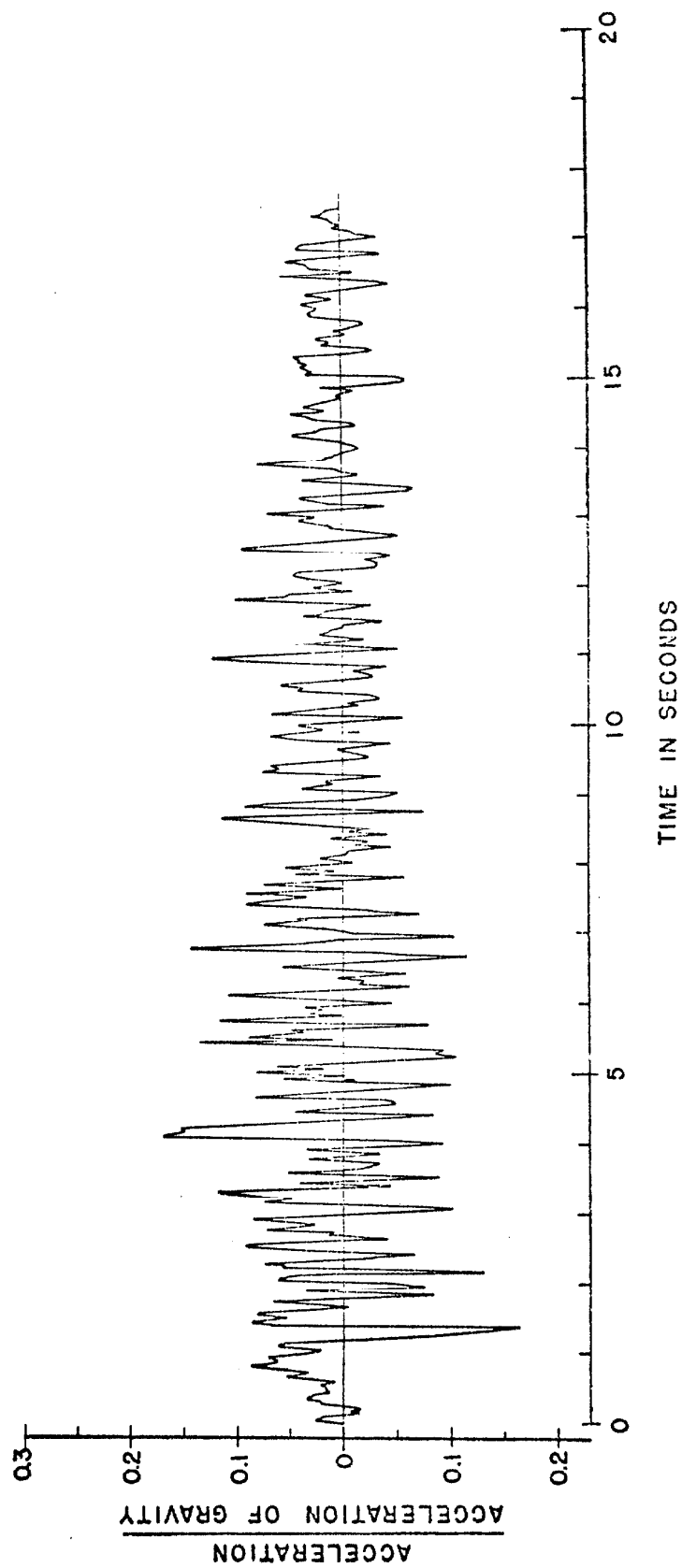


Figure 27a. Accelerogram for Taft, California; earthquake of July 21, 1952. Component S 69 E.

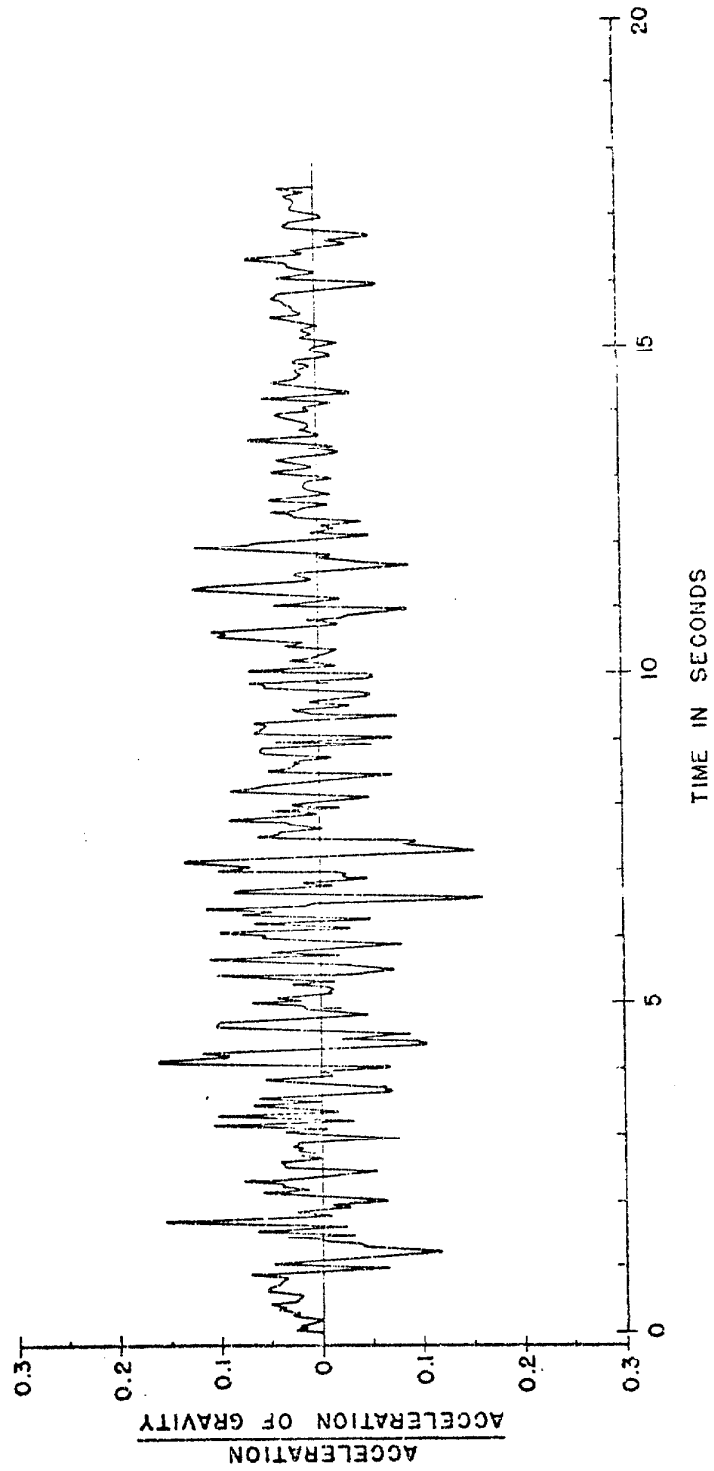


Figure 27b. Accelerogram for Taft, California; earthquake of July 21, 1952. Component N 21 E.

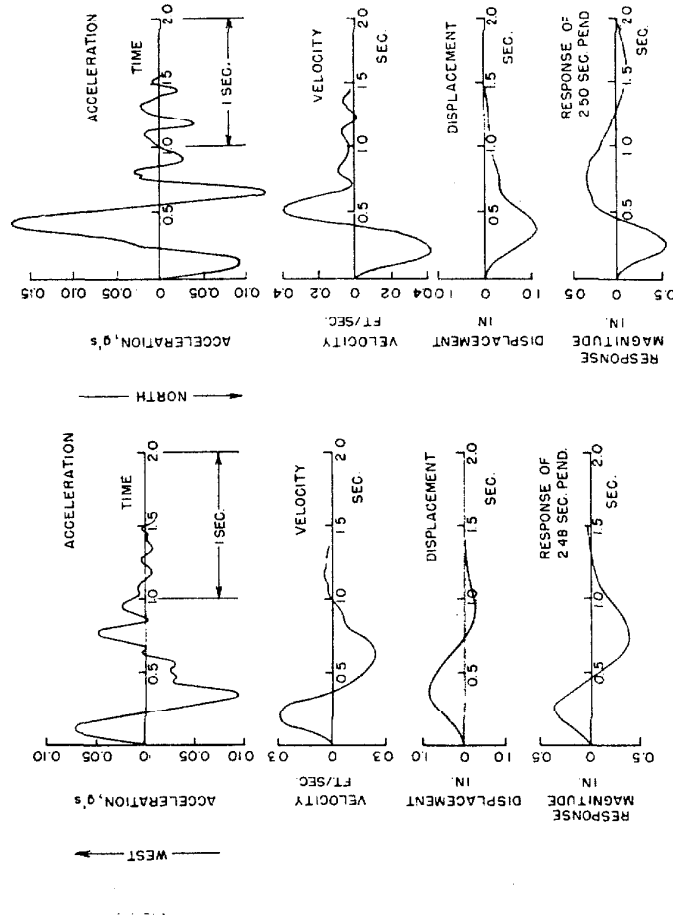


Figure 27c.

(Left) East-west components of ground motion.

(Right) North-south components of ground motion.

(See "The Port Hueneme Earthquake of March 18, 1957," by G. W. Housner and D. E. Hudson, Bull. Seismo. Soc. of Amer., Vol. 48, pp. 163-168, April 1958).

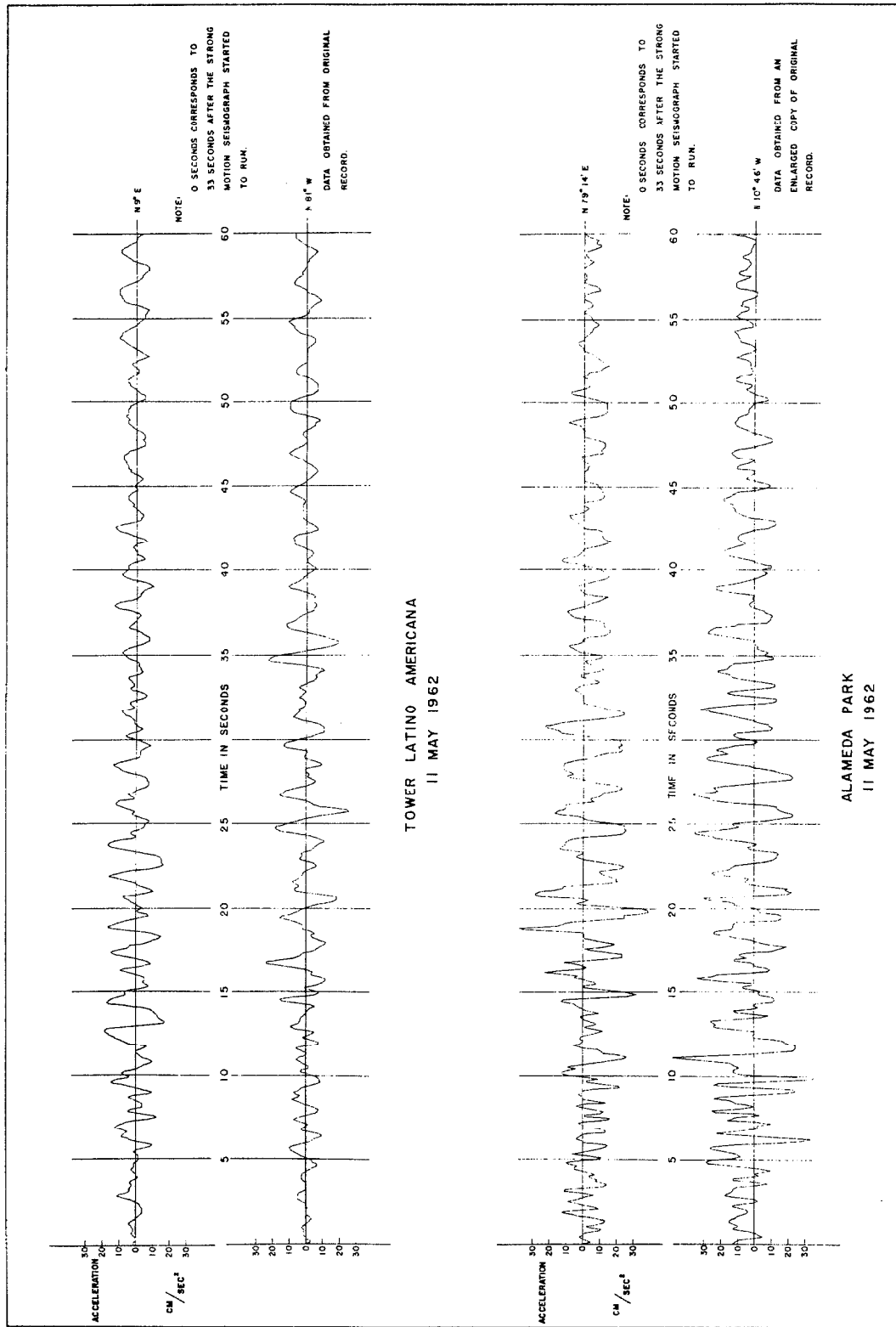


Figure 27d. Mexico City acceleration records for earthquake of 11 May 1962. (See "Mexican Earthquakes of 11 May and 19 May 1962," by P. C. Jennings, Earthquake Engineering Research Lab., C. I. T.)

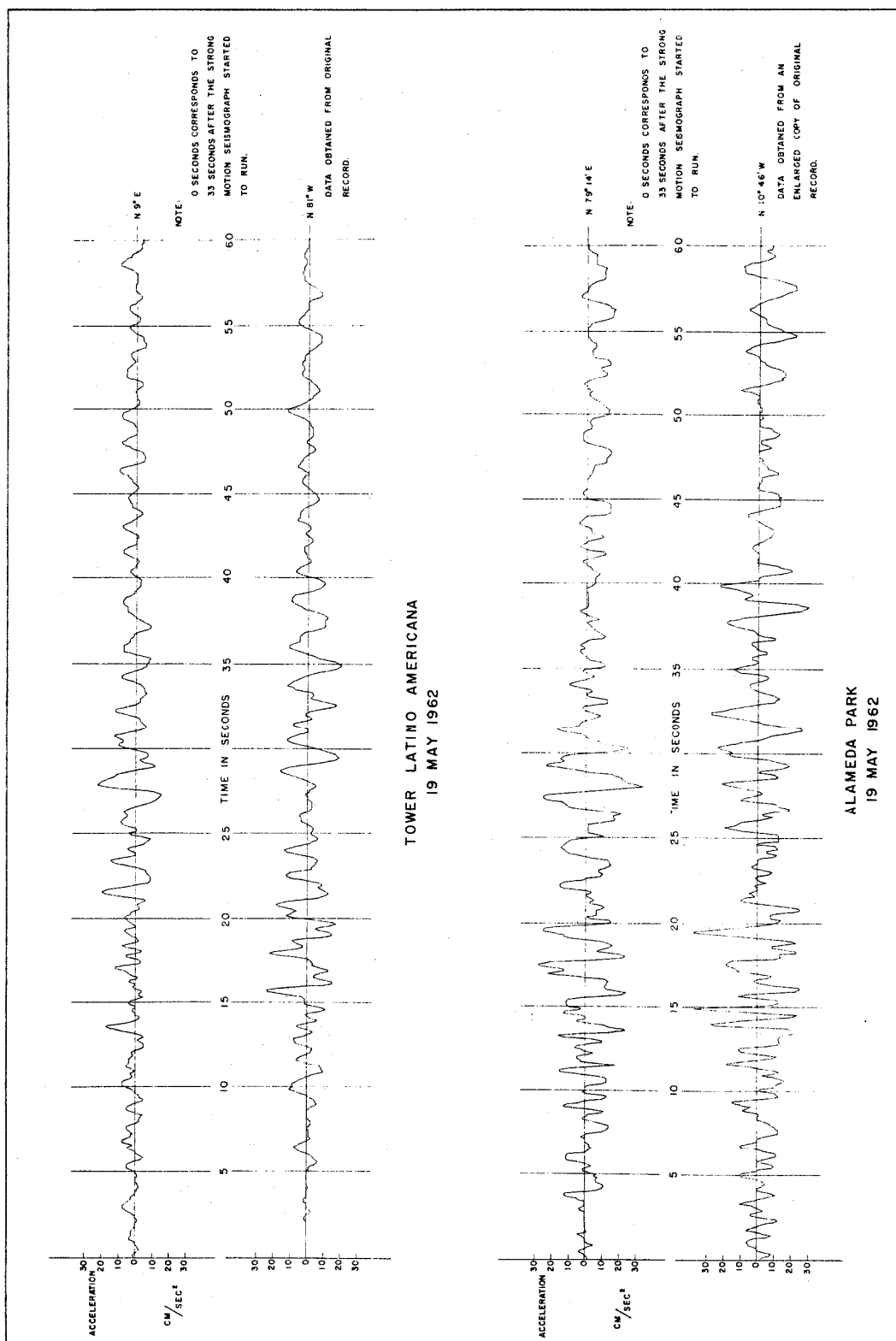


Figure 27e. Mexico City acceleration records for earthquake of 19 May 1962.

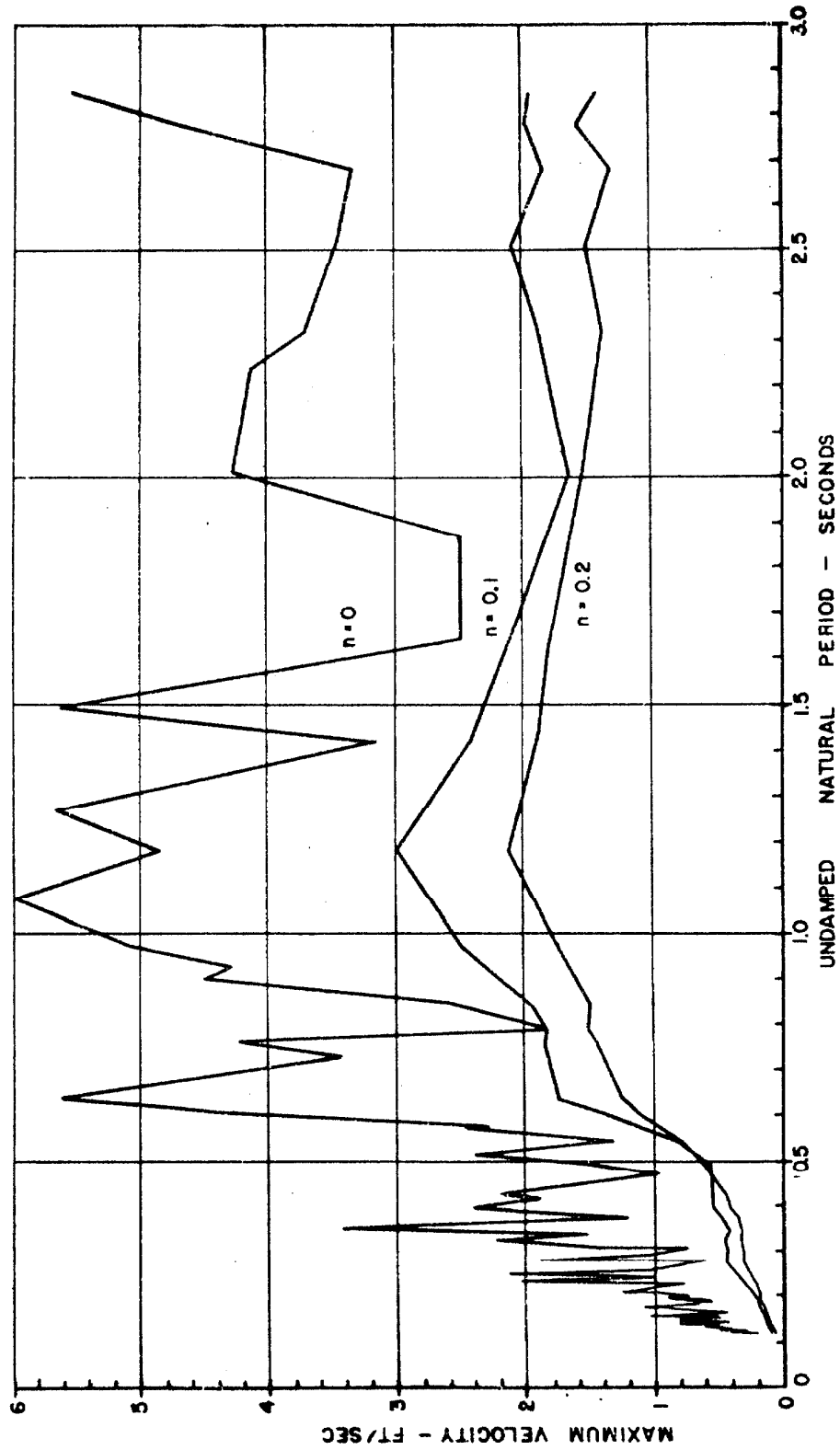


Figure 28. Velocity spectrum for Vernon, California; earthquake of March 10, 1933. Component N 08 E.

Ordinates should be multiplied by 0.525

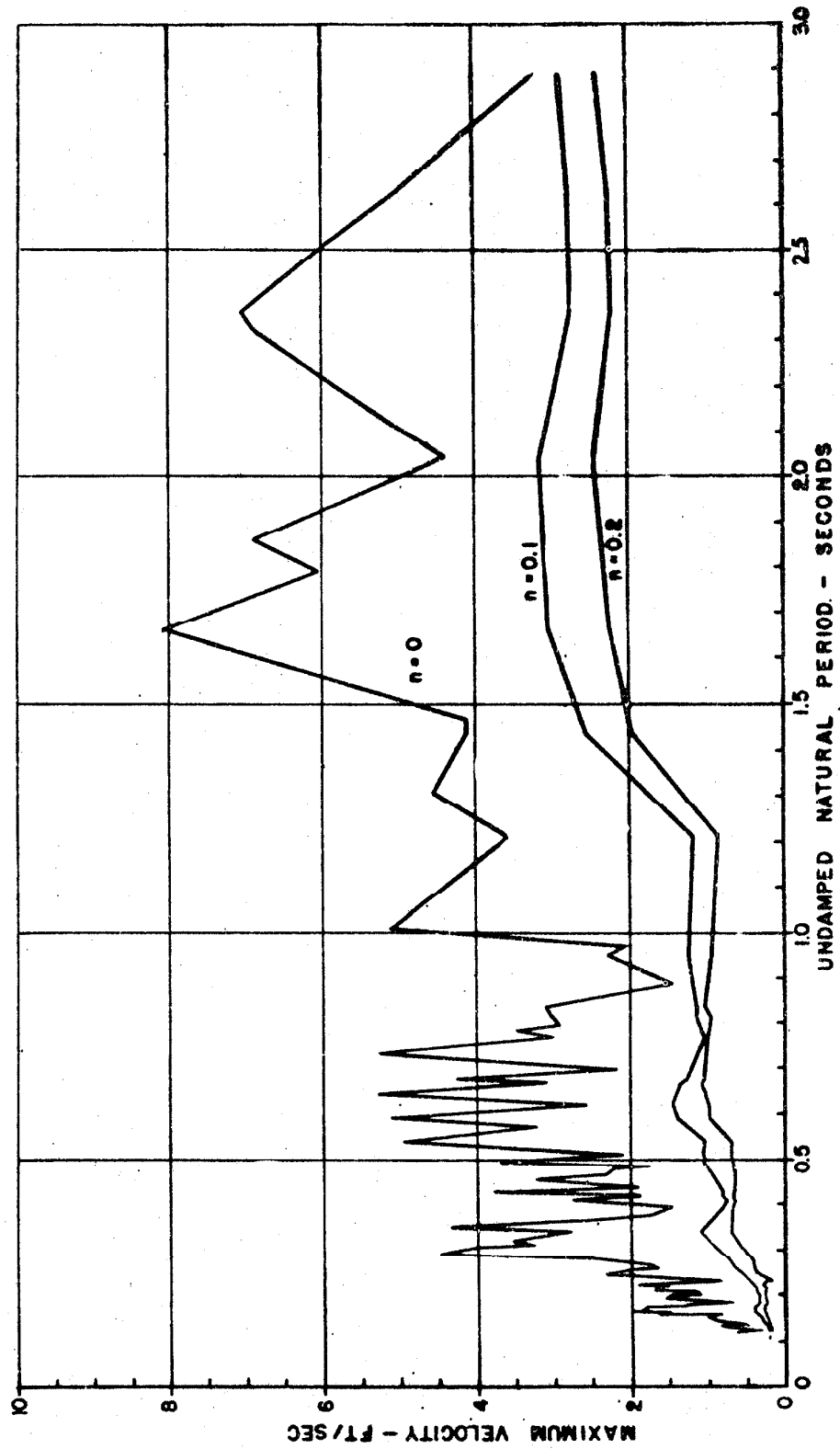


Figure 29. Velocity spectrum for Vernon, California; earthquake of March 10, 1933. Component S 82 E.

Ordinates should be multiplied by 0.472

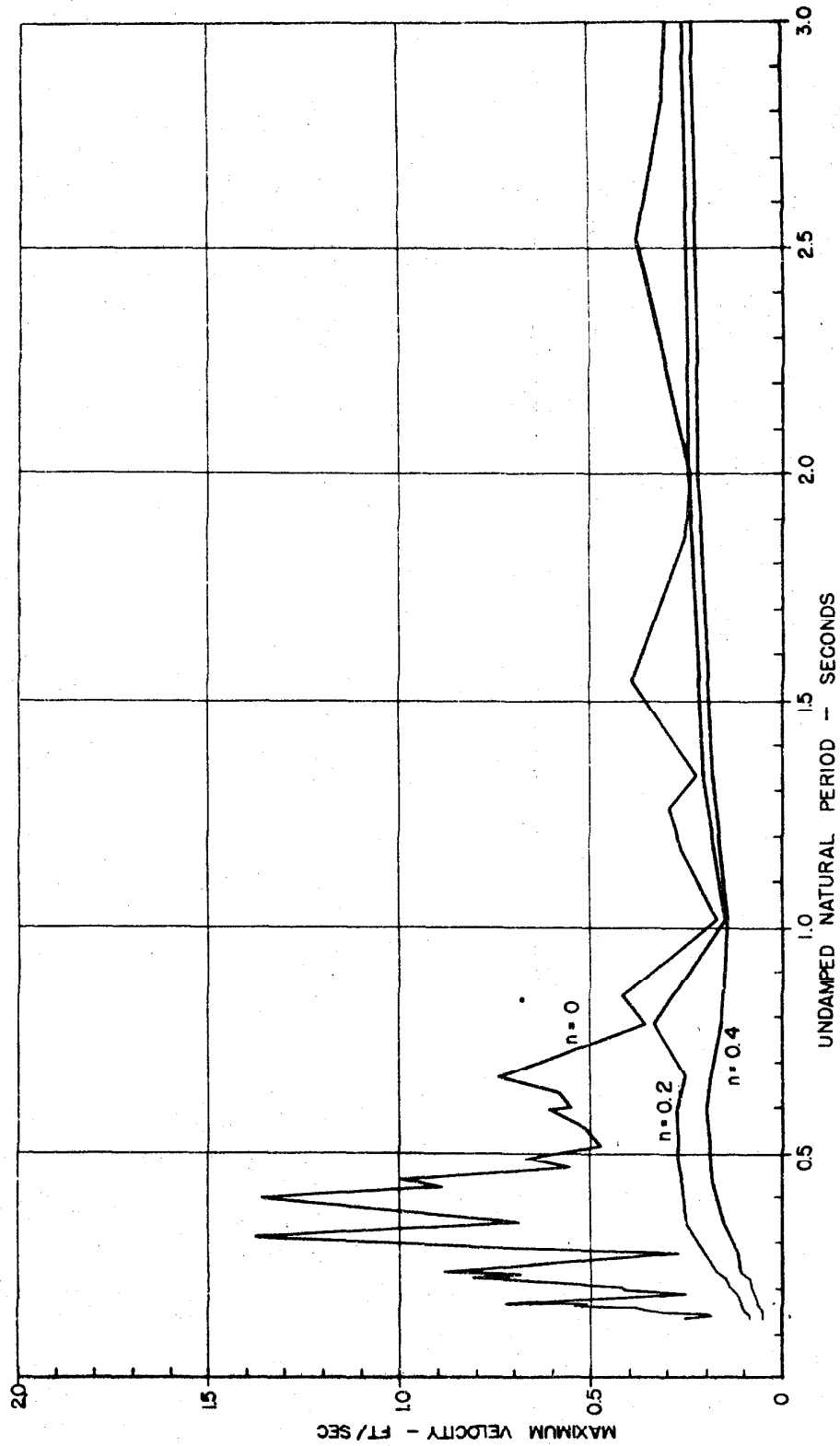


Figure 30. Velocity spectrum for Vernon, California; earthquake of Oct. 2, 1933. Component N 08 E.

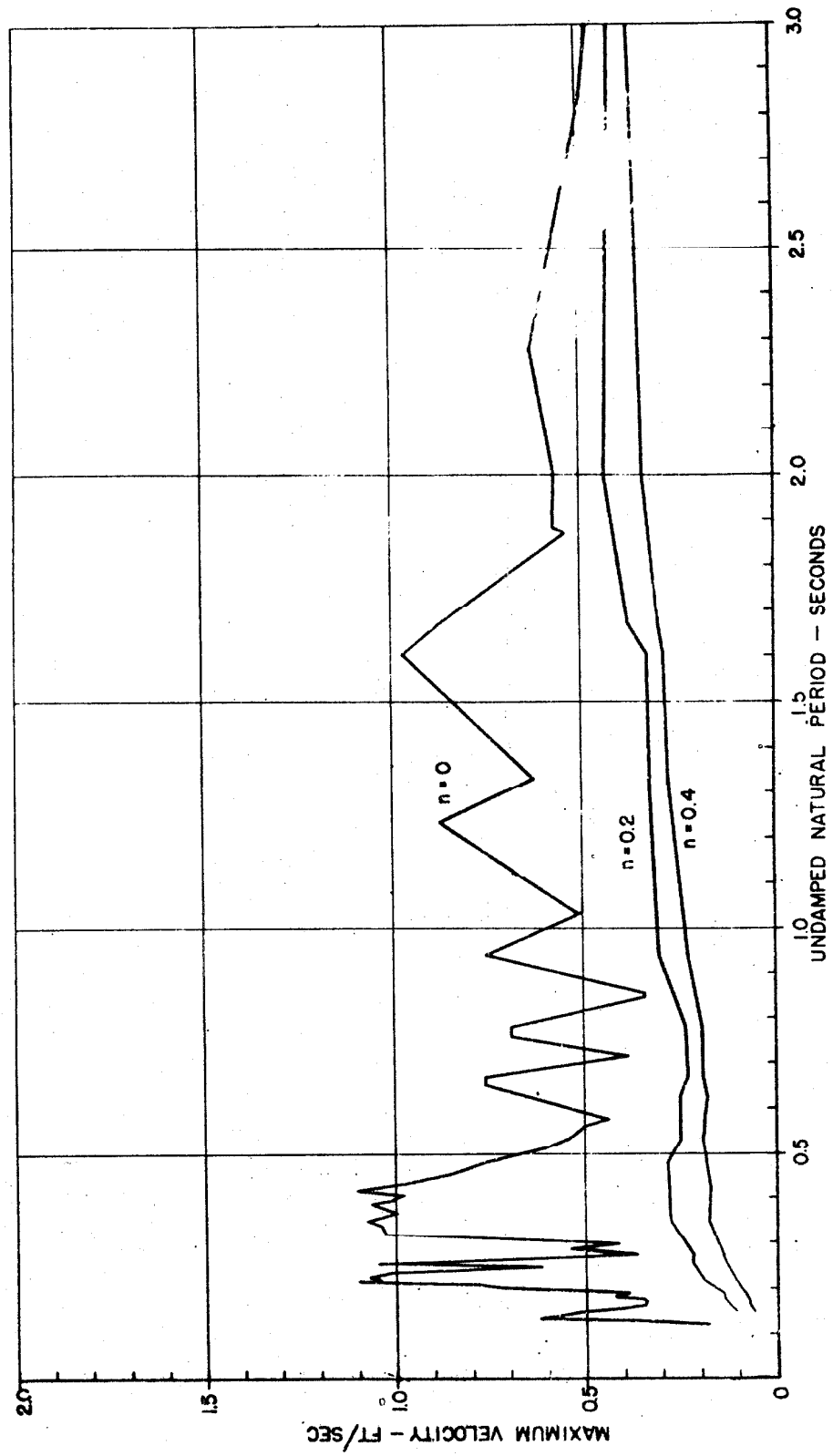


Figure 31. Velocity spectrum for Vernon, California; earthquake of Oct. 2, 1933. Component S 82 E.

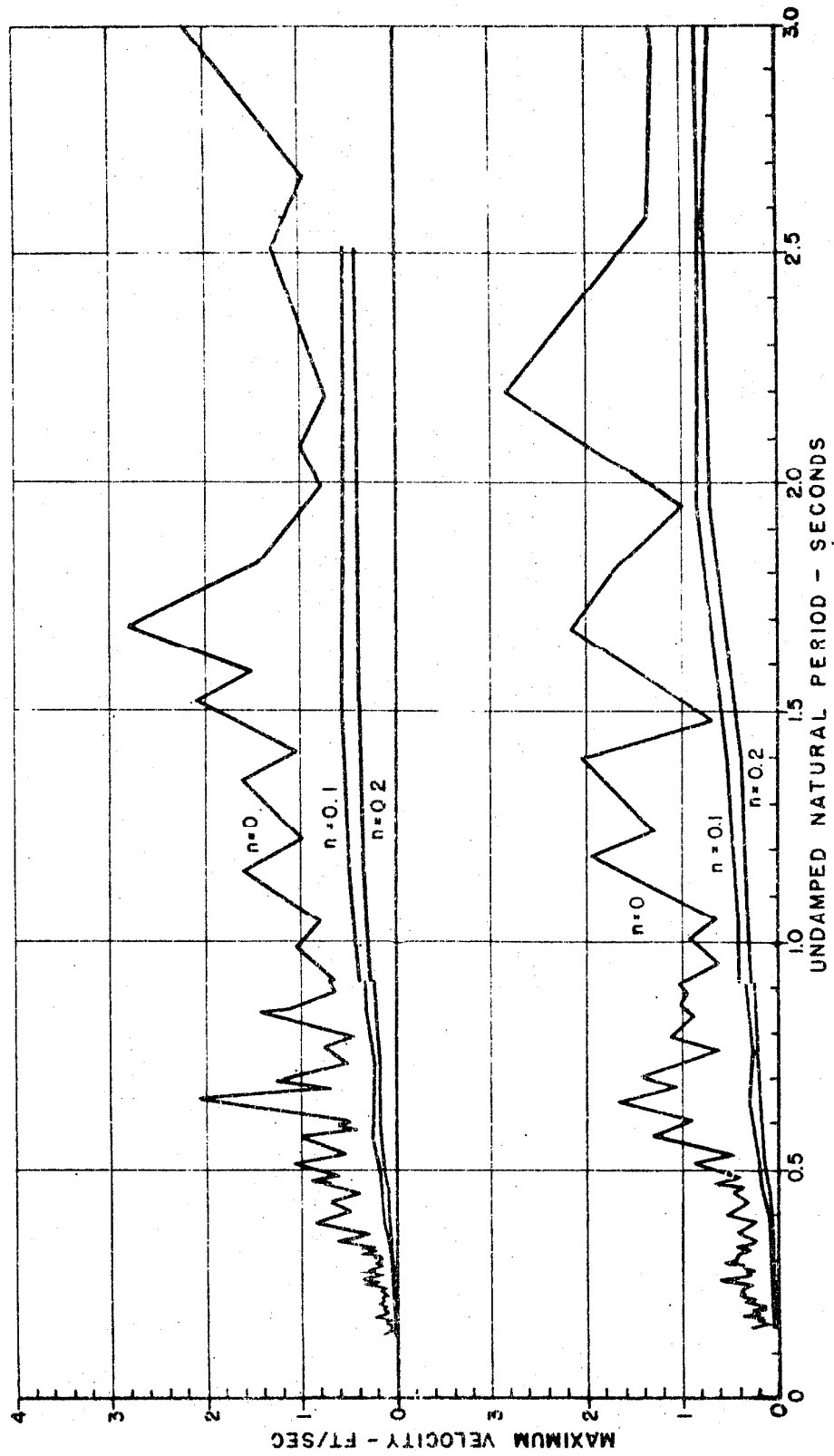


Figure 32. Velocity spectra for Los Angeles Subway Terminal; earthquake of March 10, 1933. Components: N 39 E (lower), N 51 W (upper).

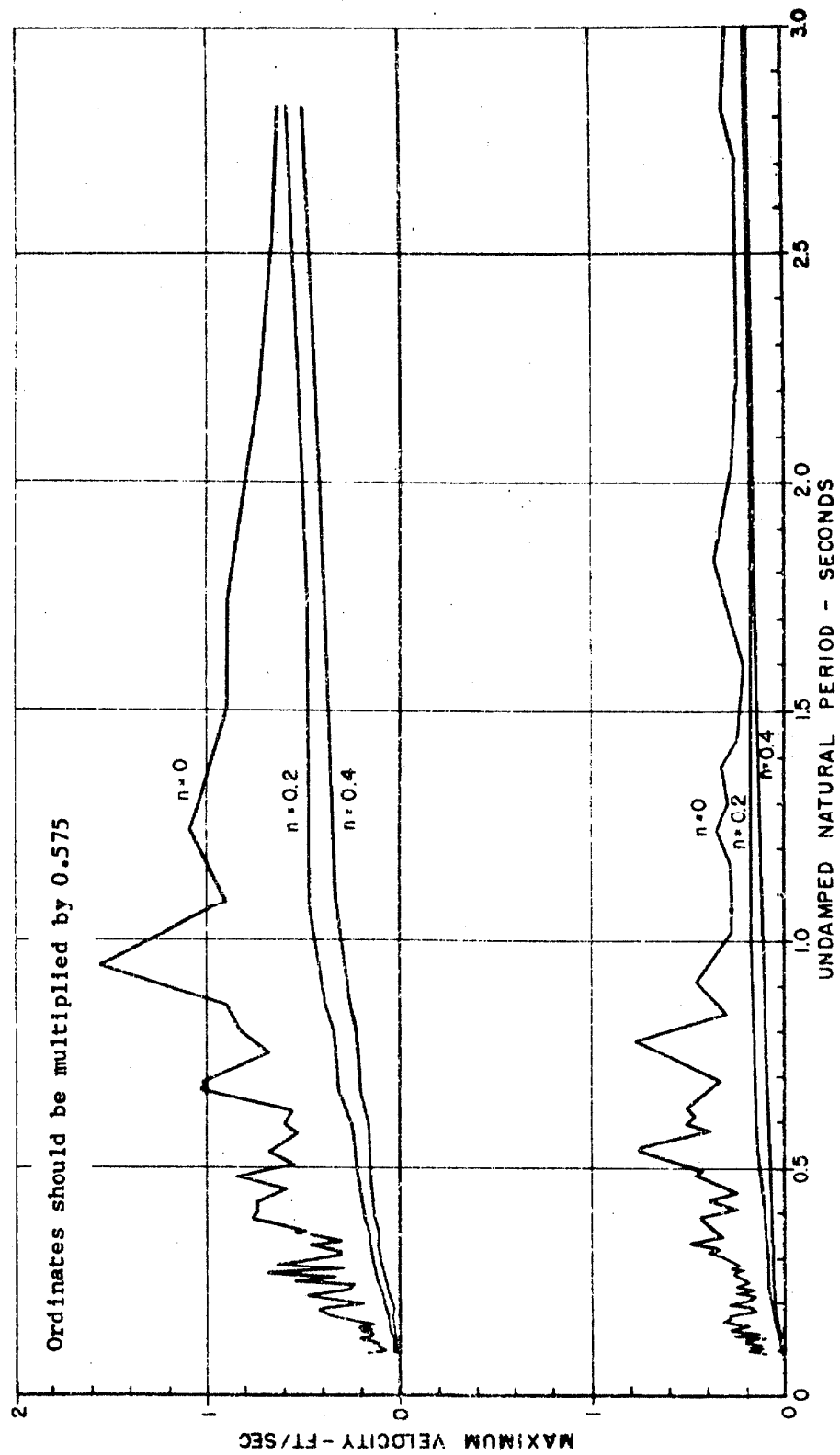


Figure 33. Velocity spectra for Los Angeles Subway Terminal; earthquake of Oct. 2, 1933. Components: N 39 E(lower), N 51 W (upper).

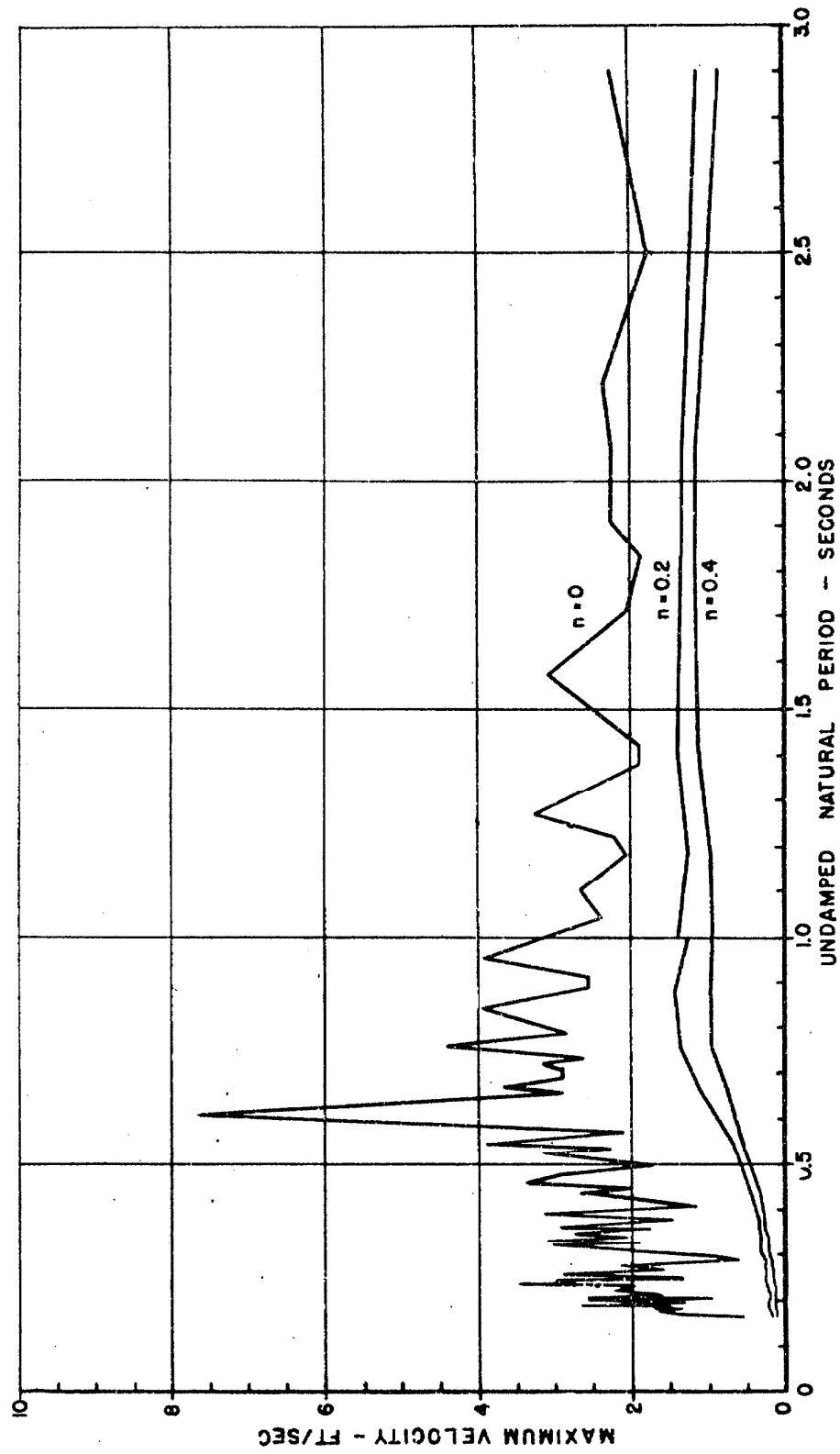


Figure 34. Velocity spectrum for El Centro, California; earthquake of Dec. 30, 1934. Component N-S.

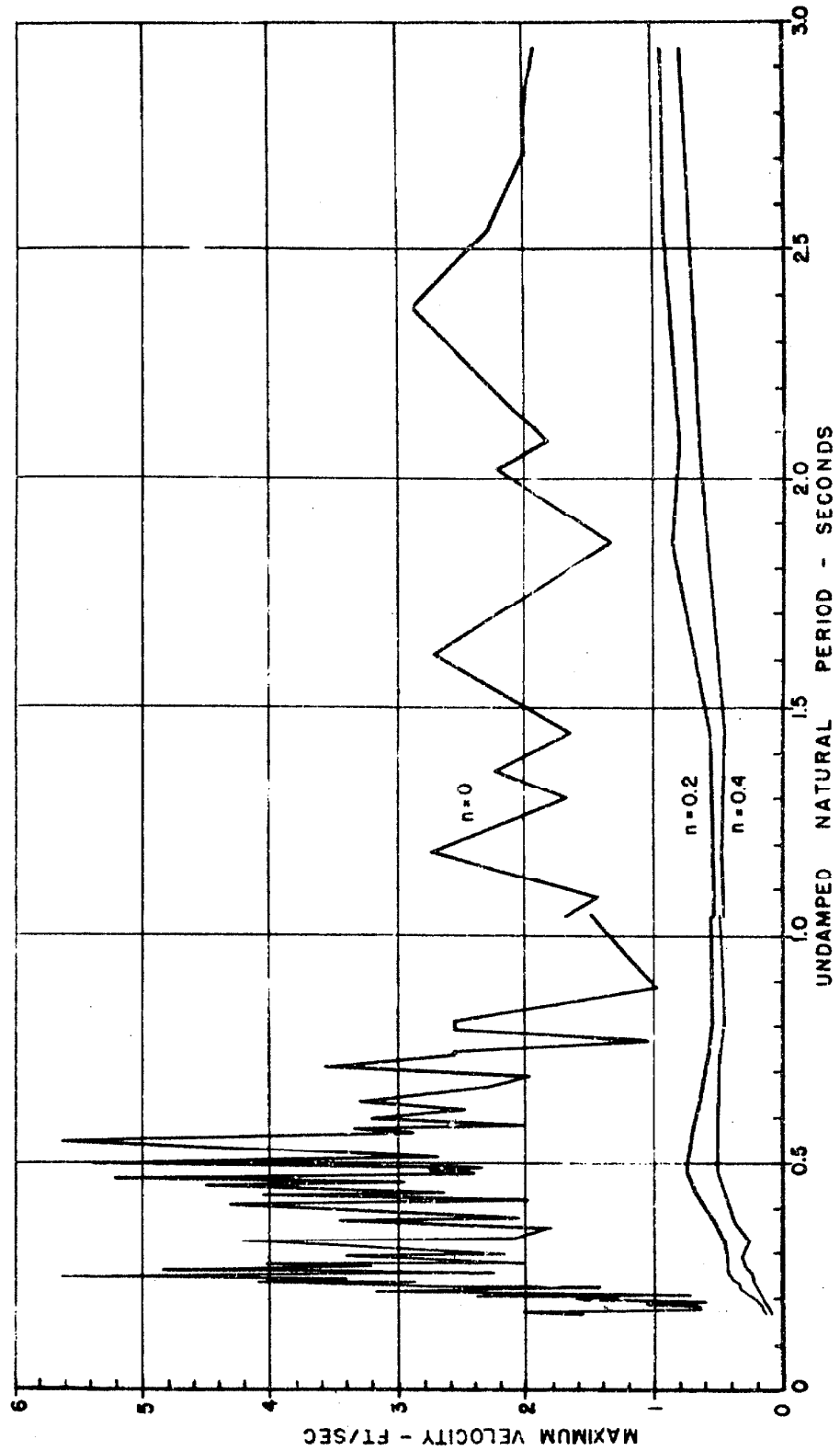


Figure 35. Velocity spectrum for El Centro, California; earthquake of Dec. 30, 1934. Component E-W.

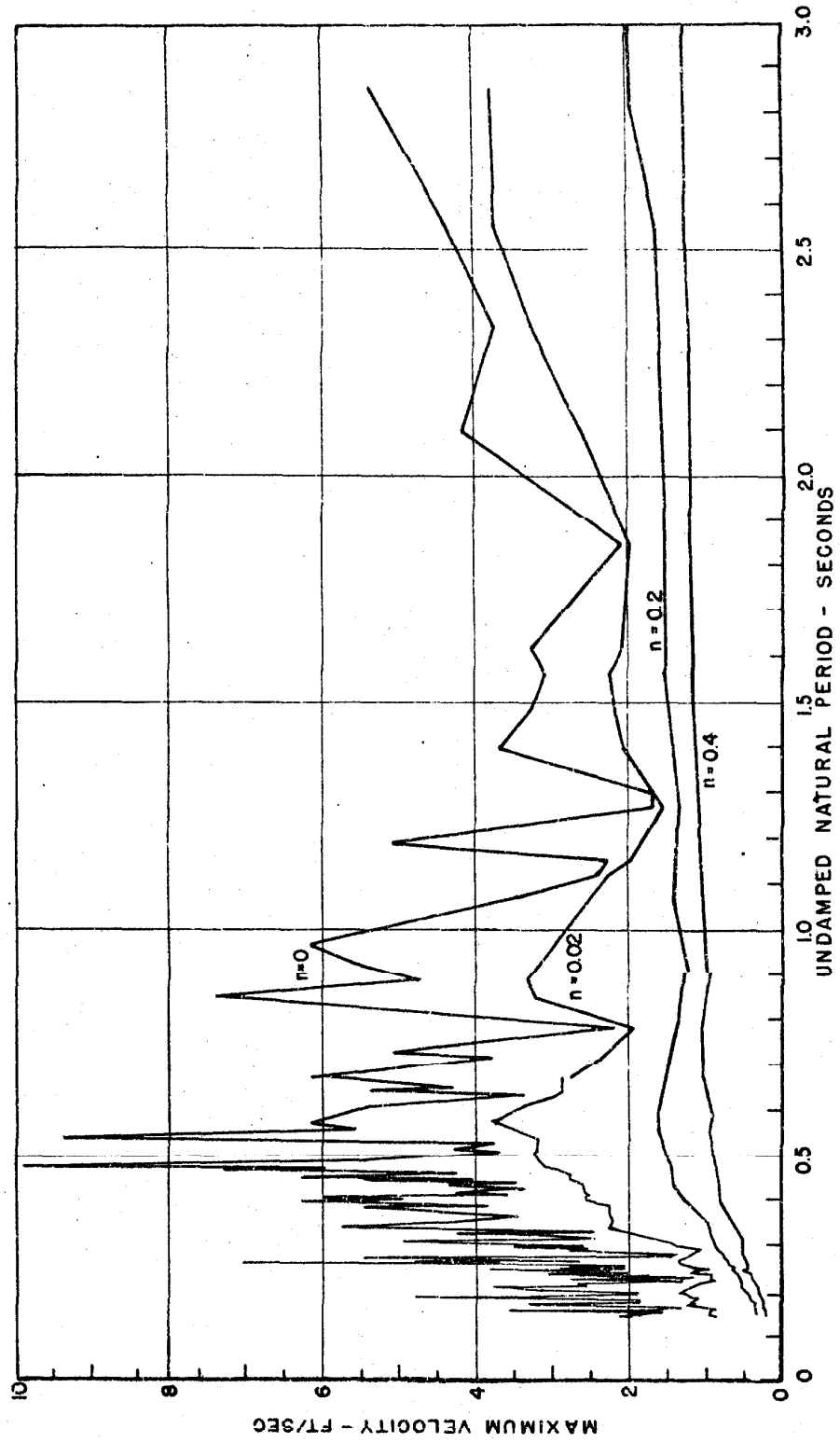


Figure 36. Velocity spectrum for El Centro, California; earthquake of May 18, 1940. Component N-S.

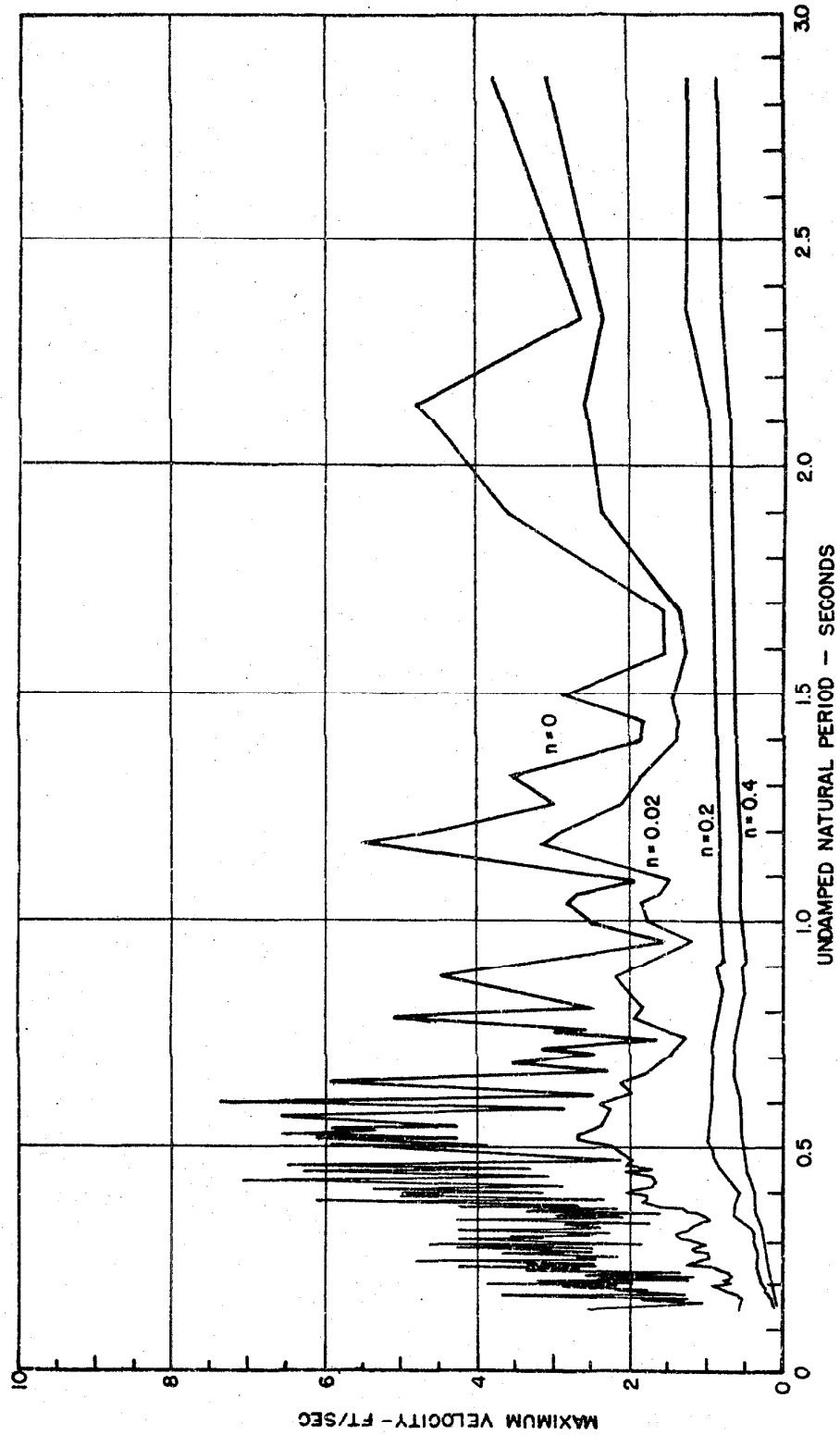


Figure 37. Velocity spectrum for El Centro, California; earthquake of May 18, 1940. Component E-W.

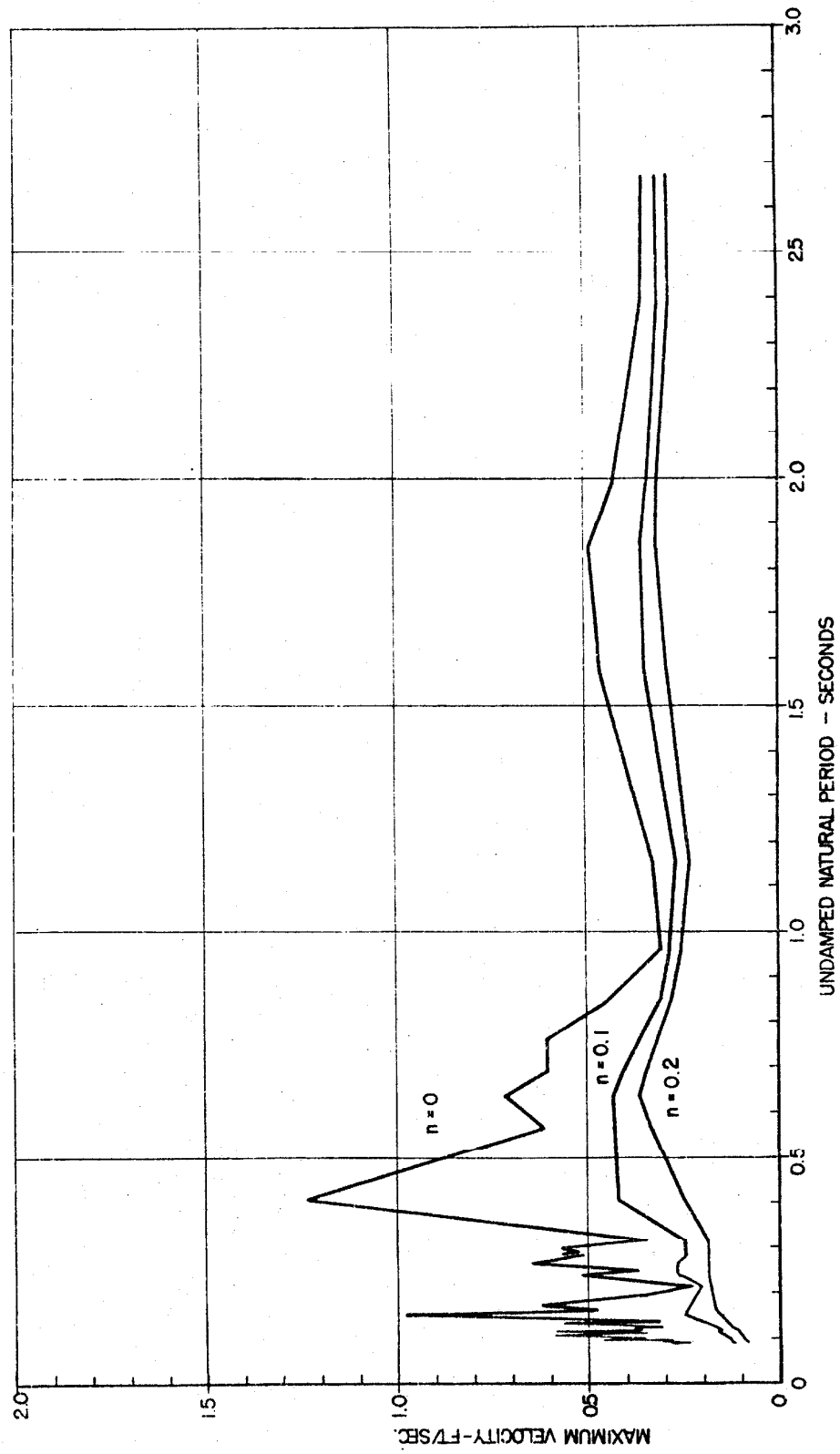


Figure 38. Velocity spectrum for Helena, Montana; earthquake of Oct. 31, 1935. Component N-S.

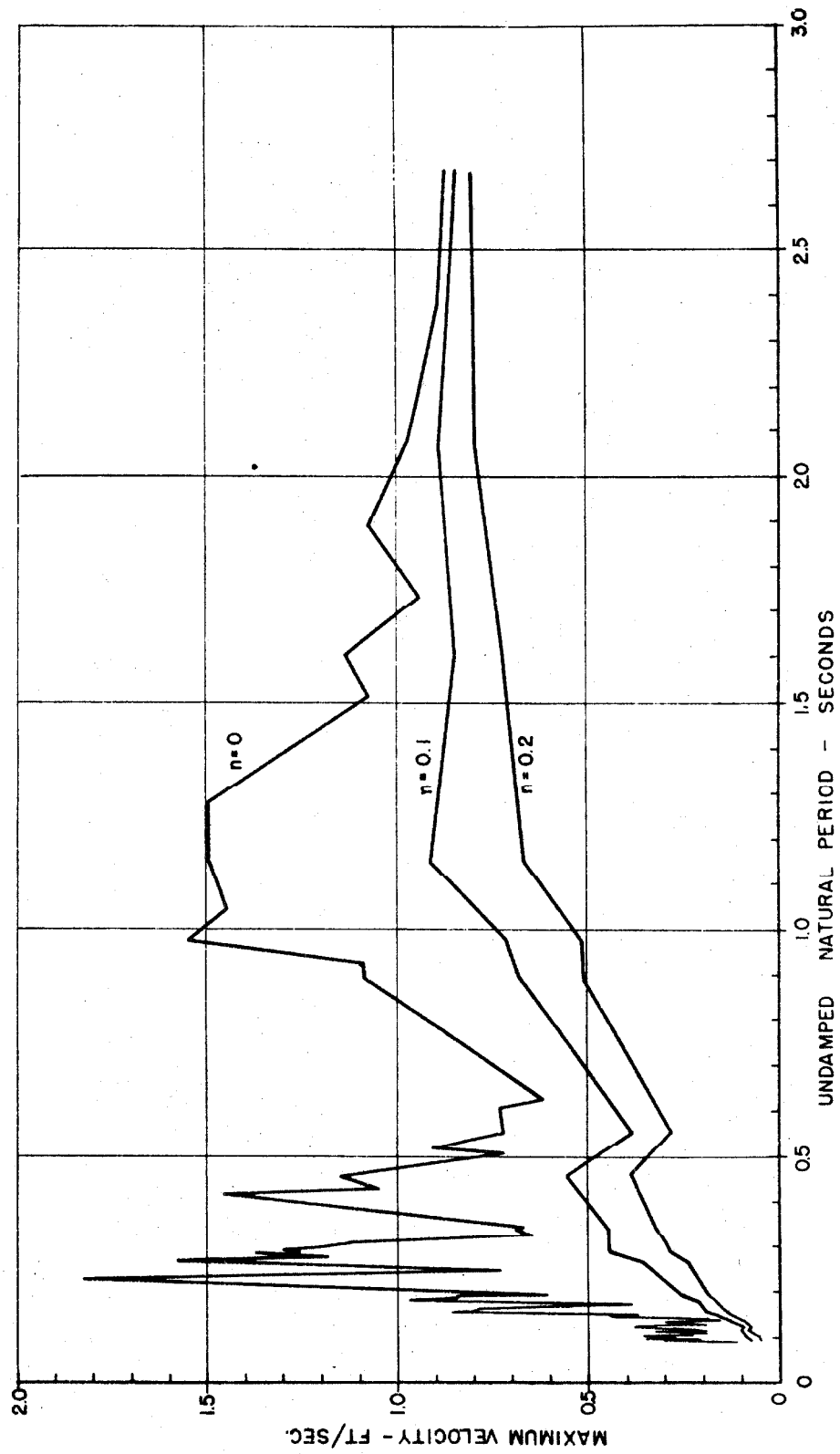


Figure 39. Velocity spectrum for Helena, Montana; earthquake of Oct. 31, 1935. Component E-W.

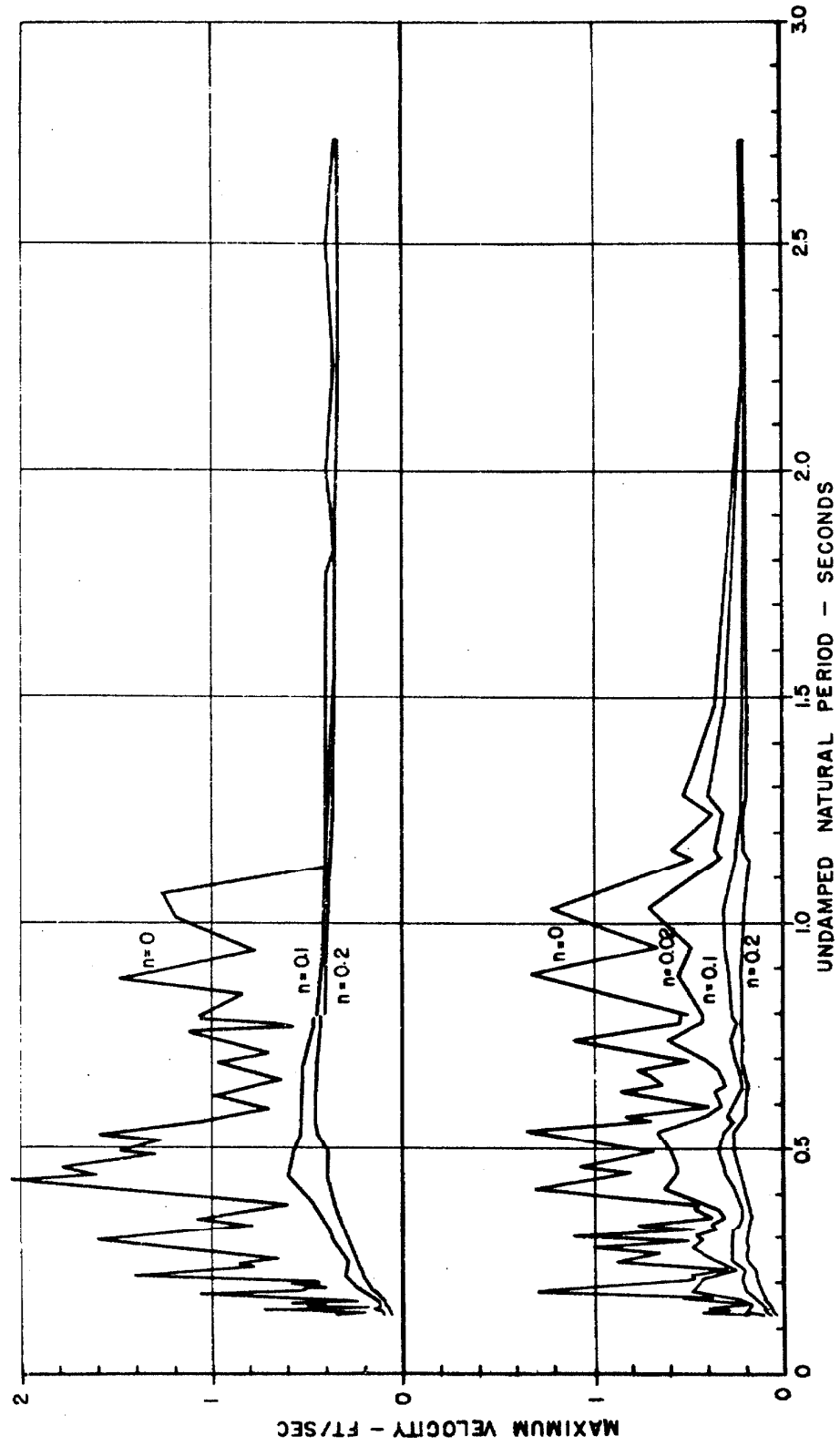


Figure 40. Velocity spectra for Ferndale, California; earthquake of Sept. 11, 1938. Components: N45E (lower), S 45 E (upper).

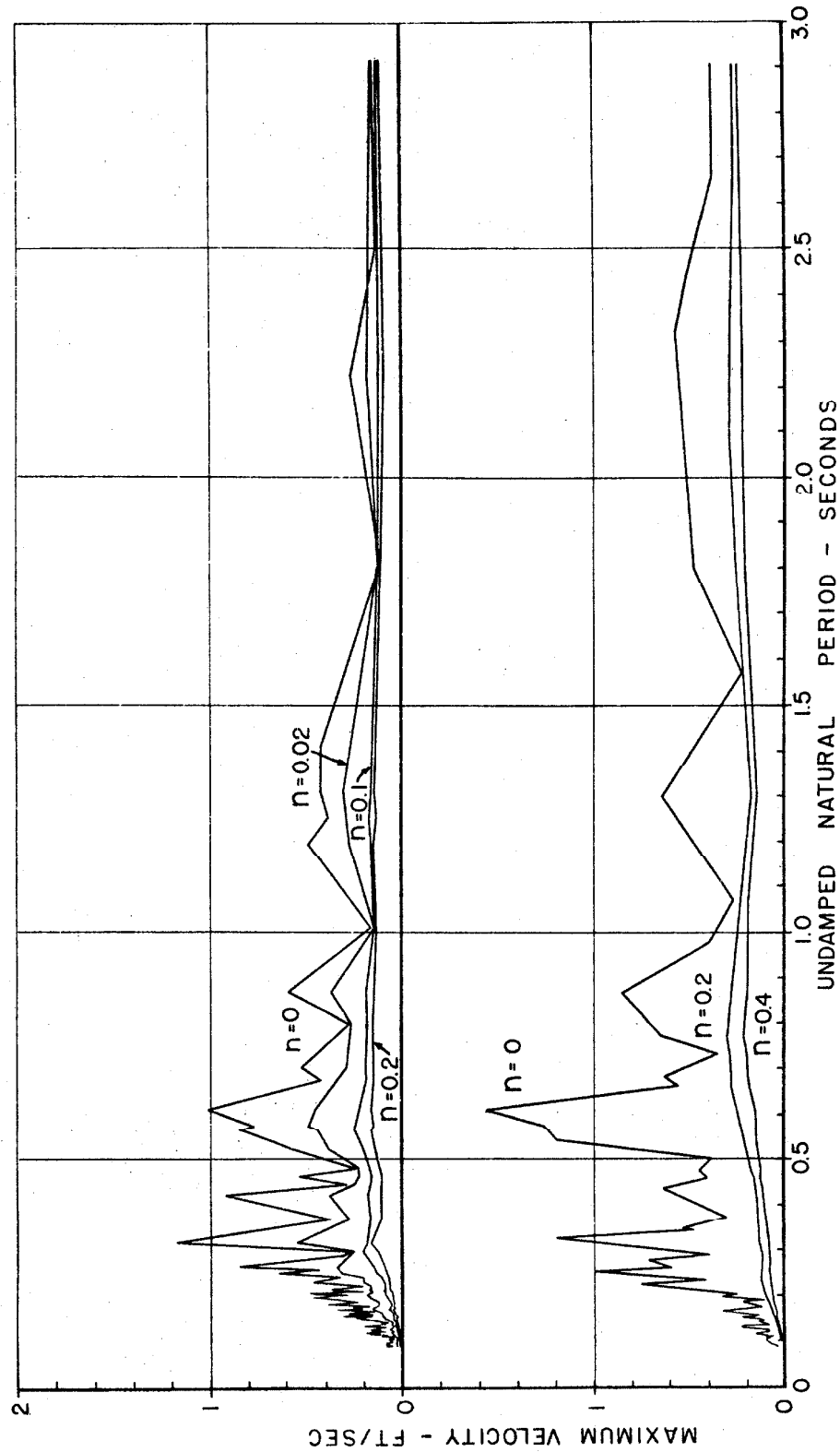


Figure 41. Velocity spectra for Ferndale, California; earthquake of Feb. 9, 1941. Components: N45E (lower), S45E (upper).

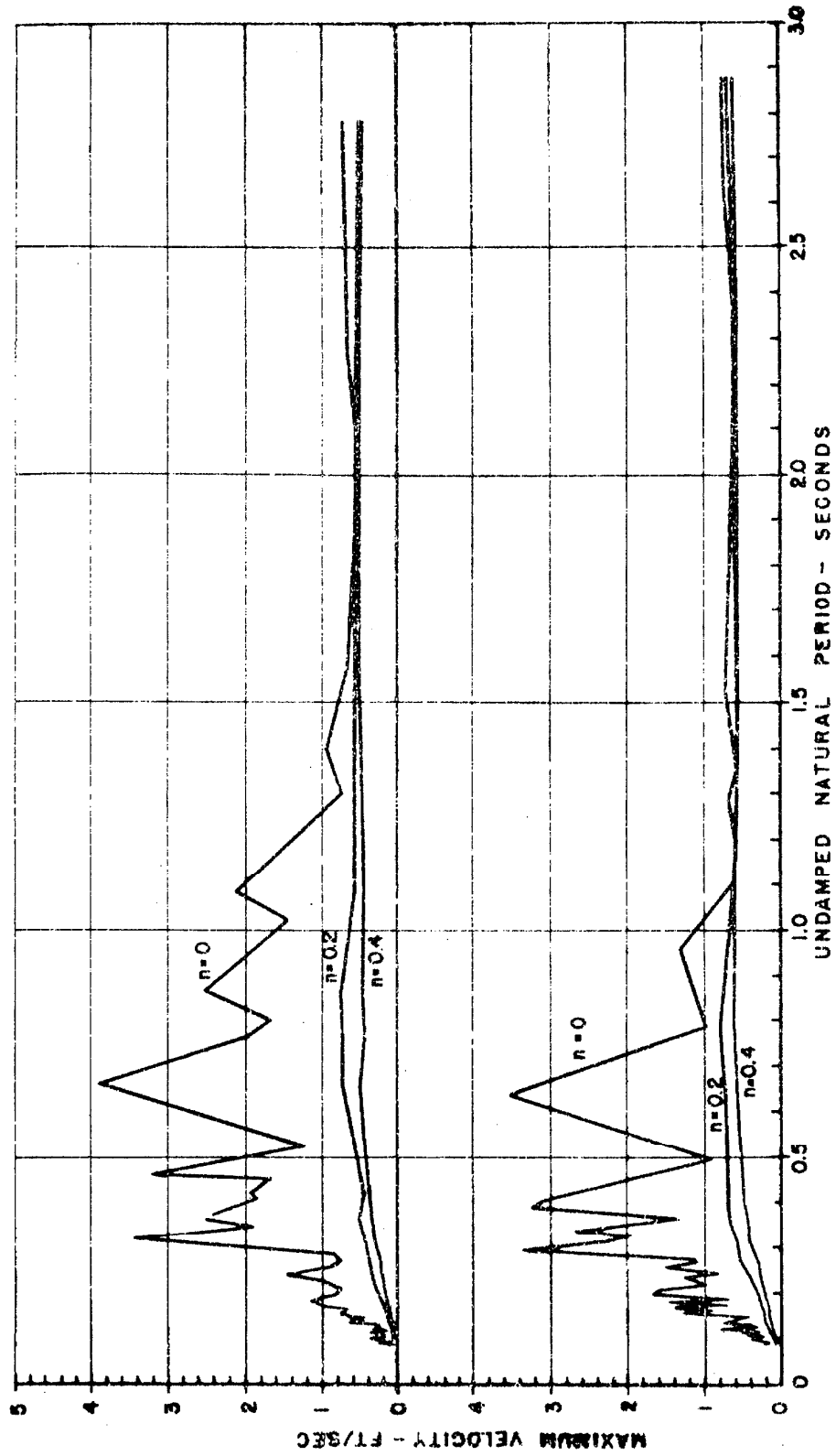


Figure 42. Velocity spectra for Ferndale, California; earthquake of Oct. 3, 1941. Components: N45E (lower), S45E (upper).

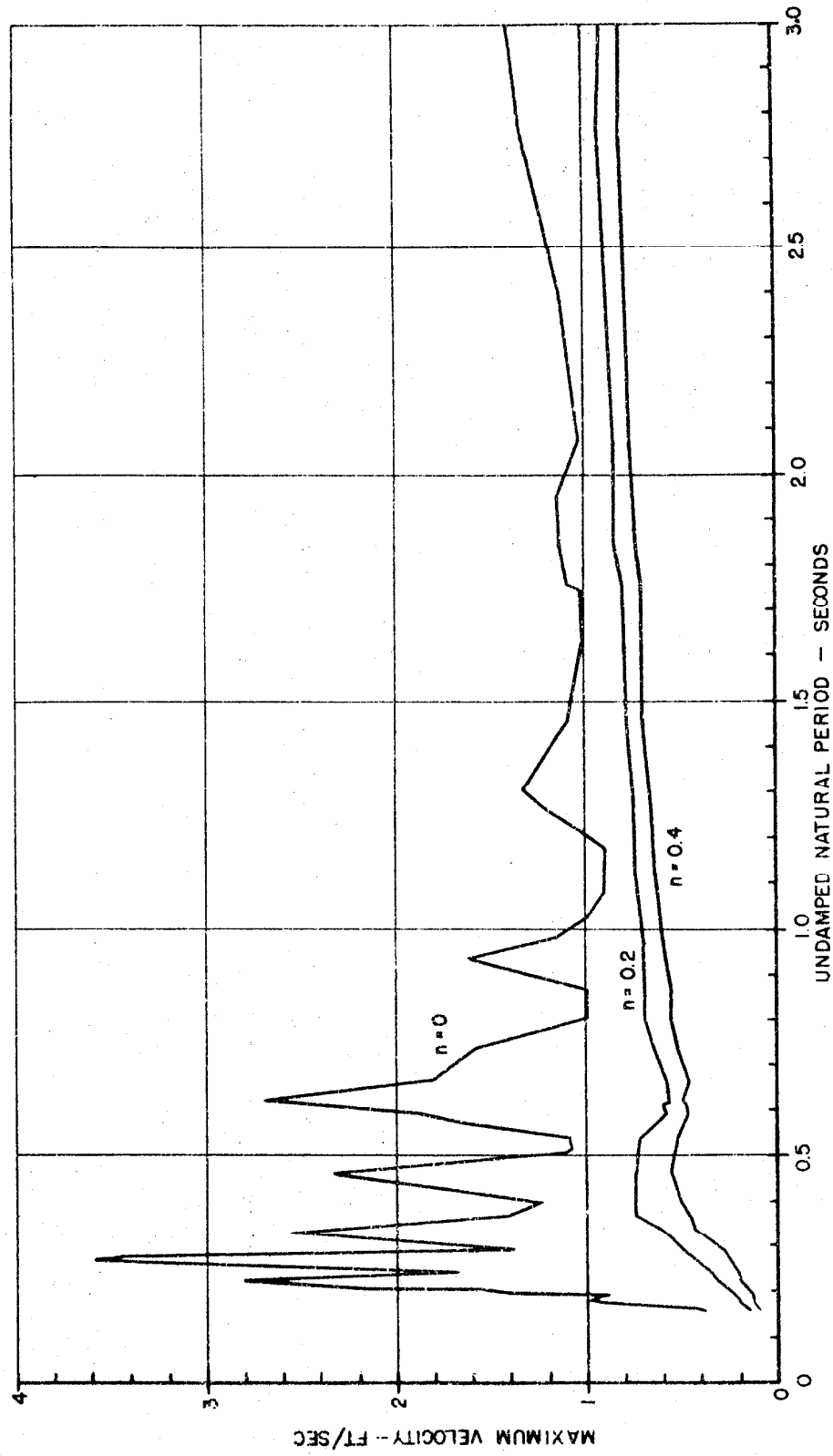


Figure 43. Velocity spectrum for Santa Barbara, California; earthquake of June 30, 1941. Component N 45 E.

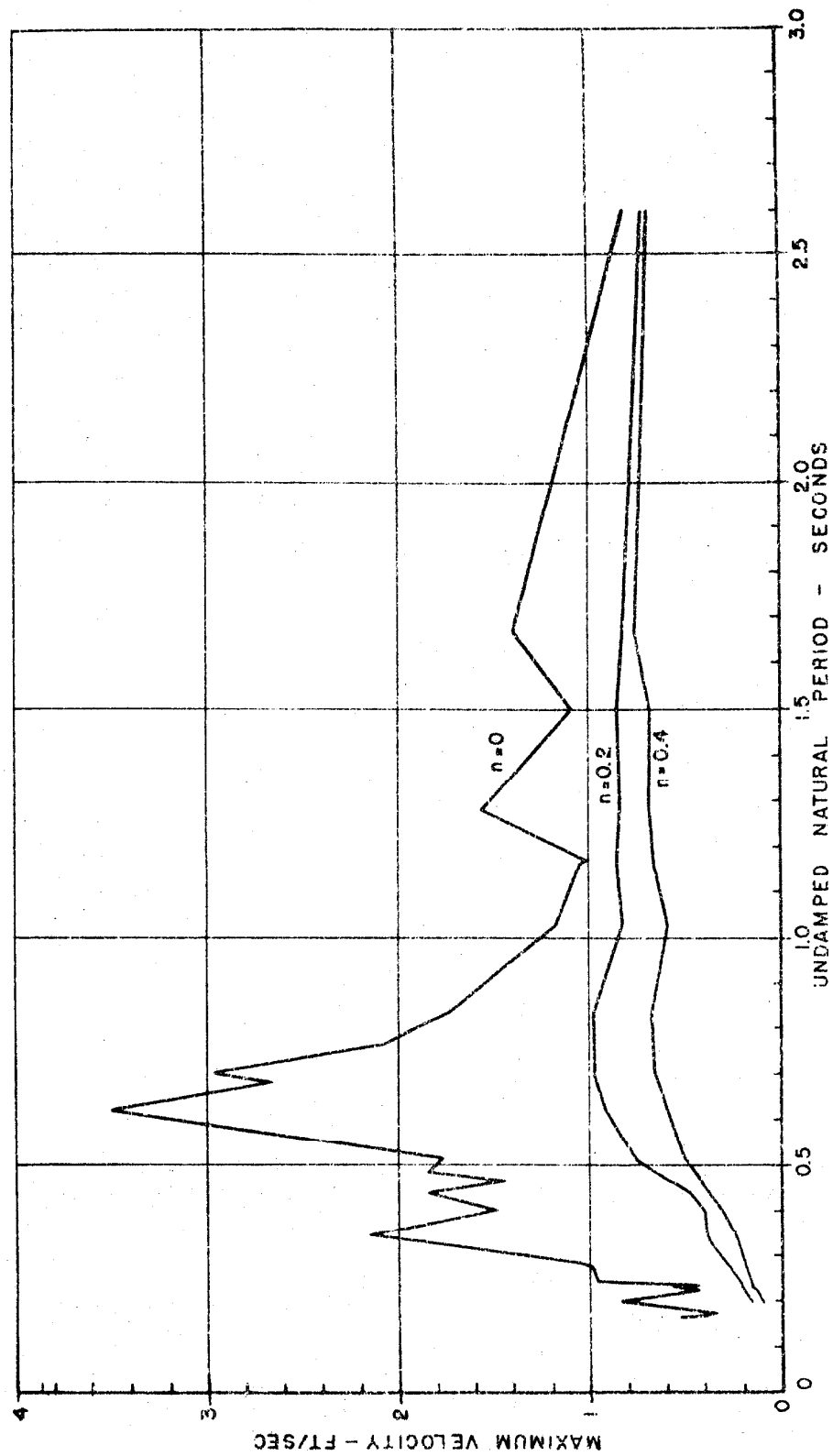


Figure 44. Velocity spectrum for Santa Barbara, California; earthquake of June 30, 1941. Component S 45 E.

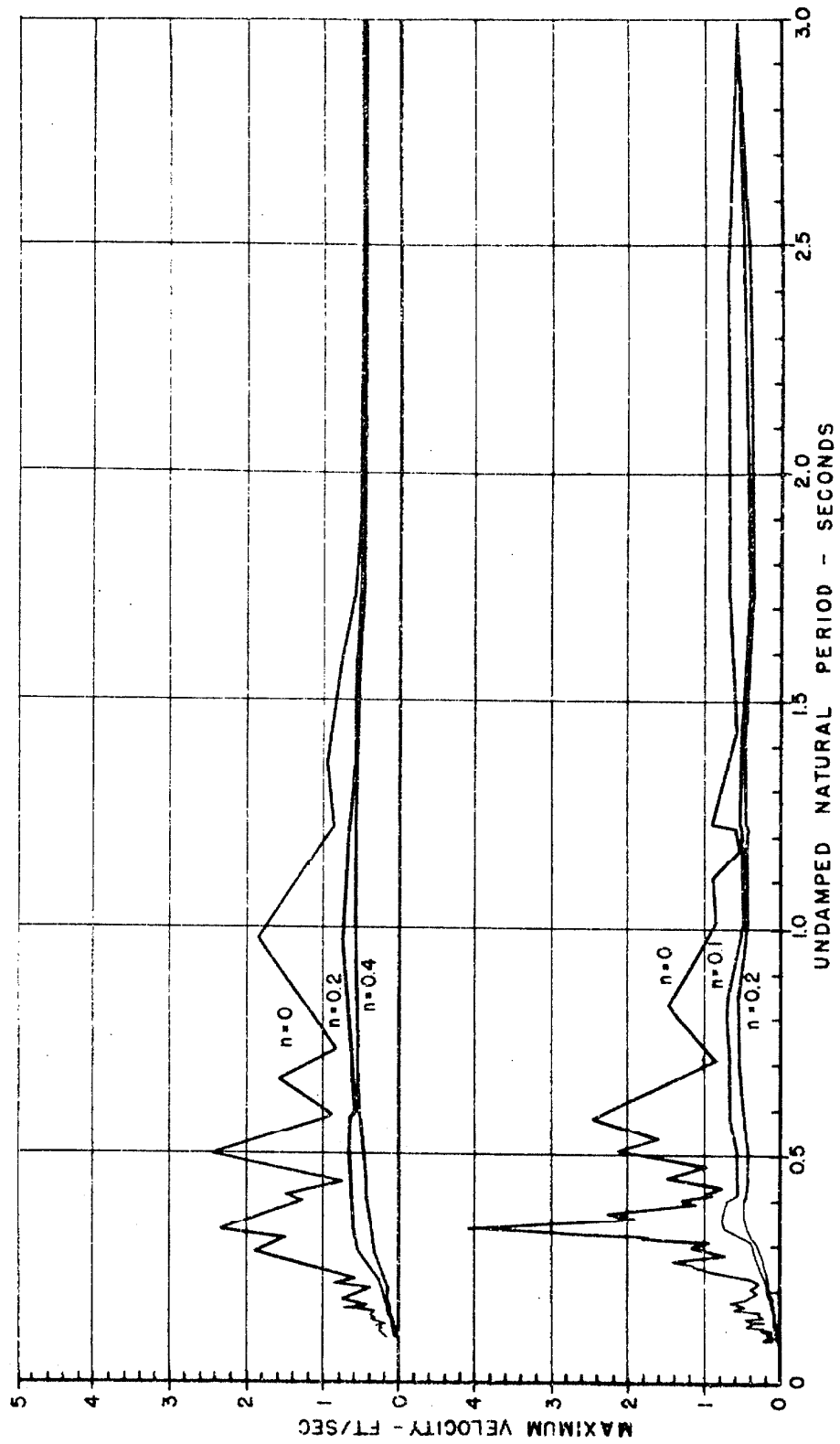


Figure 45. Velocity spectra for Hollister, California; earthquake of March 9, 1949. Components: S01 W (lower), N89 W (upper).

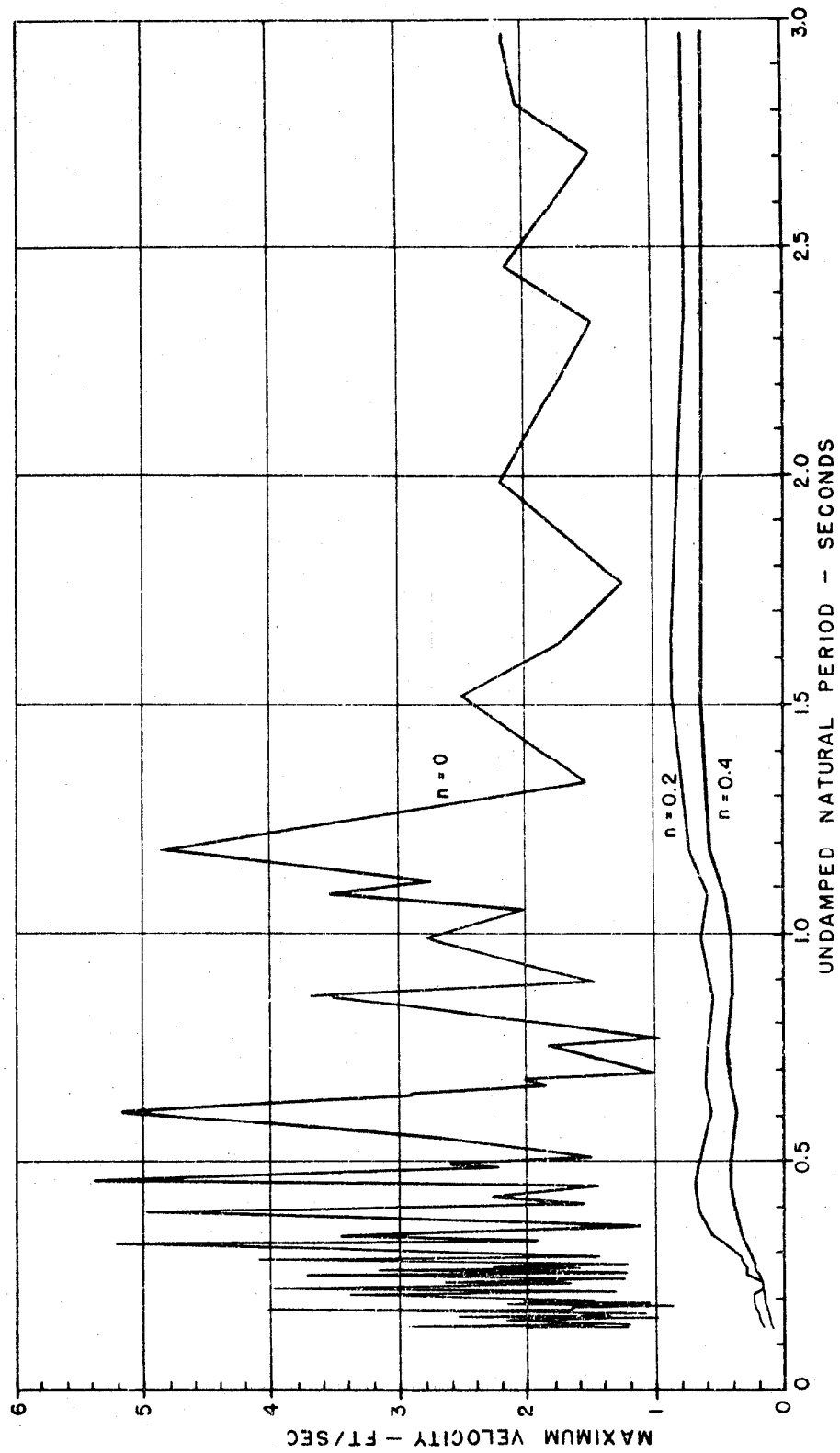


Figure 46. Velocity spectrum for Olympia, Washington; earthquake of April 13, 1949. Component S 10 E.

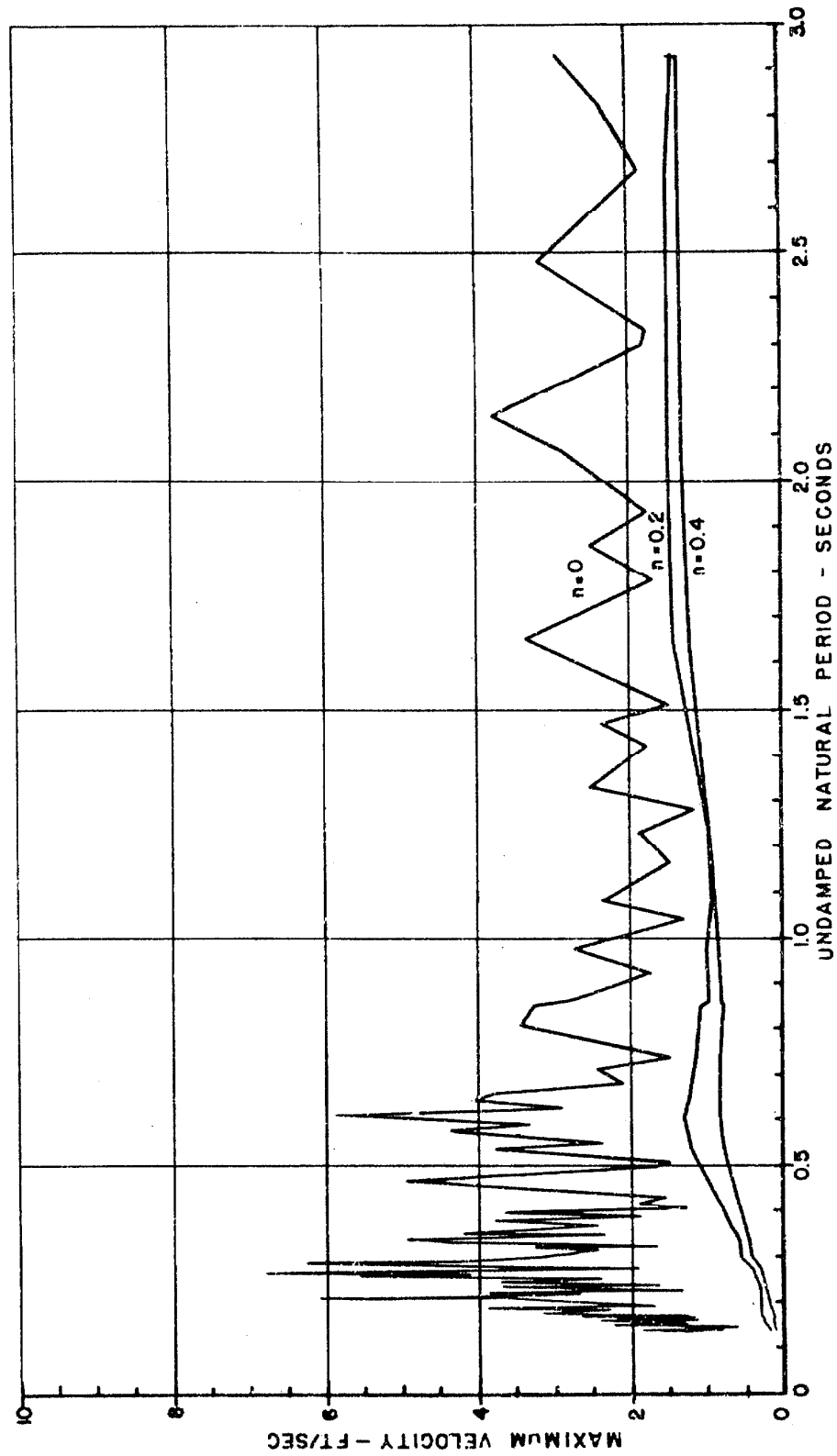


Figure 47. Velocity spectrum for Olympia, Washington; earthquake of April 13, 1949. Component S 80 W.

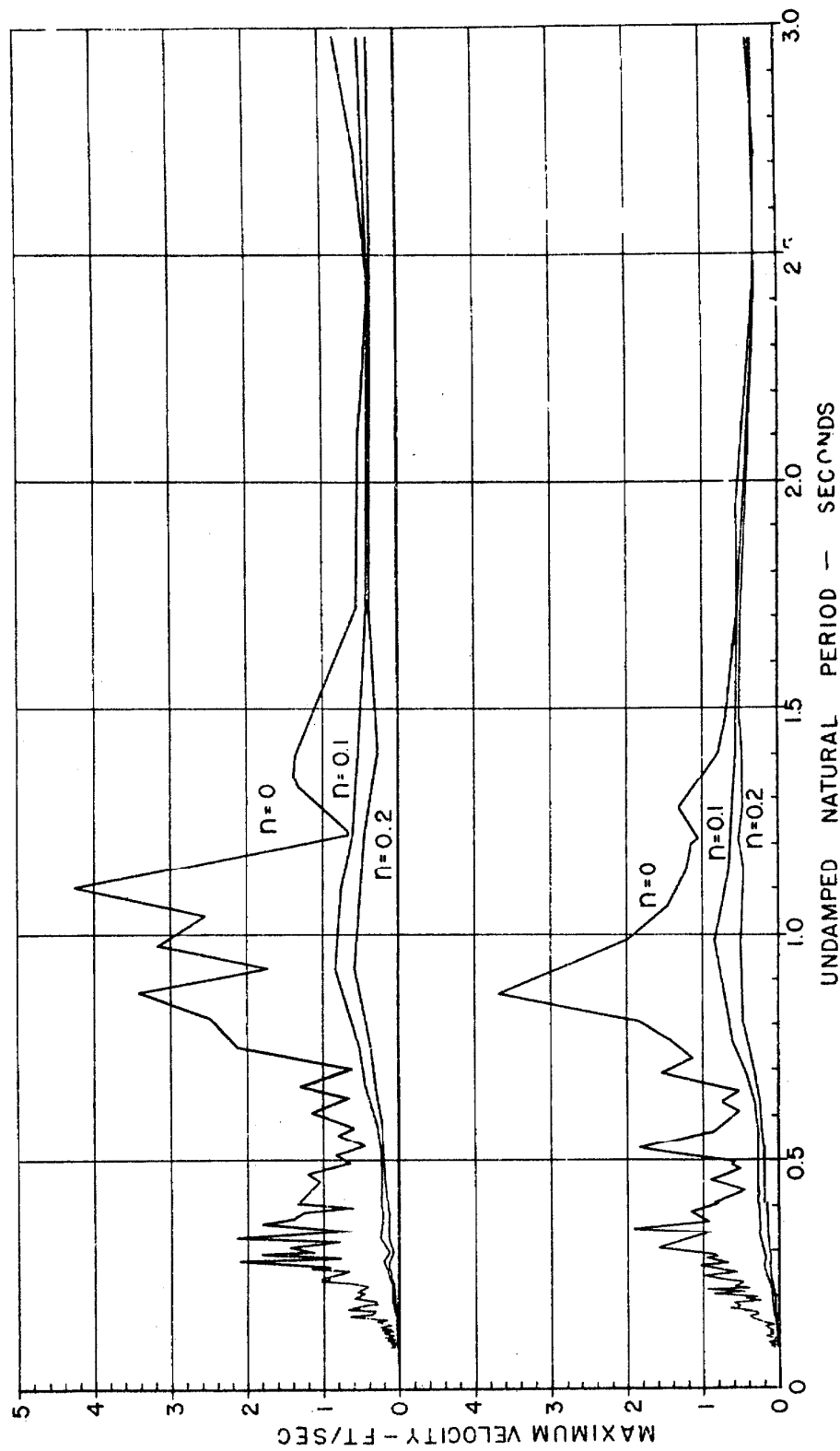


Figure 48. Velocity spectra for Seattle, Washington; earthquake of April 13, 1949. Components: N 88 W (upper), S 02 W (lower).

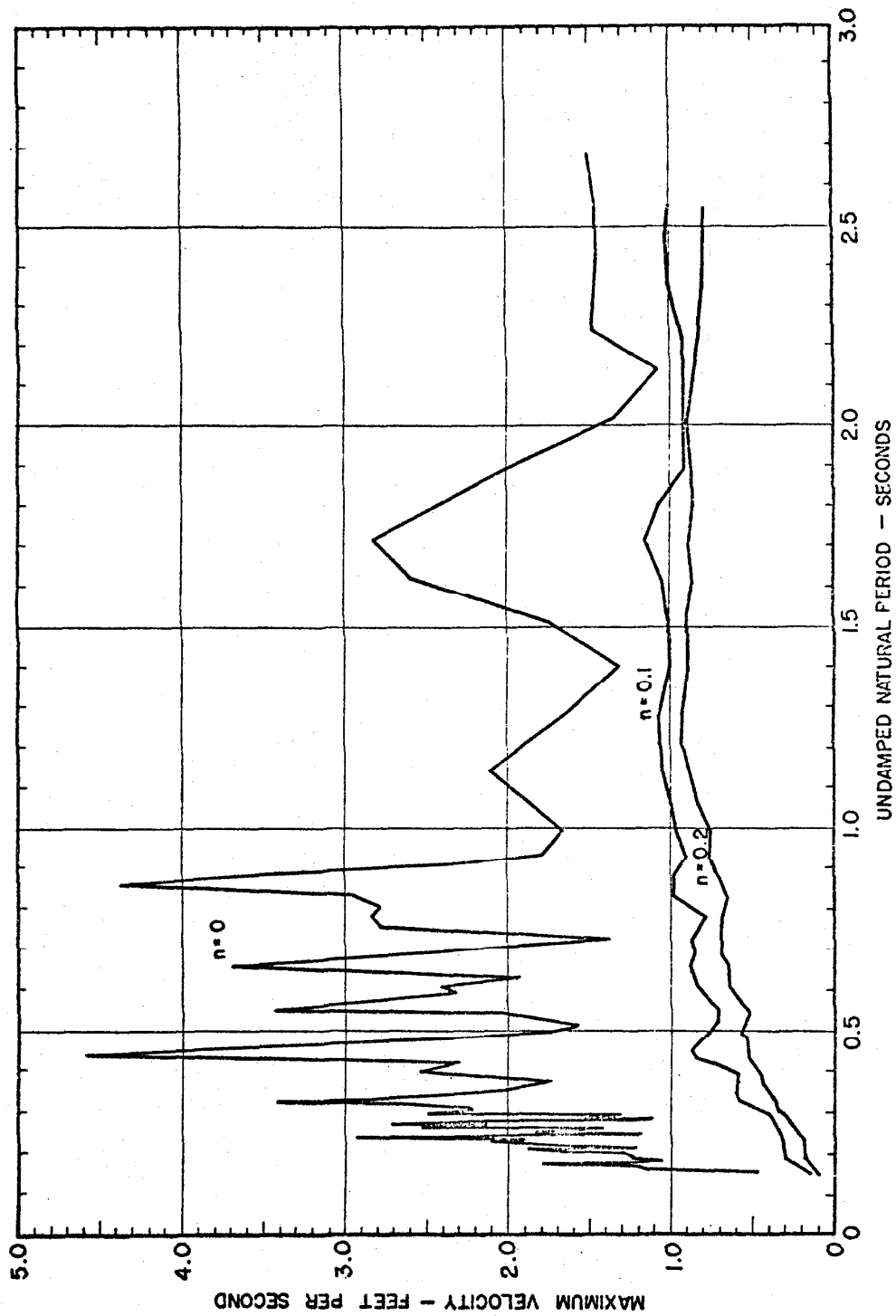


Figure 48a. Velocity spectra for Taft, California; earthquake of July 21, 1952. Component S69E.

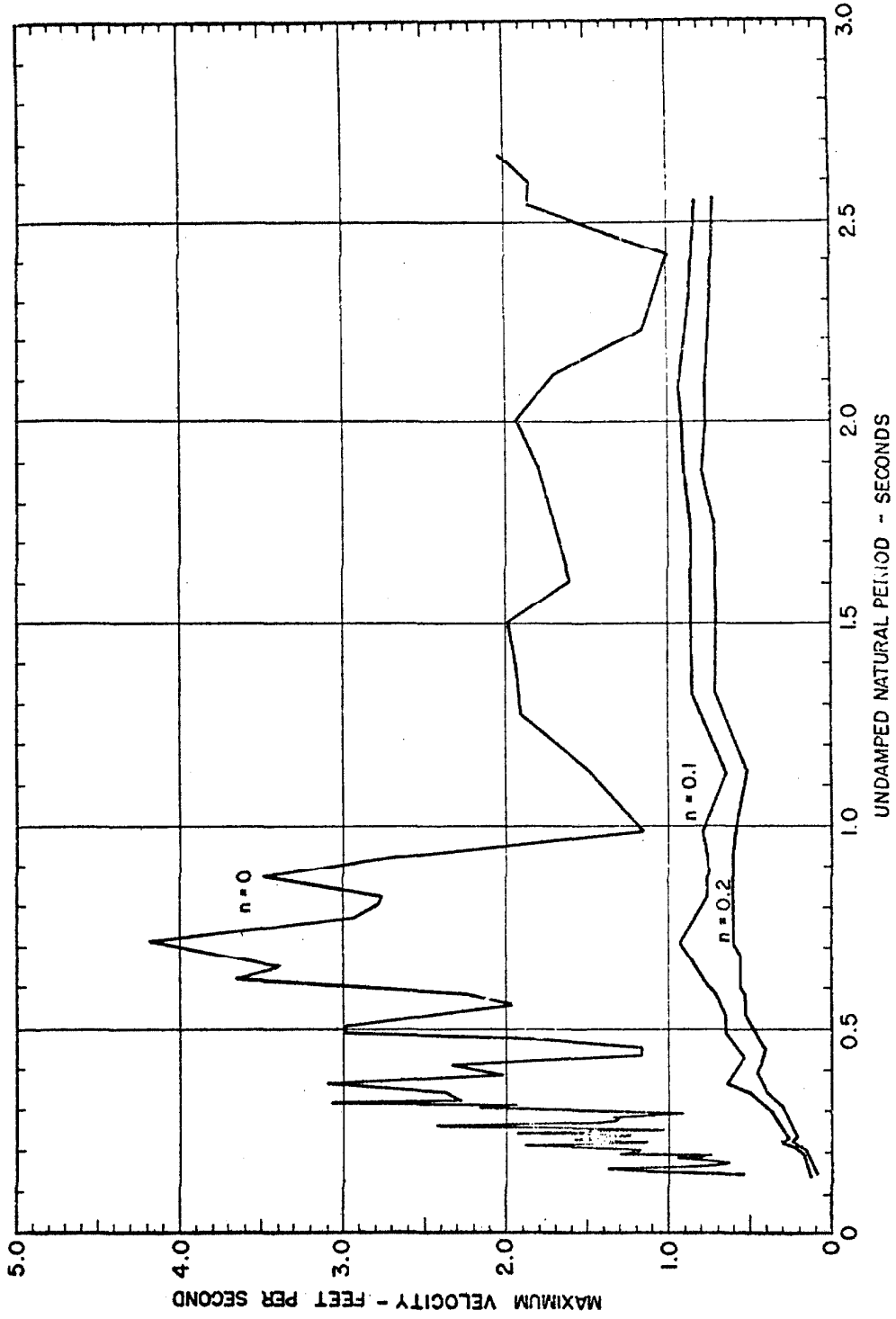
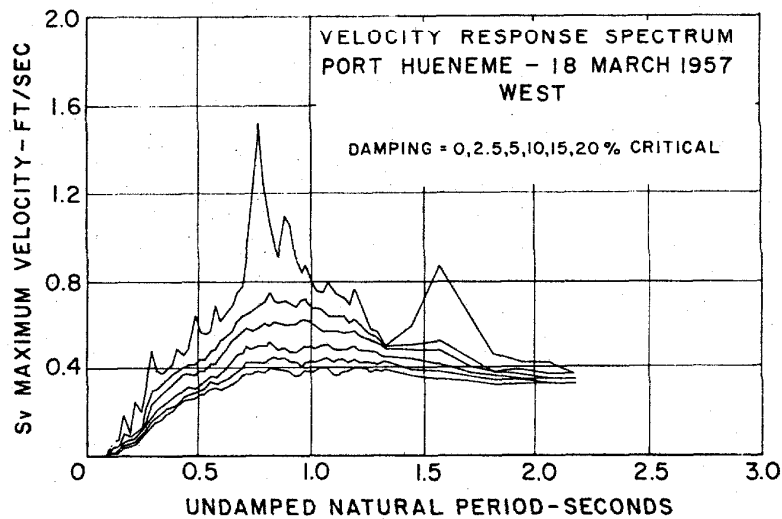
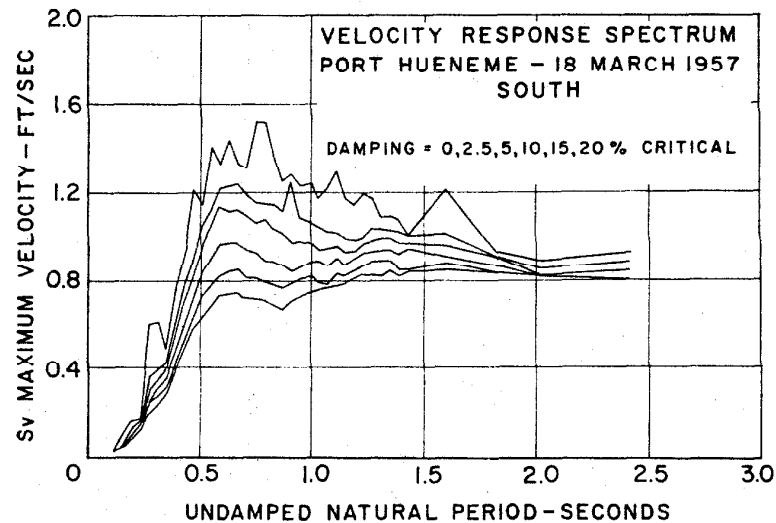


Figure 48b. Velocity spectra for Taft, California. earthquake of July 21, 1952. Component N 21 E.

67c.



East-west component. Maximum relative velocity response spectrum.



North-south component. Maximum relative velocity response spectrum.

Figure 48c.

(See "The Port Hueneme Earthquake of March 18, 1957," by G. W. Housner and D. E. Hudson, Bull. Seismo. Soc. of Amer., Vol. 48, pp. 163-168, April 1958).

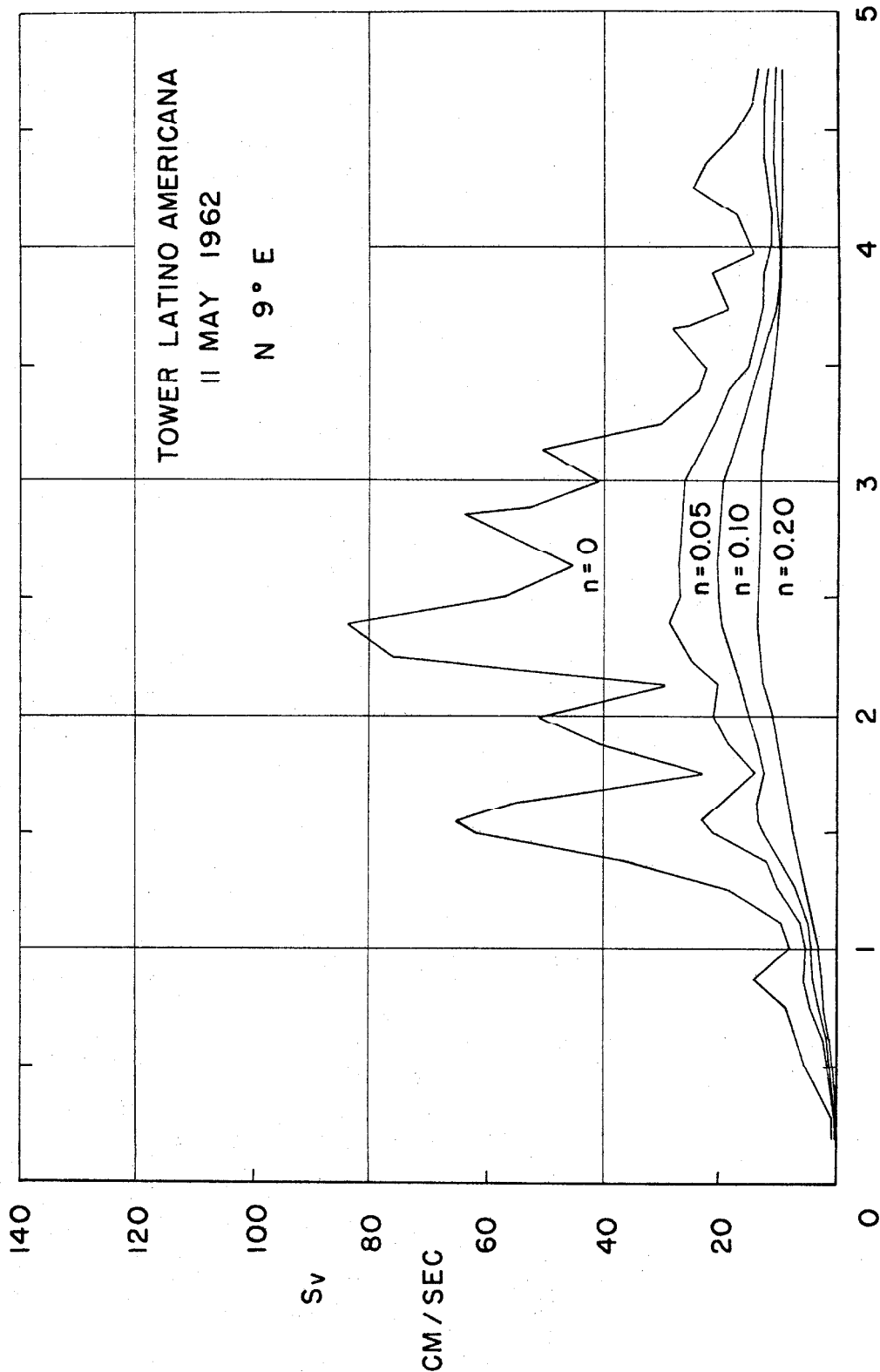


Figure 48d. Mexico City velocity spectrum for the Tower Latino Americana 11 May 1962 N9E Component. (See "Mexican Earthquakes of 11 May and 19 May 1962," by P. C. Jennings, Earthquake Engineering Research Laboratory, C.I.T.T.)

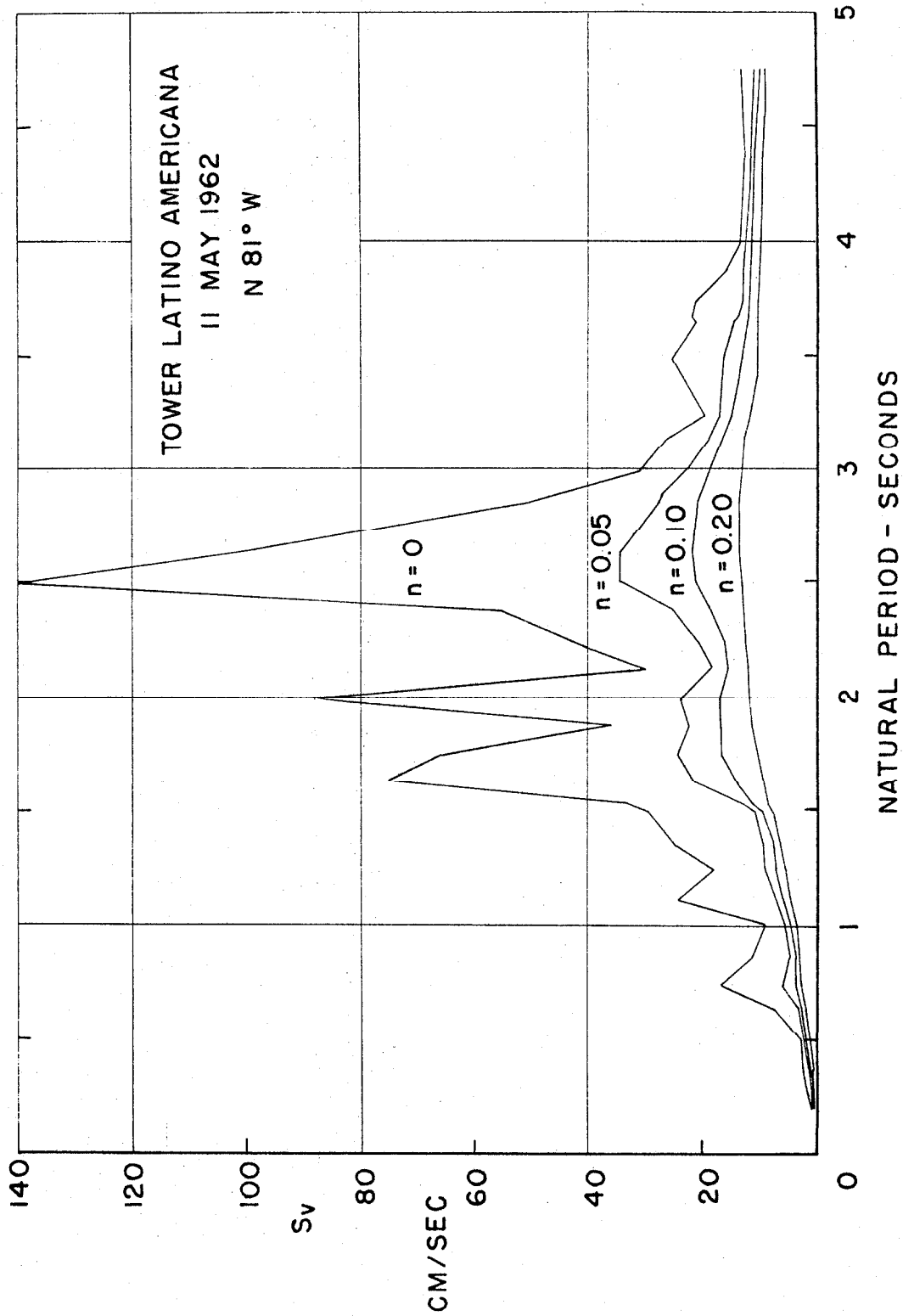


Figure 48e. Mexico City velocity spectrum for the Tower Latino Americana 11 May 1962 N81W Component. (See "Mexican Earthquakes of 11 May and 19 May 1962," by P. C. Jennings, Earthquake Engineering Research Laboratory, C.I.T.)

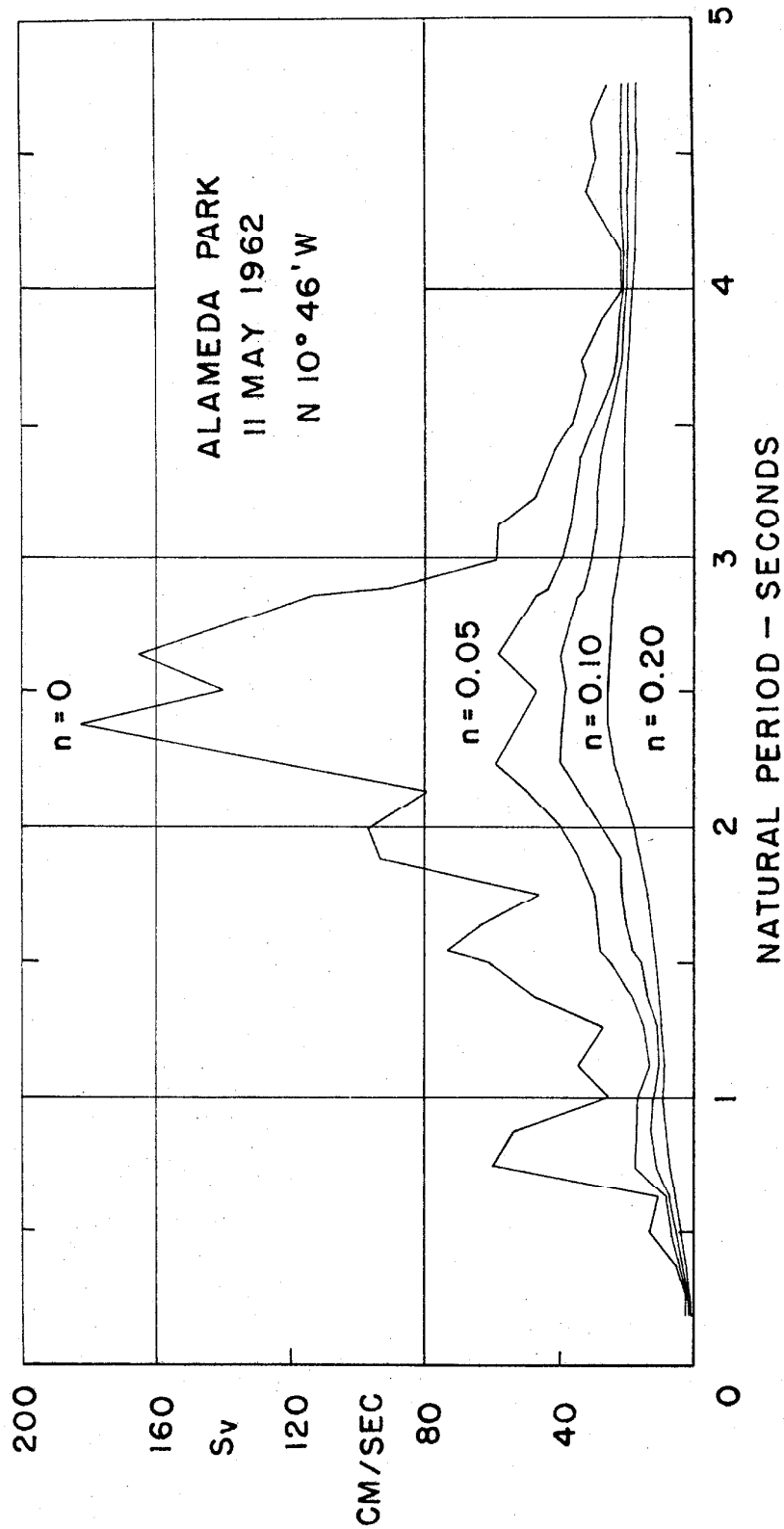


Figure 48f. Mexico City velocity spectrum for the Alameda Park 11 May 1962 N 10°46' W Component. (See "Mexican Earthquakes of 11 May and 19 May 1962," by P. C. Jennings, Earthquake Engineering Research Laboratory, C.I.T.)

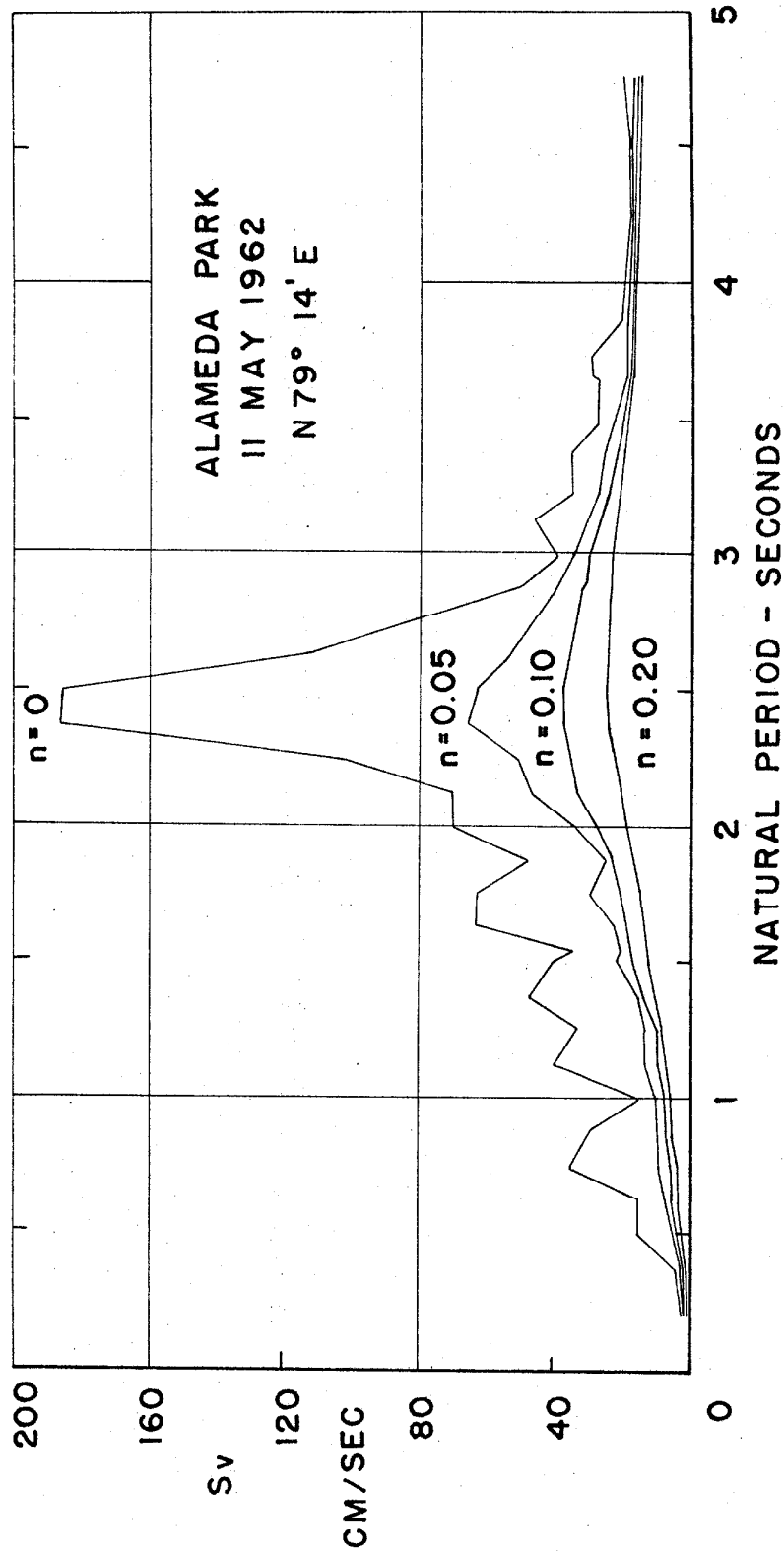


Figure 48g. Mexico City velocity spectrum for the Alameda Park 11 May 1962 N 79°14' E Component. (See "Mexican Earthquakes of 11 May and 19 May 1962," by P. C. Jennings, Earthquake Engineering Research Laboratory, C.I.T.)

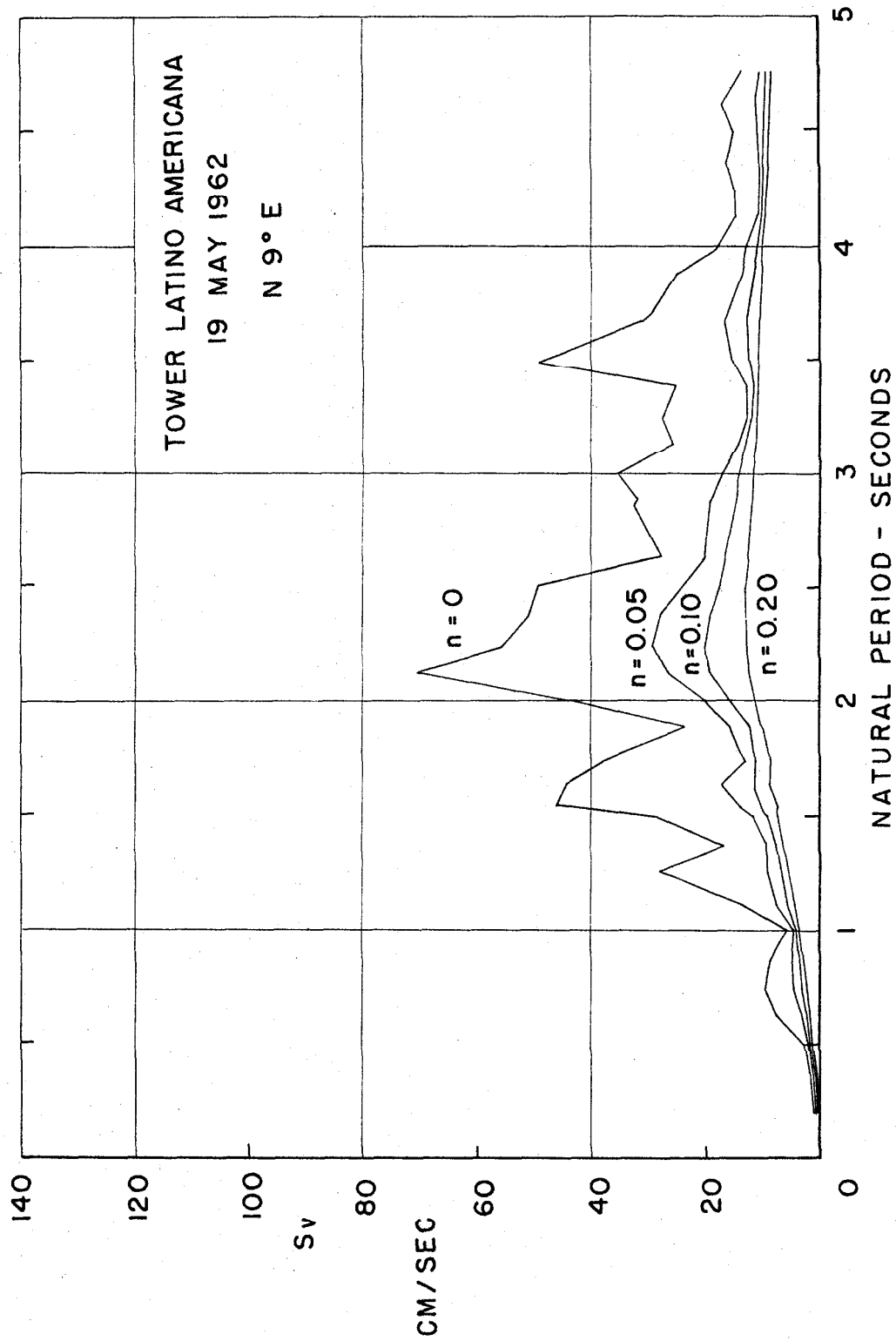


Figure 48h. Mexico City velocity spectrum for the Tower Latino Americana 19 May 1962 N 9° E Component. (See "Mexican Earthquakes of 11 May and 19 May 1962," by P. C. Jennings, Earthquake Engineering Research Laboratory, C.I.T.T.)

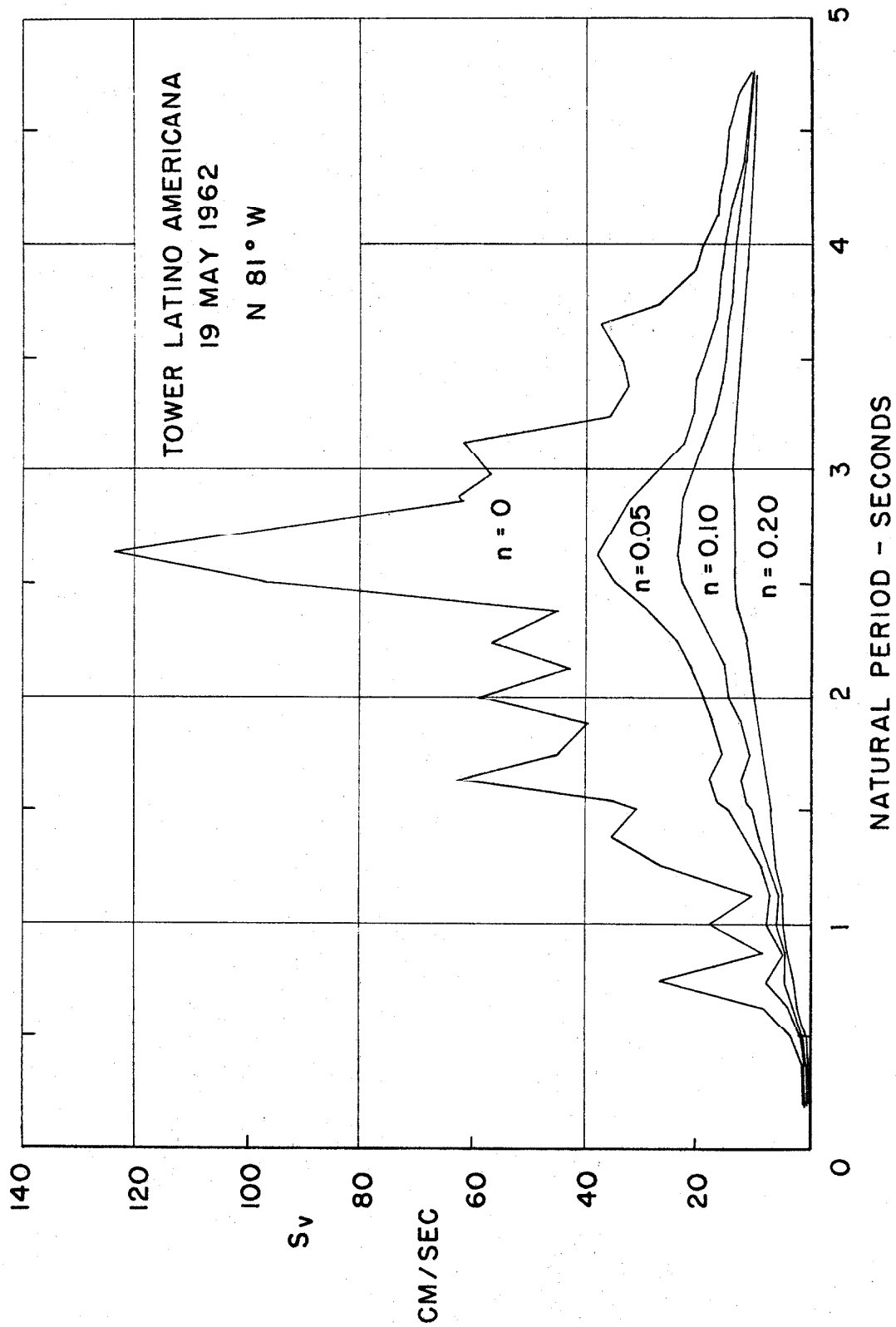


Figure 48i. Mexico City velocity spectrum for the Tower Latino Americana 19 May 1962 N81W Component. (See "Mexican Earthquakes of 11 May and 19 May 1962," by P. C. Jennings, Earthquake Engineering Research Laboratory, C.I.T.T.)

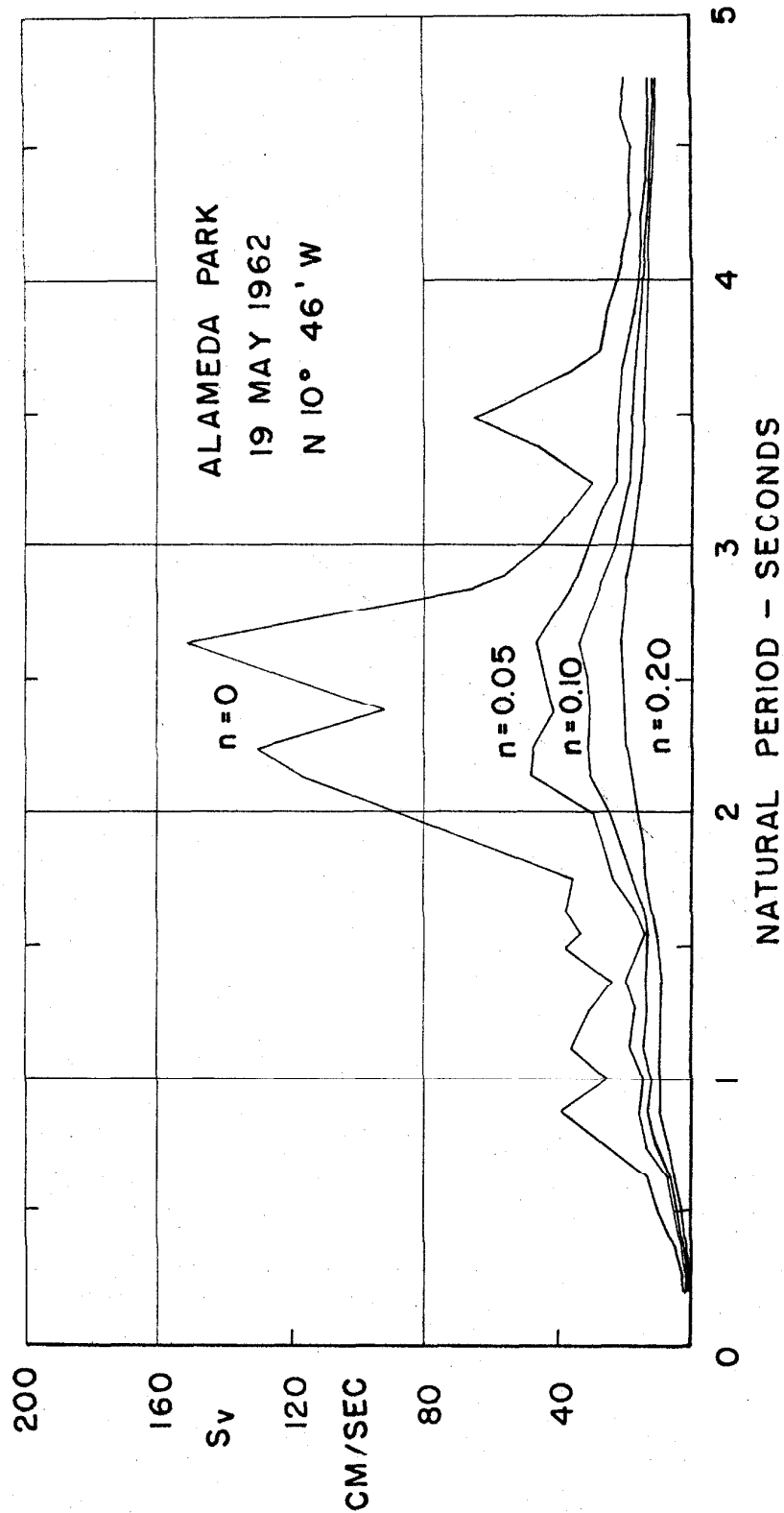


Figure 48j. Mexico City velocity spectrum for the Alameda Park 19 May 1962 N 10°46' W Component. (See "Mexican Earthquakes of 11 May and 19 May 1962," by P. C. Jennings, Earthquake Engineering Research Laboratory, C.I.T.)

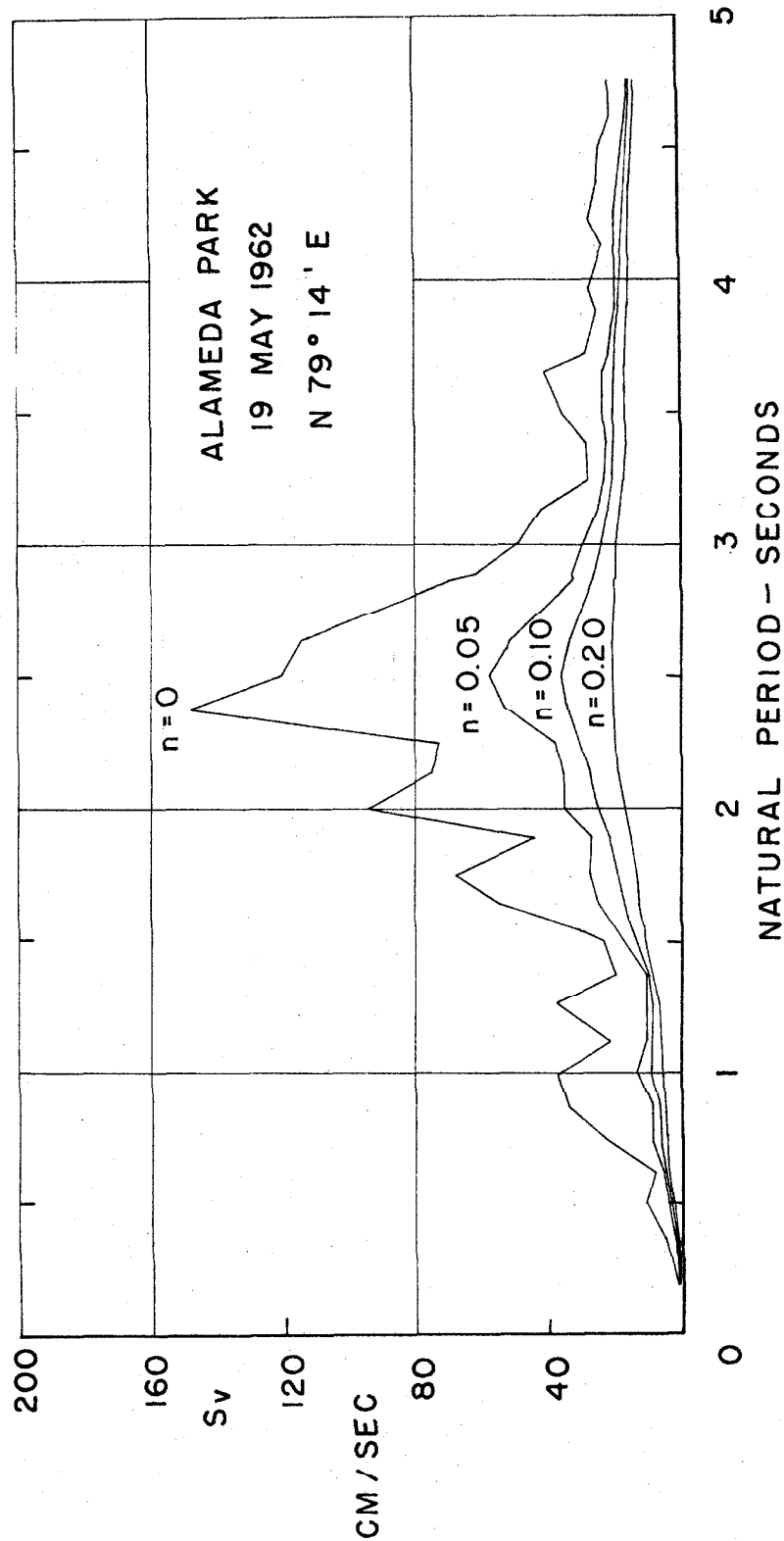


Figure 48k. Mexico City velocity spectrum for the Alameda Park 19 May 1962 N 79°14' E Component. (See "Mexican Earthquakes of 11 May and 19 May 1962," by P. C. Jennings, Earthquake Engineering Research Laboratory, C.I.T.)

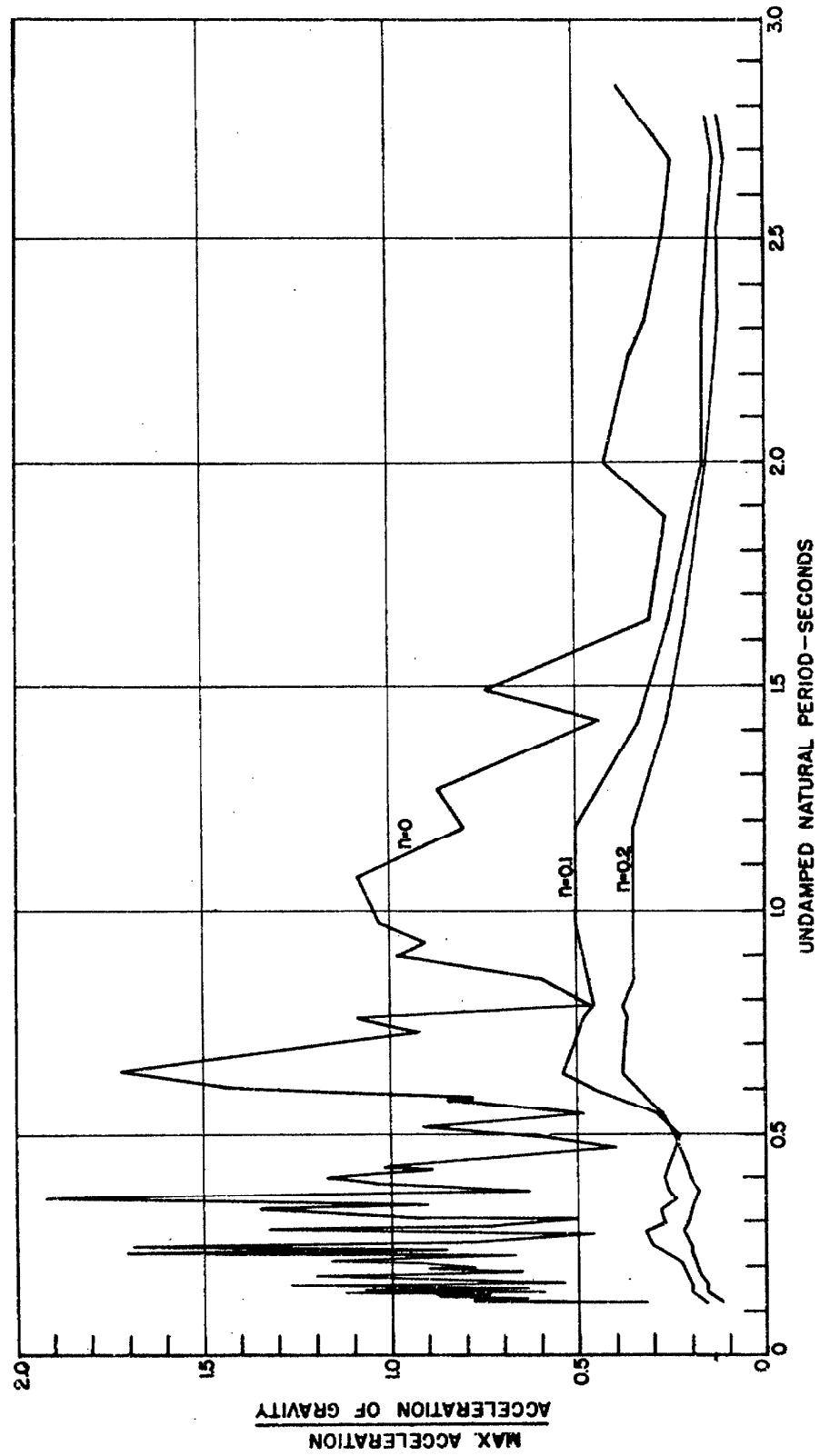


Figure 49. Acceleration spectrum for Vernon, California; earthquake of March 10, 1933. Component N08E.

Ordinates should be multiplied by 0.525

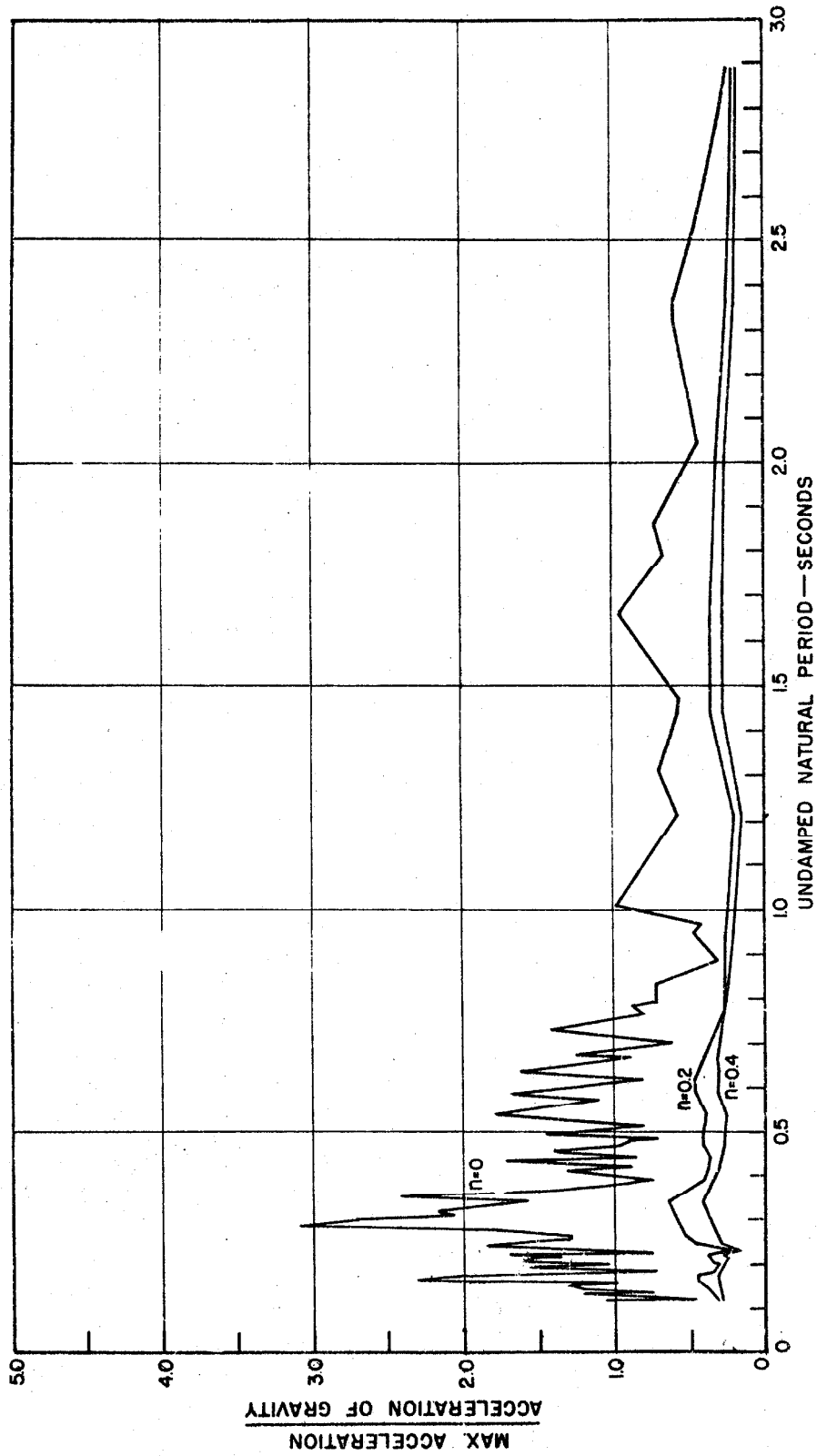


Figure 50. Acceleration spectrum for Vernon, California; earthquake of March 10, 1933. Component S82E.

Ordinates should be multiplied by 0.472

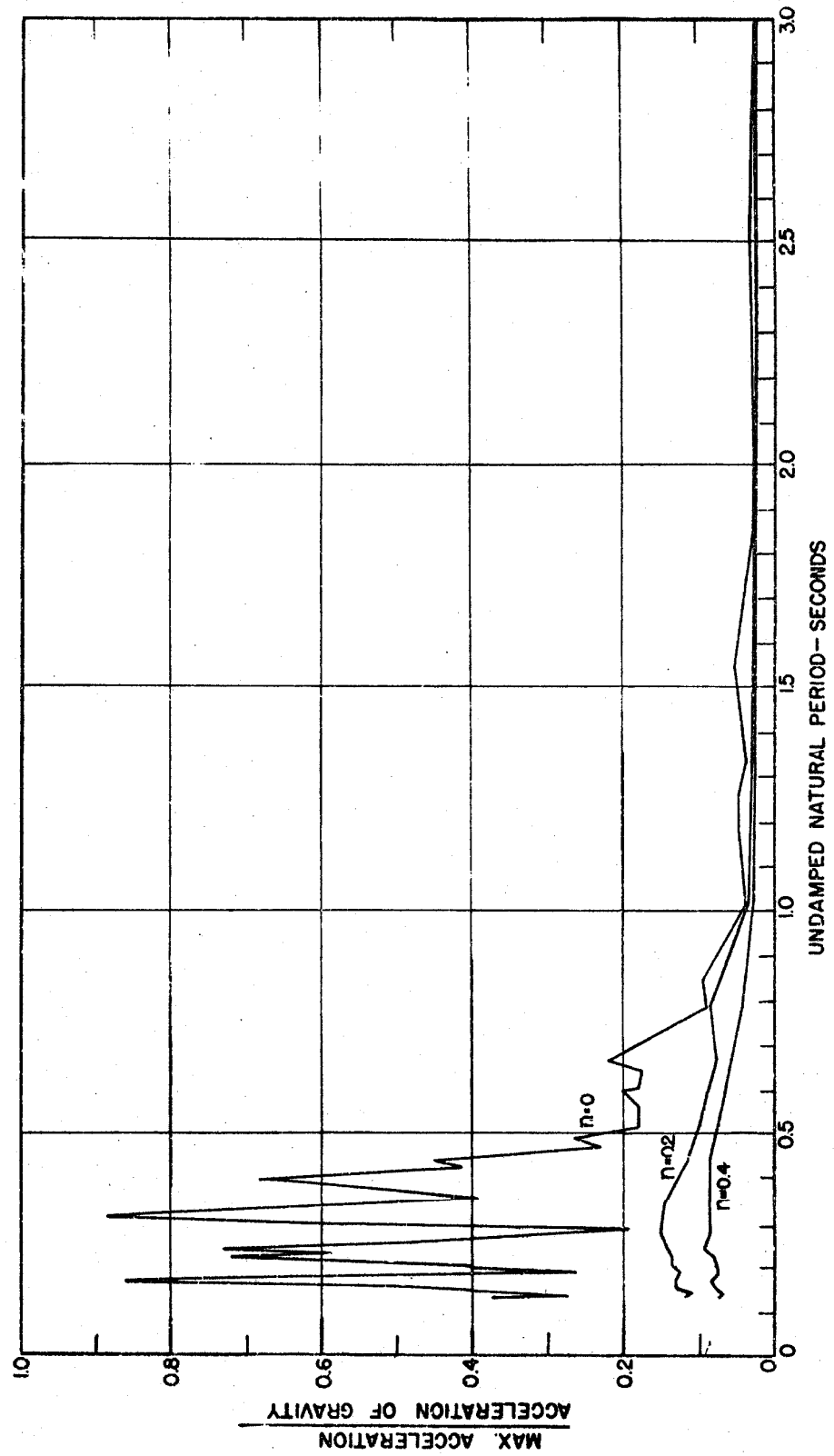


Figure 51. Acceleration spectrum for Vernon, California; earthquake of Oct. 2, 1933. Component N08E.

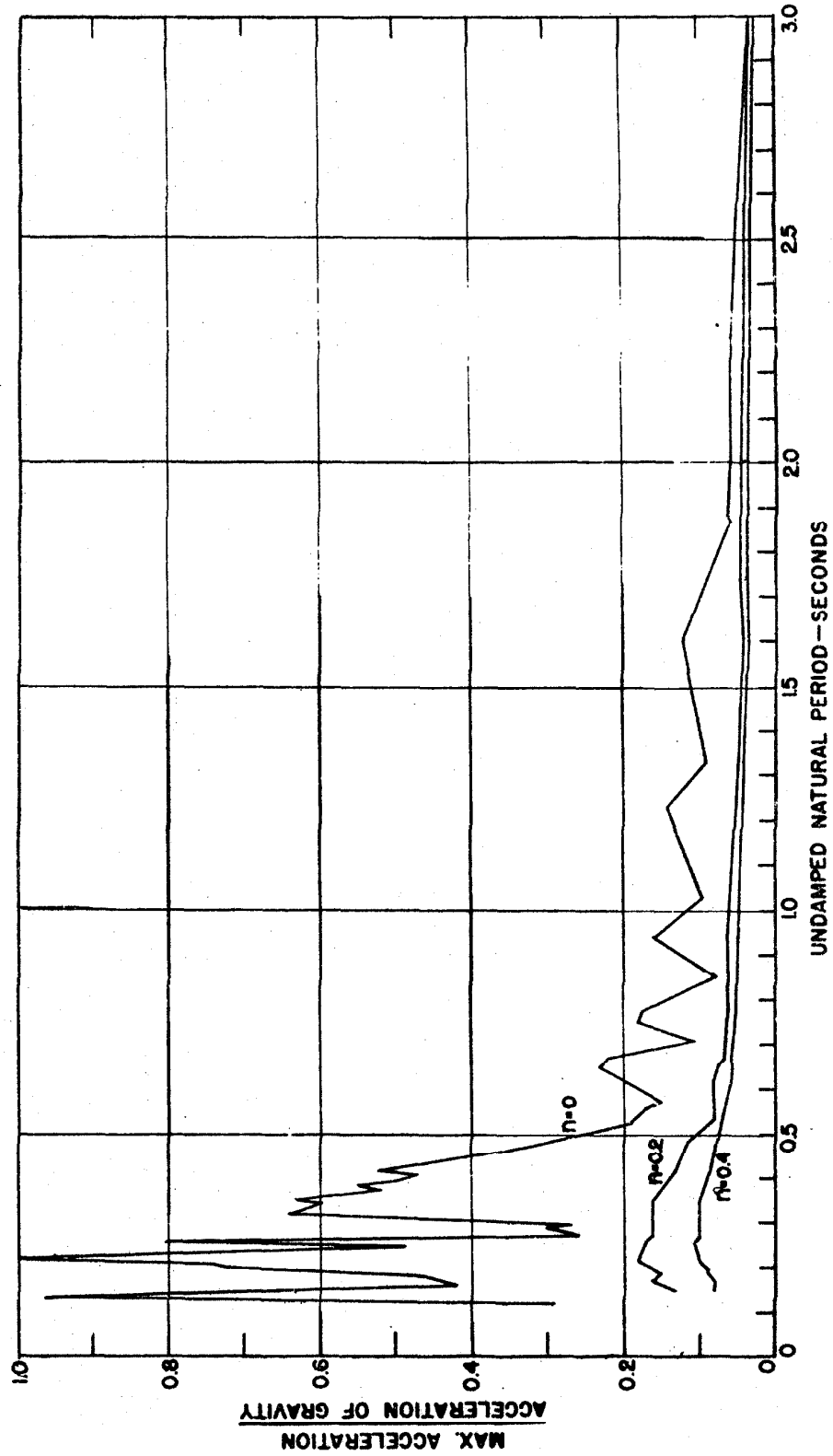


Figure 52. Acceleration spectrum for Vernon, California; earthquake of Oct. 2, 1933. Component S82E.

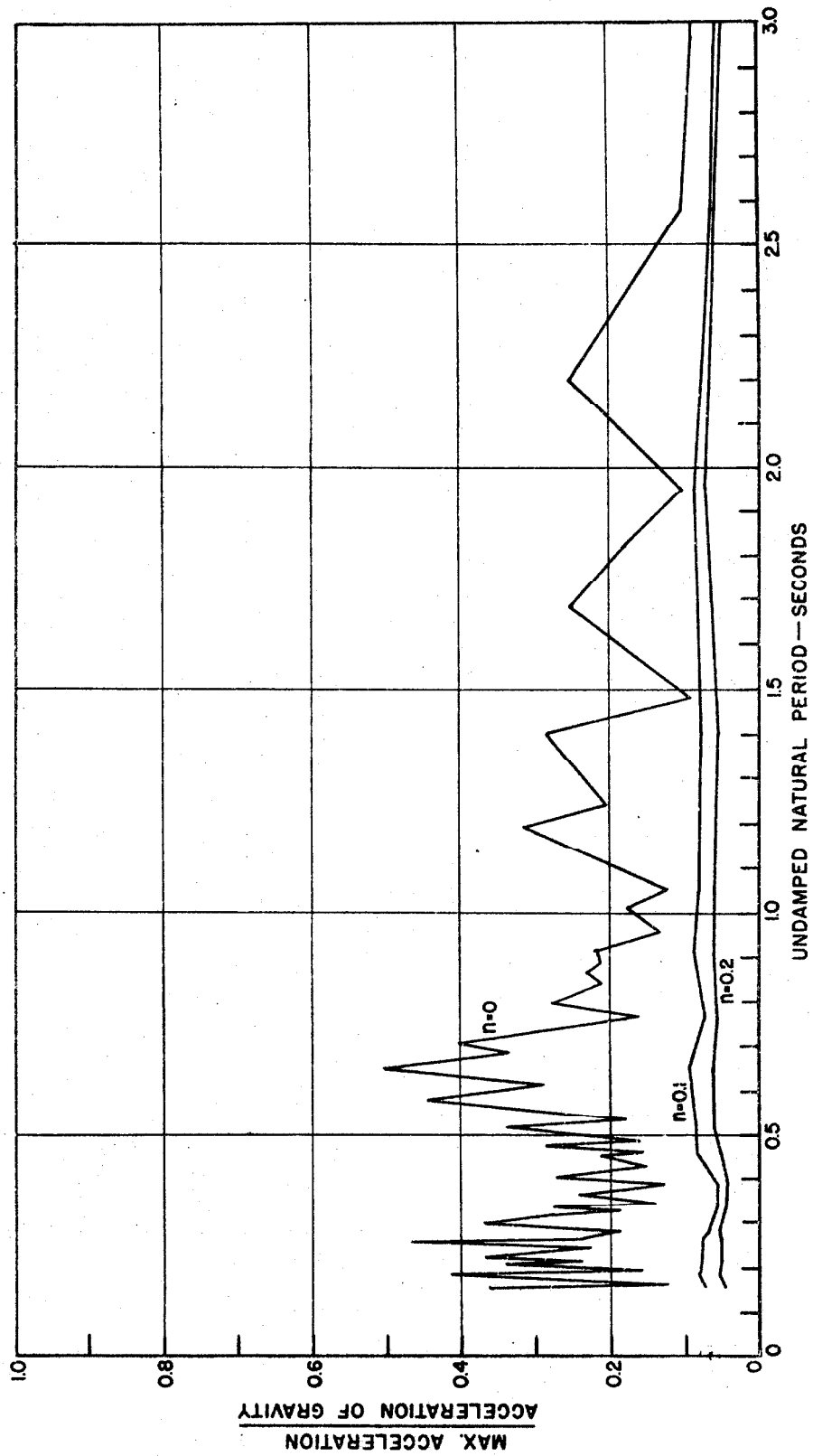


Figure 53. Acceleration spectrum for Los Angeles Subway Terminal; earthquake of March 10, 1933. Component N39E.

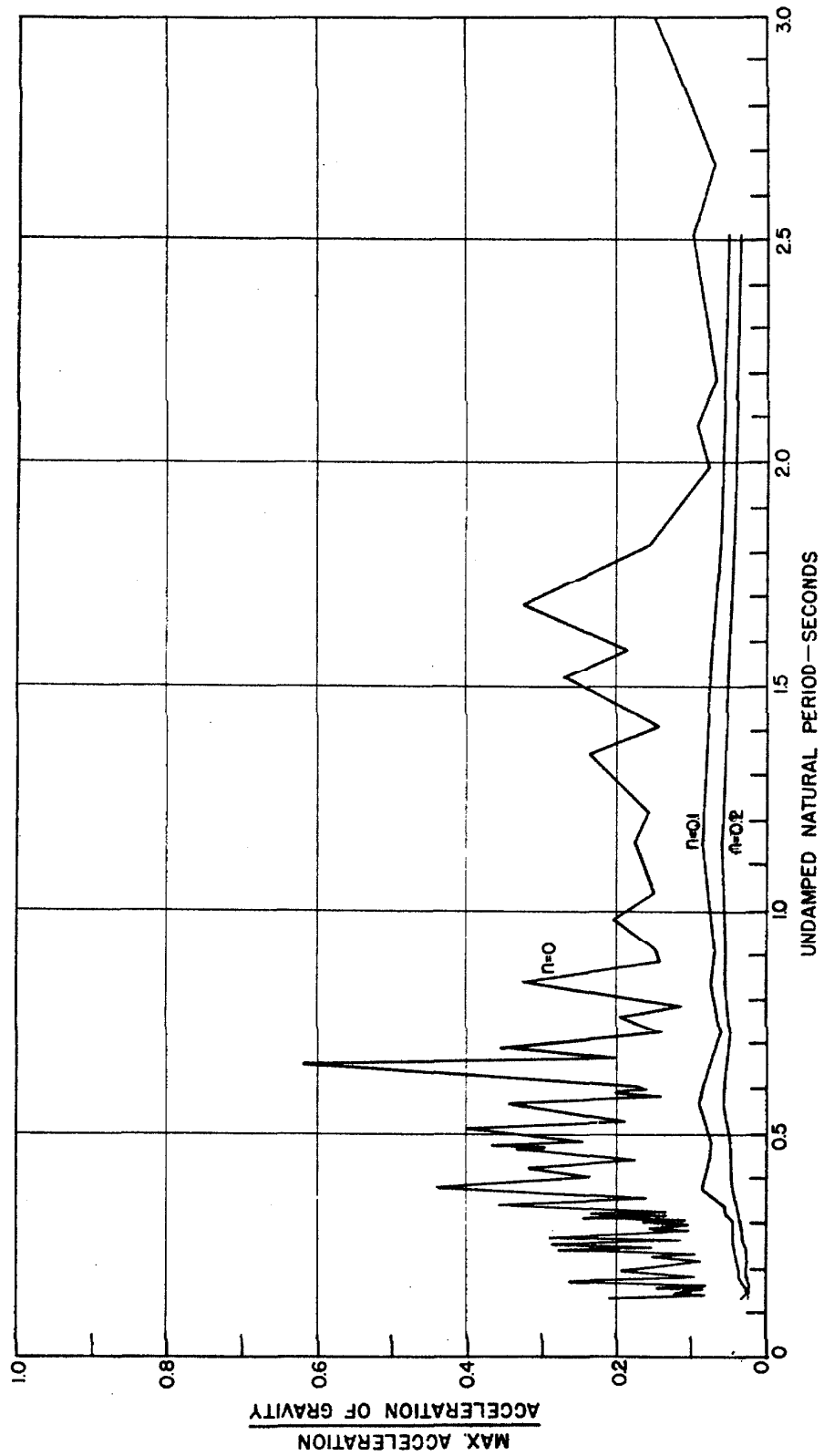


Figure 54. Acceleration spectrum for Los Angeles Subway Terminal; earthquake of March 10, 1933. Component N 51 W.

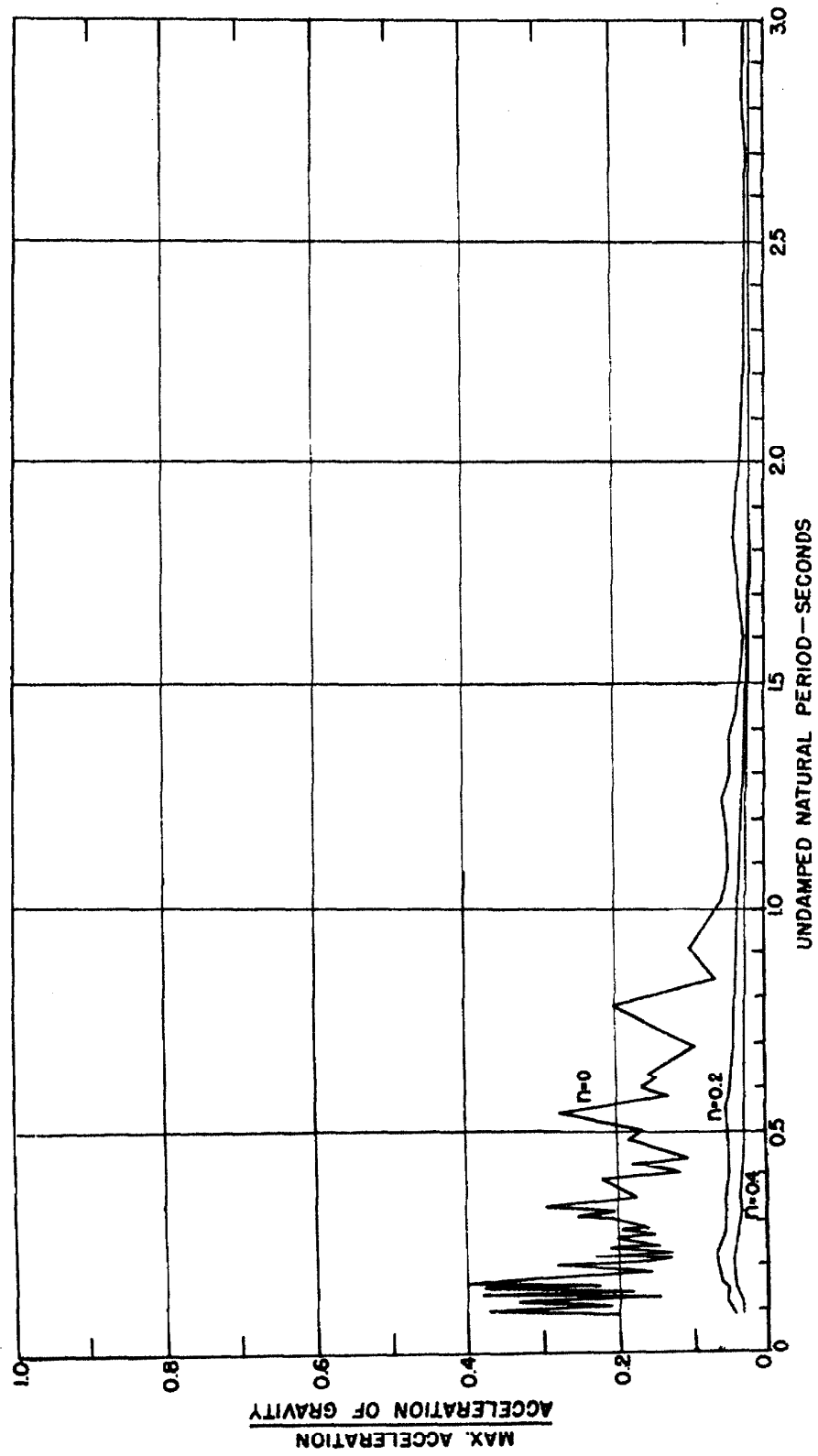


Figure 55. Acceleration spectrum for Los Angeles Subway Terminal; earthquake of Oct. 2, 1933. Component N 39 E.

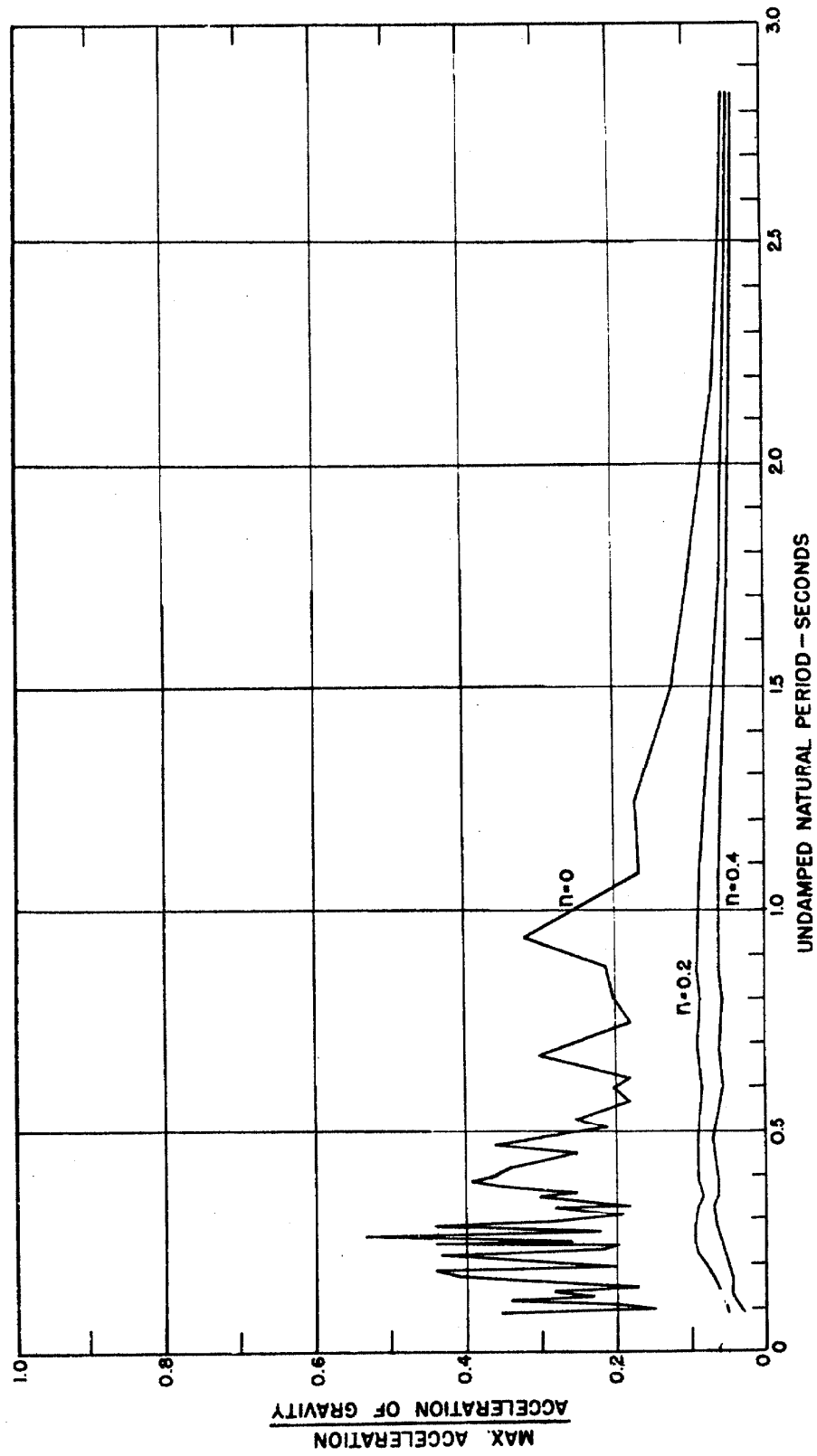


Figure 56. Acceleration spectrum for Los Angeles Subway Terminal; earthquake of Oct. 2, 1933. Component N 51 W.

Ordinates should be multiplied by 0.575

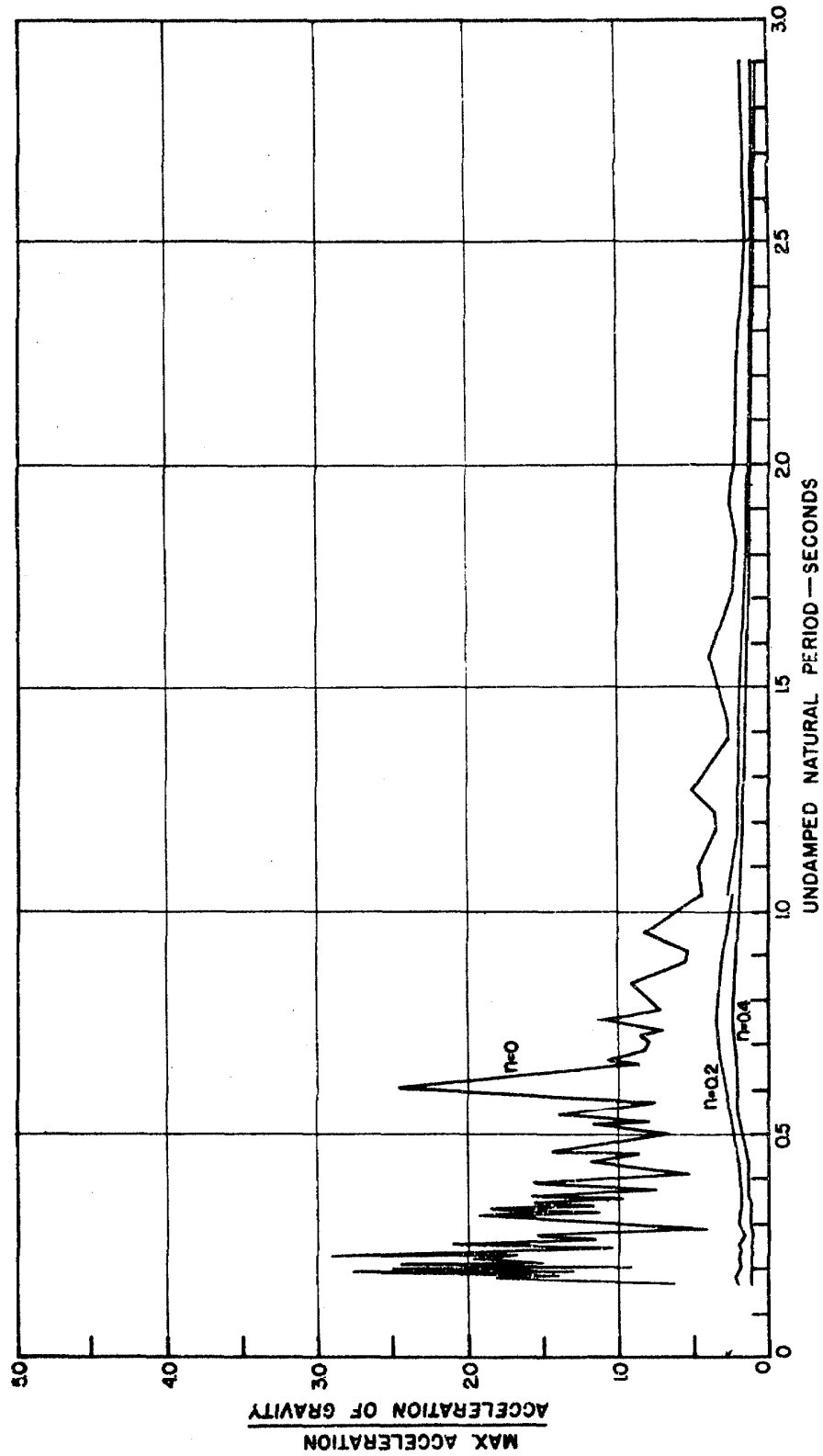


Figure 57. Acceleration spectrum for El Centro, California; earthquake of Dec. 30, 1934. Component N-S.

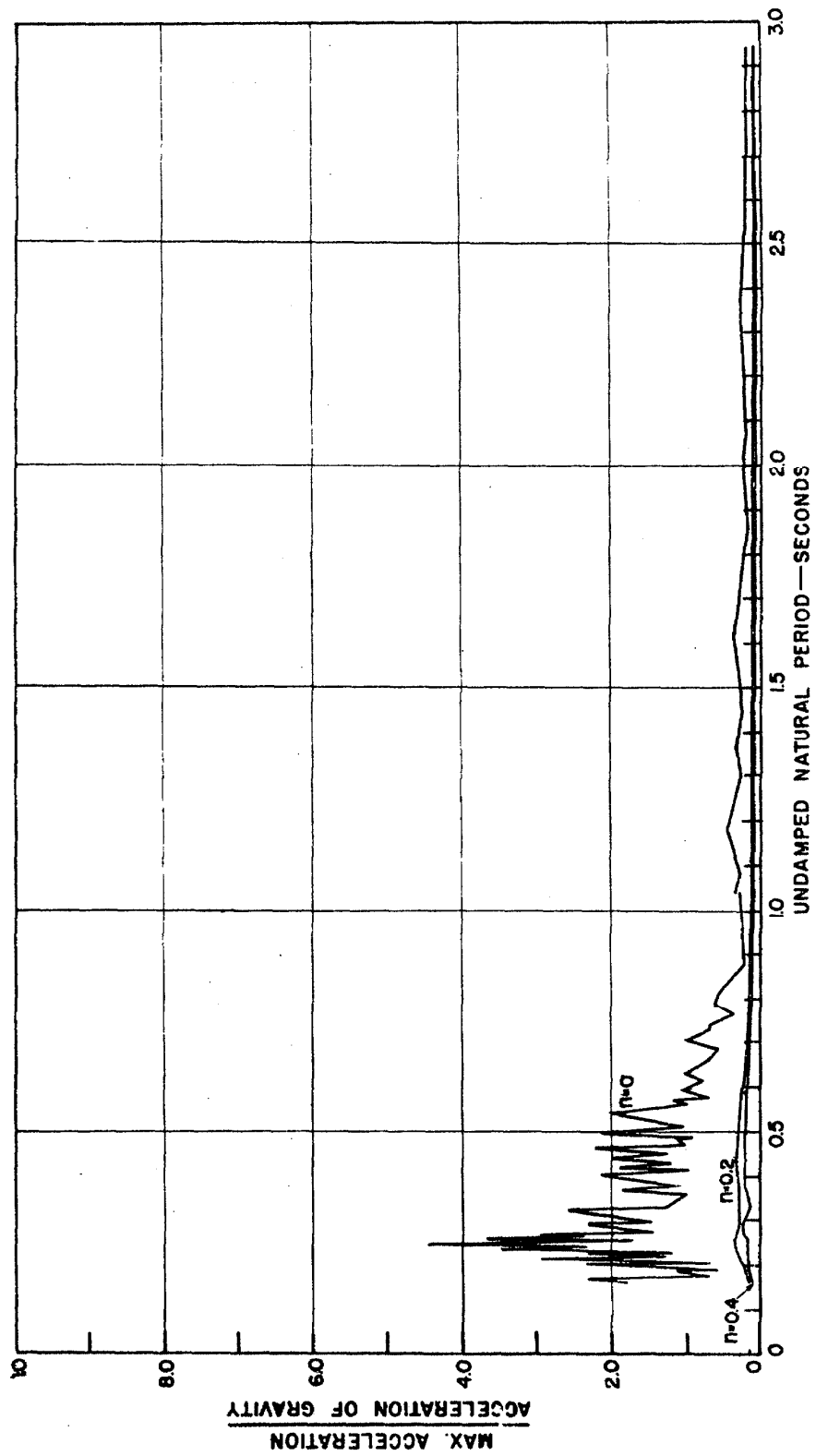


Figure 58. Acceleration spectrum for El Centro, California; earthquake of Dec. 30, 1934. Component E-W.



Figure 59. Acceleration spectrum for El Centro, California, earthquake of May 18, 1940. Component N-S.

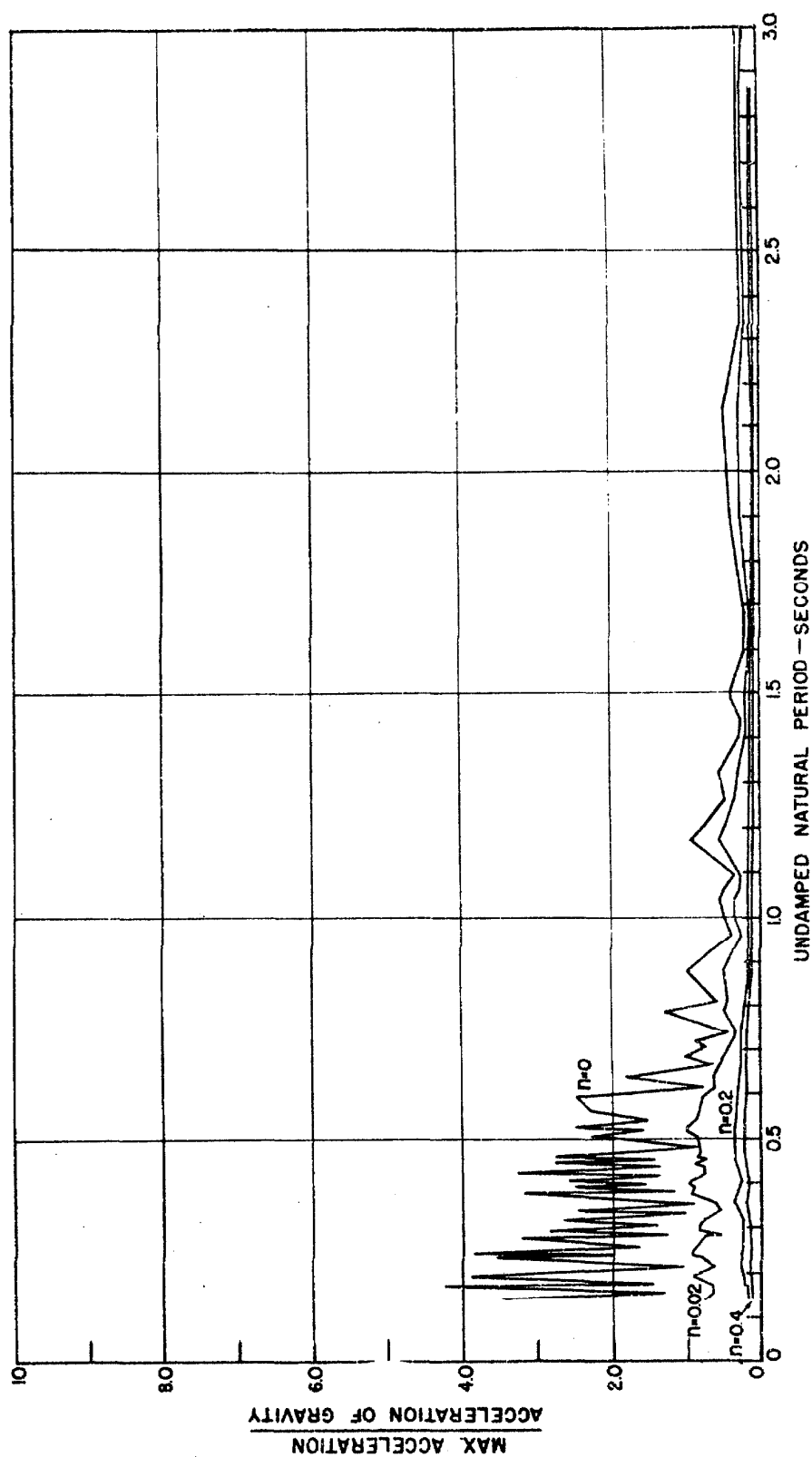


Figure 60. Acceleration spectrum for El Centro, California; earthquake of May 18, 1940. Component E-W.

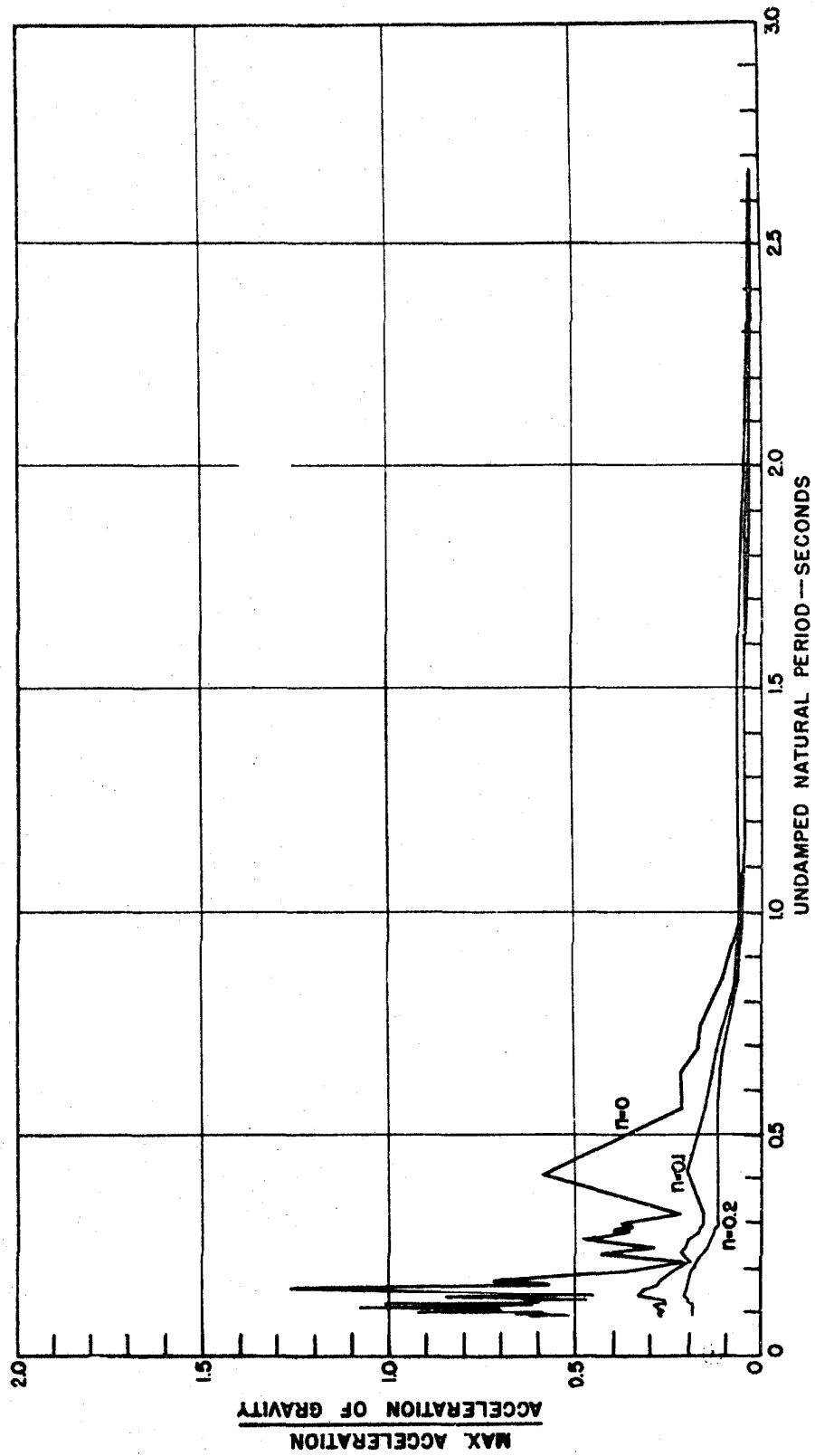


Figure 61. Acceleration spectrum for Helena, Montana; earthquake of Oct. 31, 1935. Component N-S.

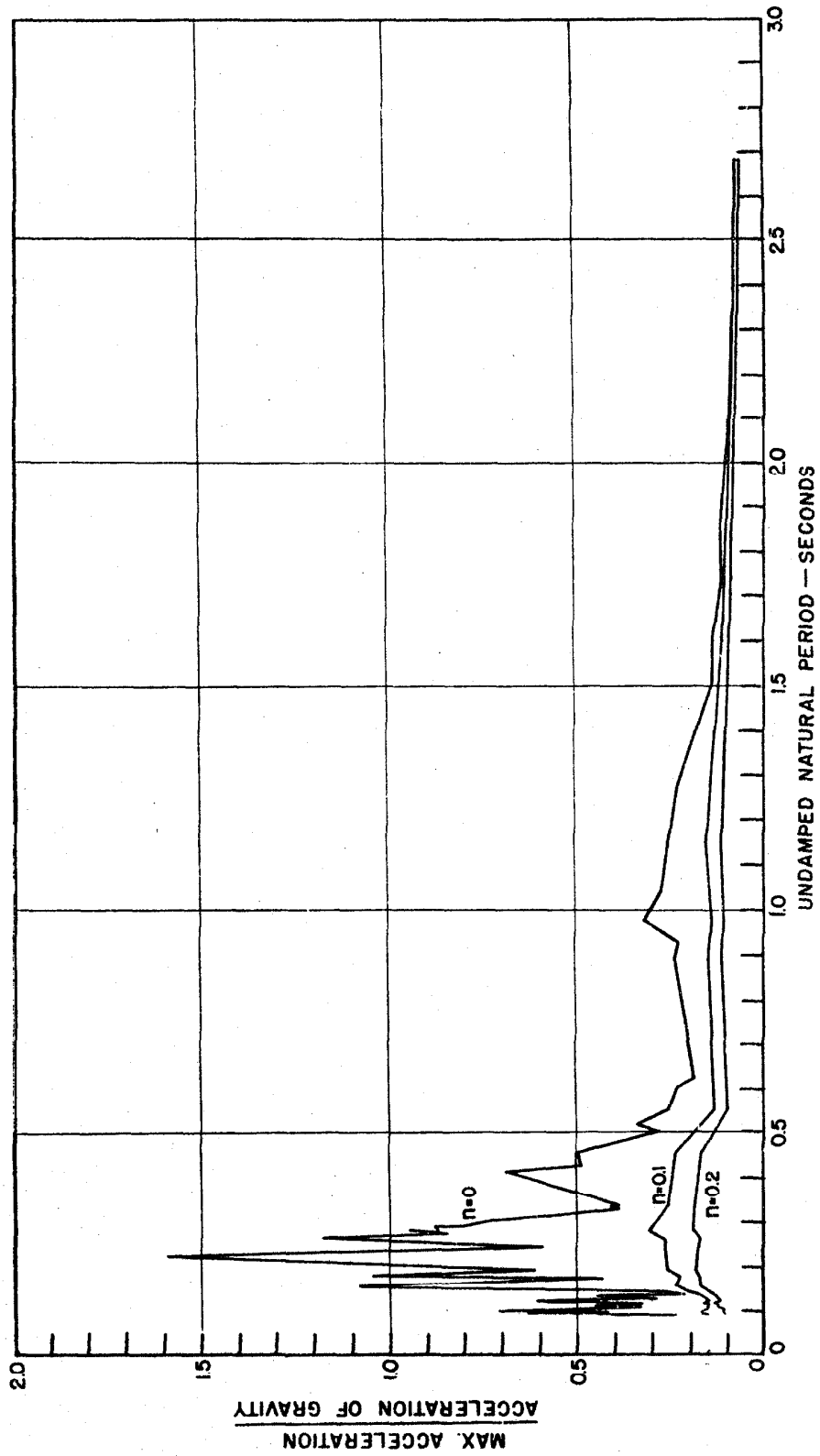


Figure 62. Acceleration spectrum for Helena, Montana; earthquake of Oct. 31, 1935. Component E-W.

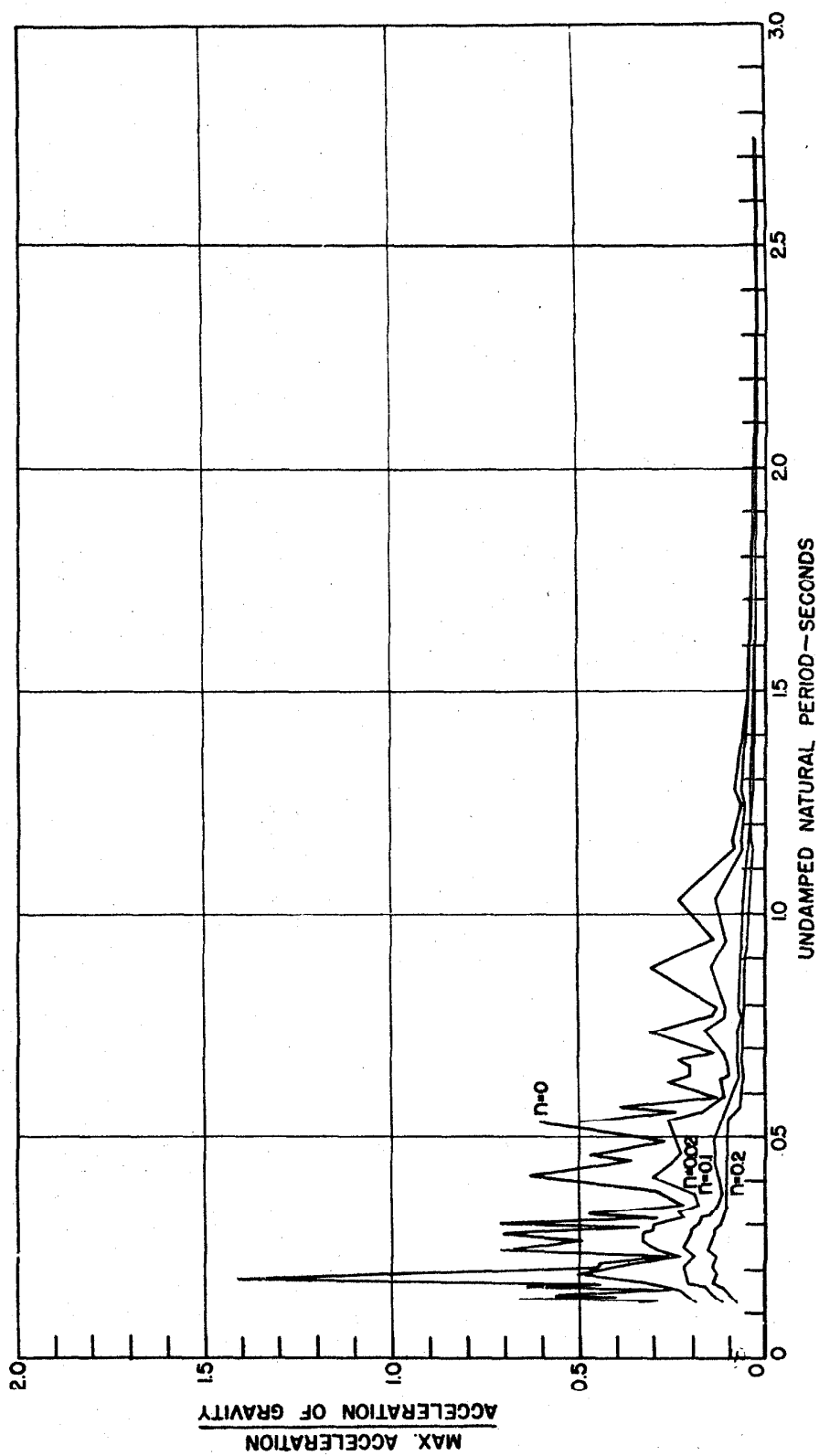


Figure 63. Acceleration spectrum for Ferndale, California; earthquake of Sept. 11, 1938. Component N45E.

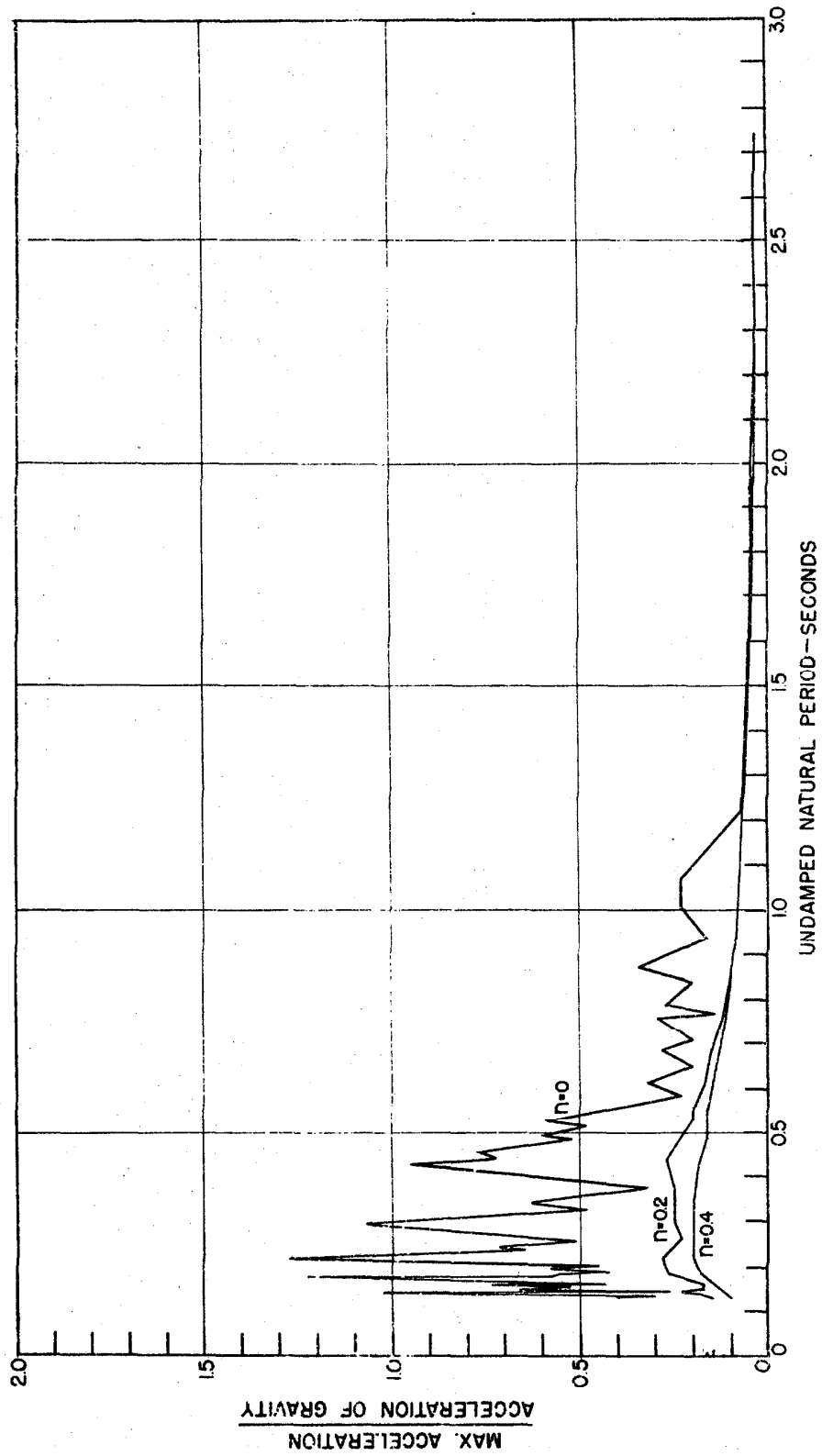


Figure 64. Acceleration spectrum for Ferndale, California; earthquake of Sept. 11, 1938. Component S 45 E.

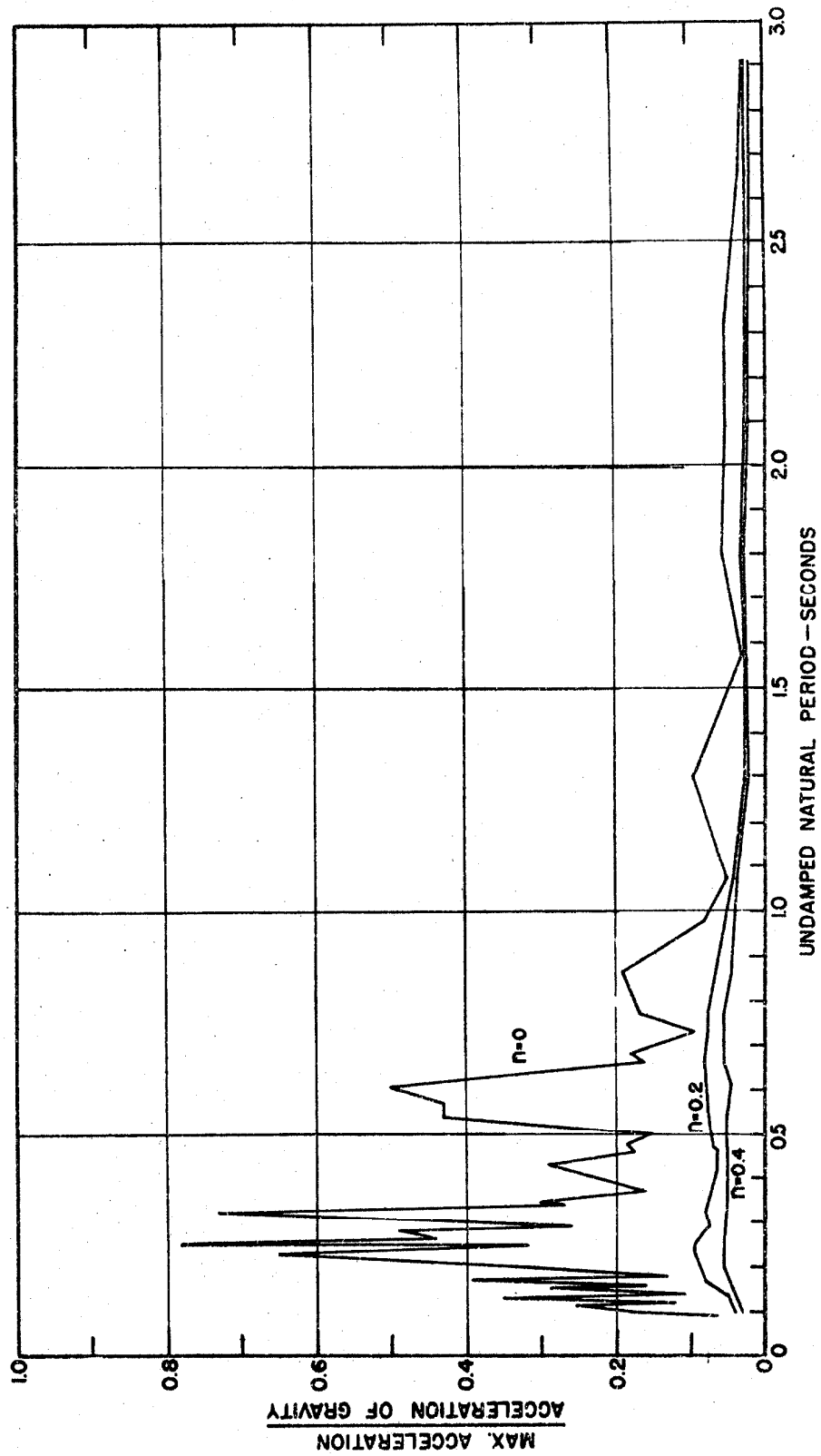


Figure 65. Acceleration spectrum for Ferndale, California; earthquake of Feb. 9, 1941. Component N45E.

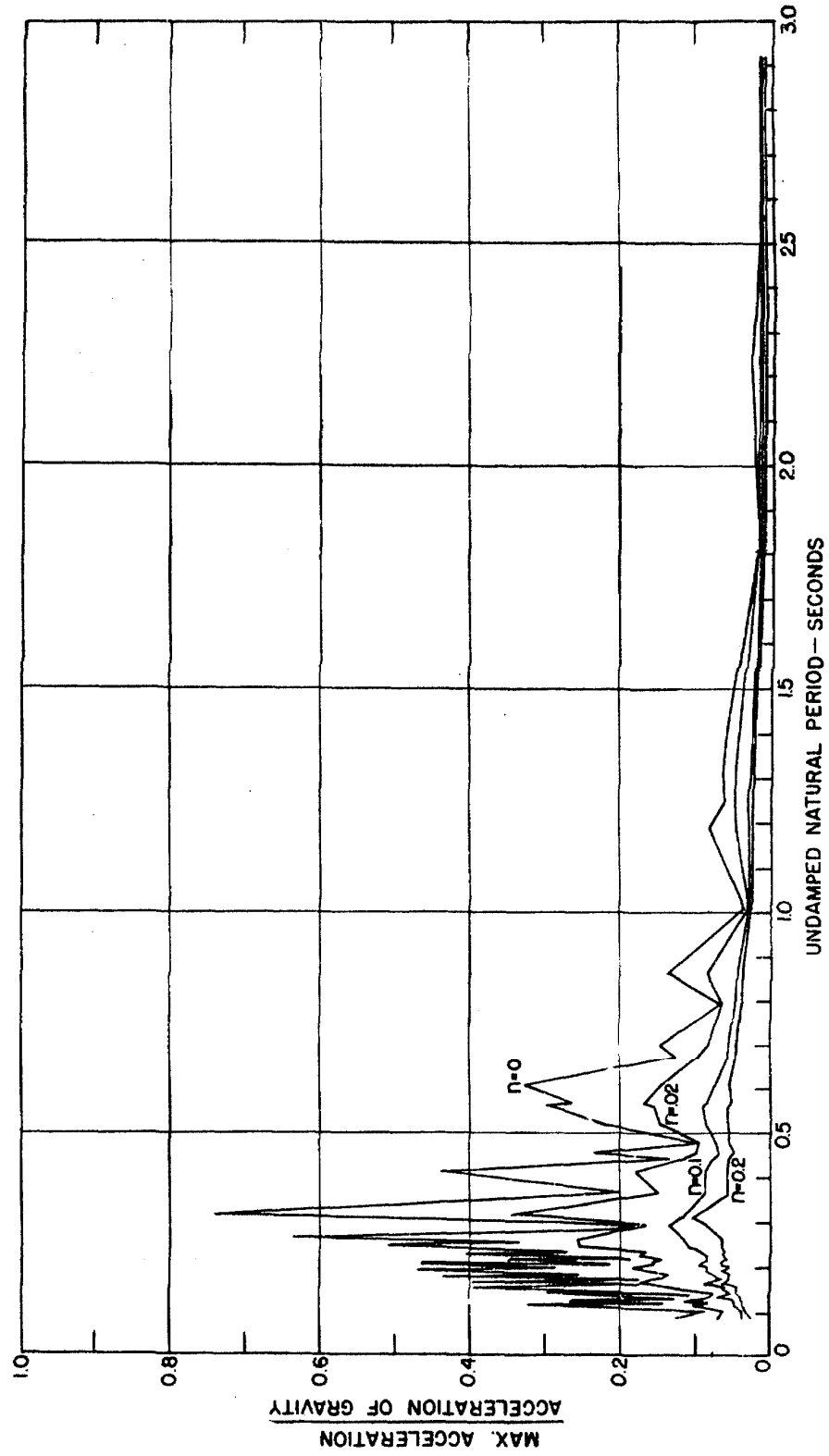


Figure 66. Acceleration spectrum for Ferndale, California; earthquake of Feb. 9, 1941. Component S45E.

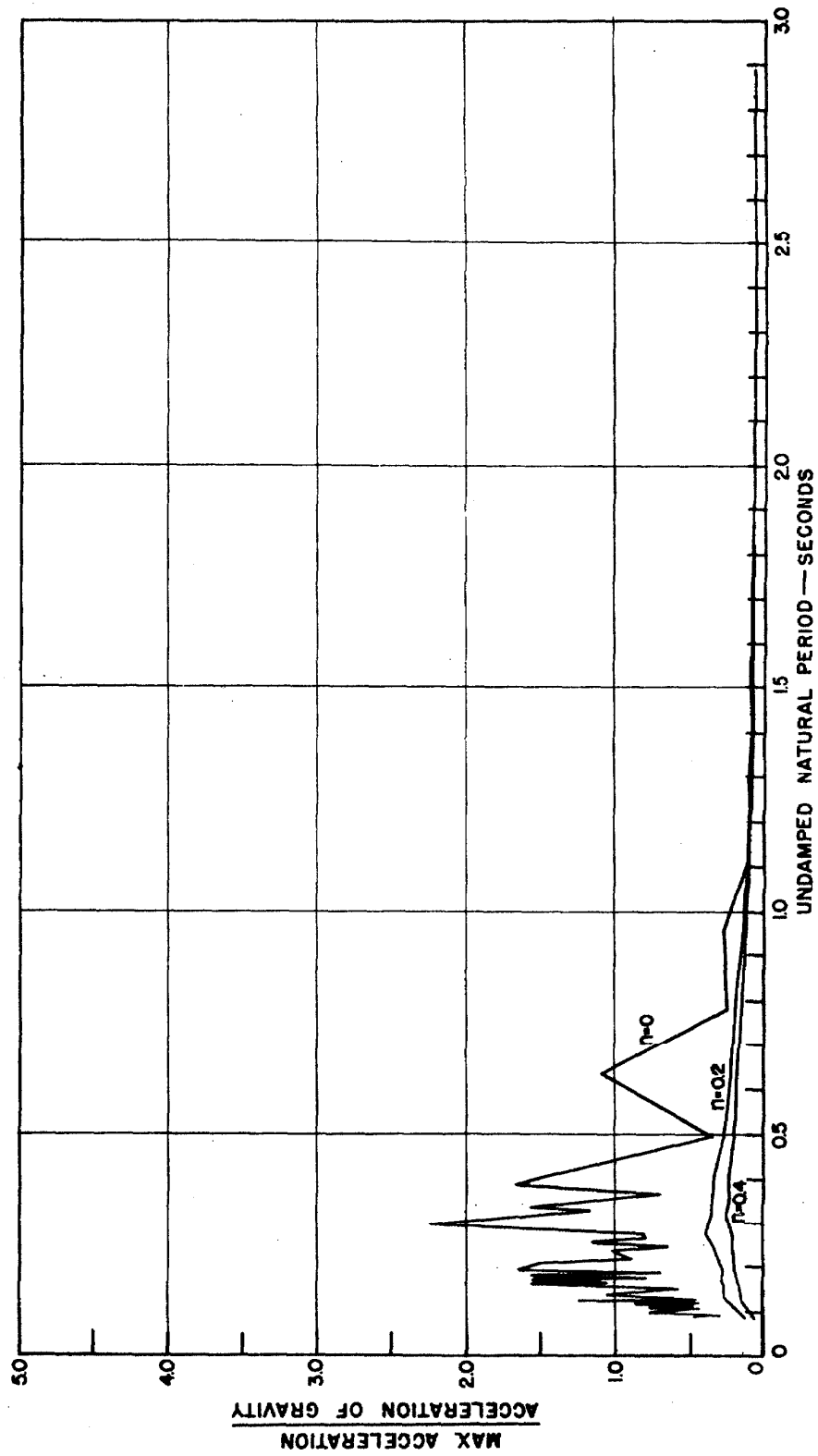


Figure 67. Acceleration spectrum for Ferndale, California; earthquake of Oct. 3, 1941. Component N45E.

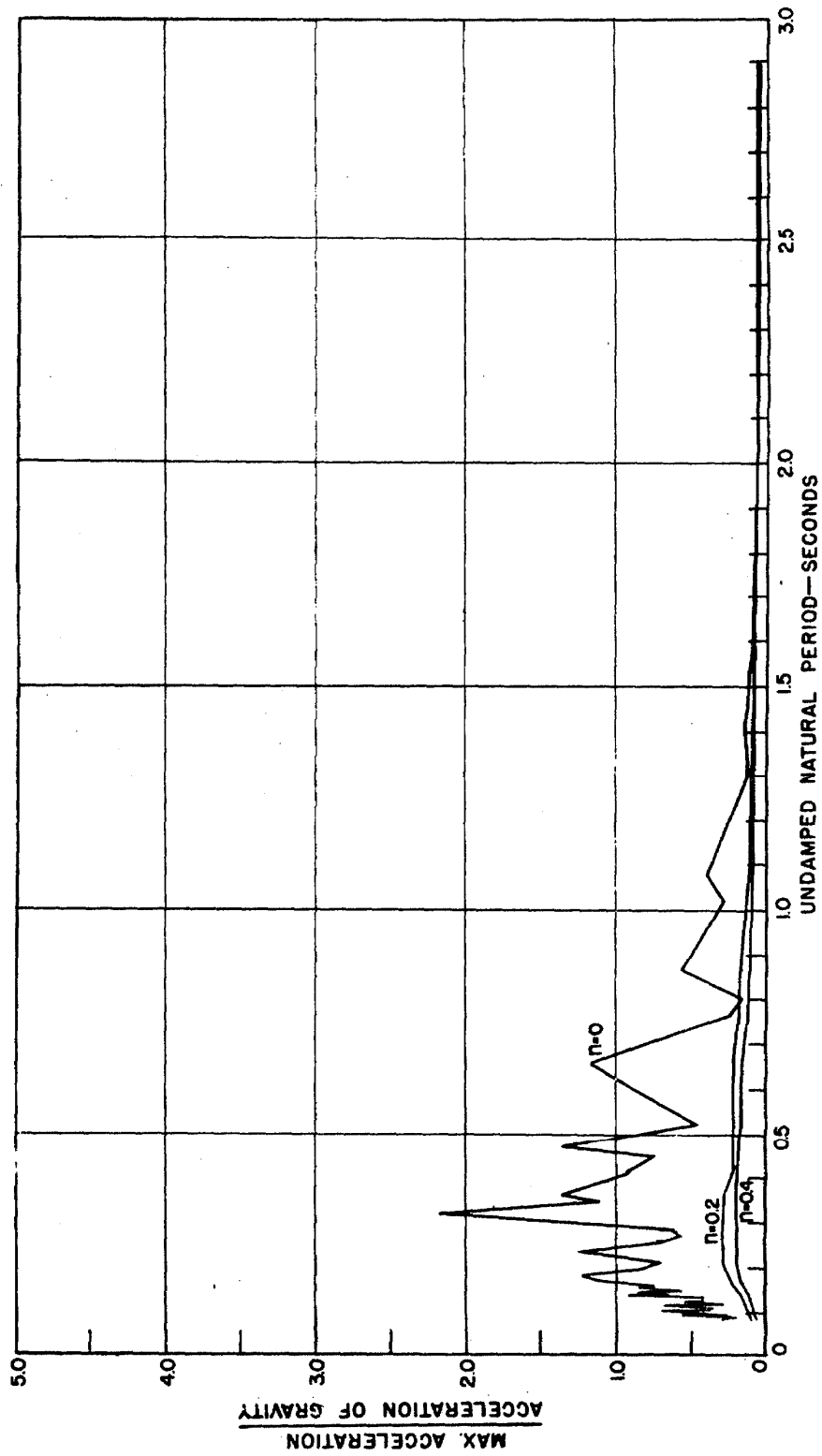


Figure 68. Acceleration spectrum for Ferndale, California; earthquake of Oct. 3, 1941. Component S45E.

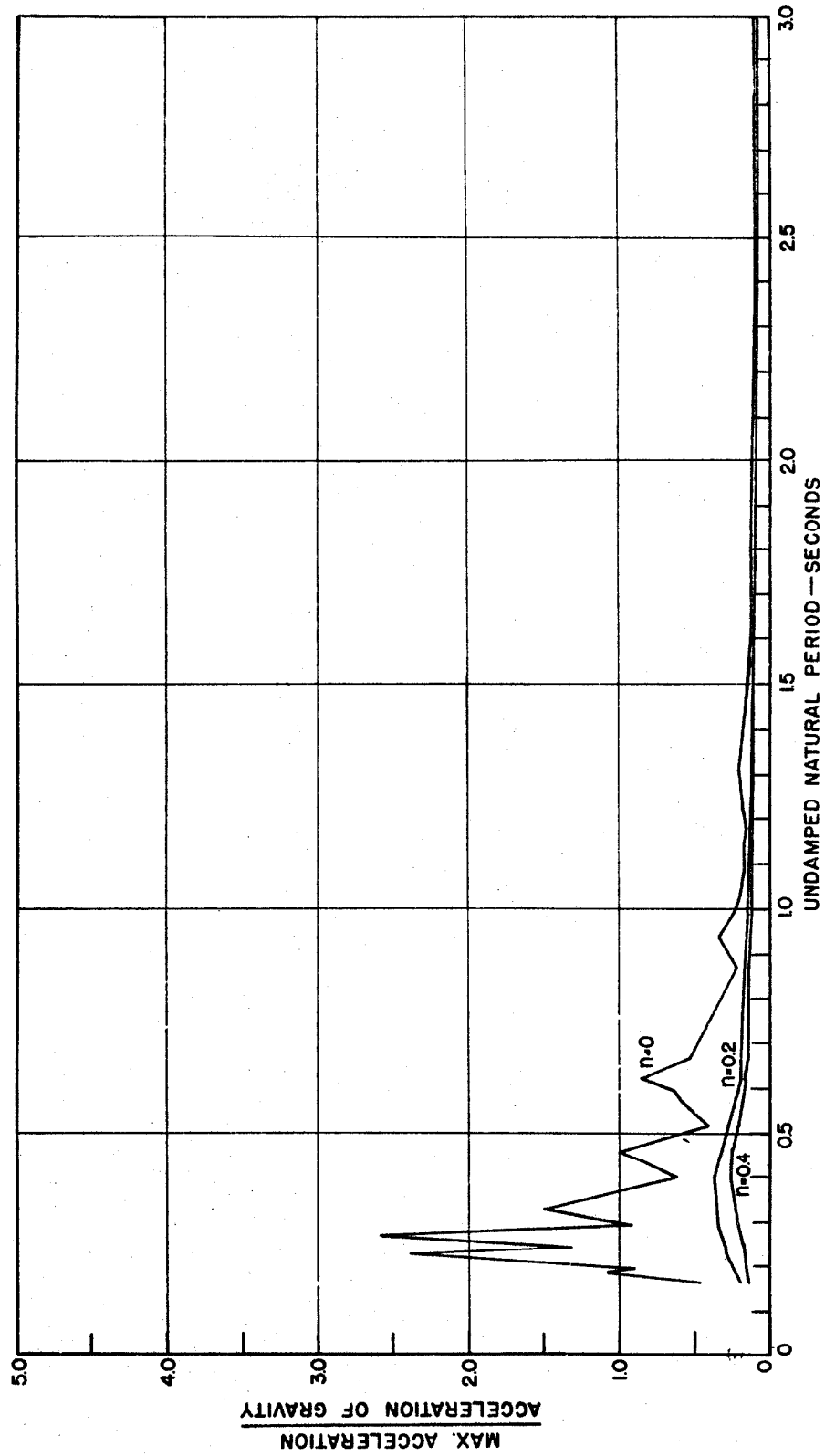


Figure 69. Acceleration spectrum for Santa Barbara, California; earthquake of June 30, 1941. Component N45E.

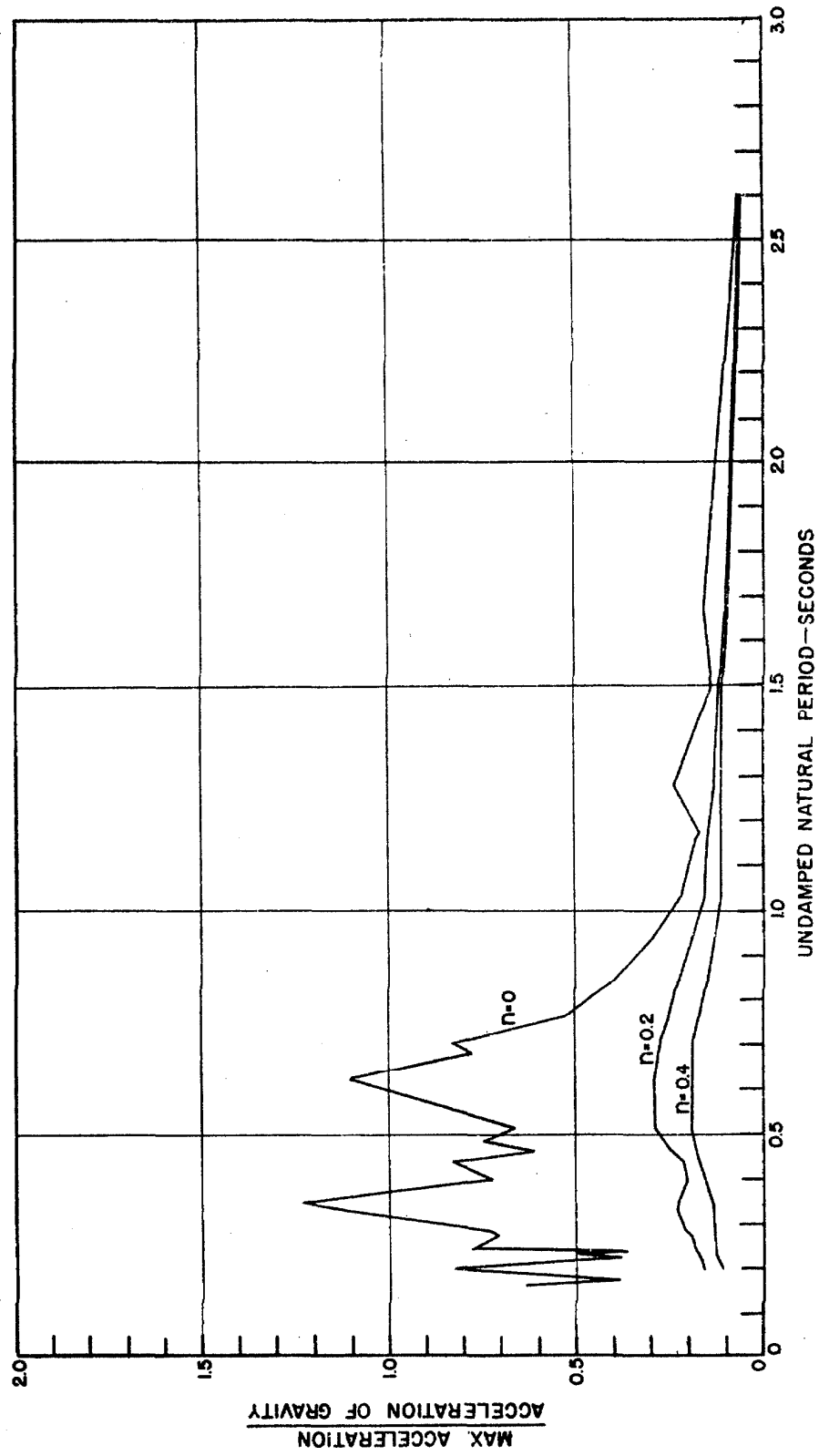


Figure 70. Acceleration spectrum for Santa Barbara, California; earthquake of June 30, 1941. Component S45E.

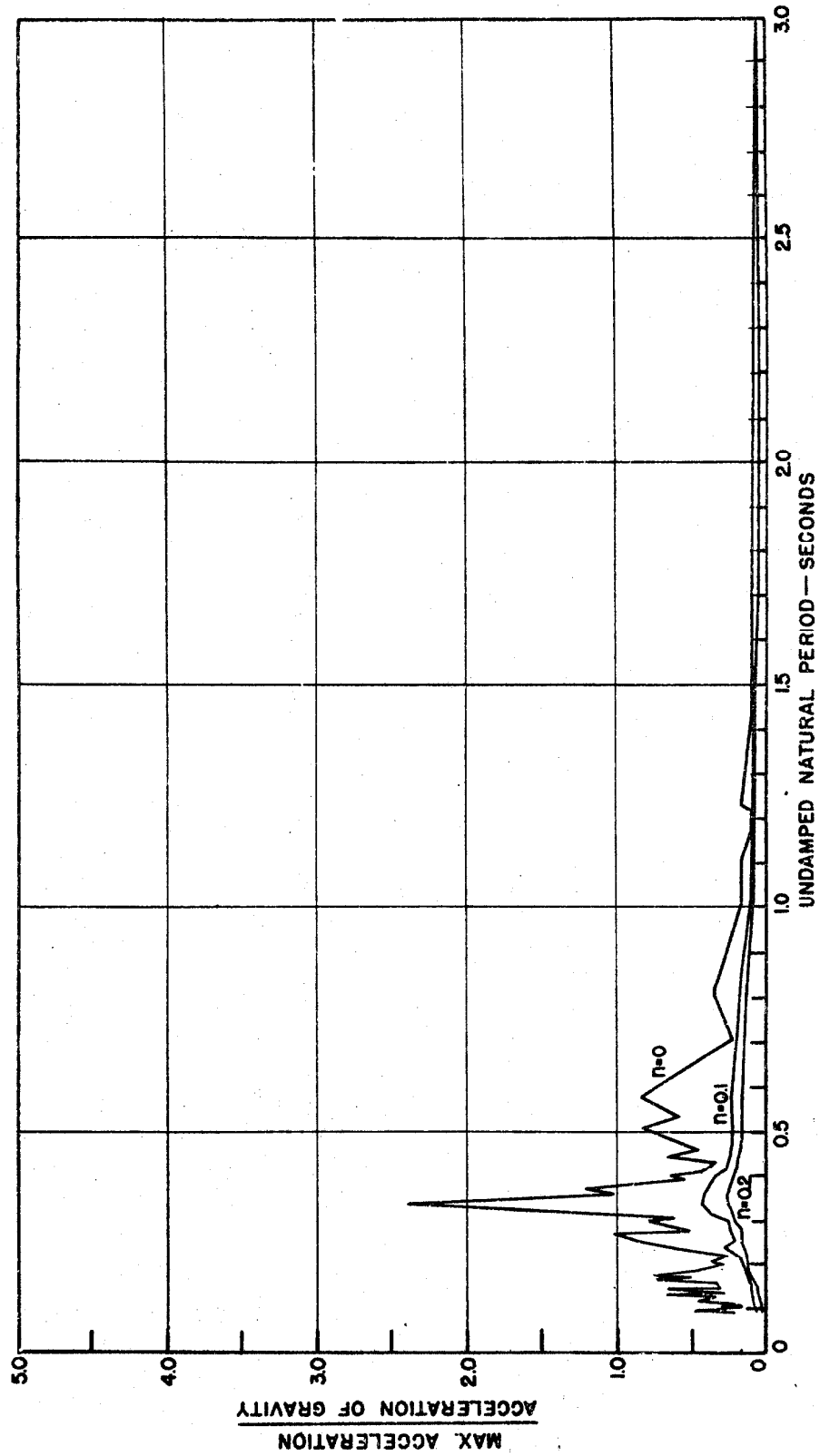


Figure 71. Acceleration spectrum for Hollister, California; earthquake of March 9, 1949. Component S01W.

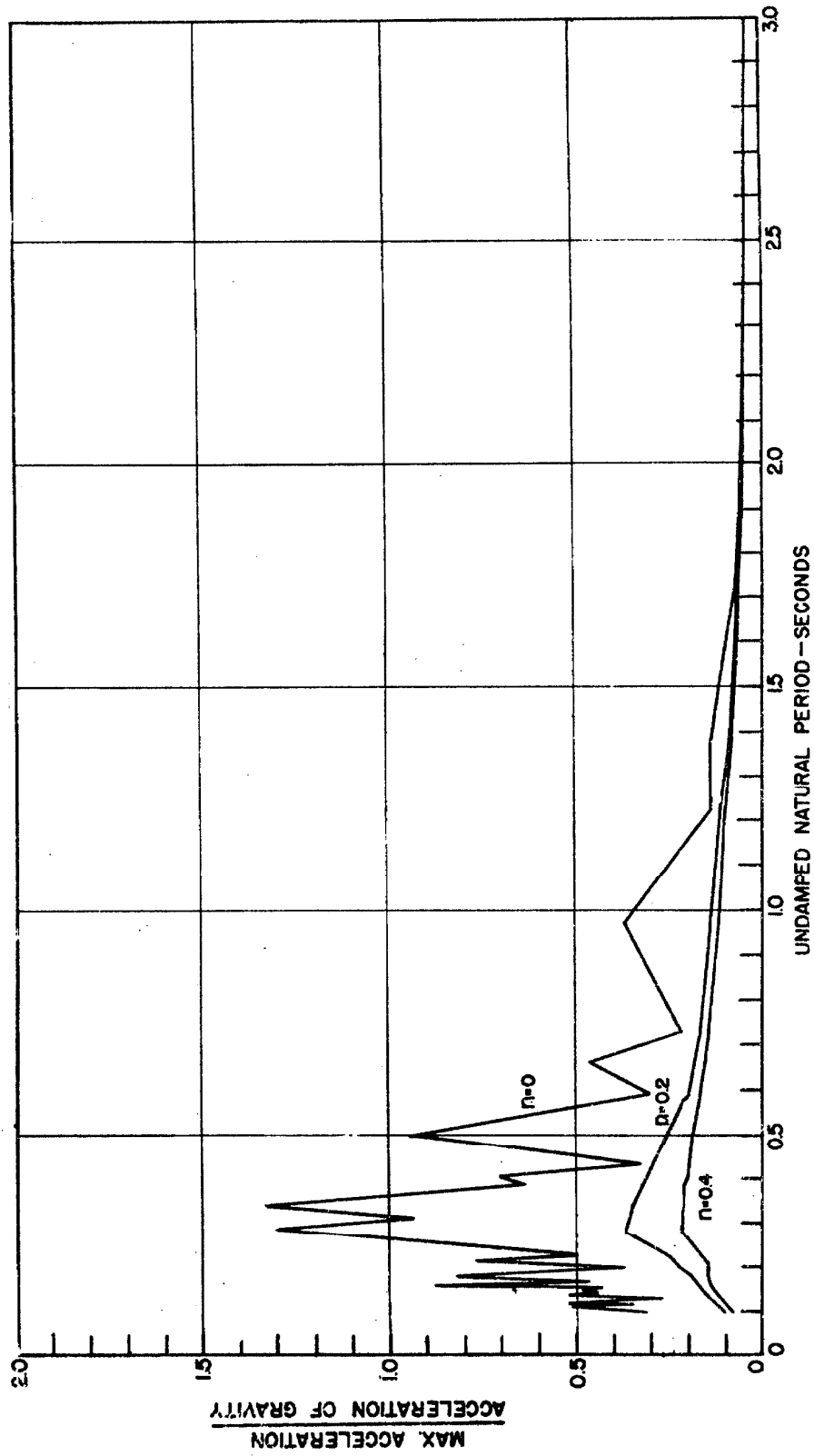


Figure 72. Acceleration spectrum for Hollister, California; earthquake of March 9, 1949. Component N89W.

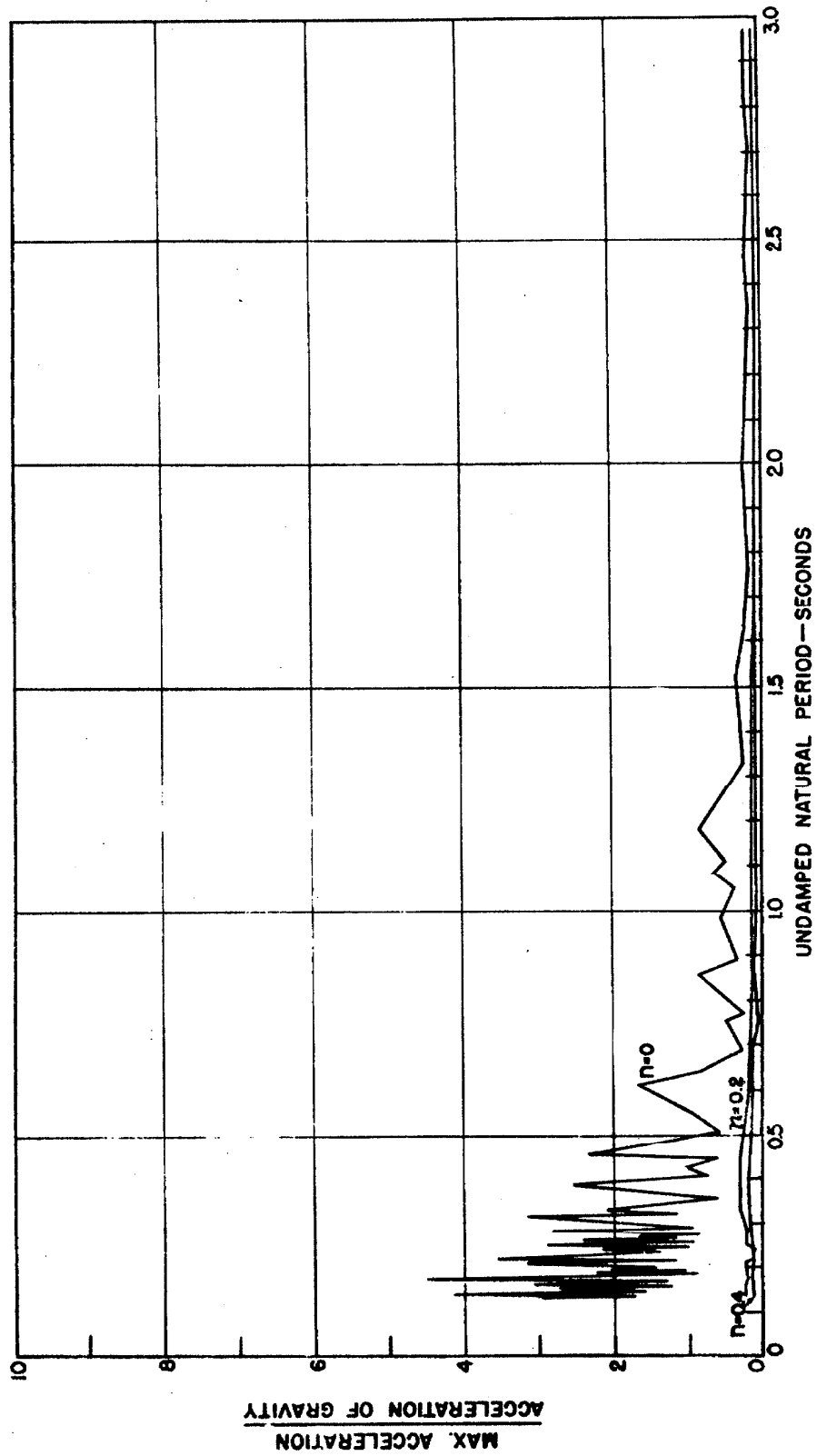


Figure 73. Acceleration spectrum for Olympia, Washington; earthquake of April 13, 1949. Component S10E.

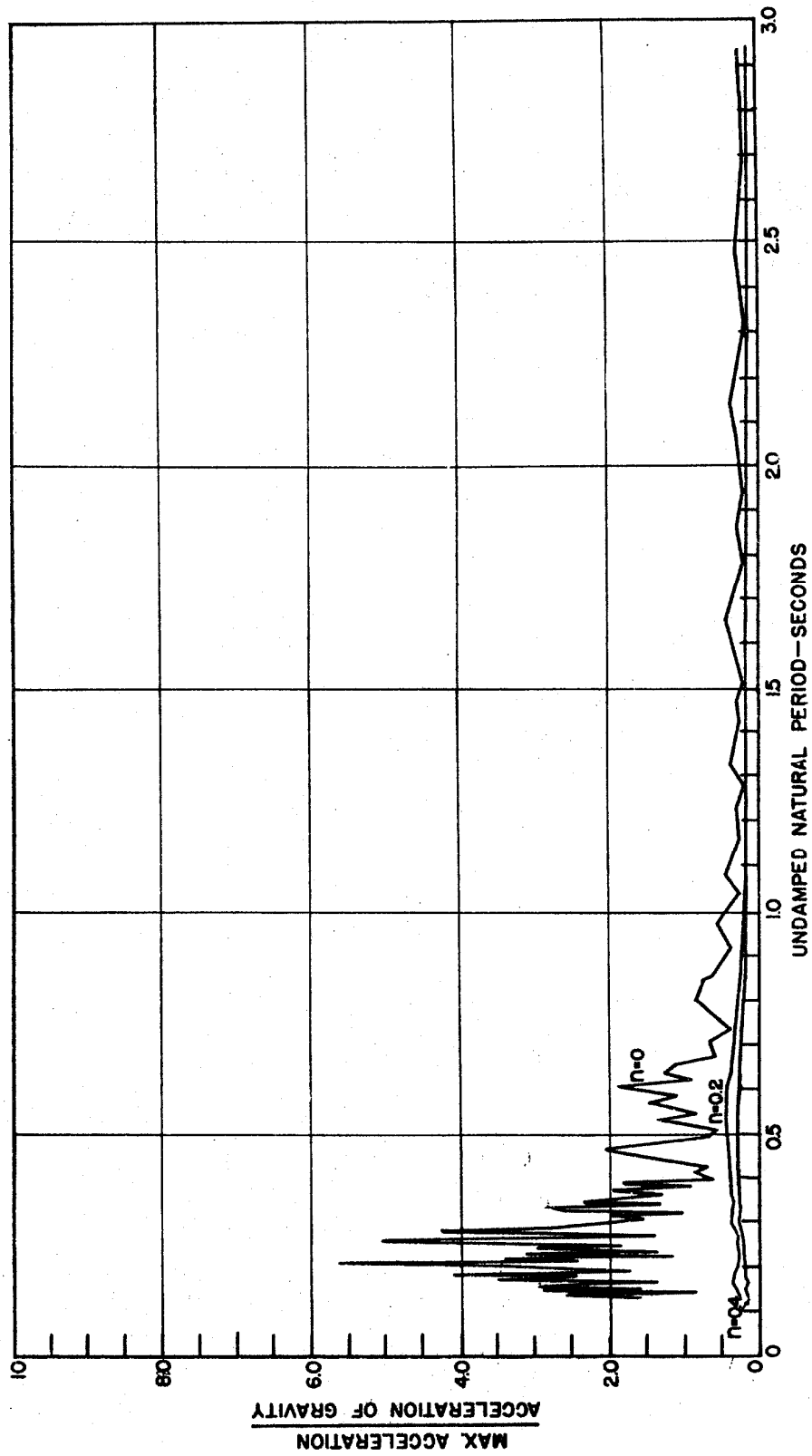


Figure 74. Acceleration spectrum for Olympia, Washington; earthquake of April 13, 1949. Component S80W.

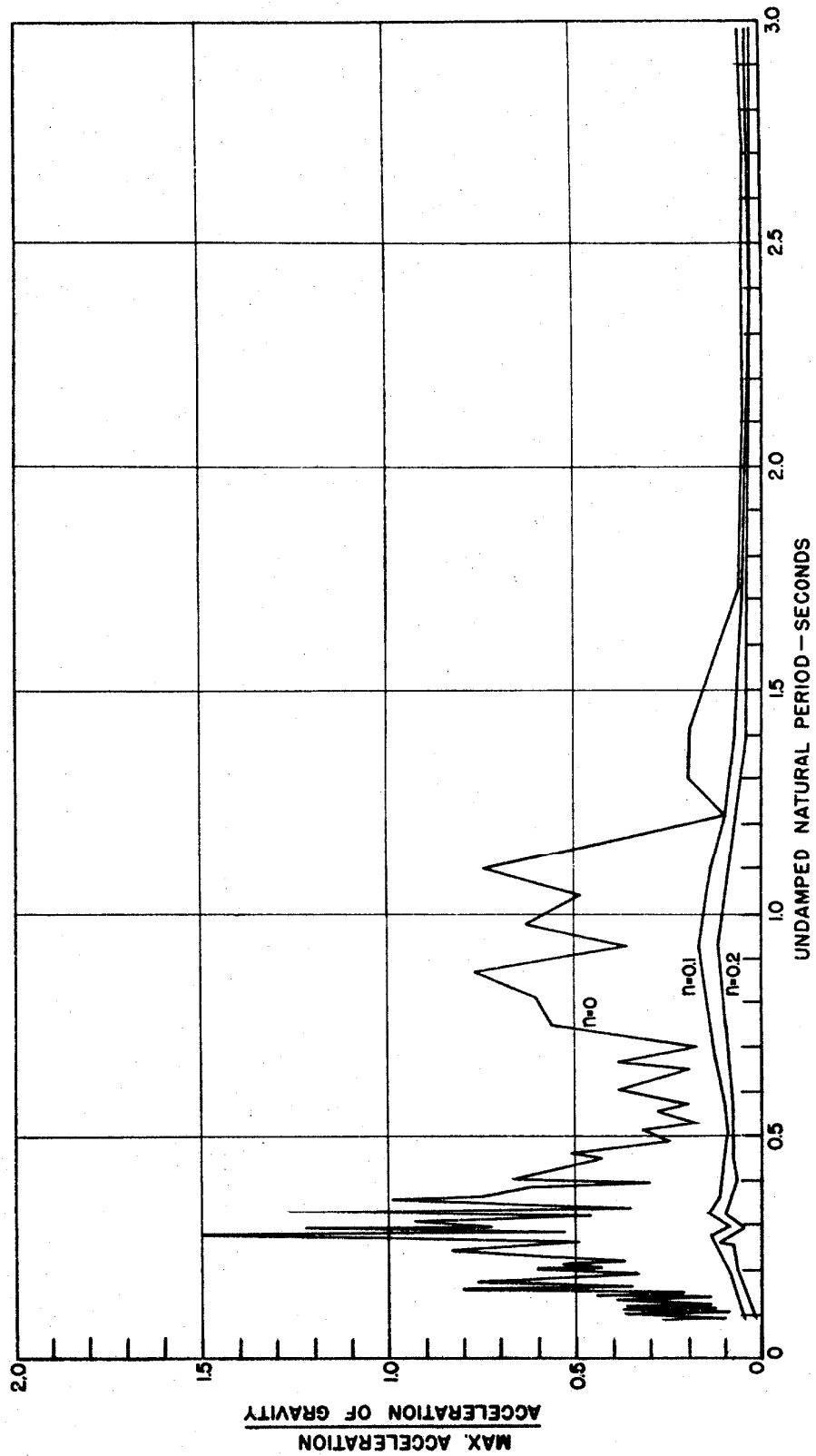


Figure 75. Acceleration spectrum for Seattle, Washington; earthquake of April 13, 1949. Component N88W.

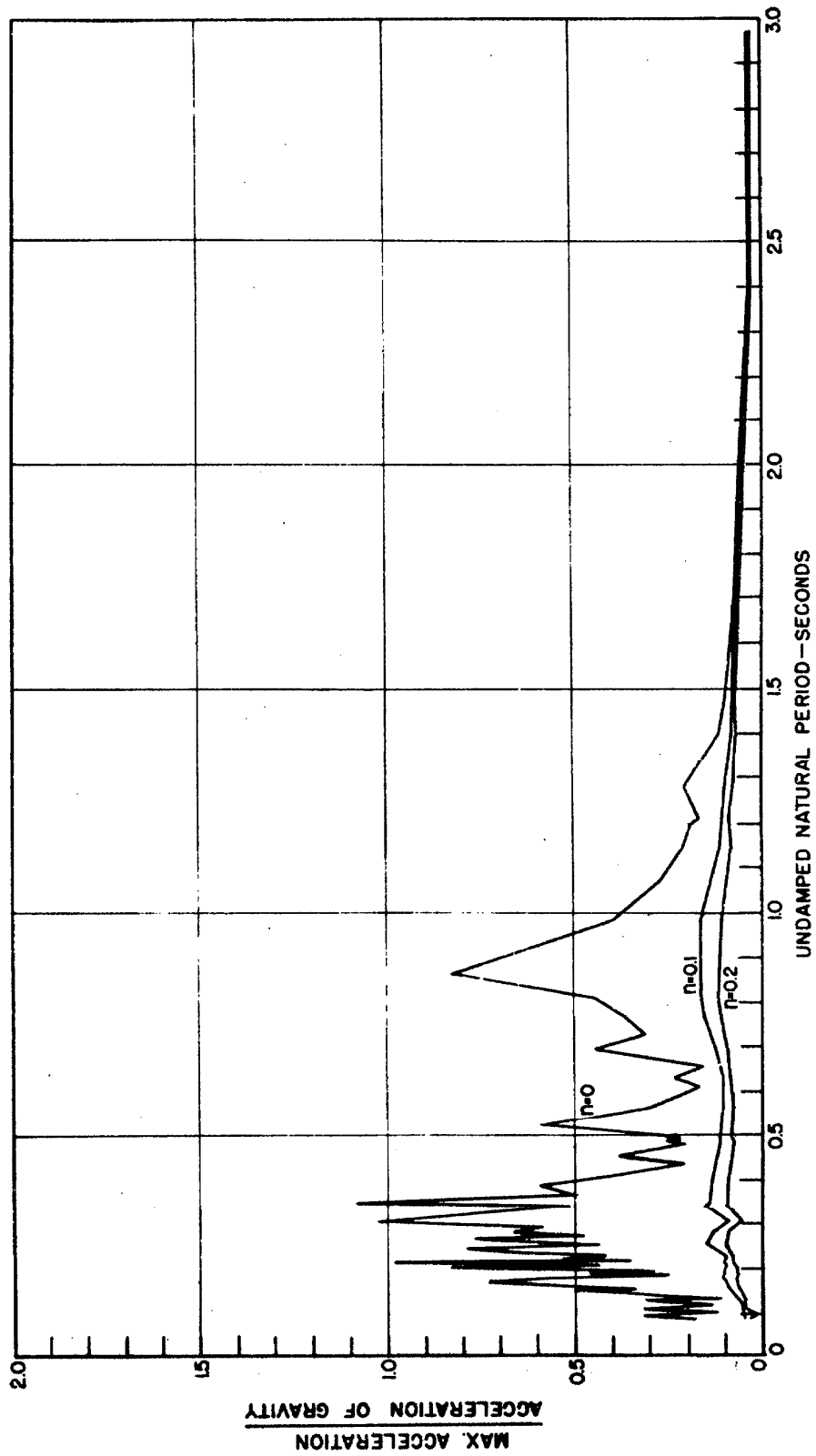


Figure 76. Acceleration spectrum for Seattle, Washington; earthquake of April 13, 1949. Component S02W.

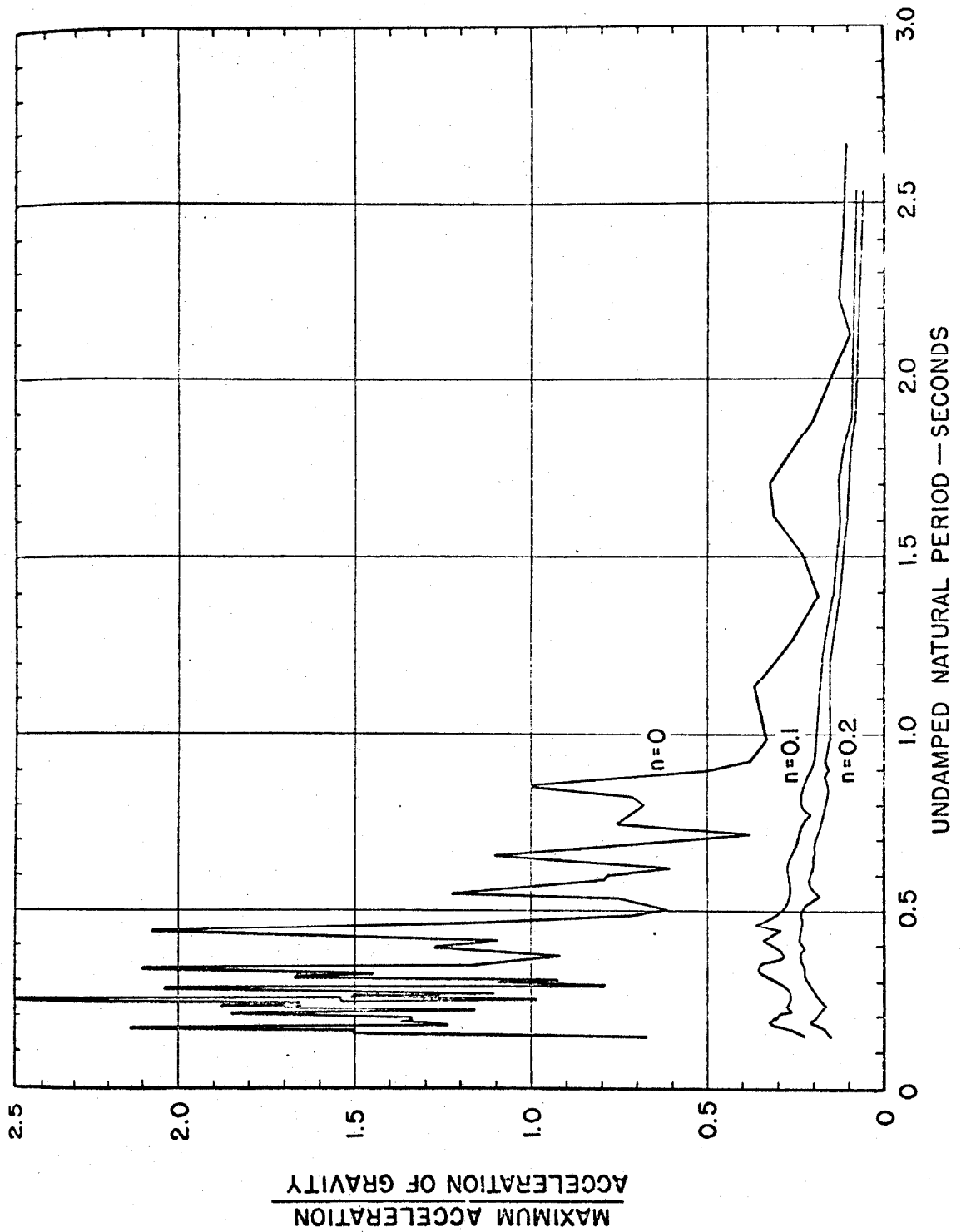


Figure 76a. Acceleration spectra for Taft, California; earthquake of July 21, 1952. Component S69E.

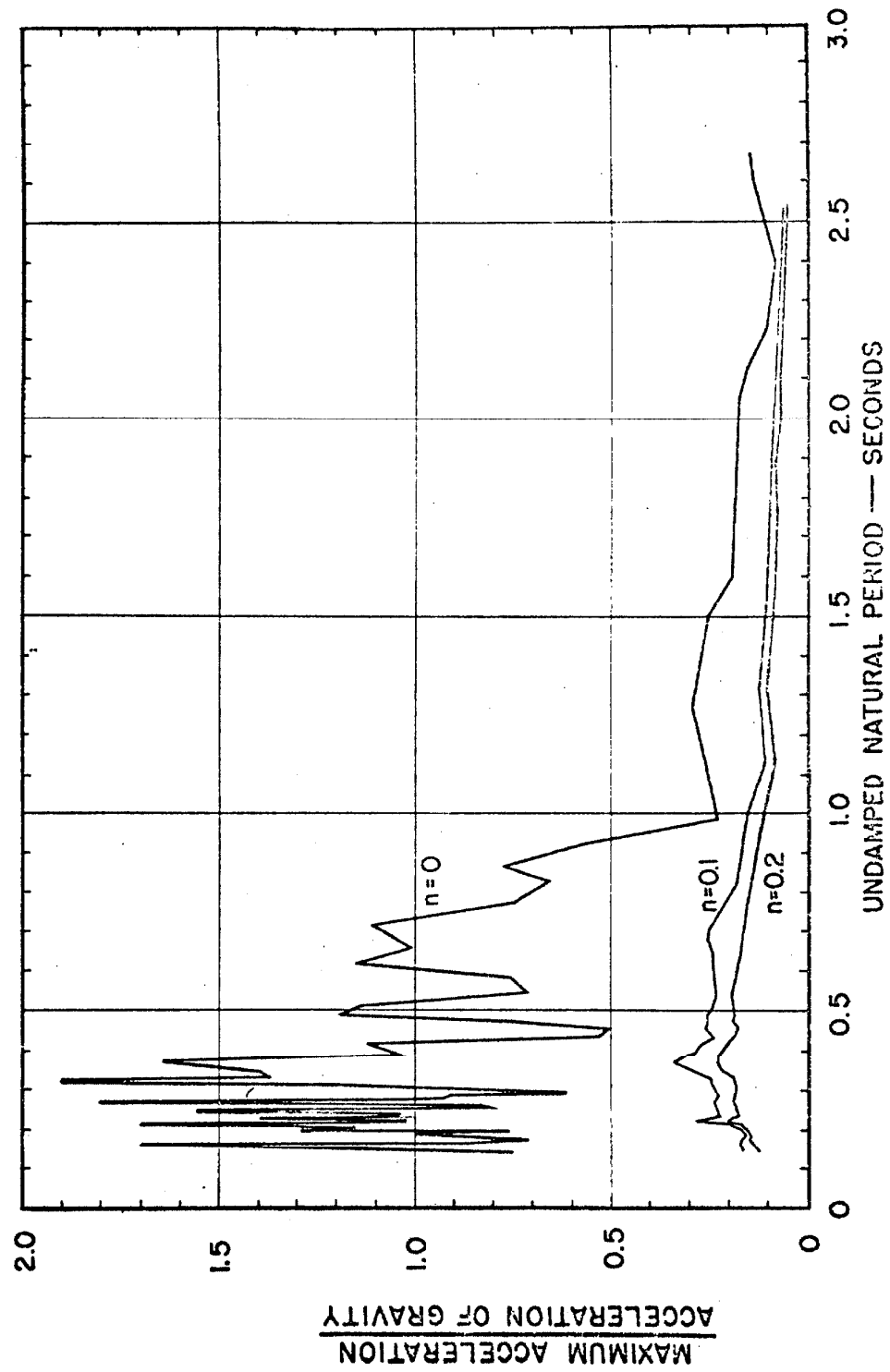
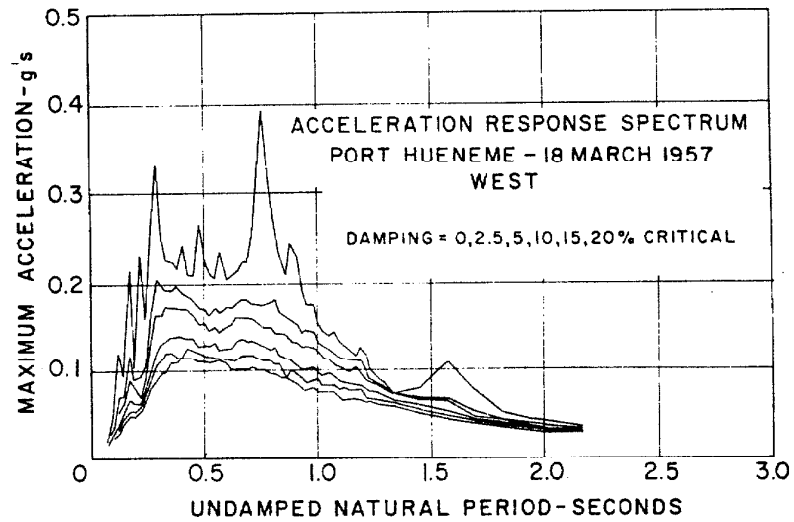
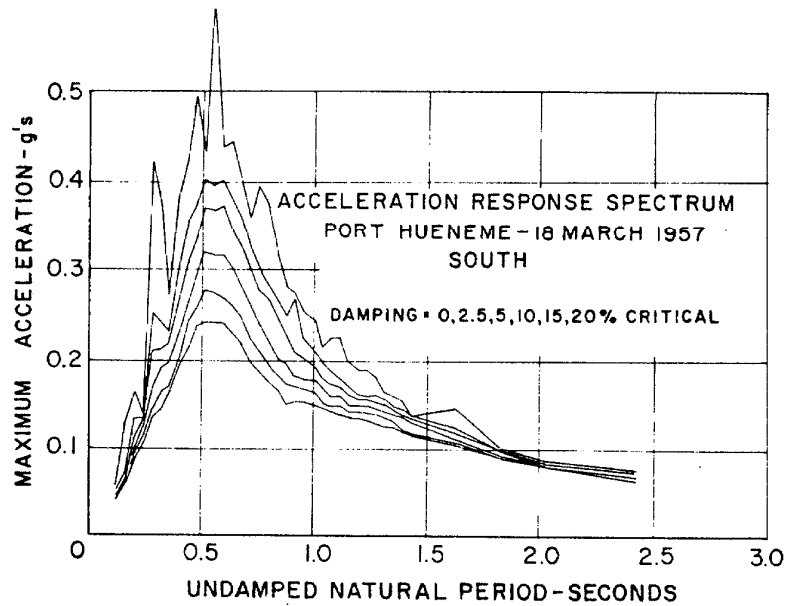


Figure 76b. Acceleration spectra for Taft, California; earthquake of July 21, 1952. Component N21E.



East-west component. Maximum absolute acceleration response spectrum.



North-south component. Maximum absolute acceleration response spectrum.

Figure 76c.

(See "The Port Hueneme Earthquake of March 18, 1957," by G. W. Housner and D. E. Hudson, Bull. Seismo. Soc. of Amer., Vol. 48, pp. 163-168, April 1958).

VI. DISCUSSION OF THE RESULTS

The spectra presented in the preceding section represent the behavior of a simple oscillator, such as the mechanical oscillator of Figure 2, under the influence of earthquake ground accelerations. From these spectra can be obtained the maximum response that would have been experienced by a particular oscillator during a particular earthquake. Such information, in itself, is of only academic interest; the real significance of the spectra is that they characterize the earthquakes as regards their effect on structures. Since a relatively large number of such spectra are now available, it should be possible to reach some conclusions concerning the general characteristics of past earthquakes. To formulate such conclusions is the purpose of this discussion.

Inspection of the strong-motion earthquake records of Figure 7 to 27 shows that the ground acceleration is extremely irregular; the chief similarity among the accelerograms is the marked irregularity exhibited by all. In a previous paper (8) it was suggested that, for this reason, earthquakes might best be analyzed as completely random phenomena — the word "random" being used in the statistical sense. Accordingly an analysis was made of a mathematical model of an earthquake, which consisted of a series of impulses random in time. The analysis showed that, above a minimum period,^{*} the undamped spectrum of such an earthquake had a mean value which was independent of the period. That the assumption of randomness was a good one was shown by the fact that average spectrum of a sample of 10 earthquake components did approach a constant value. The spectra of the individual earthquake

* The "minimum period" reflects the fact that, as the period of the oscillator approaches the time duration of the earthquake pulses, an impulsive analysis is no longer valid. It is shown in the paper referred to that, below the minimum period, the velocity will approach zero as the oscillator period approaches zero.

components and the spectrum of the mathematical model fluctuated about mean values, a probability distribution being associated with the fluctuations. On the basis of the data then available it was concluded that, for periods greater than 0.2 second, oscillators with short periods of vibration would not necessarily be more seriously affected by an earthquake than would oscillators with long periods, nor was the reverse true.

All the undamped spectra presented in Figs. 28 to 48 apparently do not follow such a trend, many appearing instead to be scattered about lines which have peaks at relatively short periods and approach constant values for longer periods. It would seem, therefore, that the results of the present investigation do not support the conclusions of the earlier study. To account for the discrepancy it is necessary to consider the methods used in the two investigations and the effect of damping.

The spectra used in the earlier study were obtained by means of the torsion pendulum analyzer described in Section IIIc. The damping in this apparatus comprised internal friction in the torsion spring, air damping of the swinging inertia bar, and a small rotational damping from the transverse damper. Since all of these effects were small, their sum was considered negligible and the results were identified as "undamped." The present results, however, were subject to precisely controlled amounts of damping, and it can be seen (e.g., Fig. 36 and 37) that the inclusion of as little as 2 percent of critical damping produces striking changes in the spectrum. First, the tendency of the mean line to peak at a short period is suppressed; second, the sensitivity of the spectrum to very small changes in period is reduced; and third, the magnitude of the response is reduced. Although no damping measurements were made on the torsion apparatus, consideration of the

magnitude of the spectrum indicates that the damping in those experiments was of the order of 2 percent of critical damping.

The conclusions of the earlier study, then, were based on damped, rather than undamped, spectra. If the damped spectra presented in Figs. 28 to 48 are considered it is seen that they are not inconsistent with the hypothesis of a spectrum consisting of points scattered about a mean value which is independent of period above a certain minimum period. There are several exceptions to this generalization. The spectra for Vernon, California, March 10, 1933 (Figs. 28 and 29); Los Angeles Subway Terminal, March 19, 1933 (Fig. 32) and October 2, 1933 (Fig. 33); and for Seattle, Washington, April 13, 1949 (Fig. 48) are departures from the trend. However, these departures are qualified by certain facts concerning the original records. The accelerograms of March 10, 1933 were the first obtained in the strong-motion program; instrument sensitivities were too high and there is some doubt as to the time at which the recording mechanisms began to function. For these reasons the records of that date are probably the least dependable of those analyzed. The first part of the Los Angeles Subway Terminal record of October 2, 1933 was also lost (9) and the spectrum is therefore incomplete. With regard to the Seattle, Washington earthquake, it is felt that the tendency of these spectra to peak at about 1.0 second period reflects the fact that the accelerograph station is located on fill and is within 25 feet of a seawall. In this sense the peak in the Seattle spectrum is a dominant ground period for this site; it would not be expected to affect the entire Seattle region.

Although the acceleration spectra of Figs. 49 to 76 are presented primarily to assist in visualizing the equivalent accelerations of the simple oscillator, it is of interest to compare them with several given by Biot (4). The components common to the two investigations are: Helena, Montana,

October 31, 1935 (E-W), and Ferndale, California, September 11, 1938 (both); the corresponding spectra are given in Figs. 62, 63 and 64 respectively. Comparison indicates that, although the acceleration spectra are in general agreement, the peak accelerations in the present undamped spectra are about 50 percent higher than those shown by Biot. From inspection of Fig. 63, which includes a spectrum for 2 percent of critical damping, it is estimated that Biot's results may have been subject to approximately 1 percent of critical damping.

The striking effectiveness of the first small increments of damping in reducing the response of an oscillator to earthquake excitation (see Figs. 36, 37, 40 and 41) leads to an interesting conclusion. It is a well-known fact in vibration theory (10, 11) that damping has its greatest effect on vibration amplitude at resonance, i.e., when the period of the disturbing force is the same as the natural period of the oscillator. By analogy it would appear that the peak responses of the undamped oscillator at certain periods are due to a condition of "quasi-resonance", which results when several earthquake acceleration pulses arrive in approximate synchronism with the motion of the oscillator. If the probability that a small group of earthquake pulses will arrive in synchronism with the oscillator motion is the same for all oscillator periods, then there should be many peaks in the response curve for the undamped oscillator and the peaks should be suppressed by the addition of damping. It can be seen from the spectra that such is the case.

In the past the theory has been advanced that a "dominant period" can be associated with a particular region and that earthquakes will be especially destructive of structures whose periods of vibration lie in the neighborhood of the dominant period. The spectra of Figs. 28 to 48, with

several exceptions, discussed above, give no indication of such a "dominant period". The damped spectra are consistent with the idea of a distribution about a mean value. In the case of the undamped spectra a study was made to see whether or not the fluctuations in spectrum value are consistent with locality. The following instances are available for comparison:

Vernon, California — March 10, 1933 and October 2, 1933.

Los Angeles Subway Terminal — March 10, 1933 and October 2, 1933.

El Centro, California — December 30, 1934 and May 19, 1940

Ferndale, California — Sept. 11, 1938; Feb. 9, 1941; and Oct. 3, 1941.

In no one of these groups of undamped spectra could a pattern be seen which might be considered characteristic of the locality.

The United States Coast and Geodetic Survey, in its series of official publications "United States Earthquakes — 19xx", summarizes the results of detailed studies of the original earthquake acceleration records. These summaries list what are described as the "outstanding" ground wave periods from each record. An attempt was made to correlate these "outstanding" periods with the local maxima of the undamped spectra. Fewer than 20 percent of the listed periods provide even approximate predictions of maximum response, and neither the maximum responses nor the predictions are consistent between different records made at a given station. It is concluded, therefore, that the concept of "dominant ground periods" is not a useful one for engineering purposes.

Several opportunities exist to compare the spectra of a given earthquake taken at two different stations. These are:

March 10, 1933 — Vernon, California and Los Angeles Subway Terminal

Oct. 2, 1933 — " " " " " "

April 13, 1949 — Seattle, Washington and Olympia, Washington

Comparison of the spectra in each of these groupings fails to reveal any characteristic resemblance that might be attributed to that particular earthquake. Additional data in the form of spectra are needed, however, since each group contains one or more earthquakes in which there is some question as to the value of the original records.

The foregoing discussion has emphasized the distinction between undamped and damped spectra and the difficulty of obtaining a truly undamped spectrum. On the other hand, since the ultimate aim of investigations such as the present one is to evolve methods for the aseismic design of structures, it is well to bear in mind that damping is present in real structures. The question remains, how much damping can be expected in engineering structures?

Very little information is available in answer to this question.

White (12) reports a damping test on a monolithic reinforced-concrete storage building. His results, when expressed in the form used here, indicate that the damping in the building was approximately 7 percent of critical. From vibration data which have been published (13) for a storage building with reinforced-concrete frame and floors and hollow-tile walls, it can be deduced that the damping in the building was approximately 14 percent of critical. The increase in damping over the monolithic structure is probably attributable to the effect of the hollow-tile walls.

The experiments referred to above were conducted at very low vibration amplitudes. Since it is probable that the damping is greater at greater amplitudes, it would be of interest to know the damping at amplitudes

experienced during a strong-motion earthquake. Large amplitude tests conducted by the Earthquake Engineering Research Institute on a four-story monolithic concrete building show damping of the order of 7-8 percent of critical. Research is also necessary on damping in buildings of other types of construction. From the meager evidence available, it appears possible that a minimum figure of the order of 5 percent of critical damping might be established as appropriate for conventional buildings. It can be seen from the spectra presented in this report that spectra so damped are consistent with the mean value hypothesis advanced at the beginning of this discussion.

For the purpose of engineering seismology qualitative scales of earthquake intensity, such as the modified Mercalli scale, are unsatisfactory because they attempt to measure intensity in terms of damage to buildings. Since buildings differ widely in design and workmanship, it is desirable to have a measure of earthquake intensity which is independent of the physical characteristics of particular buildings. Such a measure is provided by the mean value of the spectrum as defined in this report. Furthermore, the mean value of the spectrum has the advantage, for engineering purposes, that it can be related to the expected dynamic stresses and deflections in buildings.

On the basis that the mean value of the damped spectrum is the best index of the general destructiveness of an earthquake, a preliminary attempt was made to establish relative intensities. The comparison was made with the spectra for 20 percent of critical damping, since this value was common to all. While a somewhat lower amount of damping might be desirable, particularly for reinforced-concrete structures, the present comparison should

indicate the trend. The rating, in order of decreasing intensity, is:

1. El Centro, California, May 18, 1940
2. El Centro, California, Dec. 30, 1934
3. Olympia, Washington, April 13, 1949
4. Vernon, California, March 10, 1933
5. Los Angeles Subway Terminal, March 10, 1933
6. Santa Barbara, California, June 30, 1941
7. Ferndale, California, Oct. 3, 1941
8. Helena, Montana, Oct. 31, 1935
9. Hollister, California, March 9, 1949
10. Seattle, Washington, April 13, 1949
14. Los Angeles Subway Terminal, Oct. 2, 1933
11. Ferndale, California, Sept. 11, 1938
12. Vernon, California, Oct. 2, 1933
13. Ferndale, California, Feb. 9, 1941

The mean values of the damped spectra for the first four earthquakes are nearly equal, while the value for the fifth earthquake is approximately half as great. The fifth and subsequent listings are evenly spread over a wide range. This distribution, in conjunction with records of earthquake damage, suggests that the first four earthquakes listed might be described as "major" earthquakes and the remainder as "minor". The establishment of a quantitative criterion for distinguishing between "major" and "minor" earthquakes should await better knowledge of the damping which can be expected in typical buildings and comparison of the spectra for the appropriate values of damping. It should be noted that the Long Beach record of the March 1933 earthquake is not included in this study, as a satisfactory accelerogram was not obtained. The intensity of this record would have been greater than any of the 14 listed above.

Previous studies (3, 8) have indicated that the spectra are rather sensitive to inaccuracies in the methods of computation and the present study demonstrates the importance of close control over damping in experimental methods of determination. The electric analog computer provides a reliable rapid and uniform method of computing the spectra; it is the only method in which damping can conveniently be treated. For these reasons its use is indicated as the standard method for determining the spectra of future earthquakes.

VII. SUMMARY AND CONCLUSIONS

A total of 88 spectra of strong-motion earthquakes are presented. These spectra characterize the significant engineering properties of all of the strongest earthquakes recorded in the United States. The results of this investigation indicate that damping is a very important parameter in the earthquake problem. Relatively small changes of damping produce large changes in peak response, particularly when the total damping present is low. This observation is significant for two reasons. First, it emphasizes the necessity for precise control over damping in the determination of the earthquake spectrum. Because of this and because of its convenience in use, the electric analog computer is the most satisfactory means presently available for spectrum calculation. The second reason for the significance of the finding on damping is its implication for the earthquake resistance of buildings. Since damping is effective in alleviating the dynamic stresses and deflections resulting from earthquakes, it becomes of interest to know how much damping there is in each of the various types of construction. Further research on this question is essential to a more complete understanding of the earthquake problem.

It is shown that the damped spectra obtained in this investigation are consistent with an hypothesis based on the assumption that earthquakes are random disturbances; namely, that above a certain minimum period the spectrum may be considered as being distributed about a mean value which is independent of period. The implications of this conclusion for the design of earthquake-resistant structures are to be presented in a later report. It is concluded that the concept of a "dominant ground period" is not valid for engineering purposes.

It is proposed that the damped spectrum be used as a quantitative measure of earthquake intensity, since it provides an index which is independent of the design and workmanship of particular structures.

The spectra characterize the earthquakes as regards the response of structures and having the spectra it is possible to answer questions of the type: What is the general character of the response of structures of various types to such earthquakes? This report presents the basic information required for studies of this type and work is underway on this phase of the project. It is highly desirable that spectra be prepared for all future strong-motion earthquakes that are recorded.

APPENDIX A

DAMPING IN MULTIPLE-DEGREE-OF-FREEDOM SYSTEMS

It is assumed in the analytical formulation of the earthquake problem that the damping in a structure is viscous, i. e., that motions are opposed by damping forces which are proportional to velocity. Very little is known about the damping in real structures, but there is no reason to suppose that it is viscous damping. The assumption of viscous damping simplifies the mathematical treatment, and it can be justified on physical grounds. Jacobsen¹ showed that the behavior of vibrating systems with various types of damping could be satisfactorily described in terms of a viscous damping which produced an energy dissipation per cycle equivalent to that produced by the actual damping forces. This concept of "Equivalent viscous damping" is the basis for the treatment of damping in the present report.

The response of a complex structure is described in terms of a series of "normal modes", which are the configurations taken by the system when it is vibrating at one of its natural frequencies. These normal modes can always be derived for an undamped system. Rayleigh² points out that, in the case of a damped system, it is still possible to derive normal modes provided that the damping be of a restricted mathematical form. This form is not generally useful for practical problems.

Of greater significance for the present study is Rayleigh's statement³ that, for small damping, the normal modes appropriate to the undamped

-
1. L. S. Jacobsen, "Steady Forced Vibration as Influenced by Damping", Trans. A. S. M. E., 52:169 (1930)
 2. Lord Rayleigh, "Theory of Sound", Macmillan, 1937, p. 130
 3. op. cit. p. 136

system are approximately preserved. The principal effect of small damping is to produce a change in phase, so that the various parts of the system are no longer simultaneously in the same phase. This change in phase is not important for the present study because, in the application of these results to the response of complex structures, the phase will be ignored. The point of view is taken that, by assuming the maximum stresses in the various modes to occur all in the same phase, there is obtained an envelope of the worst possible conditions for design purposes. Since the distribution of stress in the structure depends on the shape of the normal modes and not on their phases, the method is satisfactory. This theory will be developed in detail in a later report.

ACKNOWLEDGEMENTS

The authors wish to express their appreciation to the staff of the Analysis Laboratory for making the electric analog computations. Thanks are due Mr. D. A. Hausmann for his help in reducing the data and preparing the figures.

REFERENCES

- (1) Lord Rayleigh, "Theory of Sound", Macmillan, New York, 1937
pp. 91-170.
- (2) Lord Rayleigh, op. cit., p. 74
- (3) G. W. Housner, "Calculating the Response of an Oscillator to Arbitrary
Ground Motion", Bull. Seism. Soc. Amer. (1941), Vol. 31, pp. 143-149.
- (4) M. A. Biot, "A Mechanical Analyzer for the Prediction of Earthquake
Stresses", Bull. Seism. Soc. Amer. (1941), Vol. 31, pp. 151-171.
- (5) H. E. Criner, G. D. McCann, and C. E. Warren, "A New Device for the
Solution of Transient Vibration Problems by the Method of Electrical-
Mechanical Analog", Journal of Applied Mechanics (1945), Vol. 12, p. 135.
- (6) G. D. McCann, "The Mechanical Transient Analyzer", National Electronics
Conference Proceedings (1946), Vol. 2, p. 372.
- (7) G. W. Housner and G. D. McCann, "The Analysis of Strong-Motion
Earthquake Records with the Electric Analog Computer", Bull. Seism.
Soc. Amer., (1949), Vol. 39, pp. 47-56.
- (8) G. W. Housner, "Characteristics of Strong-Motion Earthquakes", Bull.
Seism. Soc. Amer. (1947), Vol. 37, pp. 19-31.
- (9) U.S. Coast and Geodetic Survey, "United States Earthquakes, 1933",
Serial No. 579, p. 59.
- (10) J. P. Den Hartog, "Mechanical Vibrations", McGraw-Hill, New York, 1947.
- (11) S. P. Timoshenko, "Vibration Problems in Engineering", Van Nostrand,
New York, 1937.
- (12) M. P. White, "Friction in Buildings: Its Magnitude and Its Importance
in Limiting Earthquake Stresses", Bull. Seism. Soc. Amer. (1941),
Vol. 31, pp. 93-99.

- (13) U. S. Coast and Geodetic Survey, "Earthquake Investigations in California, 1934-1935", Special Publication No. 201, p. 125.

SAN FRANCISCO EARTHQUAKES OF MARCH 1957

ABSTRACT

Strong-motion accelerometer records were obtained from five stations located in buildings in San Francisco and Oakland. Such a group of strong-motion records from a number of stations located within a relatively small area is a most important addition to our basic information on structural effects of earthquakes.

Ground motion in the March 1957 earthquake was somewhat different from most recorded strong-motion earthquakes, in that the time durations were relatively short and peak accelerations were large for a shock of this magnitude.

Spectrum curves indicate that the influence of damping in reducing the peak values was not as marked in this earthquake as in more typical damaging earthquakes. This is a consequence of the short duration of the earthquake and the fact that the maximum structural responses occurred near the start of the motion.

ILLUSTRATIONS

	Page
Figure 1. Map showing location of U. S. Coast and Geodetic Survey strong-motion accelerometer stations	118
Figure 2. Horizontal components of ground acceleration, Golden Gate Park station	118
Figure 3. Horizontal components of ground acceleration, Building A	118
Figure 4. Horizontal components of ground acceleration, Building B	118
Figure 5. Horizontal components of ground acceleration, Building C	119
Figure 6. Horizontal components of ground acceleration, Building D	119
Figure 7. Velocity response spectrum, Golden Gate Park, N. 10 E.	119
Figure 8. Velocity response spectrum, Golden Gate Park, S. 80 E.	119
Figure 9. Velocity response spectrum, Building A, S. 81 W.	119
Figure 10. Velocity response spectrum, Building A, S. 9 E.	119
Figure 11. Velocity response spectrum, Building B, N. 9 W.	120
Figure 12. Velocity response spectrum, Building B, N. 81 E.	120
Figure 13. Velocity response spectrum, Building C, N. 45 W.	120
Figure 14. Velocity response spectrum, Building C, N. 45 E.	120
Figure 15. Velocity response spectrum, Building D, S. 64 E.	120
Figure 16. Velocity response spectrum, Building D, N. 26 E.	120
Figure 17. Acceleration response spectrum, Golden Gate Park, N. 10 E.	121
Figure 18. Acceleration response spectrum, Golden Gate Park, S. 80 E.	121
Figure 19. Acceleration response spectrum, Building A, S. 9 E.	121
Figure 20. Acceleration response spectrum, Building A, S. 81 W.	121
Figure 21. Acceleration response spectrum, Building B, N. 81 E.	121
Figure 22. Acceleration response spectrum, Building B, N. 9 W.	121
Figure 23. Acceleration response spectrum, Building C, N. 45 W.	122
Figure 24. Acceleration response spectrum, Building C, N. 45 E.	122
Figure 25. Acceleration response spectrum, Building D, N. 26 E.	122
Figure 26. Acceleration response spectrum, Building D, S. 64 E.	122

Special Report 57

CALIFORNIA DIVISION OF MINES

FERRY BUILDING, SAN FRANCISCO, 1959

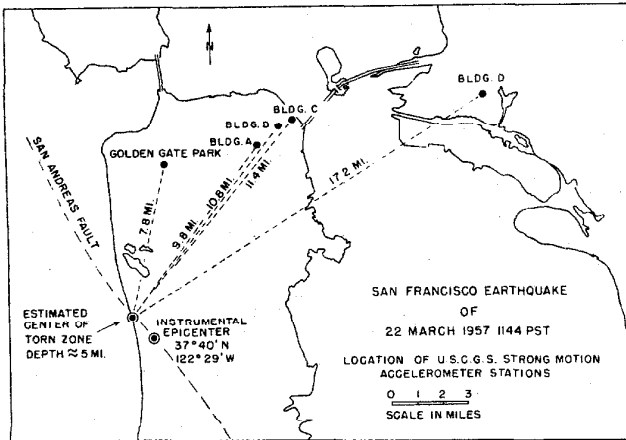


FIGURE 1.

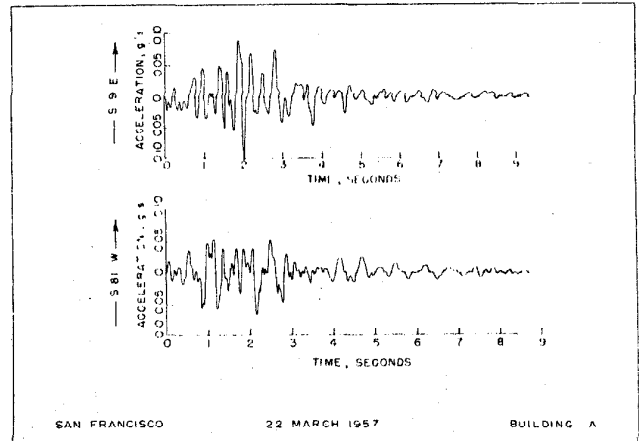


FIGURE 3.

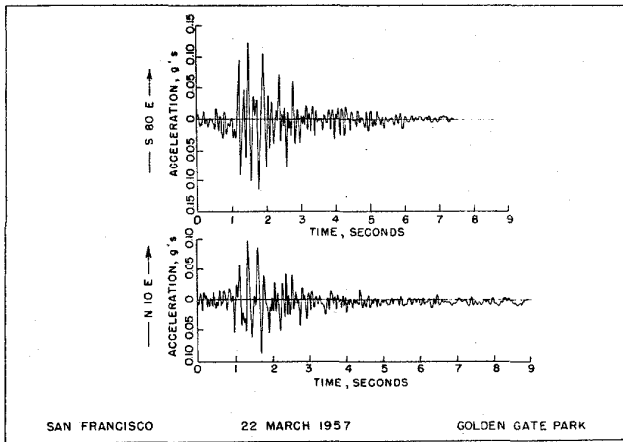


FIGURE 2.

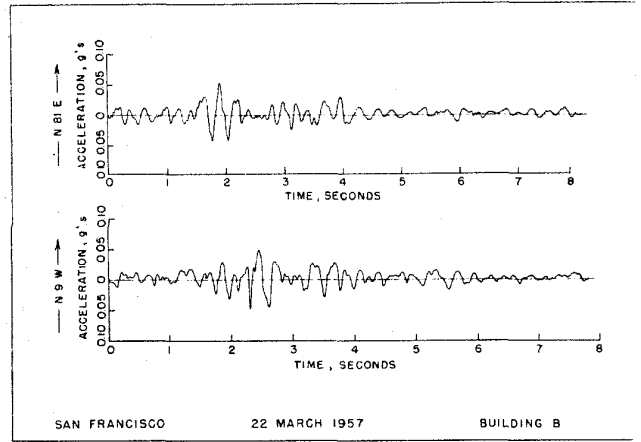


FIGURE 4.

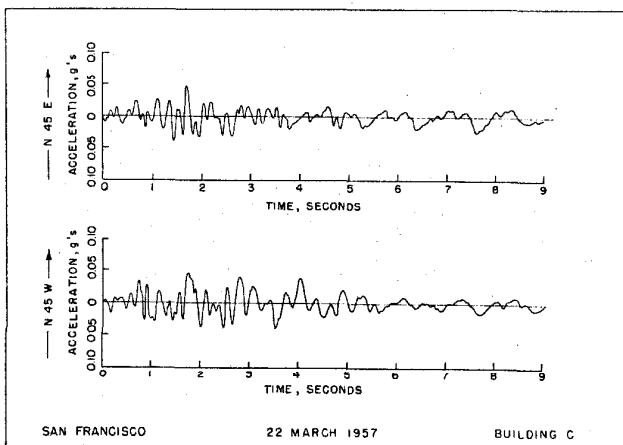


FIGURE 5.

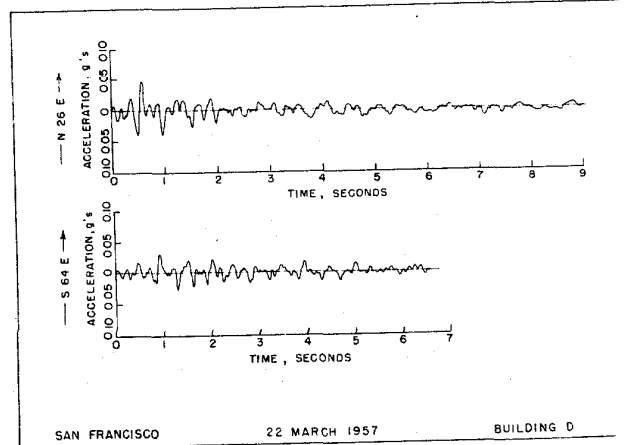


FIGURE 6.

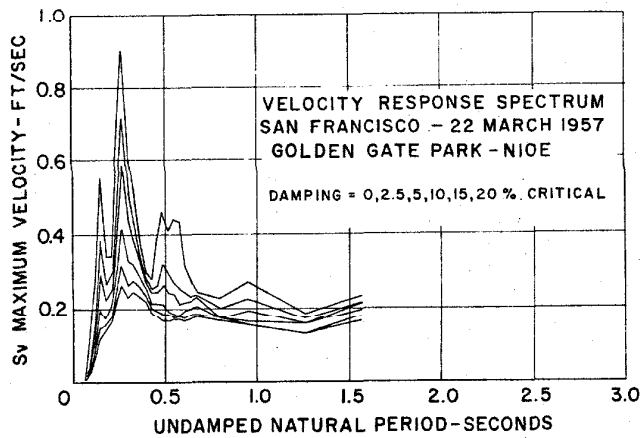


FIGURE 7.

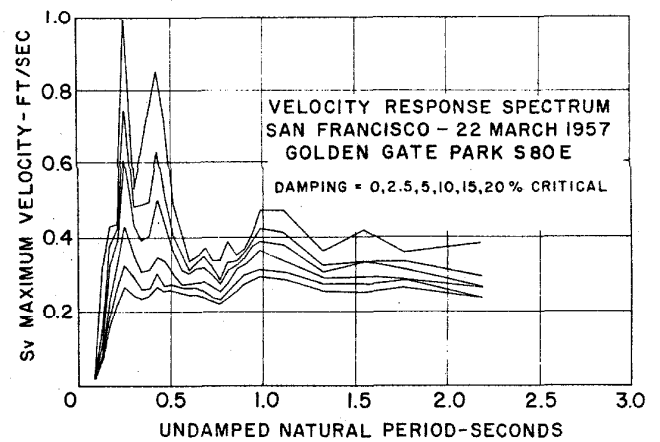


FIGURE 8.

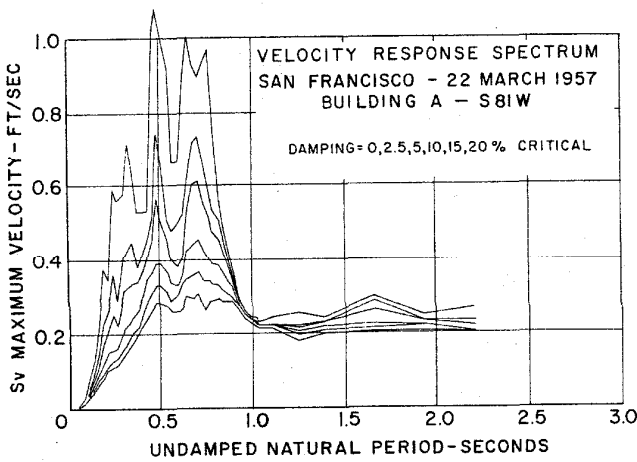


FIGURE 9.

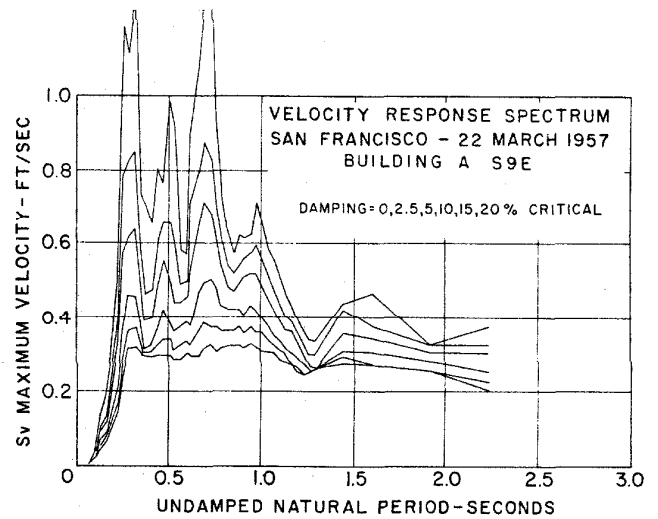


FIGURE 10.

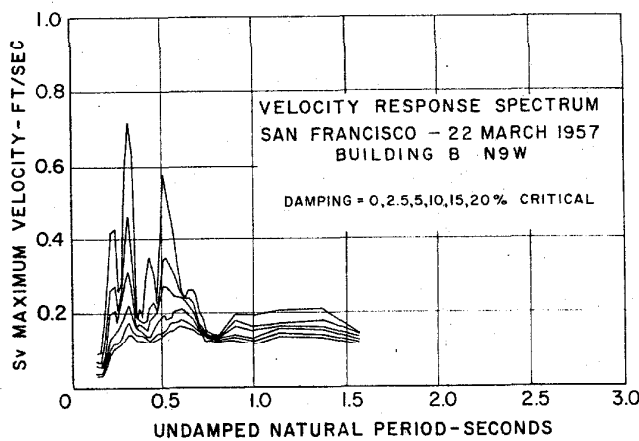


FIGURE 11.

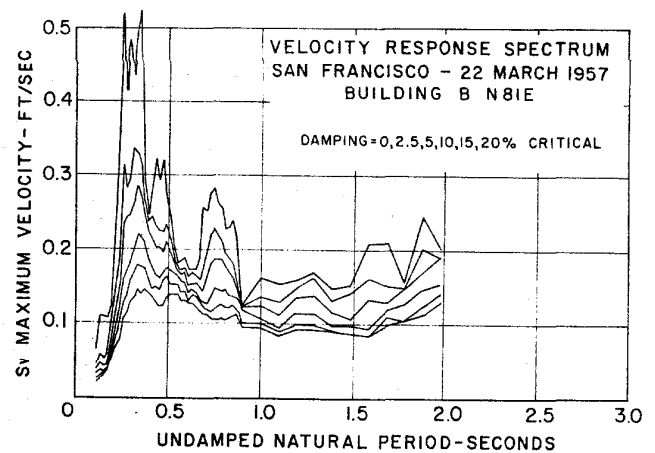


FIGURE 12.

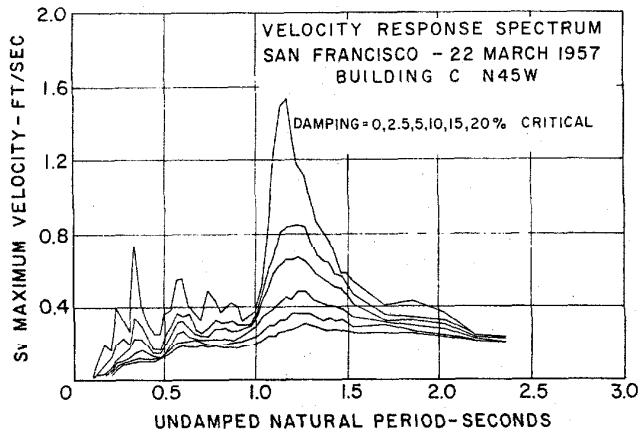


FIGURE 13.

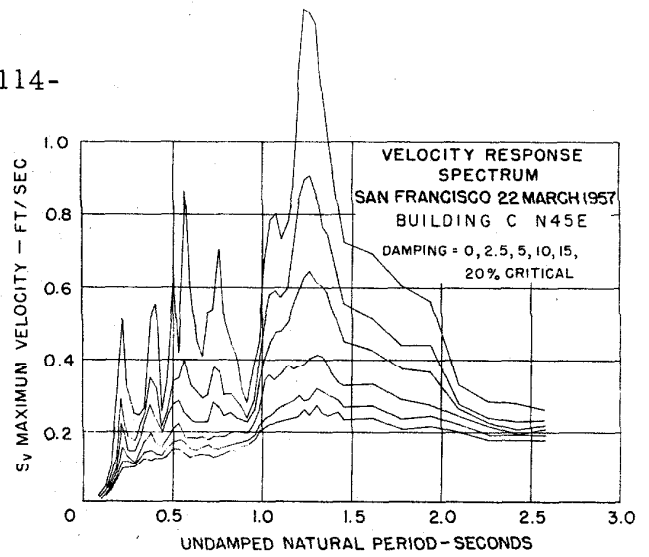


FIGURE 14.

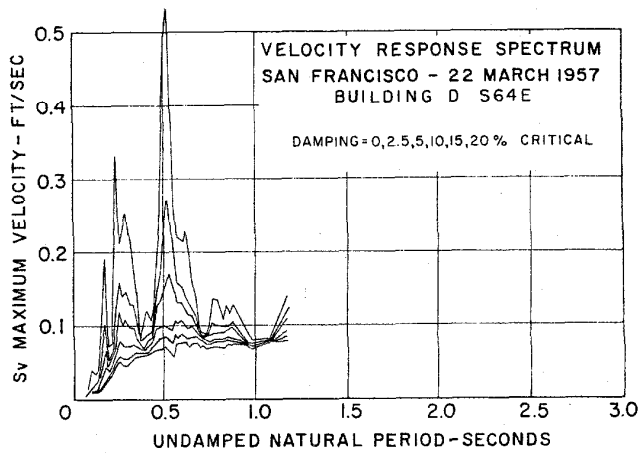


FIGURE 15.

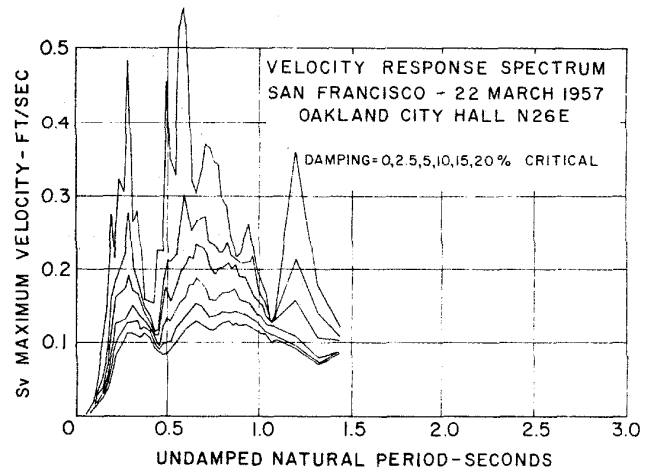


FIGURE 16.

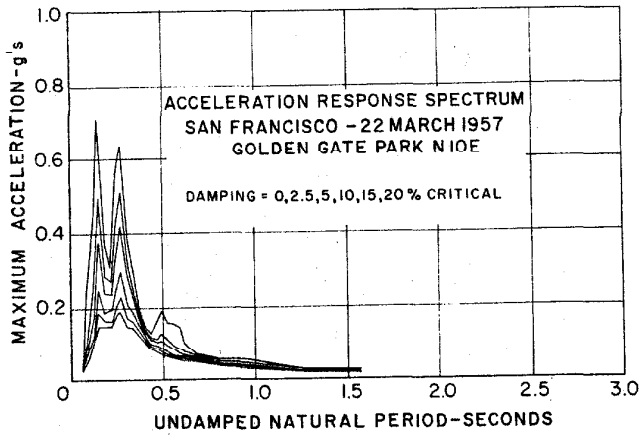


FIGURE 17.

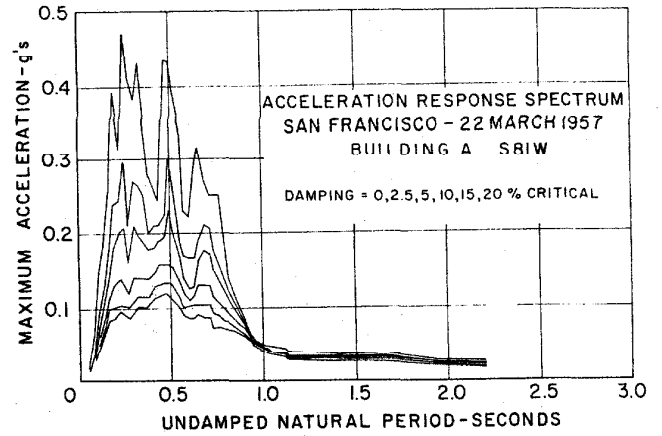


FIGURE 20.

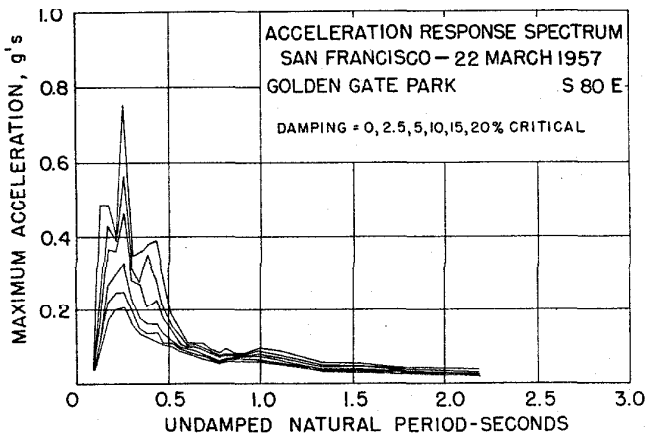


FIGURE 18.

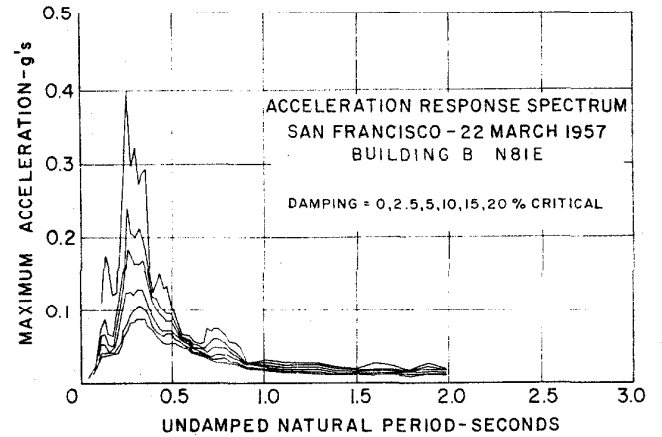


FIGURE 21.

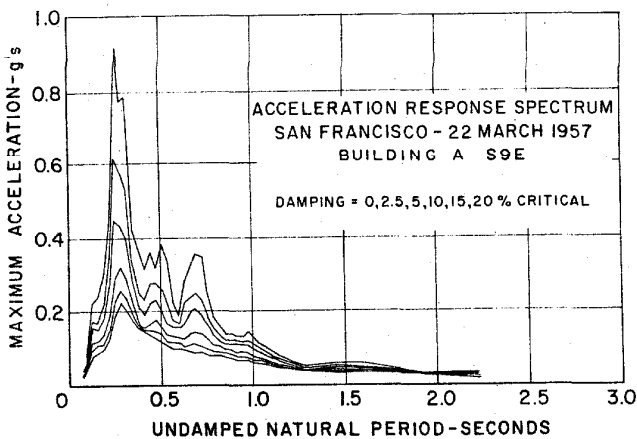


FIGURE 19.

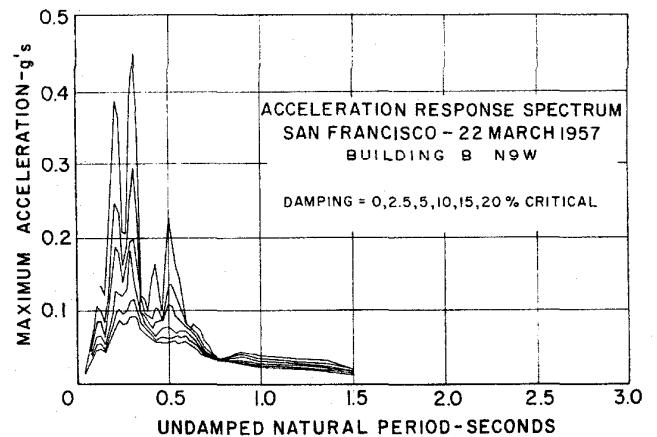


FIGURE 22.

In figures 7-16 the maximum relative velocity response spectra are shown for the various stations. These spectrum curves have been computed using the Electric Analog Spectrum Analyzer of the California Institute of Technology (Caughey and Hudson, 1955; Housner and McCann, 1949), and the data are presented in the standard form which has been used in preceding reports (Housner and Martel, and Alford, 1953; Housner, 1952, 1956). The maximum relative velocity response spectrum is defined as the maximum relative velocity between the ground support and the mass of a single degree of freedom spring-mass system of specified natural period and damping (Hudson, 1956).

In figures 17-26 the maximum acceleration response spectrum curves are shown. This is defined as the maximum absolute acceleration of the mass of a single degree of freedom spring-mass system of specified natural

period and damping, and has been computed from the velocity spectra as obtained above (Hudson, 1956).

It will be observed from all of the spectrum curves that the influence of damping in reducing the peak values was not as marked in this earthquake as in more typical earthquakes. This was a consequence of the short duration of the earthquake, and of the fact that the maximum structural responses thus occurred near the start of the motion, before damping had an opportunity to dissipate much energy. Such records emphasize again the importance which damping may have in the structural problem.

Based on the above spectrum curves, a complete analysis of the spectrum intensities at the various stations has been made, as well as a calculation of the earthquake magnitude determined from the energy released by the earthquake (Hudson and Housner, 1958).

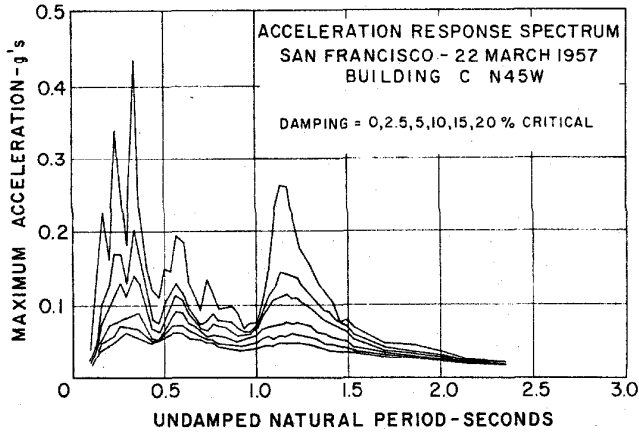


FIGURE 23.

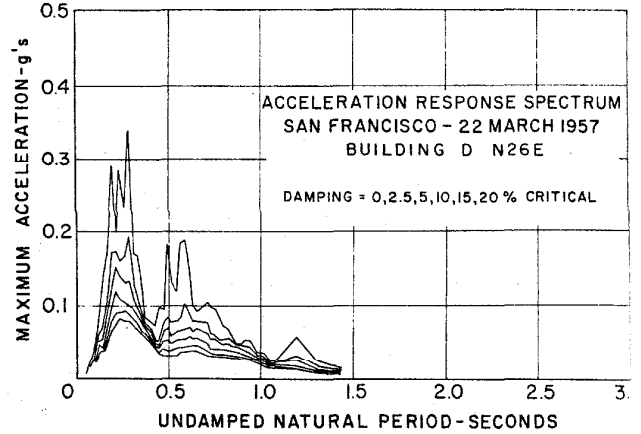


FIGURE 25.

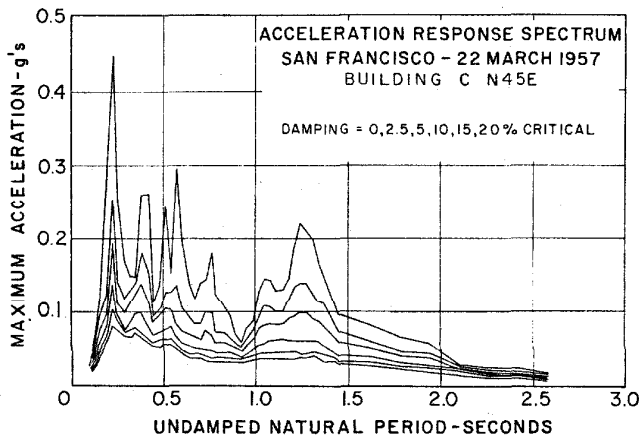


FIGURE 24.

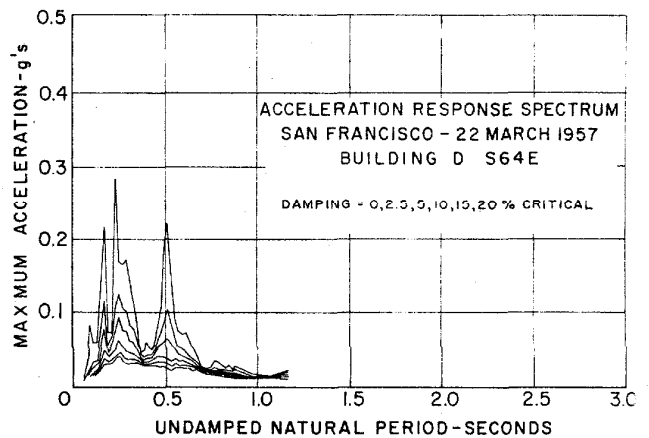


FIGURE 26.

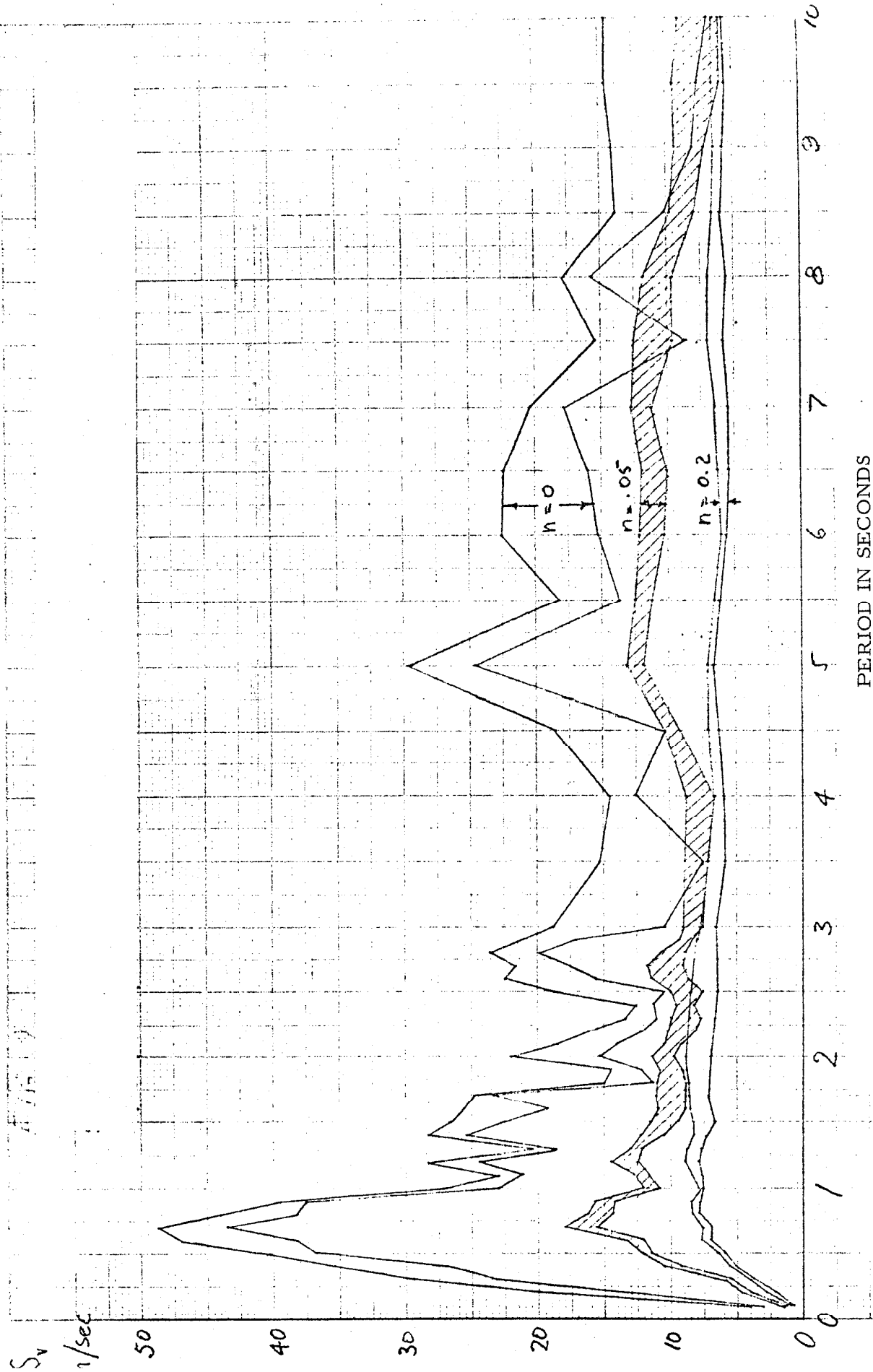
In figure 1 is shown the distribution of the strong motion accelerometer stations of the United States Coast and Geodetic Survey. Only those stations are included from which records were obtained during the earthquake of 22 March 1957 which had acceleration magnitudes of structural significance. On this same figure is shown the instrumental epicenter as reported by the Seismographic Station of the University of California, Berkeley. Additional information from foreshocks and aftershocks has indicated the approximate distance along the fault zone involved in the major tearing action. Based on this

information from the Seismographic Station, an estimated center of the torn zone has been indicated on figure 1 as the approximate origin of the major disturbance. From the same data it was estimated that the average depth of the torn area was 5 miles. This depth is not negligible compared with the distances from the epicenter to the strong-motion stations, and hence on the map the true straight-line distances from the source of major disturbance to the various strong-motion stations have been shown.

In figures 2-6 the horizontal components of ground acceleration as traced from the reproductions of the original photographic records from the strong-motion accelerometers are shown. These figures have all been arranged to have the same acceleration scale, so that the relative magnitudes at the various stations may be readily compared. It should be noted, however, that the time scales differ somewhat, as it was not feasible to completely replot the accelerograms.

APPENDIX I

Comparison of accuracy of spectrum calculations as performed independently by four persons, each of whom started with a point of the Taft, 21 July 1952 accelerogram.



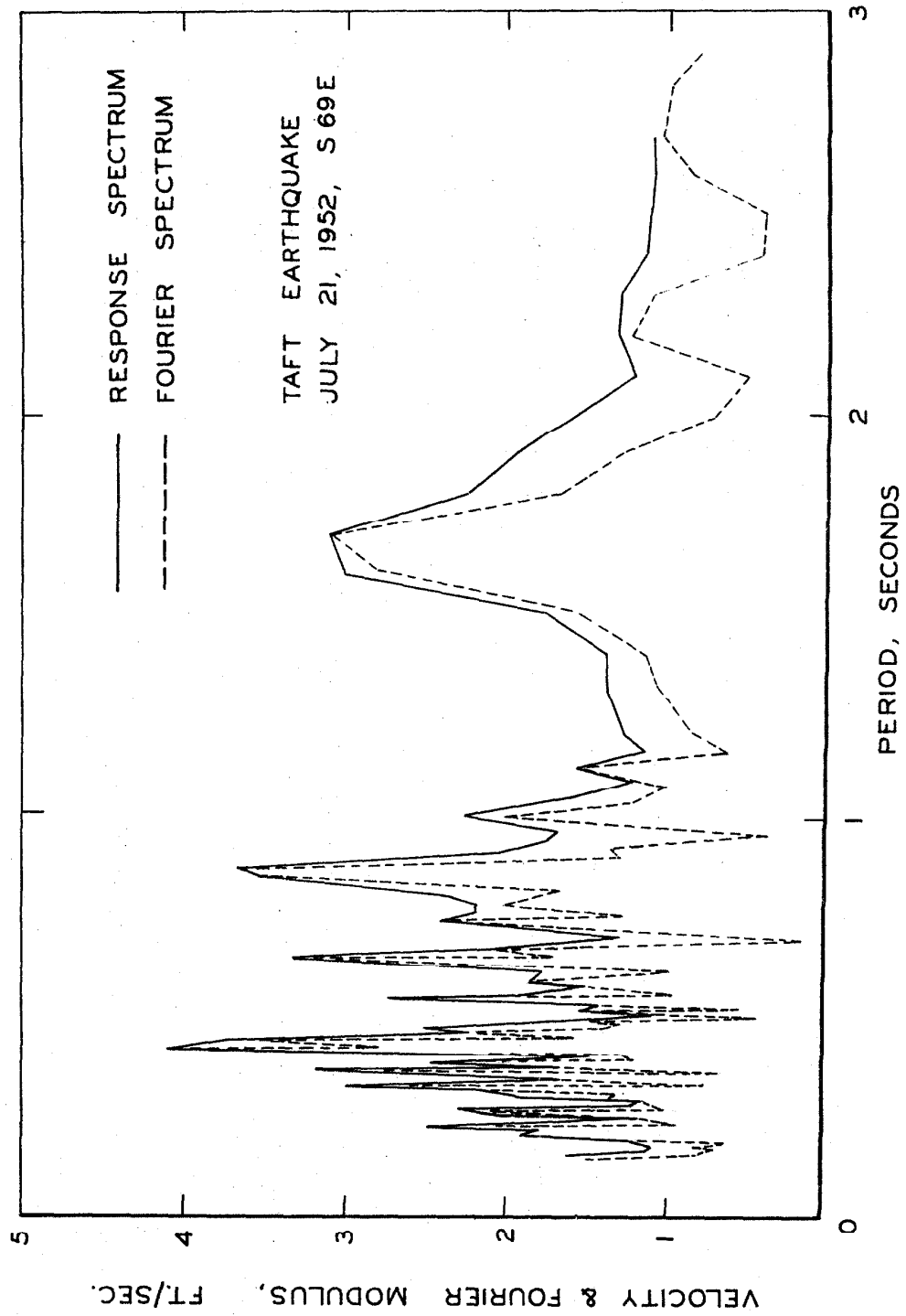
PERIOD IN SECONDS

Spread in velocity spectrum as calculated independently by four persons for 60 seconds of Taft 1952 accelerogram.

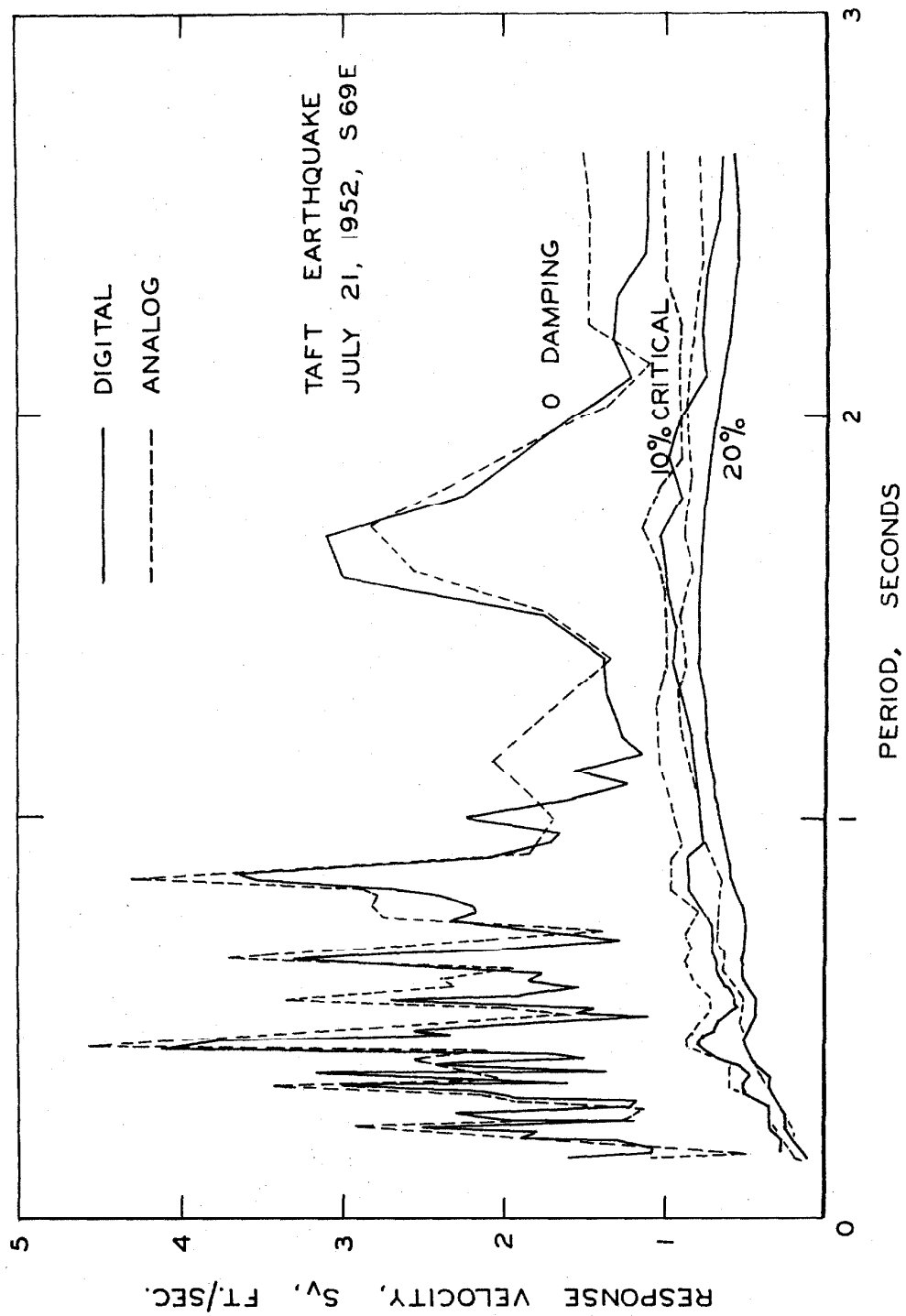
APPENDIX II

Comparison between analog and digital computer calculations, and comparison between zero damped velocity response spectrum and Fourier spectrum*.

*Hudson, D. E., "Some Problems in the Application of Spectrum Techniques to Strong-Motion Earthquake Analysis," Bull. Seism. Soc. of Amer., Vol. 52, No. 2, pp.417-430, April 1962.



COMPARISON OF FOURIER SPECTRUM AND RESPONSE SPECTRUM



COMPARISON OF DIGITAL AND ANALOG
RESPONSE SPECTRUM CALCULATIONS

APPENDIX III

INTEGRATED GROUND VELOCITY AND DISPLACEMENT*

*
Berg, Glen V. and Housner, G. W., "Integrated Velocity and Displacement of Strong Earthquake Ground Motion," Bull. of the Seism. Soc. of Amer., Vol. 51, No. 2, pp. 175-189, April 1961.

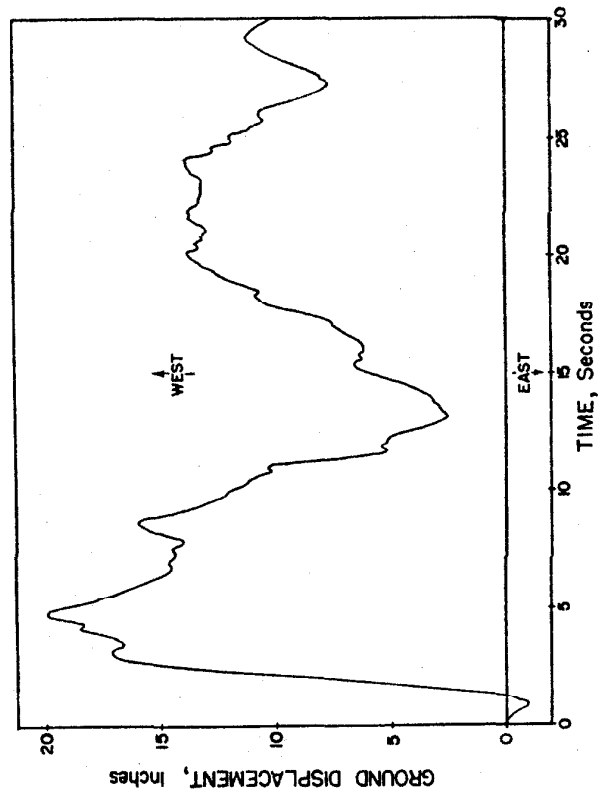
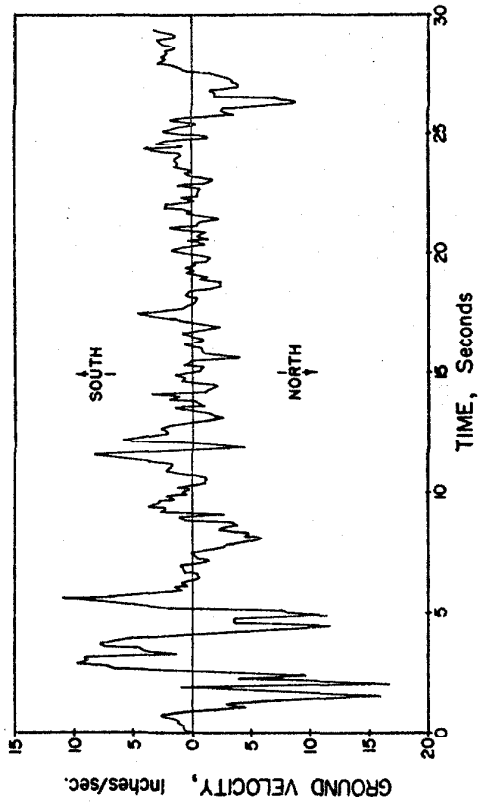


FIG. 1. El Centro, 1940, E-W component.

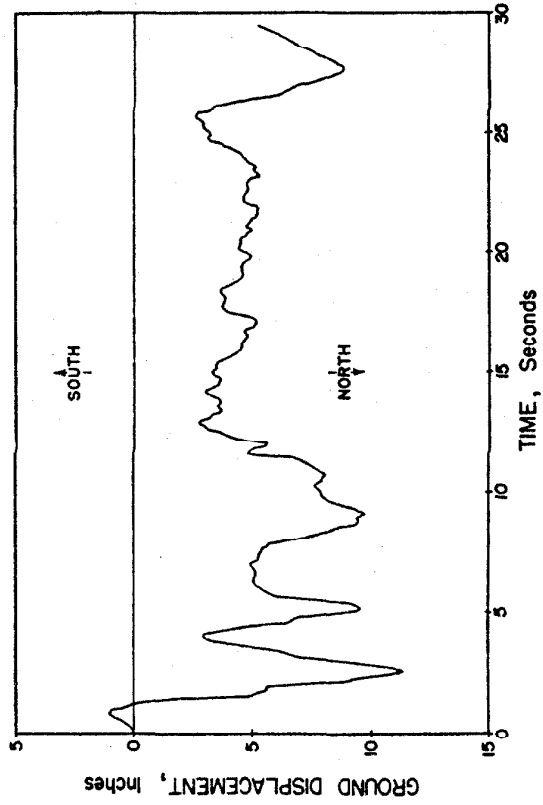
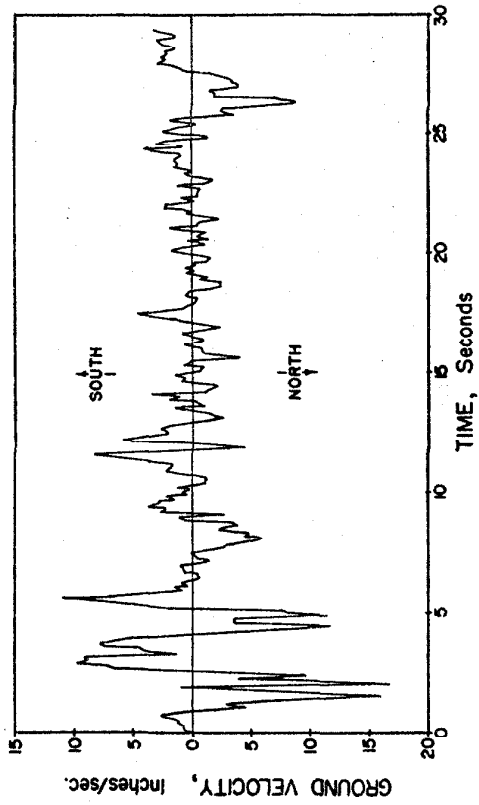


FIG. 2. El Centro, 1940, N-S component.

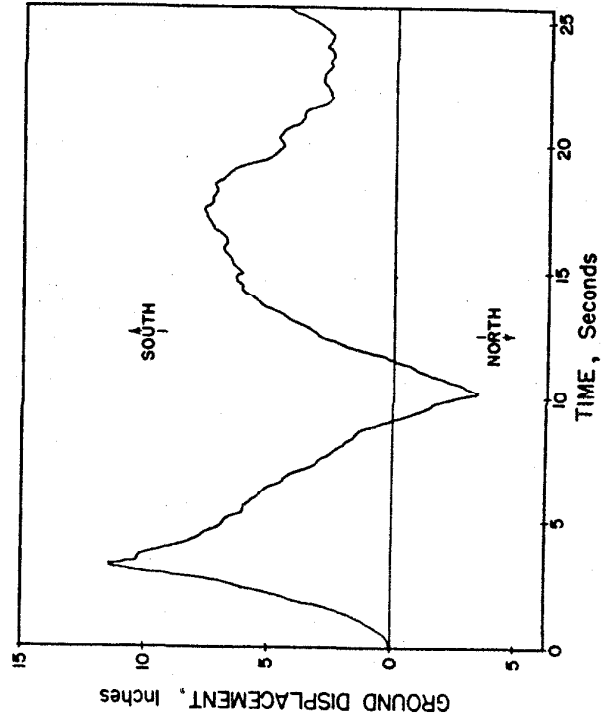
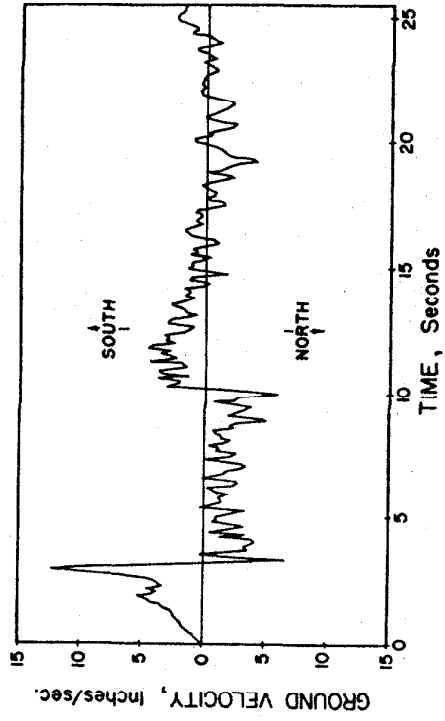


FIG. 4. El Centro, 1934, N-S component.

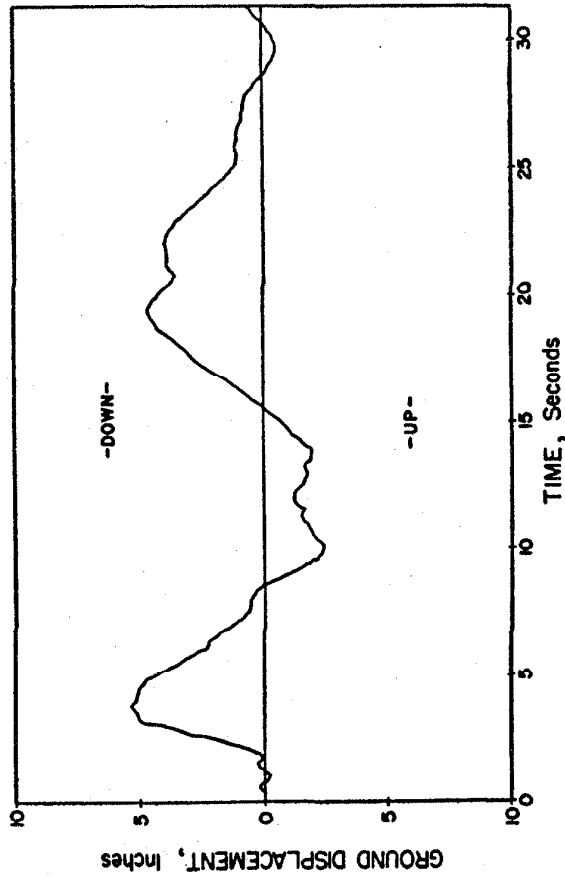
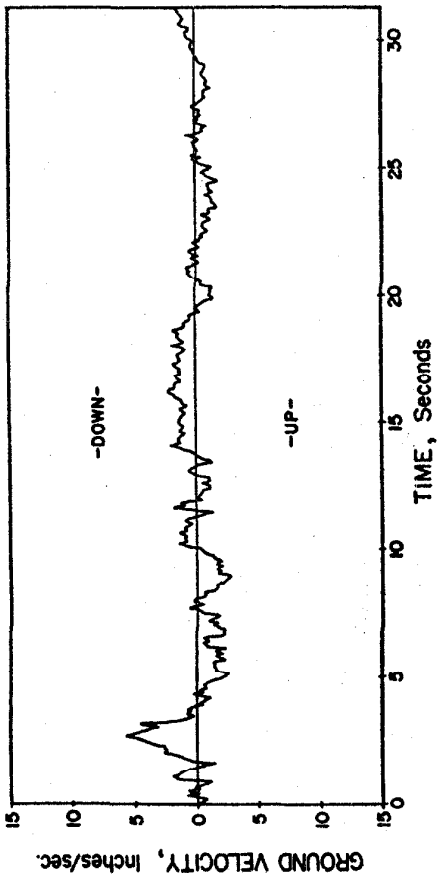


FIG. 3. El Centro, 1940, vertical component.

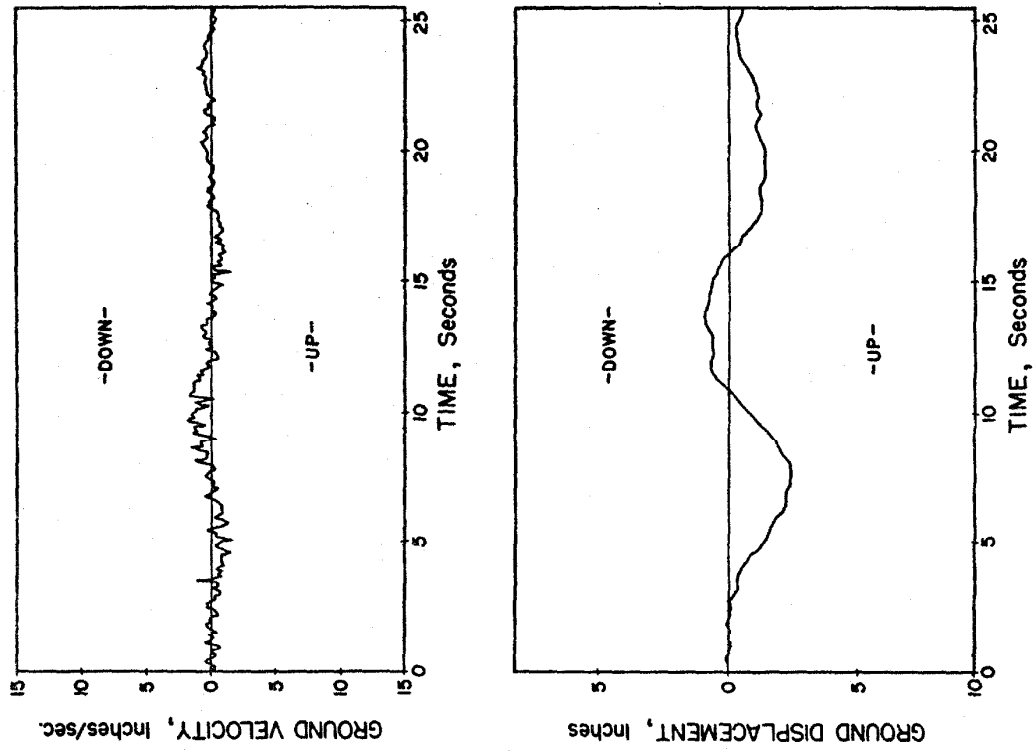


FIG. 6. El Centro, 1934, vertical component.

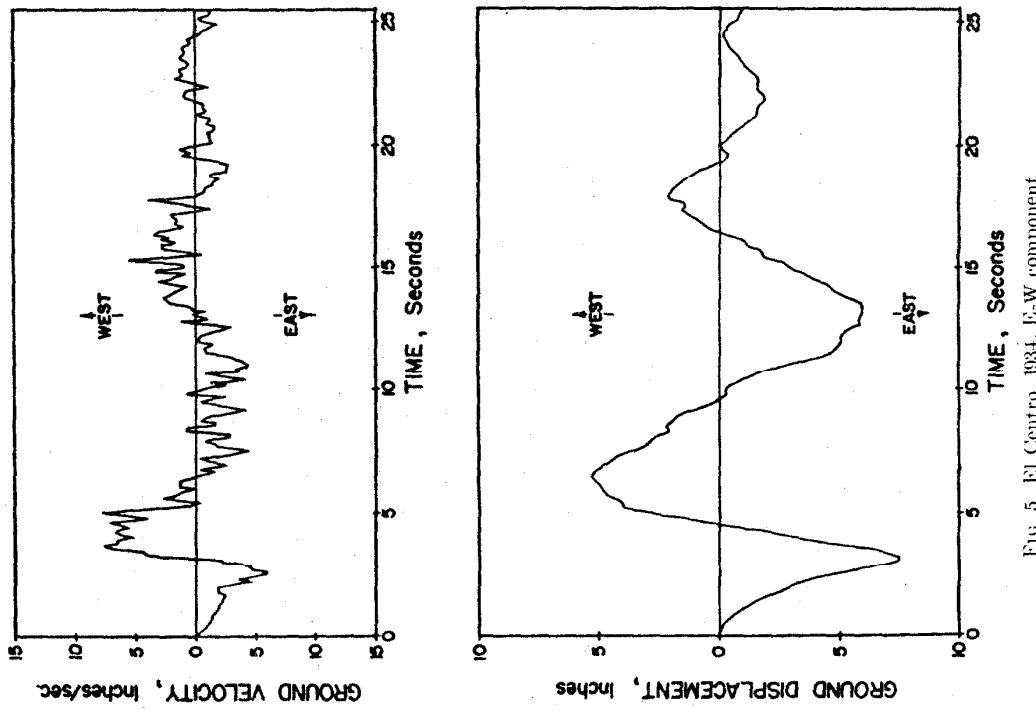


FIG. 5. El Centro, 1934, E-W component.

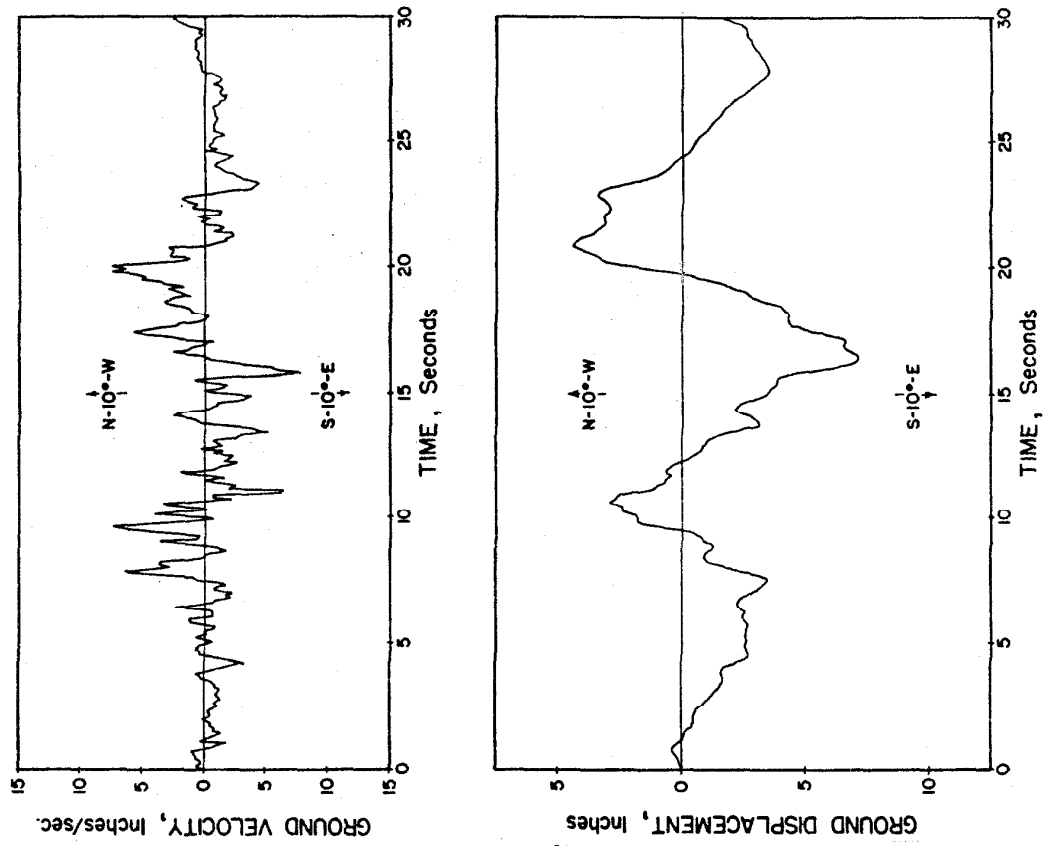


FIG. 8. Olympia, 1949, N-10°-W component.

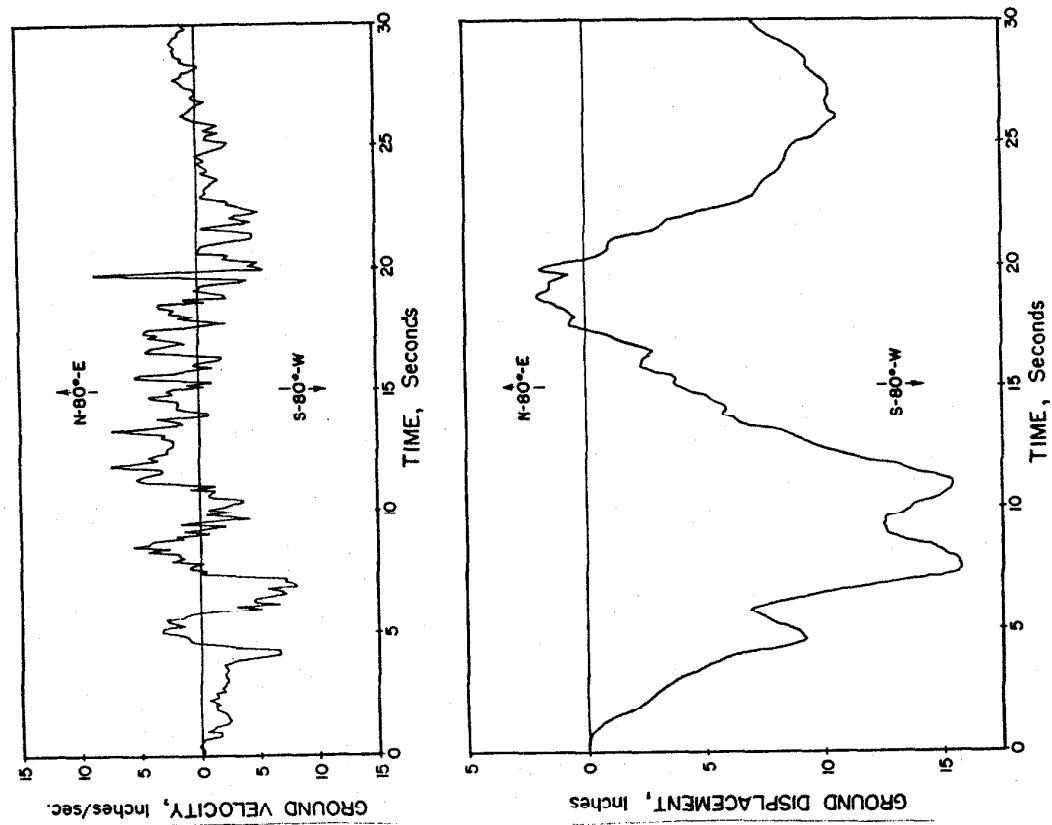


FIG. 7. Olympia, 1949, N-80°-E component.

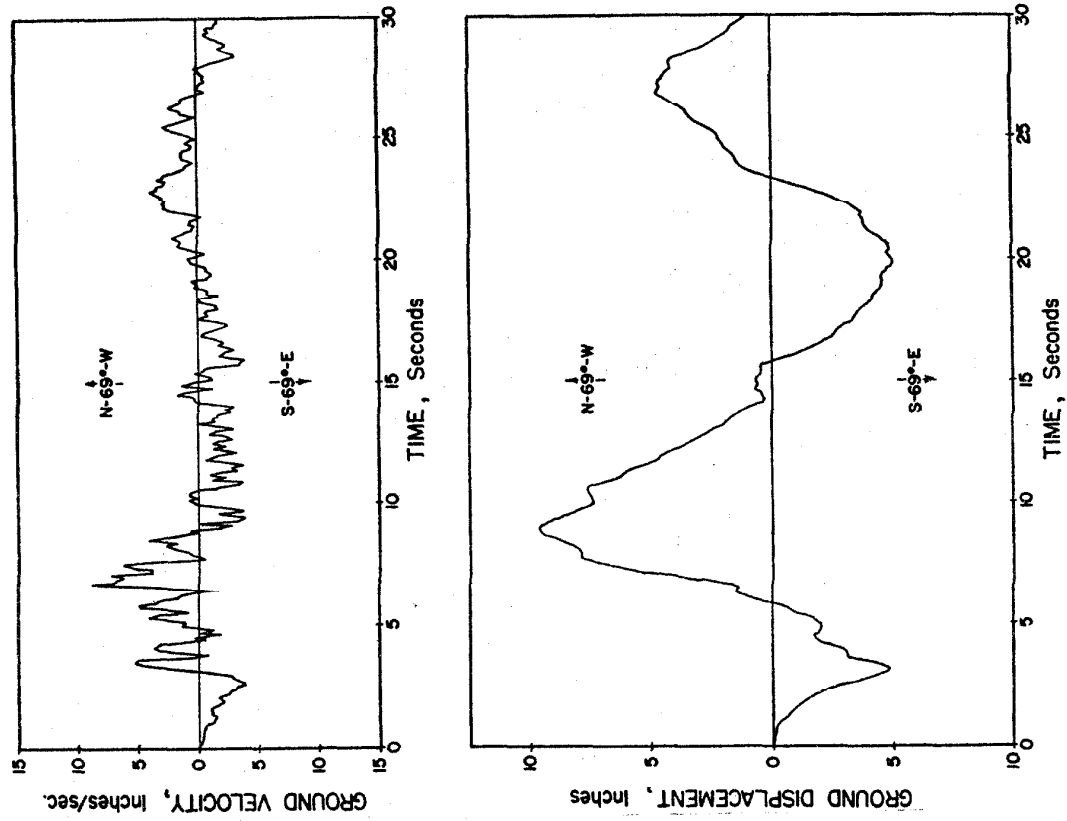


Fig. 10. Taft, 1952, N-69°W component.

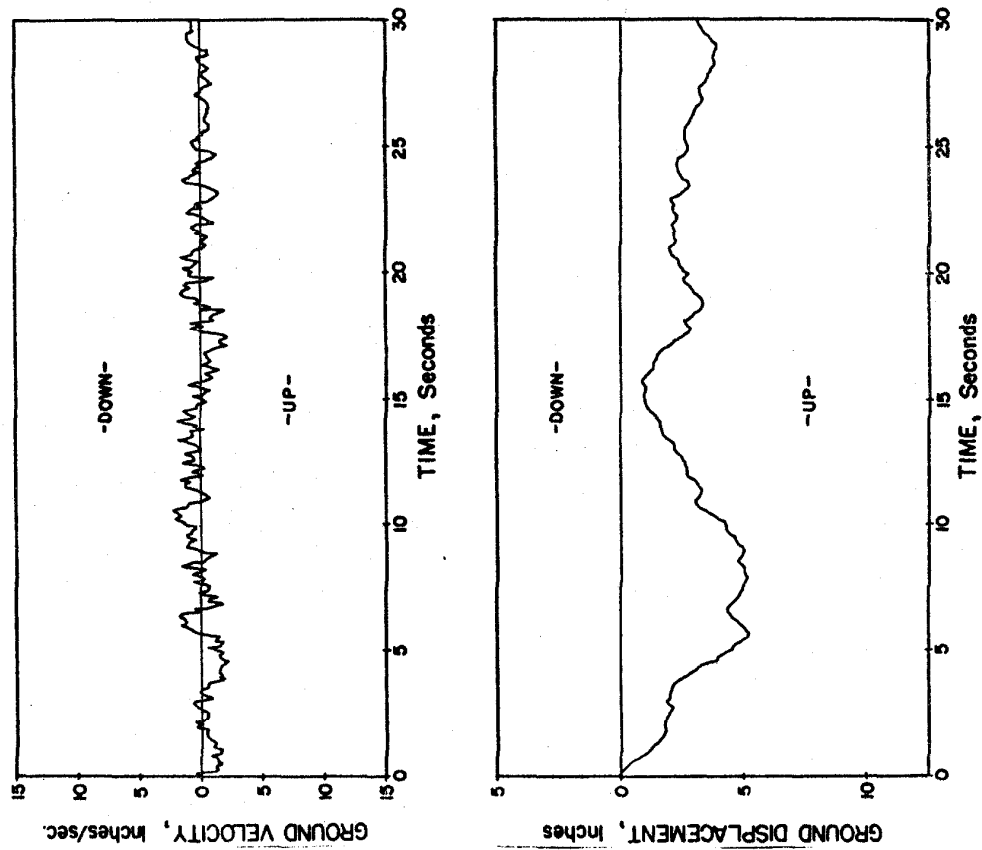


Fig. 9. Olympia, 1949 vertical component.

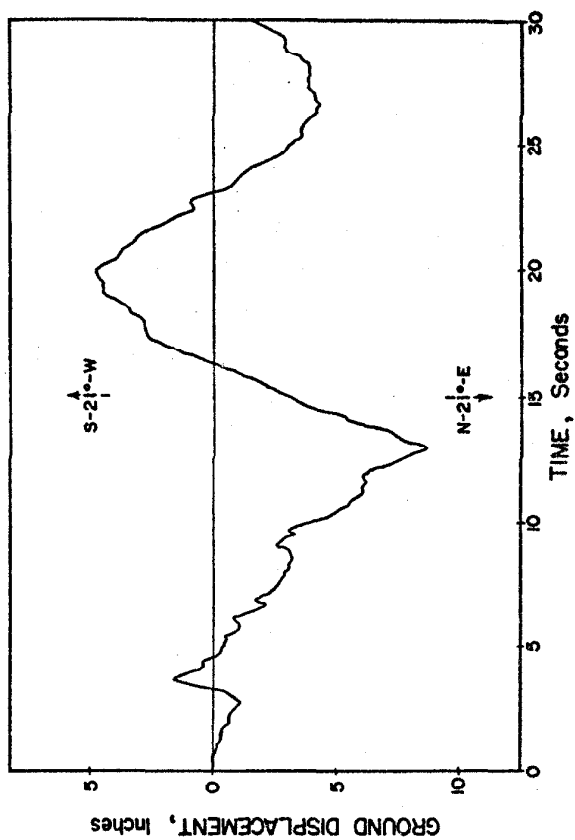
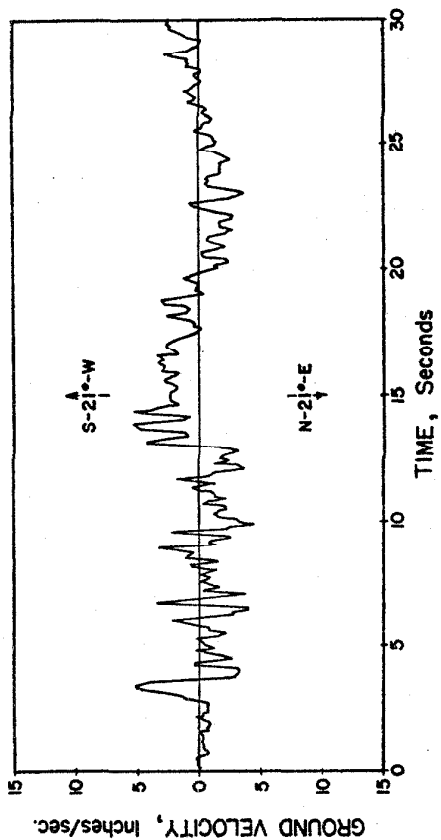


Fig. 11. Taft, 1952, N-21°-E component.

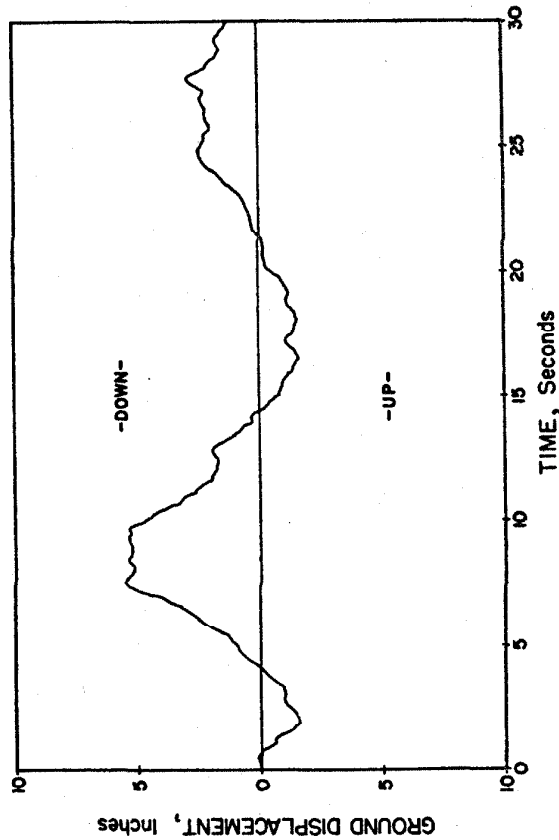
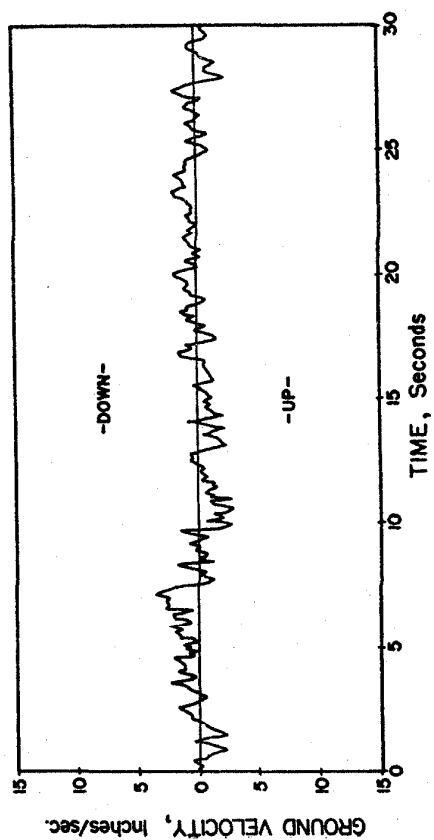


Fig. 12. Taft, 1952, vertical component.